

Fermion Interactions and Universal Behavior in Strongly Interacting Theories

Jens Braun *

Theoretisch-Physikalisches Institut, Friedrich-Schiller-Universität Jena,
Max-Wien-Platz 1, D-07743 Jena, Germany

The theory of the strong interaction, Quantum Chromodynamics (QCD), describes the generation of hadronic masses and the state of hadronic matter during the early stages of the evolution of the universe. As a complement, experiments with ultracold fermionic atoms provide a clean environment to benchmark our understanding of dynamical formation of condensates and the generation of bound states in strongly interacting many-body systems.

Renormalization group (RG) techniques offer great potential for theoretical advances in both hot and dense QCD as well as many-body physics, but their connections have not yet been investigated in great detail. We aim to take a further step to bridge this gap. A cross-fertilization is indeed promising since it may eventually provide us with an ab-initio description of hadronization, condensation, and bound-state formation in strongly interacting theories. After giving a thorough introduction to the derivation and analysis of fermionic RG flows, we give an introductory review of our present understanding of universal long-range behavior in various different theories, ranging from non-relativistic many-body problems to relativistic gauge theories, with an emphasis on scaling behavior of physical observables close to quantum phase transitions (i. e. phase transitions at zero temperature) as well as thermal phase transitions.

Contents

1	Introduction	2
2	Renormalization Group - Basic Ideas	6
3	RG Flow of Four-Fermion Interactions - A Simple Example	11
3.1	A Simple Example and the Fierz Ambiguity	11
3.2	Bosonization and the Momentum Dependence of Fermion Interactions	19
3.3	Spontaneous Symmetry Breaking and Fermion Interactions	29
3.4	A First Look at Scaling Behavior close to a Quantum Critical Point	32
3.4.1	Power-law Scaling	32
3.4.2	Essential Scaling	34
3.5	Deformations of Fermionic Theories	36
3.5.1	Many-Flavor Physics I: Chiral $SU(N_f)_L \otimes SU(N_f)_R$ Symmetry	36
3.5.2	Many-Flavor Physics II: Chiral $U(1)^{\otimes N_f}$ Symmetry	39
3.5.3	Finite Temperature	40
3.5.4	Mass-like Explicit Symmetry Breaking	45
4	Non-relativistic Quantum Field Theories	48
4.1	Cold Atomic Quantum Gases	49
4.2	Excursion: Density Functional Theory and the Renormalization Group	56
5	Gross-Neveu and Nambu-Jona-Lasinio-type Models	60
5.1	Gross-Neveu Model and Quantum Criticality	61
5.1.1	Gross-Neveu Model	61
5.1.2	Fermionic Formulation	61

* Jens Braun E-mail: j.braun@uni-jena.de

5.1.3	Partial Bosonization and the Large- N_f Limit	63
5.1.4	Quantum Critical Behavior Beyond the Large- N_f Limit	68
5.1.5	Excursion: Quantum Criticality and Asymptotic Safety	70
5.2	Nambu-Jona-Lasinio Models and QCD at Low Energies	71
5.2.1	Low-energy QCD Models and the Fierz Ambiguity	72
5.2.2	Phase Transitions in QCD Low-energy Models	76
6	Gauge Theories	82
6.1	Gauge Theories with Few and Many Fermion Flavors - A Motivation	82
6.2	The Issue of Scale Fixing in Gauge Theories	85
6.3	General Aspects of Quantum Critical Behavior in Gauge Theories	87
6.3.1	Miransky Scaling	87
6.3.2	Power-law Scaling	90
6.3.3	Beyond Miransky Scaling	92
6.4	Scaling in Low-energy Models	94
6.5	Chiral $SU(N_c)$ Gauge Theories	95
6.5.1	Renormalization Group Approach to Gauge Theories	96
6.5.2	Phases of Strongly-flavored $SU(N_c)$ Gauge Theories	98
6.5.3	Miransky Scaling	104
6.5.4	Power-law Scaling and Beyond	105
6.6	Excursion: Confinement and Chiral Symmetry Breaking	108
6.7	Fermions in Higher Representations and QED-like Theories	115
7	Summary	115
A	Conventions	116
A.1	Units	116
A.2	Minkowski- and Euclidean Space-Time	117
A.3	Fourier Transformation	117
B	Dirac Algebra	118
B.1	Clifford Algebra in $d = 4$ (Euclidean) Space-Time Dimensions	118
B.2	Clifford Algebra in $d = 3$ (Euclidean) Space-Time Dimensions	118
B.3	Fierz Transformations	118
C	$SU(N)$ Algebra	119
D	Regulator Functions and Threshold Functions	120
D.1	Regulator Functions	120
D.2	Threshold Functions for Covariant Regulators	120
D.3	Threshold Functions for Dimensionally Reduced Regulators	123
	References	124

1 Introduction

Strongly interacting fermions play a very prominent role in nature. The dynamics of a large variety of theories close to the boundary between a phase of gapped and ungapped fermions is determined by strong fermion interactions. For instance, the chiral finite-temperature phase boundary in quantum chromodynamics (QCD), the theory of the strong interaction, is governed by strong fermionic self-interactions. In the low-temperature phase the quark sector is driven to criticality due to strong quark-gluon interactions. These strong gluon-induced quark self-interactions eventually lead to a breaking of the chiral symmetry and the quarks acquire a dynamically generated mass. The chirally symmetric high-temperature phase, on the other hand, is characterized by massless quarks. The investigation of the QCD phase boundary represents one of the major research fields in physics, both experimentally and theoretically. Since the dynamics of the quarks close to the chiral phase boundary affect the equation of state of the theory, a comprehensive

understanding of the quark dynamics is of great importance for the analysis of present and future heavy-ion collision experiments at BNL, CERN and the FAIR facility [1].

While heavy-ion collision experiments provide us with information on hot and dense QCD, experiments with ultracold trapped atoms provide an accessible and controllable system where strongly-interacting quantum many-body phenomena can be investigated precisely. In contrast to the theory of strong interactions, the interaction strength can be considered a free parameter in these systems which can be tuned by hand. In fact, the interaction strength is directly proportional to the s -wave scattering length and can therefore be modulated via an external magnetic field using Feshbach resonances [2]. It is therefore possible to study quantum phenomena such as superfluidity and Bose-Einstein condensation in these systems. From a theorist's point of view, this strong degree of experimental control opens up the possibility to test non-perturbative methods for the description of strongly interacting systems.

Phases of ultracold Fermi gases at zero and finite temperature have been studied experimentally, see e. g. Refs. [3–7] as well as theoretically, see e. g. Refs. [8–27], over the past few years. In particular, studies with renormalization group (RG) methods exhibit many technical similarities to studies of QCD at finite temperature and density, see e. g. Refs. [28–33]. Physically, in both cases the phase boundary is determined by strong interactions of the fermions. While the asymptotic limits of the phase diagram of ultracold atoms for small positive and small negative (s -wave) scattering length associated with Bose-Einstein condensation and Bardeen-Cooper-Schrieffer (BCS) superfluidity [34], respectively, are under control theoretically [35–39], our understanding of the finite-temperature phase diagram in the limit of large scattering length (strong-coupling limit) is still incomplete [8, 10, 11, 14, 25, 27].

Aside from phase transitions at finite temperature, experiments with ultracold fermionic atoms provide a very clean environment for studies of *quantum phase transitions*. Experiments with a dilute gas of atoms in two different hyperfine spin states have been carried out in a harmonic trap at a finite spin-polarization [3, 4]. Since there is effectively no spin relaxation in these experiments, in contrast to most other condensed matter systems, the polarization remains constant for long times. Deforming the system by varying the polarization allows us to gain a deep insight into BCS superfluidity and its underlying mechanisms [34]. Originally, BCS theory has been worked out for systems in which the Fermi surfaces of the two spin states are identical, i. e. the polarization of the system is zero. As a function of the polarization, a *quantum phase transition* occurs at which the (fully polarized) normal phase becomes energetically more favorable than the superconducting phase [17, 20, 22]. After giving a thorough introduction on the level of (advanced) graduate students to the derivation and analysis of fermionic RG flow equations¹ in Sects. 2 and 3, we shall discuss aspects of symmetry breaking and condensate-formation in non-relativistic theories from a RG point of view in Sect. 4.1. For simplicity, we restrict ourselves to systems with a vanishing polarization. The generalization of our RG approach to spin-polarized gases is straightforward and has been discussed in Refs. [23, 40].

Phase separation between a superfluid core and a surrounding normal phase has been indeed observed in experiments with an imbalanced population of trapped spin-polarized ${}^6\text{Li}$ atoms at unitarity at MIT and Rice University [3, 4]. The density profiles measured in these experiments prove the existence of a skin of the majority atoms. A critical polarization P_c associated with a quantum phase transition has been found in both the MIT and Rice experiment. Aside from studies at zero temperature, finite-temperature studies of a spin-polarized gas have been performed at Rice University [4]. In these experiments the critical polarization, above which the superfluid core disappears, has been measured as a function of the temperature. In accordance with theoretical studies [15, 18, 23], the results from the Rice group suggest that a tricritical point exists in the phase diagram spanned by temperature and polarization, at which the

¹ Our introduction is kept on a basic level. In order to explain the derivation of fermionic RG flows, we employ a simple four-fermion theory to explain the derivation of fermionic RG flows. Our toy model already shares many aspects with more complicated theories, such as QCD. In addition to gaining first insights into symmetry breaking patterns encoded in the fixed-point structure of strongly-interacting systems, a simple four-fermion theory allows us to develop a simple terminology for the discussion of various other theories in the subsequent sections. In particular, the analysis of such a theory allows us to address many technically relevant questions such as Fierz ambiguities, the role of momentum dependences of couplings, and Hubbard-Stratonovich transformations. However, more advanced readers may readily skip Sects. 2 and 3.

superfluid-normal phase transition changes from second to first order as the temperature is lowered. Depending on the physical observable, it is in principle possible that finite-size and particle-number effects are visible in the experimental data. Concerning the critical polarization, such effects have been studied in Ref. [41].

There is indeed direct evidence that finite-size effects can alter the phase structure of a given theory. For example, Monte-Carlo studies of the $1 + 1d$ Gross-Neveu model show that the finite-temperature phase diagram of the uniform system is modified significantly due to the non-commensurability of the spatial lattice size with the intrinsic length scale of the inhomogeneous condensate [42, 43]. In particular, the phase with an inhomogeneous ground state shrinks. Such commensurability effects may be present in trapped ultracold Fermi gases as well. Since the Gross-Neveu model in $1 + 1d$ is reminiscent of QCD in many ways, the existence of a stable ground state governed by an inhomogeneous condensate is subject of an ongoing debate, see e. g. Refs. [44, 45]. In any case, it is well-known that the mass spectrum and the thermodynamics of QCD has an intriguing dependence on the volume size and the boundary conditions of the fields, see e. g. Refs. [46–57].

Our theoretical understanding of the phase structure of trapped fermions is currently mostly based on Density Functional Theory (DFT) [58] in a local density approximation (LDA) in which, for example, derivatives of densities are omitted in the ansatz for the action, see e. g. Refs. [16, 18, 19, 24, 26]. From a field-theoretical point of view, DFT corresponds to a mapping of the (effective) action of a fermionic theory onto an action which depends solely on the density. The latter then plays the role of a composite degree of freedom of fermions. Thus, the underlying idea is reminiscent of the *Hubbard-Stratonovich* transformation [59, 60] widely used in low-energy QCD models and spin systems. In any case, the introduction of an effective degree of freedom, such as the density, turns out to be advantageous for a description of theories with an inhomogeneous ground-state. Again, experiments with ultracold atoms allow us to test different approaches and approximation schemes. In Refs. [16, 24], the equation of states of the superfluid and the normal phase of a uniform system have been employed to construct a density functional which allows to study the ground-state properties of trapped Fermi gases. Such a procedure corresponds to an LDA. While there is some evidence that Fermi gases in isotropic traps can be quantitatively understood within DFT in LDA [24], the description of atoms in a highly-elongated trap in LDA seem to fail and derivatives of the density need to be taken into account [61, 62]. In the spirit of these studies, we shall discuss a functional RG approach to DFT in Sect. 4.2 which relies on an expansion of the energy density functional in terms of correlation functions and allows to include effects beyond LDA in a systematic fashion.

Heavy nuclei combine aspects of dense and hot QCD and systems of ultracold atoms. We again need to describe strong interactions between fermions, the nucleons, which form a stable bound state depending on, e. g., the number of protons and neutrons. These interactions are repulsive at short range and attractive at long range as in the case of ultracold atomic gases. Loosely speaking, heavy nuclei can be viewed as spin-polarized systems of two fermion species comparable to those systems studied in experiments with trapped spin-polarized atoms at MIT and Rice University [3, 4]. In fact, almost all nuclei have more neutrons than protons.² Therefore density profiles of protons and neutrons in heavy nuclei are evocative of the profiles associated with the two fermion states in experiments with ultracold atoms. For heavy nuclei, DFT remains currently to be the only feasible approach for a calculation of ground-state properties associated with inhomogeneous densities. State-of-the-art density functional approaches are essentially based on fitting the parameters of a given density functional such that one reproduces the experimentally determined values of the ground-state properties of various heavy nuclei [63–65]. These density functionals are then employed to describe ground-state properties of other heavy nuclei. As mentioned above, we shall briefly discuss an RG approach to DFT in Sect. 4.2, which opens up the possibility to study ground-state properties of heavy nuclei from the underlying nucleon-nucleon interactions. Such an *ab-initio* DFT approach might prove to be useful for future studies of ground-state properties of (heavy) self-bound systems.

² Protons and neutrons correspond to two different isospin states of the nucleon.

Hot and dense QCD, ultracold atoms and nuclear physics represent just three examples for systems in which the dynamics are governed by strong fermion interactions. Of course, the list can be extended almost arbitrarily. In the context of condensed-matter theory, we encounter systems such as so-called high- T_c superconductors. In this case the challenge is to describe reliably the dynamics of electrons at finite temperature in an ambient solid-state system. The so-called Hubbard model provides a theory to describe these superconductors [66, 67] and has been extensively studied with renormalization-group techniques, see e. g. Refs. [68–71]. It is worth noting that both the mechanisms as well as the techniques are remarkably similar to the ones in renormalization-group studies of gauged fermionic systems interacting strongly via competing channels [30–32], such as QCD, and of imbalanced Fermi gases in free space-time [23]. In Sect. 5, we discuss more general aspects of (non-gauged) Gross-Neveu- and Nambu-Jona-Lasinio-type models which also exhibit technical similarities to studies of condensed-matter systems. Nambu-Jona-Lasinio-type models are widely used as effective QCD low-energy models. On the other hand, Gross-Neveu-type models have been employed as toy models to study certain aspects of the QCD phase diagram but they are also related to models in condensed-matter theory, e. g. to models of ferromagnetic (relativistic) superconductors [72, 73]. In this review, we shall use Gross-Neveu- and Nambu-Jona-Lasinio-type models to discuss dynamical chiral symmetry breaking (via competing channels) and the role of momentum dependences of fermionic interactions.

In addition to fermion dynamics at finite temperature, quantum phase transitions play a prominent role in condensed-matter theory, e. g., in the context of graphene. Effective theories of graphene, such as QED_3 and the Thirring model, are expected to approach a quantum critical point when the number of fermion species, namely the number of electron species, is varied [74, 75]. RG studies of these effective theories, see e. g. Refs. [74–76], are closely related to studies of quantum phase transitions in QCD [29–31, 77–79]. Similar to the situation in QED_3 , a quantum phase transition from a chirally broken to a conformal phase is expected in QCD when the number of (massless) quark flavors is increased. Studies of the dependence on the number of fermion species seem to be a purely academic question. Depending on the theory under consideration, however, such a deformation of the theory may allow us to gain insights into the dynamics of fermions close to a phase boundary in a controlled fashion. For example, the gauge coupling in QCD becomes small when the number of quark flavors is increased and therefore perturbative approaches in the gauge sector become meaningful. Moreover, an understanding of strongly-flavored QCD-like gauge theories is crucial for applications beyond the standard-model, namely for so-called walking technicolor scenarios for the Higgs sector [80–88]. In Sect. 6, we shall discuss chiral symmetry breaking in gauge theories with N_f fermion flavors. In particular, we shall present a detailed discussion of the scaling behavior of physical observables close to the quantum phase transition which occurs for large N_f .

Our discussion shows that systems of strongly interacting fermions play indeed a very prominent role in nature and that their dynamics determine the behavior of a wide class of physical systems with seemingly substantial differences. However, our discussion also shows that the underlying mechanisms of symmetry breaking and the applied techniques are very similar in these different fields. Therefore a phenomenological and technical cross-fertilization offers great potential to gain a better understanding of the associated physical processes. As outlined, examples include an understanding of the dynamical generation of hadron masses as well as of the dynamical formation of condensates and bound-states in ultracold gases from first principles. The main intent of the present review is to give a general introduction to the underlying mechanisms of symmetry breaking and bound-state formation in strongly-interacting fermionic theories. In particular, we aim to give a thorough introduction into the scaling behavior of physical observables close to critical points, ranging from power-law scaling behavior to essential scaling. As a universal tool for studies of quantum field theories we employ mainly Wilsonian-type renormalization-group techniques [89–95]. For concrete calculations we shall use the so-called Wetterich equation [95] which we briefly introduce in the next section. Reviews focussing on various different aspects of renormalization-group approaches can be found in Refs. [96–110].

2 Renormalization Group - Basic Ideas

We begin with a brief introduction of the basic ideas of RG approaches including a discussion of the Wetterich equation. The latter describes the scale dependence of the quantum effective action which underlies our studies in this and the following sections.

In perturbation theory, the correlation functions of a given quantum field theory contain divergences which can be removed by a renormalization prescription. The choice of such a prescription defines a renormalization scheme and renders all (coupling) constants of a given theory scheme-dependent. Since the renormalized (coupling) constants are nothing but mathematical parameters, their values can be arbitrarily changed by changing the renormalization prescription. We stress that these renormalized constants should not be confused with physical observables such as, for example, the phase transition temperature or the *physical* mass of a particle. Physical observables are, of course, invariant under a variation of the renormalization prescription, provided we have not truncated the perturbation series. If we consider a truncated perturbation series, we find that there is a residual dependence on the renormalization scheme which can be controlled to some extent by the so-called "Principle of Minimum Sensitivity" [111], see also discussion below.

At this point we are then still free to perform additional finite renormalizations. This results in different *effective* renormalization prescriptions. A given renormalization prescription can then be considered as a particular reordering of the perturbative expansion which expresses it in terms of new renormalized constants [112]. Let us assume that the transformations between the finite renormalizations can be parametrized by introducing an auxiliary single mass scale μ . This scale corresponds to a UV (cutoff) scale at which the parameters of the theory are fixed. A set of RG equations for a given theory then describes the changes of the renormalized parameters of this theory (e. g. the coupling constant) induced by a variation of the auxiliary mass scale μ . The set of renormalization *transformations* is called the renormalization group.

Let us now consider a (renormalized) microscopic theory at some large momentum scale Λ defined by a (classical) action S . Wilson's basic idea of the renormalization group is to start with such a classical action S and then to integrate out successively all fluctuations from high to low momentum scales [89–91]. This procedure results in an action which depends on an IR regulator scale, say k , which plays the role of a reference scale. The values of the (scale-dependent) couplings defining this action on the different scales are related by continuous RG transformations. We shall refer to the change of a coupling under a variation of the scale k as the RG flow of the coupling. In this picture, *universality* means that the RG flow of the couplings is governed by a *fixed point*. The possibility of identifying fixed points of a theory makes the RG such a powerful tool for studying statistical field theories as well as quantum field theories. As we shall discuss below, critical behavior near phase transitions is intimately linked to the fixed-point structure of the theory under consideration.

In this review we employ a non-perturbative RG flow equation, the Wetterich equation [95], for the so-called effective average action in order to analyze critical behavior in physical systems. The effective average action Γ_k depends on an intrinsic momentum scale k which parameterizes the Wilsonian RG transformations. We note that such an approach is based on the fact that an infinitesimal RG transformation (i. e. an RG step), performed by an integration over a single momentum shell of width Δk , is finite. For this reason we are able to integrate out all quantum fluctuations through an infinite sequence of such RG steps. The flow equation for Γ_k then describes the continuous trajectory from the microscopic theory S at large momentum scales to the full quantum effective action (macroscopic theory) at small momentum scales. Thus, it allows us to cover physics over a wide range of scales.

Here, we only discuss briefly the derivation and the properties of the RG flow equation for the effective average action Γ_k ; for details we refer to the original work by Wetterich [95]. The scale-dependent effective action Γ_k is a generalization of the (quantum) effective action Γ but only includes the effects of fluctuations with momenta $p^2 \gtrsim k^2$. Therefore Γ_k is sometimes called a coarse-grained effective action since quantum fluctuations on length scales smaller than $1/k$ are integrated out. The underlying idea is to calculate the generating functional Γ of one-particle irreducible (1PI) graphs of a given theory by starting at an

ultraviolet (UV) scale Λ with the microscopic (classical) action S and then successively integrating out quantum fluctuations by lowering the scale k . The quantum effective action Γ is then obtained in the limit $k \rightarrow 0$. In other words, the coarse-grained effective action Γ_k interpolates between the classical action S at the UV scale Λ and the 1PI generating functional Γ in the infrared limit (IR) $k \rightarrow 0$. The starting point for the derivation of the flow equation of Γ is a UV- and IR-regularized generating functional Z_k for the Greens functions:³

$$Z_k[J] = \int_{\Lambda} \mathcal{D}\phi(\{p_i\}) e^{-S[\phi] - \Delta S_k[\phi] + J^T \cdot \phi} \equiv e^{W_k[J]}, \quad (1)$$

where $\{p_i\} \equiv \{p_0, \dots, p_d\}$ and W_k is the scale-dependent generating functional for the connected Greens functions. The field variable ϕ as well as the source J are considered as generalized vectors in field space and are defined as

$$\phi = \begin{pmatrix} \psi \\ \bar{\psi}^T \\ \varphi \\ \vdots \end{pmatrix} \quad \text{and} \quad J^T = (\bar{\eta}, \eta^T, j, \dots). \quad (2)$$

Moreover, we have introduced a generalized scalar product in field space: $J^T \cdot \phi \equiv \int d^d x \{ \bar{\eta} \psi + \dots \}$. Here, the field ψ represents a Dirac spinor, and φ denotes a real-valued scalar field. The dots indicate that other types of fields, e. g. gauge-fields, are allowed as well. For non-relativistic theories of fermions, the generating functional can be defined accordingly. We assume that the theory is well-defined by a UV-regularized generating functional: The index Λ indicates that we only integrate over fields $\phi(\{p_i\})$ with momenta $|p| \lesssim \Lambda$, i. e. we implicitly take $\phi(\{p_i\}) = 0$ for $|p| > \Lambda$. To regularize the infrared modes a cutoff term has been inserted into the path integral. It is defined as

$$\Delta S_k[\phi] = \frac{1}{2} \sum_{a,b} \int \frac{d^d p}{(2\pi)^d} \phi_a(\{-p_i\}) R_k^{ab}(\{p_i\}) \phi_b(\{p_i\}) \equiv \frac{1}{2} \phi^T \cdot R_k \cdot \phi, \quad (3)$$

where R_k is a matrix-valued regulator function. Through the insertion of the cutoff term, we have defined a generating functional which now depends on the scale k .

The cutoff function R_k has to fulfill three conditions. Since R_k has been introduced to regularize the IR, it must fulfill

$$\lim_{\frac{p^2}{k^2} \rightarrow 0} R_k(\{p_i\}) > 0, \quad (4)$$

where $p^2 = p_0^2 + \dots + p_{d-1}^2$. Second, the function R_k must vanish in the IR-limit, i. e. for $k \rightarrow 0$:

$$\lim_{\frac{k^2}{p^2} \rightarrow 0} R_k(\{p_i\}) = 0. \quad (5)$$

This condition ensures that we obtain the 1PI generating functional for $k \rightarrow 0$. Third, the cutoff function should obey

$$\lim_{k \rightarrow \Lambda} R_k(\{p_i\}) \rightarrow \infty \quad (6)$$

for fixed p^2 . This property guarantees that $\Gamma_{k \rightarrow \Lambda} \rightarrow S$ for $k \rightarrow \Lambda$.

In this review, we shall always use cutoff functions which can be written in terms of a dimensionless regulator shape function $r(p^2/k^2)$. For simple relativistic scalar theories, we may choose

$$R_k(p^2) \propto p^2 r\left(\frac{p^2}{k^2}\right). \quad (7)$$

³ Throughout this review we work in Euclidean space-time. We refer the reader to App. A for details on our conventions.

For studies of theories with chiral fermions, it is convenient to employ a cutoff function which *preserves* chiral symmetry. An appropriate choice is [113]

$$R_k^\psi(\{p_i\}) \propto \not{p} r_\psi\left(\frac{p^2}{k^2}\right). \quad (8)$$

On the other hand, for non-relativistic fermionic many-body problems the choice of the cutoff function should respect the presence of a Fermi surface. An appropriate choice for such a cutoff function is given by [27]

$$R_k^\psi(\vec{p}^2) = k^2 r_\psi(\mathcal{Z}) \quad \text{with} \quad \mathcal{Z} = (\vec{p}^2 - \mu)/k^2, \quad (9)$$

where, for instance,

$$r_\psi(\mathcal{Z}) = (\text{sign}(\mathcal{Z}) - \mathcal{Z})\theta(1 - |\mathcal{Z}|). \quad (10)$$

The chemical potential of the fermions is given by μ and defines the associated Fermi surface. This choice for the regulator function arranges the momentum-shell integrations around the Fermi surface, i. e. modes with momenta $(\vec{p}^2 - \mu) \geq k^2$ remain unchanged while the momenta of modes with $(\vec{p}^2 - \mu) < k^2$ are cut off.

For scalar field theories, the presence of a cutoff function of the form $\sim R_k(p^2)$ is in general not problematic. For gauge theories, however, it causes difficulties due to condition (4) which essentially requires that the cutoff function acts like a mass term for small momenta. Therefore the cutoff function necessarily breaks gauge symmetry. We stress that this observation does by no means imply that such an approach cannot be applied to gauge theories. In fact, it is always necessary to fix the gauge in order to treat gauge theories perturbatively within a path-integral approach. This gauge-fixing procedure also breaks gauge invariance. Gauge-invariant results are then obtained by resolving Ward-Takahashi identities. Consequently, we can think of the cutoff function as an additional source of gauge-symmetry breaking. In analogy to perturbation theory, one then needs to deal with *modified* Ward-Takahashi identities in order to recover gauge invariance [114–119]. In addition, there are essentially two alternatives: first, one can construct manifestly gauge-invariant flows as proposed in [108, 120, 121]. Second, we can apply special (useful) gauges, such as the background-field gauge [122, 123]. We refer the reader to Ref. [105] for a detailed introduction to RG flows in gauge theories.

The coarse-grained effective action Γ_k can in principle be obtained from the IR-regularized functional $W_k[J]$ in a standard fashion, see, e. g., the standard textbook derivation of the quantum effective action Γ in Refs. [112, 123]. However, we employ here a *modified* Legendre transformation to calculate the coarse-grained effective action:⁴

$$\Gamma_k[\Phi] = \sup_J \{-W_k[J] + J^T \cdot \Phi\} - \Delta S_k[\Phi]. \quad (11)$$

The so-called classical field Φ is implicitly defined by the supremum prescription. The modification of the Legendre transformation is necessary for the connection of Γ_k with the classical action S in the limit $k \rightarrow \Lambda$. From this definition of Γ_k we find the RG flow equation of the coarse-grained effective action, the so-called Wetterich equation [95], by taking the derivative with respect to the scale k :

$$\partial_t \Gamma_k[\Phi] = \frac{1}{2} \text{STr} \left[\Gamma_k^{(2)}[\Phi] + R_k \right]^{-1} \cdot (\partial_t R_k) = \frac{1}{2} \text{Tr} \left[\text{Bubble} \right], \quad (12)$$

⁴ Note that a functional obtained by an ordinary Legendre transformation, e. g. $\Gamma[\Phi] = \sup_J \{-W[J] + J^T \cdot \Phi\}$, is convex. However, the coarse-grained effective action Γ_k is not necessarily convex for finite k due to the insertion of the cutoff term. Since $R_k \rightarrow 0$ for $k \rightarrow 0$, convexity is recovered in the limit $k \rightarrow 0$.

with $t = \ln(k/\Lambda)$ being the RG “time” and $\Gamma^{(2)} \equiv \Gamma^{(1,1)}$. The $(n + m)$ -point functions are defined as follows:

$$\Gamma_k^{(n,m)}[\Phi] = \overbrace{\frac{\overrightarrow{\delta}}{\delta\Phi^T} \cdots \frac{\overrightarrow{\delta}}{\delta\Phi^T}}^{n\text{-times}} \Gamma_k[\Phi] \overbrace{\frac{\overleftarrow{\delta}}{\delta\Phi} \cdots \frac{\overleftarrow{\delta}}{\delta\Phi}}^{m\text{-times}} . \quad (13)$$

Thus, $\Gamma_k^{(1,1)}$ is matrix-valued in field space. The super-trace arises since Φ contains both fermionic as well as bosonic degrees of freedom and it provides a minus sign in the fermionic subspace of the matrix. The double-line in Eq. (12) represents the *full* propagator of the theory which includes the *complete* field dependence. The solid black dot in the loop stands for the insertion of $\partial_t R_k$. The structure of the flow equation reveals that the regulator function R_k specifies the Wilsonian momentum-shell integrations, such that the RG flow of Γ_k is dominated by fluctuations with momenta $|p| \simeq k$.

The flow equation (12) has been obtained by taking the derivative of Γ_k with respect to the scale k . However, we have not taken into account a possible scale dependence of the classical field Φ yielding a term $\sim \partial_t \Phi_k$ on the right-hand side of Eq. (12). We stress that the inclusion of this term is a powerful extension of the flow equation discussed here, since it allows to bridge the gap between microscopic and macroscopic degrees of freedom in the RG flow, e. g. between quarks and gluons and hadronic degrees of freedom, without any fine-tuning [28, 124, 125]. More technically speaking, this extension makes it possible to perform continuous Hubbard-Stratonovich transformations in the RG flow. We shall not employ these techniques here since they do not provide us with additional insights into the fermionic fixed-point structure to which the scope of the present review is limited. For details concerning such an extension of the flow equation (12), we refer the reader to Refs. [28, 104, 105, 124–127]. In Ref. [32] these so-called re-bosonization techniques⁵ have been employed for a first-principles study of the QCD phase boundary.

As should be the case for an *exact* one loop flow [128], the Wetterich equation (12) is linear in the inverse of the full propagator. Moreover, it is a nonlinear functional differential equation, since it involves the inverse of the second functional derivative of the effective action. We stress, however, that the loop in Eq. (12) is not a simple perturbative loop since it depends on the *full* propagator. In fact, it can be shown that arbitrarily high loop-orders are summed up by integrating this flow equation [128]. Nonetheless it is possible and sometimes even technically convenient to rewrite (12) in a form which is reminiscent of the textbook form of the one-loop contribution to the effective action:

$$\partial_t \Gamma_k[\Phi] = \frac{1}{2} \text{STr} \tilde{\partial}_t \ln \left(\Gamma_k^{(1,1)}[\Phi] + R_k \right) . \quad (14)$$

Here, $\tilde{\partial}_t$ denotes a formal derivative acting only on the k -dependence of the regulator function R_k . Replacing $\Gamma_k^{(1,1)}$ by the (scale-independent) second functional derivative of the classical action, $S^{(1,1)}$, we can perform the integration over the RG scale k analytically and obtain the standard one-loop expression for the effective action:

$$\Gamma_{1\text{-loop}}[\Phi] = S_{\text{UV}}[\Phi] + \frac{1}{2} \text{STr} \ln S^{(1,1)}[\Phi] , \quad (15)$$

where

$$S_{\text{UV}}[\Phi] = S[\Phi] - \frac{1}{2} \text{STr} \ln \left(S^{(1,1)}[\Phi] + R_\Lambda \right) . \quad (16)$$

Here, the second term on the right-hand side corresponds to the boundary condition for the RG flow at the UV scale Λ , which renders $\Gamma_{1\text{-loop}}$ finite.

From a technical point of view, the representation (14) turns out to be a convenient starting point for our studies of the fixed-point structure of four-fermion interactions. In order to calculate flow equations

⁵ In the context of QCD these techniques are sometimes referred to as “dynamical hadronization”.

of four-fermion interactions, we decompose the inverse regularized propagator $\Gamma_k^{(1,1)}[\Phi]$ on the right-hand side of the flow equation into a field-independent (\mathcal{P}_k) and a field-dependent (\mathcal{F}_k) part,

$$\Gamma_k^{(1,1)}[\Phi] + R_k = \mathcal{P}_k + \mathcal{F}_k. \quad (17)$$

We can then expand the flow equation in powers of the fields according to

$$\begin{aligned} \partial_t \Gamma_k &= \frac{1}{2} \text{STr} \left\{ \tilde{\partial}_t \ln(\mathcal{P}_k + \mathcal{F}_k) \right\} \\ &= \frac{1}{2} \text{STr} \left\{ \tilde{\partial}_t \left(\frac{1}{\mathcal{P}_k} \mathcal{F}_k \right) \right\} - \frac{1}{4} \text{STr} \left\{ \tilde{\partial}_t \left(\frac{1}{\mathcal{P}_k} \mathcal{F}_k \right)^2 \right\} + \frac{1}{6} \text{STr} \left\{ \tilde{\partial}_t \left(\frac{1}{\mathcal{P}_k} \mathcal{F}_k \right)^3 \right\} + \dots \end{aligned} \quad (18)$$

The powers of $\frac{1}{\mathcal{P}_k} \mathcal{F}_k$ can be calculated by simple matrix multiplications. The flow equations for the various couplings can now be obtained by comparing the coefficients of the four-fermion operators on the right-hand side of Eq. (18) with the couplings specified in the definition of the effective action. In other words, the flow equation of higher n -point functions are obtained straightforwardly from the flow equation (12) (or, equivalently, from Eq. (18)) by taking the appropriate number of functional derivatives. From this, we observe that the RG flow of the n -point function depends in general on the flow of the $(n+1)$ - and $(n+2)$ -point function. This means that we obtain an infinite tower of coupled flow equations by taking functional derivatives of the flow equation (12). In most cases we are not able to solve this infinite tower of flow equations. Thus, we need to truncate the effective action and restrict it to include only correlation functions with N_{max} external fields. However, such a *truncation* poses severe problems: first, the system of flow equations is no longer closed and, second, neglecting higher n -point functions may render the flow unstable in the IR region of strongly coupled theories. For example in QCD, one would naively expect that contributions from higher n -point functions are important.

Finding reliable truncations of the effective action is the most difficult step and requires a lot of physical insight. We stress that an expansion in terms of n -point functions must not be confused with an expansion in some small parameter as in perturbation theory. The assumption here is that the influence of neglected operators on the already included operators is small. Once we have chosen a truncation for studying a given theory, we need to check its reliability. One possibility for such a check is to extend the truncation by including additional operators and then check if the results obtained from this new truncation are in agreement with the earlier results. If this is not the case, one must rethink the chosen truncation. However, even if the results are not sensitive to the specific set of additional operators added to the truncation, this does not necessarily mean that one has included all relevant operators in the calculation. A second possibility to assess the reliability of a given truncation is to exploit the fact that physical observables should not depend on the regularization scheme. Since the scheme is specified by the cutoff function, the physical observables should be independent of this choice. In the present approach the scheme is defined by our choice for the regulator function R_k . Thus, we can vary R_k and then check if the results depend on the choice of the cutoff function. If this is the case, an extension of the truncation might be required. In addition to a simple variation of regulator functions, we may actually exploit the dependence on R_k to *optimize* the truncated RG flow of a given theory. For example, an optimization criterion can be based on the size of the gap induced in the effective propagator $(\Gamma_k^{(1,1)}[\Phi] + R_k)^{-1}$, see Refs. [129–131]. We then denote those regulators to be optimized for which the gap is maximized with respect to the cutoff scheme. In addition to such an optimization of RG flows within a given regulator class, a more general criterion has been put forward in Ref. [104]. The latter defines the optimized regulator to be the one for which the regularized theory is already closest to the full theory at $k=0$, for a given gap induced in the effective propagator $(\Gamma_k^{(1,1)}[\Phi] + R_k)^{-1}$. This optimization criterion yields an RG trajectory which defines the shortest path in theory space between the UV theory at $k=\Lambda$ and the full theory at $k=0$. Both optimization criteria naturally encompass the so-called ‘‘Principle of Minimum Sensitivity’’. However, in contradistinction to the ‘‘Principle of Minimum Sensitivity’’, the optimization of (truncated) RG flows does not rely on the existence of extremal values of physical observables which may arise from a variation of

the regularization scheme. For a detailed discussion of optimization criteria and properties of optimized RG flows, we refer the reader to Refs. [104, 129–131].

Nonetheless, even an approximate solution of the flow equation (12) can describe non-perturbative physics reliably, provided the relevant degrees of freedom in the form of RG relevant operators are kept in the ansatz for the effective action.

3 RG Flow of Four-Fermion Interactions - A Simple Example

In this section we discuss a simple four-fermion theory which already allows us to gain some important insight into the mechanisms of symmetry breaking in strongly-interacting theories. A study of a simple four-fermion theory is useful for many reasons. First, it allows us to highlight various methods and technical aspects such as Fierz ambiguities, (partial) bosonization and the role of explicit symmetry breaking. Second, a confrontation of this model study with our analysis of symmetry breaking in gauge theories is instructive: To be specific, we will consider the mechanisms of chiral symmetry breaking to point out the substantial differences between these theories.

3.1 A Simple Example and the Fierz Ambiguity

In this section we discuss the basic concepts and problems in describing strongly-interacting fermionic theories, with a particular emphasis on the application of RG approaches. To this end, we employ a Nambu–Jona-Lasinio-type model. Such models play a very prominent role in theoretical physics. Originally, the Nambu–Jona-Lasinio (NJL) model has been used as an effective theory to describe spontaneous symmetry breaking in particle physics based on an analogy with superconducting materials [132, 133], see Ref. [134] for a review. RG methods have been extensively employed to study critical behavior in QCD with the aid of NJL-type models, see e. g. Refs. [33, 53, 55, 100, 113, 135–139]. Usually these model studies rely on a (partially) bosonized version of the action. We shall discuss aspects of bosonization in Sect. 3.2. For the sake of simplicity we start with a purely fermionic formulation of the NJL model with only one fermion species. This model has been extensively studied at zero temperature with the functional RG in Refs. [77, 140]. In particular, the ambiguities arising from Fierz transformations have been explicitly worked out and discussed. We shall follow the discussion in Refs. [77, 140] but extend it with respect to issues arising at finite temperature and for a finite (explicit) fermion mass. In addition, we exploit this model to discuss general aspects of theories with many fermion flavors as well as quantum critical behavior.

In the following we consider a simple ansatz for the effective action in $d = 4$ Euclidean space-time dimensions:

$$\Gamma_{\text{NJL}}[\bar{\psi}, \psi] = \int d^4x \left\{ Z_\psi \bar{\psi} i \not{\partial} \psi + \frac{1}{2} \bar{\lambda}_\sigma [(\bar{\psi} \psi)^2 - (\bar{\psi} \gamma_5 \psi)^2] \right\}, \quad (19)$$

where $\bar{\lambda}_\sigma$ is the bare four-fermion coupling and Z_ψ is the so-called fermionic wave-function renormalization. The coupling $\bar{\lambda}_\sigma$ is considered to be RG-scale dependent. Here, we consider four-fermion couplings as fundamental parameters. However, in other theories fermionic self-interactions might be fluctuation-induced. In QCD, for example, they are induced by two-gluon exchange and are therefore not fundamental as we shall discuss in Sect. 6, see also Refs. [28–32, 78]. We would like to add that the NJL model in $d = 4$ is perturbatively non-renormalizable. In the following we define it with a fixed UV cutoff Λ . Also the regularization scheme therefore belongs to the definition of the model. We shall come back to this issue in Sects. 3.2 and 5.1.

Our ansatz (19) for the effective action can be considered as the leading order approximation in a systematic expansion in derivatives. The associated small parameter of such an expansion is the so-called anomalous dimension $\eta_\psi = -\partial_t \ln Z_\psi$ of the fermion fields. If this parameter is small, then such a derivative expansion is indeed justified. We shall come back to this issue below. In any case, we will drop terms in our studies which are of higher order in derivatives, such as terms $\sim (\bar{\psi} i \not{\partial} \psi)^2$.

The action (19) is clearly invariant under simple phase transformations,

$$\psi(x) \longmapsto e^{i\alpha}\psi(x), \quad (20)$$

but also under chiral U(1) transformations (axial phase transformations),

$$\psi(x) \longmapsto e^{i\gamma_5\alpha}\psi(x), \quad \bar{\psi}(x) \longmapsto \bar{\psi}(x) e^{i\gamma_5\alpha}, \quad (21)$$

where α is an arbitrary “rotation” angle. A necessary condition for the chiral symmetry of the NJL model is the absence of explicit mass terms for the fermion fields in the action, such as $\sim \bar{\psi}\bar{m}\psi$. As we shall discuss in more detail below, the chiral symmetry can be still broken spontaneously, if a finite vacuum expectation value $\langle \bar{\psi}\psi \rangle$ is generated by loop corrections associated with (strong) fermionic self-interactions. Breaking of chiral symmetry in the ground state of the theory is then indicated by a dynamically generated mass term for the fermions. This mass term is associated, e. g., with a constituent quark mass in low-energy models of QCD and similar to the gap in condensed-matter theory. The relation between the strength of the four-fermion interactions and the symmetry properties of the ground-state are discussed in detail in Sects. 3.2 and 3.3.

We may now ask whether the action (19) is complete or whether other four-fermion couplings, such as a vector interaction $\sim (\bar{\psi}\gamma_\mu\psi)^2$, can be generated dynamically due to quantum fluctuations. We first realize that the four-fermion interaction in our ansatz (19) can be expressed in terms of a vector and axial-vector interaction term with the aid of so-called Fierz transformations, see App. B for details:

$$[(\bar{\psi}\psi)^2 - (\bar{\psi}\gamma_5\psi)^2] = \frac{1}{2} [(\bar{\psi}\gamma_\mu\gamma_5\psi)^2 - (\bar{\psi}\gamma_\mu\psi)^2]. \quad (22)$$

This ambiguity in the representation of a four-fermion interaction term arises due to the fact that an arbitrary $d \times d$ -matrix M can be expanded in terms of a complete and orthonormalized set $\{O^{(1)}, \dots, O^{(n)}\}$ of $d \times d$ -matrices as follows:

$$M_{ab} = \sum_{j=1}^n O_{ab}^{(j)} \text{tr}(O_j M) \equiv \sum_{j=1}^n O_{ab}^{(j)} \sum_{c,d} \left(O_{cd}^{(j)} M_{dc} \right) \quad \text{with } \text{tr}(O^{(j)} O^{(k)}) = \mathbb{1}_d \delta_{jk}. \quad (23)$$

The expansion of a combination of two matrices $M^{(1)}$ and $M^{(2)}$ then reads (say for fixed b and c)

$$(M_{bc})_{ad} \equiv M_{ad} := M_{ab}^{(1)} M_{cd}^{(2)} = \sum_{j=1}^n O_{ad}^{(j)} \sum_{e,f} (M_{ce}^{(2)} O_{ef}^{(j)} M_{fb}^{(1)}). \quad (24)$$

In the case of four-fermion interactions we may classify the basis elements O_i according to the transformation properties of the corresponding interaction terms $(\bar{\psi}O_i\psi)^2$, i. e. scalar channel, vector channel, tensor channel, axial-vector channel and pseudo-scalar channel. To be specific, we choose $O_S = \mathbb{1}_d$, $O_V = \gamma_\mu$, $O_T = \frac{1}{\sqrt{2}}\sigma_{\mu\nu} = \frac{i}{2\sqrt{2}}[\gamma_\mu, \gamma_\nu]$, $O_A = \gamma_\mu\gamma_5$ and $O_P = \gamma_5$ as basis elements of the Clifford algebra defined by the γ matrices, see App. B for details. To obtain Eq. (22) we then simply apply Eq. (24) to the matrix products $(\mathbb{1})_{ab}(\mathbb{1})_{cd}$ and $(\gamma_5)_{ab}(\gamma_5)_{cd}$, respectively. Thus, a Fierz transformation can be considered as a reordering of the fermion fields. We stress that this is by no means related to quantum effects but a simple algebraic operation. Nonetheless it suggests that other four-fermion couplings compatible with the underlying symmetries of our model exist and are potentially generated by quantum effects.

With our choice for the set of basis elements $\{O_S, \dots, O_P\}$ it is straightforward to write down the most general ansatz for the effective action Γ_{NJL} which is compatible with the underlying symmetries of the model, i. e. the symmetries with respect to U(1) phase transformations, U(1) chiral transformations and Lorentz transformations:⁶

$$\Gamma_{\text{NJL}}[\bar{\psi}, \psi] = \int d^4x \left\{ Z_\psi \bar{\psi} i \not{\partial} \psi + \frac{1}{2} \bar{\lambda}_S [(\bar{\psi}\psi)^2 - (\bar{\psi}\gamma_5\psi)^2] - \frac{1}{2} \bar{\lambda}_V [(\bar{\psi}\gamma_\mu\psi)^2] - \frac{1}{2} \bar{\lambda}_A [(\bar{\psi}\gamma_\mu\gamma_5\psi)^2] \right\}. \quad (25)$$

⁶ Note that $(\bar{\psi}O_T\psi)^2$ is not invariant under chiral U(1) transformations.

Because of Eq. (22) only two of the three couplings $\bar{\lambda}_\sigma$, $\bar{\lambda}_V$ and $\bar{\lambda}_A$ are independent. Thus, it suffices to consider the following action with implicitly redefined four-fermion couplings:

$$\Gamma_{\text{NJL}}[\bar{\psi}, \psi] = \int d^4x \left\{ Z_\psi \bar{\psi} i \not{\partial} \psi + \frac{1}{2} \bar{\lambda}_\sigma [(\bar{\psi}\psi)^2 - (\bar{\psi}\gamma_5\psi)^2] - \frac{1}{2} \bar{\lambda}_V [(\bar{\psi}\gamma_\mu\psi)^2] \right\}. \quad (26)$$

Note that we could have also chosen to remove, e. g., the vector-channel interaction term with the aid of Eq. (22) at the expense of getting the axial-vector interaction. From a phenomenological point of view it is tempting to attach a physical meaning to, e. g., the vector-channel interaction and interpret it as an effective mass term for vector bosons V_μ as done in mean-field studies of Walecka-type models [141]: $\bar{\lambda}_V (\bar{\psi}\gamma_\mu\psi)^2 \sim \bar{m}_V^2 V_\mu V_\mu + \dots$. However, the present analysis shows that one has to be careful to attach such a phenomenological interpretation to this term since the Fierz transformations allow us to remove this term completely from the action, see also Sect. 3.2.

In this section we drop a possible momentum dependence of the four-fermion couplings. Thus, we only take into account the leading term of an expansion of the four-fermion couplings in powers of the dimensionless external momenta $|p_i|/k$, e. g.

$$\Gamma^{(2,2)}[\bar{\psi}, \psi](p_1, p_2, p_3) \equiv \bar{\lambda}_V(p_1, p_2, p_3) = \bar{\lambda}_V(0, 0, 0) + \mathcal{O}\left(\frac{|p_i|}{k}\right). \quad (27)$$

In momentum space, the corresponding interaction term in the expansion of the effective action (26) in terms of fermionic self-interactions then assumes the following form, see App. A for our conventions of the Fourier transformation:

$$\Gamma_{\text{NJL}}[\bar{\psi}, \psi] = \dots - \frac{1}{2} \bar{\lambda}_V \prod_{i=1}^3 \int \frac{d^4 p_i}{(2\pi)^4} \bar{\psi}(p_1) \gamma_\mu \psi(p_2) \bar{\psi}(p_3) \gamma_\mu \psi(p_1 - p_2 + p_3) - \dots, \quad (28)$$

where $\bar{\lambda}_V \equiv \bar{\lambda}_V(0, 0, 0)$ and correspondingly for the other four-fermion interaction terms in Eq. (26). Note that only three of the four four-momenta p_1, \dots, p_4 are independent due to momentum conservation. We stress that we also apply this expansion at finite temperature T , see Sect. 3.5.3. In this case, it then corresponds to an expansion in powers of the dimensionless Matsubara modes $\nu_n/k = (2n+1)\pi T/k$ and $|\vec{p}|/k$. Thus, we assume that $T/k \ll 1$.

The approximation (27) does not permit a study of properties of bound states of fermions, such as meson masses in QCD, in the chirally broken regime; such bound states manifest themselves as momentum singularities in the four-fermion couplings in Minkowski space. Nonetheless, the point-like limit can still be a reasonable approximation for $T/k \ll 1$. In the chirally symmetric regime above the chiral phase transition it allows us to gain some insight into the question how the theory approaches the regime with broken chiral symmetry in the ground state [30–32]. In Sect. 3.2 we shall discuss how the momentum dependence of the fermionic interactions can be conveniently resolved in order to gain access to the mass spectrum in the regime with broken chiral symmetry.

Let us now compute the RG flow equations, i. e. the so-called β functions, for the four-fermion couplings in the point-like limit. To this end, we compute the second functional derivative of the effective action with respect to the fields

$$\Phi \equiv \Phi(q) := \begin{pmatrix} \psi(q) \\ \bar{\psi}^\text{T}(-q) \end{pmatrix} \quad \text{and} \quad \Phi^\text{T} \equiv \Phi^\text{T}(-q) := (\psi^\text{T}(-q), \bar{\psi}(q)), \quad (29)$$

see also Eq. (13), and evaluate it for *homogeneous* (constant) background fields $\bar{\Psi}$ and Ψ . In momentum space this means that we evaluate $\Gamma_{\text{NJL}}^{(1,1)}$ at

$$\psi(p) = \Psi (2\pi)^4 \delta^{(4)}(p) \quad \text{and} \quad \bar{\psi}(p) = \bar{\Psi} (2\pi)^4 \delta^{(4)}(p), \quad (30)$$

where Ψ and $\bar{\Psi}$ on the right-hand side denote the homogeneous background fields. Following Eq. (17), we then split the resulting matrix into a field-independent part and a part which depends on Ψ and $\bar{\Psi}$. To detail

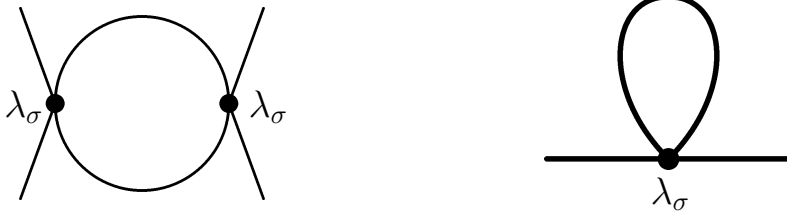


Fig. 1 Left diagram: 1PI Feynman diagram associated with the λ_σ^2 -term on the right-hand side of the RG flow equation (33). Note that our (functional) RG study includes resummations of this diagram to arbitrary order in λ_σ . Right diagram: 1PI Feynman diagram associated with the RG running of the fermionic wave-function renormalization Z_ψ .

the derivation of flow equations of four-fermion interactions in a simple manner, we first restrict ourselves to the simplified ansatz (19) of the effective action. In this case, the so-called (regularized) propagator matrix \mathcal{P}_k and the fluctuation matrix \mathcal{F}_k read

$$\mathcal{P}_k = \begin{pmatrix} 0 & -Z_\psi \not{p}^T (1 + r_\psi) \\ -Z_\psi \not{p} (1 + r_\psi) & 0 \end{pmatrix} (2\pi)^4 \delta^{(4)}(p - p') \quad (31)$$

and

$$\mathcal{F}_k = \begin{pmatrix} \mathcal{F}_{11} & \mathcal{F}_{12} \\ \mathcal{F}_{21} & \mathcal{F}_{22} \end{pmatrix} (2\pi)^4 \delta^{(4)}(p - p'), \quad (32)$$

respectively, where

$$\begin{aligned} \mathcal{F}_{11} &= -\bar{\lambda}_\sigma [\bar{\Psi}^T \bar{\Psi} - \gamma_5 \bar{\Psi}^T \bar{\Psi} \gamma_5], \quad \mathcal{F}_{22} = -\bar{\lambda}_\sigma [\Psi \Psi^T - \gamma_5 \Psi \Psi^T \gamma_5], \\ \mathcal{F}_{12} &= -\bar{\lambda}_\sigma [(\bar{\Psi} \Psi) - \gamma_5 (\bar{\Psi} \gamma_5 \Psi) + \Psi \bar{\Psi} - \gamma_5 \Psi \bar{\Psi} \gamma_5]^T = -\mathcal{F}_{21}^T. \end{aligned}$$

Since we evaluated $\Gamma_{\text{NJL}}^{(1,1)}$ for constant fields, both \mathcal{P}_k and \mathcal{F}_k are diagonal in momentum space. At this point it is not yet necessary to specify the regulator function exactly.

The RG flow equation for $\bar{\lambda}_\sigma$ can now be computed straightforwardly by comparing the coefficients of the four-fermion interaction terms on the right-hand side of Eq. (18) with the couplings included in our ansatz (19). From the fluctuation matrix \mathcal{F}_k it is clear that only the term $\text{tr}(\mathcal{P}_k^{-1} \mathcal{F}_k)^2 \sim (\bar{\psi} O_i \psi)^2$ in Eq. (18) contributes to the RG flow of the four-fermion coupling $\bar{\lambda}_\sigma$. For this initial study, we simply take the four-fermion terms on the right-hand side of the flow equation “as they appear” and ignore Fierz transformations of these terms. We then find

$$\beta_{\lambda_\sigma} \equiv \partial_t \lambda_\sigma = (2 + 2\eta_\psi) \lambda_\sigma - 16v_4 l_1^{(\text{F}), (4)}(0; \eta_\psi) \lambda_\sigma^2, \quad (33)$$

where $v_d^{-1} = 2^{d+1} \pi^{d/2} \Gamma(d/2)$, i. e. $v_4 = 1/(32\pi^2)$. Here, we have defined the dimensionless renormalized coupling

$$\lambda_\sigma = (Z_\psi)^{-2} k^2 \bar{\lambda}_\sigma. \quad (34)$$

The so-called threshold function $l_1^{(\text{F}), (d)}$ corresponds to a one-particle irreducible (1PI) Feynman diagram, see left diagram in Fig. 1, and describes the decoupling of massive and also thermal modes in case of finite-temperature studies. Moreover, the regularization-scheme dependence is encoded in these threshold functions, see App. D for their definitions.

In Fig. 2 we show a sketch of the β_{λ_σ} -function for vanishing temperature. Apart from a Gaussian fixed point, $\lambda_\sigma^{\text{GauB}} = 0$, we find a second non-trivial fixed point λ_σ^* :

$$\lambda_\sigma^* = \frac{1}{8v_4 l_1^{(\text{F}), (4)}(0; 0)} + \mathcal{O}(\eta_\psi^*). \quad (35)$$

In the present leading-order approximation of the derivative expansion we have $\eta_\psi \equiv 0$, see below. We then find

$$\lambda_\sigma^* = 8\pi^2 \quad (36)$$

for an optimized (linear) regulator function (for which $l_1^{(F),(d)}(0;0) = 2/d$) and

$$\lambda_\sigma^* = 4\pi^2 \quad (37)$$

for the sharp cutoff (for which $l_1^{(F),(d)}(0;0) = 1$). It is instructive to have a closer look at Eq. (33). This flow equation represents an ordinary differential equation which can be solved analytically for $\eta_\psi = 0$. Its solution reads

$$\lambda_\sigma(k) = \lambda_\sigma^{\text{UV}} \left[\left(\frac{\Lambda}{k} \right)^\Theta \left(1 - \frac{\lambda_\sigma^{\text{UV}}}{\lambda_\sigma^*} \right) + \frac{\lambda_\sigma^{\text{UV}}}{\lambda_\sigma^*} \right]^{-1}, \quad (38)$$

where

$$\Theta := - \frac{\partial(\partial_t \lambda_\sigma)}{\partial \lambda_\sigma} \Big|_{\lambda_\sigma^*} \quad (\eta_\psi \equiv 0) \quad 2. \quad (39)$$

In order to derive Eq. (38), it is convenient to expand the right-hand side of Eq. (33) about the fixed-point λ_σ^* . The physical meaning of the so-called critical exponent Θ will be discussed in more detail below. In Sect. 3.4.1 we will then see that this exponent governs the scaling behavior of physical observables close to a quantum critical point.

For $\lambda_\sigma^{\text{UV}} = \lambda_\sigma^*$, we find that $\lambda_\sigma(k)$ does not depend on the RG scale k as it should be: $\lambda_\sigma(k) = \lambda_\sigma^*$. Choosing an initial value $\lambda_\sigma^{\text{UV}} < \lambda_\sigma^*$ at the initial UV scale Λ , the solution (38) of the flow equation predicts that the theory becomes non-interacting in the infrared regime ($\lambda_\sigma \rightarrow 0$ for $k \rightarrow 0$), i. e. chiral symmetry remains unbroken in this case, see Fig. 2. For $\lambda_\sigma^{\text{UV}} > \lambda_\sigma^*$, we find that the four-fermion coupling λ_σ increases rapidly and diverges eventually at a finite scale k_{SB} : $1/\lambda_\sigma(k_{\text{SB}}) \rightarrow 0$. This behavior of the coupling and the associated fixed-point structure are tightly linked to the question whether chiral symmetry is broken in the ground state or not: The value of the non-trivial fixed-point can be considered as a critical value of the coupling which separates the chirally symmetric regime and the regime with a broken chiral symmetry in the ground state. We shall discuss this in more detail in Sects. 3.2, 3.3 and 3.4.

In the derivation of the flow equation (33) we have dropped contributions arising from four-fermion interactions with different transformation properties, e. g. a vector-channel interaction. From the expansion (18) of the flow equation, we can indeed read off that contributions to the flow of four-fermion couplings other than $\bar{\lambda}_\sigma$ might be generated, even though they have not been included in the truncation (19): the matrix multiplications on the right-hand side of Eq. (18) mix the contributions from the propagator \mathcal{P}_k , which is proportional to γ_μ , with the contributions from the field-dependent part \mathcal{F}_k :

$$\bar{\lambda}_\sigma^2 \text{tr} \{ \gamma_\mu \psi \bar{\psi} \gamma_\mu \psi \bar{\psi} \} = -\bar{\lambda}_\sigma^2 (\bar{\psi} \gamma_\mu \psi) (\bar{\psi} \gamma_\mu \psi). \quad (40)$$

This term obviously contributes to the flow of the $\bar{\lambda}_V$ -coupling.⁷ Moreover, contributions of this type couple the flow equations of the various four-fermion interactions to one another. Thus, quantum fluctuations induce a vector-channel interaction, even though we have not included such an interaction term initially. This observation explains why we need to include a basis which is complete with respect to Fierz transformations, such as in the effective action (25). We stress that the effective action (25) is closed in the sense that no contributions to four-fermion interactions, which are *not* covered by the truncation, are generated in the RG flow: any other pointlike four-fermion interaction compatible with the underlying symmetries of the theory can be written in terms of the interactions included in these effective actions by means of Fierz transformations.

⁷ At first glance, it seems possible that a term could arise in the calculation with opposite sign to the term in Eq. (40), so that both would cancel each other. We are aware of this and stress that Eq. (40) should serve only as a motivation. As the full calculation of the NJL model shows (see below), not all terms which couple the RG flows of the different couplings drop out in the end.

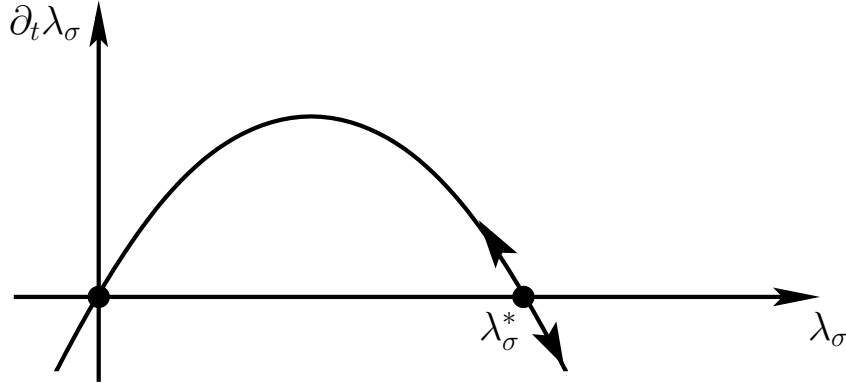


Fig. 2 Sketch of the β_{λ_σ} function of the four-fermion interaction for zero temperature (black/solid line). The arrows indicate the direction of the RG flow towards the infrared.

In the point-like limit the RG flow of the four-fermion coupling is completely decoupled from the RG flow of fermionic n -point functions of higher order. For example, 8-fermion interactions do not contribute to the RG flow of the coupling $\bar{\lambda}_\sigma$ in this limit. Using the one-loop structure of the Wetterich equation, this statement can be proven diagrammatically: it is not possible to construct a one-loop diagram with only for external legs out of fermionic n -point functions ($n > 4$) which are compatible with the underlying chiral symmetry.

Up to now we have only discussed the running of a four-fermion coupling. We have not yet discussed how to compute the running of the wave-function renormalization Z_ψ . In general, the flow equation for Z_ψ can be obtained from $\Gamma_{\text{NJL}}^{(1,1)}$ evaluated for a spatially varying background field,

$$\psi(p) = \Psi (2\pi)^4 \delta^{(4)}(p + Q) \quad \text{and} \quad \bar{\psi}(p) = \bar{\Psi} (2\pi)^4 \delta^{(4)}(p - Q),$$

where Q denotes the external momentum.⁸ The Q -dependent second functional derivative $\Gamma_{\text{NJL}}^{(1,1)}$ can still be split into a field-independent and a field-dependent part. However, the latter is no longer diagonal in momentum space. The flow equations for the wave-function renormalizations can then be computed by comparing the coefficients of the terms bilinear in fermionic fields which appear on the right-hand side of Eq. (18) with the kinetic terms in the ansatz for the effective action. In our present approximation, we find that the RG running of Z_ψ is trivial, i. e.

$$\partial_t Z_\psi = 0. \tag{41}$$

Thus, the associated anomalous dimensions $\eta_\psi = -\partial_t \ln Z_\psi$ is zero. In fact, this follows immediately from the associated 1PI Feynman diagram, see diagram on the right in Fig. 1, which has only one internal fermion line.⁹ In the following we therefore set the wave-function renormalization to one, $Z_\psi \equiv 1$, which implies $\eta_\psi \equiv 0$.

Let us now turn to the effective action (26). The flow equations of the various couplings can be derived along the same lines as the RG equation for the λ_σ -coupling detailed above. We find

$$\partial_t \lambda_\sigma = 2\lambda_\sigma - 8v_4 l_1^{(\text{F}), (4)}(0; 0) [\lambda_\sigma^2 + 4\lambda_\sigma \lambda_V + 3\lambda_V^2], \tag{42}$$

$$\partial_t \lambda_V = 2\lambda_V - 4v_4 l_1^{(\text{F}), (4)}(0; 0) [\lambda_\sigma^2 + 2\lambda_\sigma \lambda_V + \lambda_V^2], \tag{43}$$

⁸ These choices correspond to plane waves in position space.

⁹ The momentum of the ingoing and outgoing fermion (line) is identical, namely Q in our conventions. Due to momentum conservation, the loop momentum integration is then independent of Q . Recall that we consider the four-fermion coupling in the point-like limit.

where the dimensionless (renormalized) couplings are defined as

$$\lambda_\sigma = k^2 \bar{\lambda}_\sigma, \quad \text{and} \quad \lambda_V = k^2 \bar{\lambda}_V. \quad (44)$$

In the derivation of the flow equations for λ_σ and λ_V also terms of the type $\sim (\bar{\psi} \gamma_\mu \gamma_5 \psi)^2$ and

$$[(\bar{\psi} \sigma_{\mu\nu} \psi)^2 - (\bar{\psi} \sigma_{\mu\nu} \gamma_5 \psi)^2] \quad (45)$$

appear. While the latter vanishes identically, see also App. B, the former can be completely transformed into a scalar-pseudoscalar and vector-interaction channel with the aid of the Fierz transformation (22). In fact, any four-fermion interaction term appearing in the derivation of the flow equations for the present system can be unambiguously rewritten in terms of these two interaction channels. Thus, the above RG flows are closed with respect to Fierz transformations. Due to Eq. (22) we could have also used, e. g., a scalar-pseudoscalar and an axial-vector interaction to describe the properties of our simplified theory without loss of physical information. The present choice for a complete basis of four-fermion interactions is one of several possibilities.

Our flow equations for λ_σ and λ_V agree with the results found in Refs. [140, 142]. The RG flow of the couplings λ_σ and λ_V is governed by three fixed points $\mathcal{F}_i = (\lambda_\sigma^*, \lambda_V^*)$ which are given by¹⁰

$$\mathcal{F}_1 \equiv \mathcal{F}_{\text{GauB}} = (0, 0), \quad \mathcal{F}_2 = (3\zeta, \zeta), \quad \mathcal{F}_3 = (-32\zeta, 16\zeta), \quad (46)$$

where

$$\zeta = \frac{1}{32v_4 l_1^{(F),(4)}(0; 0)}. \quad (47)$$

These fixed-points are of phenomenological importance. First of all, they might be related to (quantum) phase transitions. Second, we can define sets of initial values for the RG flows of the couplings λ_σ and λ_V for which we find condensate formation associated with (chiral) symmetry breaking in the IR, as we shall discuss in detail in the two subsequent sections. The existence of such sets of initial conditions is not a generic feature of fermionic models but also appears in (chiral) gauge theories. In QCD and QED₃, four-fermion interactions are generated dynamically due to strong quark-gluon interactions, see our discussion in Sect. 6.

We can classify the various fixed points according to their directions in the space spanned by the couplings. To this end, we first linearize the RG flow equations of the couplings near a fixed point:

$$\partial_t \lambda_i = \sum_j B_{ij} (\lambda_j - \lambda_j^*) + \dots, \quad \text{where} \quad B_{ij} = \left. \frac{\partial_t \lambda_i}{\partial \lambda_j} \right|_{\lambda_i = \lambda_i^*} \quad (48)$$

and $i, j \in \{\sigma, V\}$. We refer to B as the *stability* matrix. The two eigenvectors \vec{v}_i and eigenvalues $\Theta^{(i)}$ (critical exponents) of this matrix essentially determine the RG evolution near a fixed point:¹¹

$$\partial_t \vec{v}_i = B \cdot \vec{v}_i =: -\Theta^{(i)} \vec{v}_i. \quad (49)$$

The solution of the RG flow in the fixed-point regime is then given by

$$\lambda_i = \lambda_i^* + \sum_j c_j (\vec{v}_j)_i \left(\frac{k_0}{k} \right)^{\Theta^{(j)}}. \quad (50)$$

Here, the c_j 's define the initial conditions at the scale k_0 . From the solution of the linearized flow it becomes apparent that positive critical exponents, $\Theta^{(j)} > 0$, correspond to RG relevant, i. e. infrared repulsive, directions. On the other hand, negative critical exponents $\Theta^{(j)} < 0$ correspond to RG irrelevant,

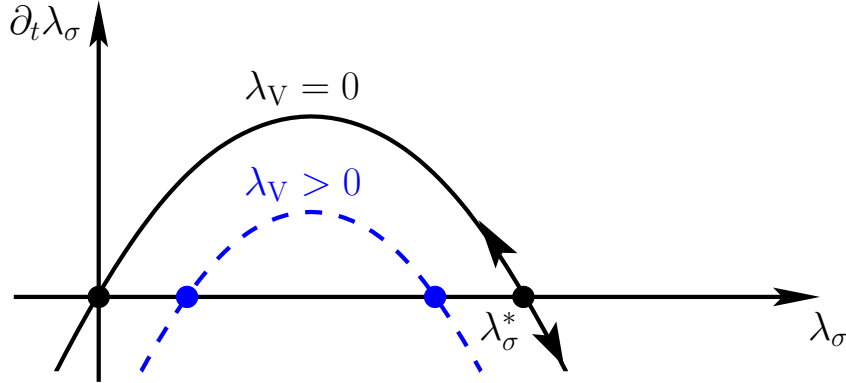


Fig. 3 Sketch of the β_{λ_σ} -function of the four-fermion interaction for $\lambda_V = 0$ (black line) and $\lambda_V > 0$ (blue/dashed line). The arrows indicate the direction of the RG flow towards the infrared.

i. e. infrared attractive, directions. The classification of marginal directions associated with vanishing critical exponents requires to consider higher orders in the expansion about the fixed point.

Using the flow equations (42) and (43), we find that the Gaussian fixed point has two IR attractive directions; the eigenvalues are $\Theta_{\mathcal{F}_1} \equiv \Theta_{\text{GauB}} = \{-2, -2\}$. The fixed points \mathcal{F}_2 with $\Theta_{\mathcal{F}_2} = \{2, -5/2\}$ and \mathcal{F}_3 with $\Theta_{\mathcal{F}_3} = \{2, -10\}$ have both one IR attractive and one IR repulsive direction. We would like to add that the fixed-point values of the four-fermion couplings are *not* universal quantities as the dependence of their RG flows on the threshold function indicates. However, the statement about the mere existence of these fixed points is *universal*, because the regulator-dependent factor $l_1^{(F),(d)}(0; 0)$ is a positive number for any regulator. Moreover, the critical exponents Θ_i themselves are universal. The latter can be indeed related to the exponents associated with (quantum) phase transitions, as we shall discuss in Sect. 3.4. Therefore the accuracy of the critical exponents can be used to measure the quality of a given truncation as has been done in the context of scalar field theories, see e. g. Refs. [106, 143–146]. In a pragmatic sense, the computation of critical exponents allows us to estimate how well the dynamics close to a phase transition are captured within our ansatz for the effective action.

Let us conclude our discussion with a comparison of the RG flows (42) and (43) obtained from a complete basis of four-fermion interactions with the RG flow equation (33) from our single-channel approximation. We immediately observe that setting $\lambda_V \rightarrow 0$ in Eq. (42) does not yield the flow equation (33). Thus, the values of the non-trivial fixed point of this coupling are not identical but differ by a factor of two.¹² For a finite λ_σ , we find that the vector-channel interaction is dynamically generated due to quantum fluctuations even if we have initially set the vector-channel interaction to zero. In fact, a finite λ_σ -coupling shifts the parabola associated with the β -function of the coupling λ_V , and vice versa, see Fig. 3. Thus, the λ_σ -coupling can potentially induce critical behavior in the vector-channel, i. e. a diverging four-fermion coupling. We shall discuss this in more detail in Sect. 3.3 after we have clarified the physical meaning of diverging four-fermion couplings in the subsequent section.

¹⁰ One might naively expect four fixed points. In order to show that our system of flow equations has only three fixed points, we redefine the λ_σ -coupling according to $\lambda_\sigma \rightarrow (\lambda_\sigma - \lambda_V)$. The flow equation for the vector coupling then has only one fixed point which depends on the value of the (new) λ_σ -coupling. However, the β -function of the latter is now cubic in λ_σ when we evaluate it at the fixed-point value of the λ_V -coupling. Thus, the system indeed has only three fixed points.

¹¹ In other words, the critical exponents are simply the zeroes of the (characteristic) polynomial $\det(B + \Theta \mathbb{1})$.

¹² The RG flow also generates axial-vector channel interactions which, in the present (Fierz) basis of four-fermion interactions, reduce the prefactor of the term $\propto \lambda_\sigma^2$ in Eq. (42) by a factor of two.

3.2 Bosonization and the Momentum Dependence of Fermion Interactions

In this section we study the NJL model with one fermion species in a partially bosonized form. Partial bosonization of fermionic theories is a well-established concept which makes use of the so-called *Hubbard-Stratonovich* transformation [59, 60]. The advantage of a partially bosonized formulation of NJL-type models over their purely fermionic formulation is that it allows us to include the momentum dependence of four-fermion interactions in a simple manner. Therefore it opens up the possibility to study conveniently the mass spectrum of a theory which emerges from the spontaneous breakdown of its underlying symmetries, e. g. the chiral symmetry. As a bonus, it relates the *Ginzburg-Landau* picture of spontaneous symmetry breaking, as known from statistical physics, with dynamical bound-state formation in strongly-interacting fermionic theories.

In the following we derive the RG flow equations for the partially bosonized version of this theory and discuss dynamical chiral symmetry breaking. In particular, we explain the mapping of the (partially) bosonized equations onto the RG equations of the four-fermion couplings in the purely fermionic description of our model. This finally allows us to relate the fixed-point structure of the purely fermionic formulation to spontaneous (chiral) symmetry breaking.

The generating functional Z reads¹³

$$Z \propto \int \mathcal{D}\psi \mathcal{D}\bar{\psi} e^{-S[\bar{\psi}, \psi]} \quad (51)$$

with the action

$$S[\bar{\psi}, \psi] = \int d^4x \left\{ Z_\psi \bar{\psi} i \not{\partial} \psi + \frac{1}{2} \bar{\lambda}_\sigma [(\bar{\psi}\psi)^2 - (\bar{\psi}\gamma_5\psi)^2] - \frac{1}{2} \bar{\lambda}_V [(\bar{\psi}\gamma_\mu\psi)^2] - \frac{1}{2} \bar{\lambda}_A [(\bar{\psi}\gamma_\mu\gamma_5\psi)^2] \right\}. \quad (52)$$

see also Eq. (25). As discussed in the previous section, this action is over-complete in the sense that only two of the three couplings $\bar{\lambda}_\sigma$, $\bar{\lambda}_V$ and $\bar{\lambda}_A$ are independent. We shall come back to this issue in the partially bosonized formulation below.

Our NJL model possesses a chiral symmetry, see Eq. (21), which can be broken dynamically, if a finite vacuum expectation value $\langle \bar{\psi}\psi \rangle$ is generated. This is associated with the *Nambu-Goldstone* theorem [132, 133, 147, 148] which relates a spontaneously broken continuous symmetry of a given theory to the existence of massless states in the spectrum. To apply this theorem to the present model, we need to compute the vacuum expectation value of the commutator of the so-called chiral charge Q_5 , which is the generator of the chiral symmetry transformations, and the composite field $\bar{\psi}i\gamma_5\psi$:

$$\langle [iQ_5, \bar{\psi}i\gamma_5\psi] \rangle \propto \langle \bar{\psi}\psi \rangle \quad \text{with} \quad Q_5 = \frac{1}{2} \int d^3x \bar{\psi}\gamma_0\gamma_5\psi. \quad (53)$$

We observe that the generator Q_5 does not commute with the field $\bar{\psi}i\gamma_5\psi$, if the vacuum expectation value of $\bar{\psi}\psi$ is finite. Thus, the chiral symmetry of our model can be indeed broken spontaneously. Following the *Nambu-Goldstone* theorem this implies the existence of a *massless* pseudo-scalar *Nambu-Goldstone* boson in the channel of the composite field $\bar{\psi}i\gamma_5\psi$. Since the action S does not contain such a state, the massless state must be a bound state. We refer to this type of boson as a *pion* in the context of QCD, see Sect. 5. At this point we have traced the question of chiral symmetry breaking back to the existence of a finite expectation value of the composite field $\bar{\psi}\psi$.

Formally, we may introduce auxiliary fields in the path integral by introducing an exponential factor into the integrand of the generating functional. This is known as a *Hubbard-Stratonovich* transformation. To bosonize the scalar-pseudoscalar interaction channel we use

$$\mathcal{N} \int \mathcal{D}\phi_1 \mathcal{D}\phi_2 \mathcal{D}V_\mu \mathcal{D}A_\mu e^{-\int d^4x \left\{ \frac{1}{2} \bar{m}_\sigma^2 \bar{\phi}^2 + \frac{1}{2} \bar{m}_V^2 V_\mu V_\mu + \frac{1}{2} \bar{m}_A^2 A_\mu A_\mu \right\}} = 1, \quad (54)$$

¹³ For convenience, we do not display the source terms for the fields here and in the following.

where we have combined the scalar fields into the $O(2)$ vector $\vec{\phi}^T = (\phi_1, \phi_2)$, where ϕ_1 and ϕ_2 are real-valued scalar fields.¹⁴ The fields ϕ_1 , ϕ_2 , V_μ and A_μ are auxiliary fields (which have no dynamics so far), \mathcal{N} is a normalization factor, and the constants \bar{m}_σ , \bar{m}_V^2 and \bar{m}_A^2 remain arbitrary for the moment. Multiplying the integrand of the generating functional with such a factor leaves the Greens functions of the theory unchanged. We now shift the integration variables in the so-modified generating functional according to¹⁵

$$\begin{aligned}\phi_1 &\rightarrow \phi_1 + \frac{i\bar{h}_\sigma}{\sqrt{2}\bar{m}_\sigma^2} (\bar{\psi}\psi), & \phi_2 &\rightarrow \phi_2 - \frac{i\bar{h}_\sigma}{\sqrt{2}\bar{m}_\sigma^2} (\bar{\psi}i\gamma_5\psi), \\ V_\mu &\rightarrow V_\mu - \frac{\bar{h}_V}{\bar{m}_V^2} (\bar{\psi}\gamma_\mu\psi), & A_\mu &\rightarrow A_\mu - \frac{\bar{h}_A}{\bar{m}_A^2} (\bar{\psi}\gamma_\mu\gamma_5\psi).\end{aligned}\quad (55)$$

where we have introduced the auxiliary constants \bar{h}_σ , \bar{h}_V and \bar{h}_A . The new generating functional then reads

$$Z \propto \int \mathcal{D}\phi_1 \mathcal{D}\phi_2 \mathcal{D}V_\mu \mathcal{D}A_\mu \mathcal{D}\psi \mathcal{D}\bar{\psi} e^{-S[\bar{\psi}, \psi, \phi_1, \phi_2, V_\mu, A_\mu]} \quad (56)$$

with the so-called partially bosonized action

$$\begin{aligned}S[\bar{\psi}, \psi, \phi_1, \phi_2, V_\mu, A_\mu] &= \int d^4x \left\{ Z_\psi \bar{\psi} i \not{\partial} \psi + \frac{1}{2} \bar{m}_\sigma^2 \vec{\phi}^2 + \frac{\bar{h}_\sigma}{\sqrt{2}} \bar{\psi} (\vec{\tau} \cdot \vec{\phi}) \psi \right. \\ &\quad \left. + \frac{1}{2} \bar{m}_V^2 V_\mu V_\mu - \bar{h}_V \bar{\psi} \not{V} \psi + \frac{1}{2} \bar{m}_A^2 A_\mu A_\mu - \bar{h}_A \bar{\psi} \not{\gamma}_\mu \gamma_5 A_\mu \psi \right\}.\end{aligned}\quad (57)$$

Here, we have introduced $\vec{\tau} = (i \cdot \mathbf{1}, \gamma_5)$ in order to define a chirally invariant Yukawa interaction. To obtain the (partially) bosonized action in this convenient form, we have exploited the fact that \bar{m}_σ , \bar{m}_V^2 and \bar{m}_A^2 as well as \bar{h}_σ , \bar{h}_V and \bar{h}_A are arbitrary parameters. To be specific, we have chosen

$$\bar{\lambda}_\sigma \stackrel{!}{=} \frac{\bar{h}_\sigma^2}{2\bar{m}_\sigma^2}, \quad \bar{\lambda}_V \stackrel{!}{=} \frac{\bar{h}_V^2}{\bar{m}_V^2} \quad \text{and} \quad \bar{\lambda}_A \stackrel{!}{=} \frac{\bar{h}_A^2}{\bar{m}_A^2}.\quad (58)$$

Instead of a four-fermion interactions, there are now Yukawa-type interactions and mass terms for the auxiliary fields. The interaction between the fermions is mediated by the bosonic fields $\vec{\phi}$, V_μ and A_μ , see Fig. 4. It is clear that the point-like approximation of the four-fermion interactions is only meaningful in the limit of large boson mass terms, $m_i^2 \gg \Lambda^2 \geq p^2$ with $i \in \{\sigma, V, A\}$, where p is a typical momentum of the composite boson. We would like to emphasize that the Yukawa couplings and their associated mass terms are not independent in the pointlike limit: Only their ratio has a physical meaning which is due to our choice (58).

The new action (57) is symmetric under a simultaneous chiral transformation of the fermions and the composite fields. While the transformation of the fermionic fields is given by Eq. (21), the scalar fields, which are of our particular interest, transform according to

$$\vec{\phi} \mapsto \begin{pmatrix} \cos(2\alpha) & \sin(2\alpha) \\ -\sin(2\alpha) & \cos(2\alpha) \end{pmatrix} \vec{\phi}, \quad (59)$$

where α is an arbitrary rotation angle. The group of transformations defined by this matrix is simply the $O(2)$ rotation group. Note that the chiral transformation of the scalar fields follows immediately from the transformation properties of $\bar{\psi}\psi$ and $\bar{\psi}\gamma_5\psi$.

¹⁴ Alternatively, we could have introduced a complex field $\varphi = (\phi_1 + i\phi_2)/\sqrt{2}$: $\bar{m}_\sigma^2 \varphi^* \varphi = \bar{m}_\sigma^2 \vec{\phi}^2/2$.

¹⁵ For historical reasons we include a factor of $\sqrt{2}$ in the shift of the scalar fields; such a factor is usually present in studies of theories with only one fermion species, such as QED, where one rather deals with a complex (charged) scalar field $\varphi = (\phi_1 + i\phi_2)/\sqrt{2}$.



Fig. 4 Left diagram: Representation of a four-fermion interaction ($i \in \{\sigma, V, A\}$) in the purely fermionic formulation of our NJL model. In general, the vertex function has a non-trivial momentum dependence. Right diagram: The Feynman diagram has the same external lines as the one on the left. However, the vertex function has been replaced by a boson propagator (dashed line) which mediates the interaction. This illustrates the situation in the partially bosonized version of the NJL model.

From the equations of motion of the bosonic field it follows that

$$\frac{\delta S}{\delta \phi_1(x)} = \bar{m}_\sigma^2 \phi_1(x) + i \frac{\bar{h}_\sigma}{\sqrt{2}} \bar{\psi} \psi = 0, \quad \frac{\delta S}{\delta \phi_2(x)} = \bar{m}_\sigma^2 \phi_2(x) + \frac{\bar{h}_\sigma}{\sqrt{2}} \bar{\psi} \gamma_5 \psi = 0, \quad (60)$$

$$\frac{\delta S}{\delta V_\mu(x)} = \bar{m}_V^2 V_\mu(x) - \bar{h}_V \bar{\psi} \gamma_\mu \psi = 0, \quad \frac{\delta S}{\delta A_\mu(x)} = \bar{m}_A^2 A_\mu(x) - \bar{h}_A \bar{\psi} \gamma_\mu \gamma_5 \psi = 0. \quad (61)$$

Inserting the solutions of these equations of motion into the action (57) and using Eq. (58), we immediately recover the original action (57). From a phenomenological point of view, the solutions of the equations of motion allow us to consider the bosonic fields as bound-states of the fermion fields. In particular, they relate the vacuum expectation value of $\bar{\psi}\psi$ to that of the scalar field ϕ_1 , $\langle \bar{\psi}\psi \rangle \sim \langle \phi_1 \rangle$. From our consideration of the Nambu-Goldstone theorem, see Eq. (53), we then conclude that chiral symmetry breaking is indicated by a finite expectation value of the field ϕ_1 . Strictly speaking, chiral symmetry breaking is signaled by a finite expectation value of the field $\vec{\phi}$, where $|\langle \vec{\phi} \rangle|$ defines a circle in the two-dimensional space spanned by the fields ϕ_1 and ϕ_2 . The points on this circle are related to each other by chiral transformations, i. e. $O(2)$ rotations in the space of the chiral components, see Eq. (59). In any case, the fermions acquire a finite mass once the expectation value of ϕ_1 is finite, as can be seen from an evaluation of their equation of motion at a finite value of $\langle \phi_1 \rangle$:

$$\left. \frac{\delta S}{\delta \bar{\psi}(x)} \right|_{\substack{\phi_1 = \langle \phi_1 \rangle \\ \phi_2 = 0}} = (i\not{\partial} + im_\psi) \psi(x) = 0 \quad \text{with} \quad m_\psi = \frac{\bar{h}_\sigma}{\sqrt{2}Z_\psi} \langle \phi_1 \rangle. \quad (62)$$

Thus, the fermions *condense* for $\langle \phi_1 \rangle > 0$ and their finite mass term m_ψ signals the spontaneous breakdown of chiral symmetry in the physical ground state of the theory. Note that the chiral symmetry is still present on the level of the microscopic theory.

The discussed (chiral) symmetry breaking pattern plays an important role in various fields of research. In condensed-matter physics, such a mass term is associated with a fermion gap. In low-energy QCD, it plays the role of a constituent quark mass. By contrast, in the electroweak theory it is considered as the (current) quark mass. The ground-state value $\langle \phi_1 \rangle$ does not necessarily have to be homogeneous, i. e. spatially constant. In fact, inhomogeneous condensates have been identified in some parts of the phase diagram of the Gross-Neveu model in $d = 2$ at finite temperature and large values of the chemical potential in the large- N_f limit [42]; the status for higher-dimensional fermionic models is a subject of ongoing work, see e. g. Refs. [44, 45]. In the following, however, we shall assume that the ground state of the theory is homogeneous.

Let us now critically discuss the partially bosonized form of our NJL model. From its action we may already conclude that a non-trivial ground state of the theory, i. e. a finite expectation value $\langle \vec{\phi} \rangle$, is tightly

linked to the sign of the term bilinear in the scalar fields:¹⁶ $\bar{m}_\sigma^2 < 0$ seems to necessarily imply that $|\langle \vec{\phi} \rangle| > 0$. To establish this relation and to discuss issues related to Fierz transformations, we briefly analyze the model in a mean-field approximation. In fermionic models with more than one fermion species, this approximation is often referred to as the large- N_f approximation, see e. g. Ref. [150].

In the action (57) the fermions appear only as bilinears. Thus, they can be integrated out straightforwardly and we obtain a purely bosonic effective action:

$$\Gamma_{\text{MF}}[\phi_1, \phi_2, V_\mu, A_\mu] = \int d^4x \left\{ \frac{1}{2} \bar{m}_\sigma^2 \vec{\phi}^2 + \frac{1}{2} \bar{m}_V^2 V_\mu V_\mu + \frac{1}{2} \bar{m}_A^2 A_\mu A_\mu \right\} - \text{Tr} \ln \left[Z_\psi i \not{\partial} + \frac{\bar{h}_\sigma}{\sqrt{2}} (\vec{\tau} \cdot \vec{\phi}) - \bar{h}_V \gamma_\mu V_\mu - \bar{h}_A \gamma_\mu \gamma_5 A_\mu \right], \quad (63)$$

where

$$\text{Tr} \mathcal{O} = \text{tr}_D \int d^4x \langle x | \mathcal{O} | x \rangle. \quad (64)$$

Here, tr_D sums over Dirac indices. In general, this purely bosonic action is highly nonlocal since the bosonic fields depend on the space-time coordinates. In the following we neglect such a dependence and evaluate the bosonic action (57) for constant background fields $\bar{\phi}_1$, $\bar{\phi}_2$, \bar{V}_μ and \bar{A}_μ . We also set the wavefunction renormalization of the fermion fields to one, $Z_\psi = 1$. This yields the effective potential U :

$$\Gamma_{\text{MF}}[\bar{\phi}_1, \bar{\phi}_2, \bar{V}_\mu, \bar{A}_\mu] = \int d^4x U(\bar{\phi}_1, \bar{\phi}_2, \bar{V}_\mu, \bar{A}_\mu). \quad (65)$$

The (homogeneous) ground state can be obtained from a variation of the effective potential with respect to the fields evaluated at the physical ground state. Assuming for simplicity that the vacuum expectation values of the vector bosons and the axial-vector boson are zero, we find¹⁷

$$\langle \phi_1 \rangle = 4 \frac{\bar{h}_\sigma^2}{2\bar{m}_\sigma^2} \int \frac{d^4p}{(2\pi)^4} \frac{\langle \phi_1 \rangle}{p^2 + \frac{1}{2} \bar{h}_\sigma^2 \langle \phi_1 \rangle^2}. \quad (66)$$

We immediately realize that the prefactor on the right-hand side is directly related to the four-fermion coupling $\bar{\lambda}_\sigma$, see Eq. (58). Depending on the value of the four-fermion coupling $\bar{\lambda}_\sigma = \bar{h}_\sigma^2 / (2\bar{m}_\sigma^2)$, Eq. (66) has apart from a trivial solution, $\langle \phi_1 \rangle = 0$, a non-trivial solution for $\langle \phi_1 \rangle$. Since the integral on the right-hand side of Eq. (58) is divergent, we have to regularize it. We employ a sharp UV cutoff $\Lambda \gg m_\psi$ for the four-momenta which permits a comparison of our results with the ones from the previous section. The fermion mass m_ψ is then determined by the following implicit equation:

$$\left(4\pi^2 \left(\frac{2\bar{m}_\sigma^2}{\bar{h}_\sigma^2 \Lambda^2} \right) - 1 \right) = \left(\frac{m_\psi^2}{\Lambda^2} \right) \ln \left(\frac{m_\psi^2}{\Lambda^2} \right), \quad (67)$$

¹⁶ Let us add a word of caution on the meaning of $\langle \vec{\phi} \rangle$ in the present work. For this discussion we put our theory in a finite volume V . We then have $\langle \vec{\phi} \rangle = 0$, independent of our choice for the parameters \bar{h}_σ and \bar{m}_σ . Depending on our choice for \bar{h}_σ and \bar{m}_σ , however, we may have $\langle |\vec{\phi}| \rangle = 0$. In order to obtain a finite expectation value $\langle \vec{\phi} \rangle$ in a finite volume, we may allow for a finite external source for, e. g., the scalar field ϕ_1 , such that $\langle \vec{\phi}^T \rangle = (\langle \phi_1 \rangle, 0)$. In a field-theoretical model of ferromagnetism, such an external source plays the role of an external magnetic field. Considering now the limit of a vanishing source term before taking the limit $V \rightarrow \infty$, we encounter $\langle \vec{\phi} \rangle = 0$ also for $V \rightarrow \infty$. Considering first the limit $V \rightarrow \infty$ and then the limit of a vanishing source term, however, the expectation value $\langle \vec{\phi}^T \rangle = (\langle \phi_1 \rangle, 0)$ remains finite in the infinite-volume limit, see e. g. Ref. [149] for a detailed discussion. In our effective-action approach we *implicitly* take these two limits in the “correct” order to obtain a finite expectation value $\langle \vec{\phi} \rangle$. In infinite volume, this is ensured by expanding the effective action about, e. g., a finite value of $\langle \vec{\phi}^T \rangle = (\langle \phi_1 \rangle, 0)$. From now on, we shall always assume that the two limits have been taken in such a way that $\langle \vec{\phi} \rangle$ remains finite, provided that the parameters \bar{h}_σ and \bar{m}_σ have been chosen accordingly. In our present case, the (continuous) chiral symmetry of the ground state is then said to be broken spontaneously.

¹⁷ Here, we evaluate the so-called gap equation for $\langle \vec{\phi}^T \rangle = (\langle \phi_1 \rangle, 0)$. Equivalent ground states with $\langle \vec{\phi}^T \rangle = (\langle \phi_1 \rangle \neq 0, \langle \phi_2 \rangle \neq 0)$ are related to this ground state by means of a chiral transformation.

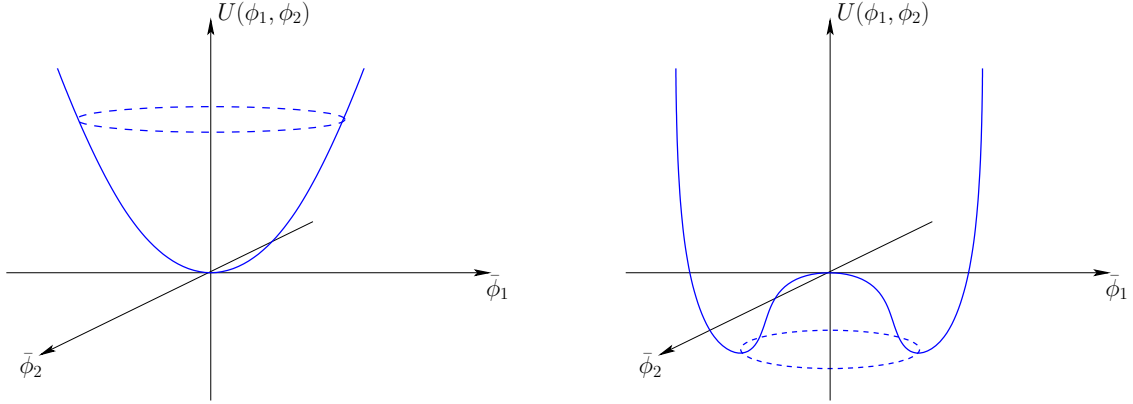


Fig. 5 Sketch of the mean-field order-parameter potential $U(\vec{\phi}_1, \vec{\phi}_2)$. The left panel depicts the shape of the potential in the chirally symmetric phase ($\langle \bar{\psi}\psi \rangle \sim |\langle \vec{\phi} \rangle| = 0$, $\lambda_\sigma \leq \lambda_\sigma^{\text{crit.}}$). The shape of the potential in a phase with broken chiral symmetry in the ground state ($|\langle \vec{\phi} \rangle| > 0$, $\lambda_\sigma > \lambda_\sigma^{\text{crit.}}$) is shown in the right panel.

where m_ψ is defined in Eq. (62). Thus, the fermions acquire a finite mass due to the spontaneous breakdown of chiral symmetry, if we choose

$$\lambda_\sigma = \bar{\lambda}_\sigma \Lambda^2 = \frac{\bar{h}_\sigma^2 \Lambda^2}{2\bar{m}_\sigma^2} > 4\pi^2. \quad (68)$$

From this inequality we can read off a critical value for the dimensionless four-fermion coupling $\lambda_\sigma = \bar{\lambda}_\sigma \Lambda^2$:

$$\lambda_\sigma^{\text{crit.}} = 4\pi^2. \quad (69)$$

It is instructive to repeat this analysis with the optimized regulator function that we have also employed in the previous section. Using Eqs. (15) and (351), the gap equation (66) assumes the following form:

$$\langle \phi_1 \rangle = 4 \frac{\bar{h}_\sigma^2}{2\bar{m}_\sigma^2} \int \frac{d^4 p}{(2\pi)^4} \left[\frac{\langle \phi_1 \rangle}{p^2 + \frac{1}{2}\bar{h}_\sigma^2 \langle \phi_1 \rangle^2} - \frac{\langle \phi_1 \rangle}{\Lambda^2 + \frac{1}{2}\bar{h}_\sigma^2 \langle \phi_1 \rangle^2} \right] \theta(\Lambda^2 - p^2). \quad (70)$$

Note that the second term in the square brackets is absent when we choose a sharp cutoff. From Eq. (70) we obtain

$$\lambda_\sigma^{\text{crit.}} = 8\pi^2. \quad (71)$$

Our results for the critical value $\lambda_\sigma^{\text{crit.}}$ can be identified with the value of the non-trivial fixed point of the four-fermion coupling, which we have computed in the previous section, see e. g. Eqs. (36), (37) and (46). In fact, we find that the critical values given in Eqs. (69) and (71) are identical to the fixed-point values given in Eqs. (37) and (36), respectively. The role of the critical value as a fixed point becomes apparent from the fact that the theory is (strongly) interacting for $\lambda_\sigma = \lambda_\sigma^{\text{crit.}}$ but remains massless and ungapped on all scales.

In Fig. 5 we show a sketch of the mean-field effective potential $U(\vec{\phi}_1, \vec{\phi}_2, 0, 0) \equiv U(\vec{\phi}_1, \vec{\phi}_2, 0, 0)$ for $\lambda_\sigma > \lambda_\sigma^{\text{crit.}}$ (spontaneous breakdown of chiral symmetry) and for $\lambda_\sigma < \lambda_\sigma^{\text{crit.}}$ (chirally symmetric phase). This effective potential simply corresponds to a *Ginzburg-Landau* effective potential for the order parameter fields.

A word of caution on the parameter dependence of the model needs to be added here: Our analysis indicates that the Yukawa couplings and the boson masses are not independent input parameters of the partially bosonized theory at the UV scale Λ . In fact, Eq. (67) suggests that the fermion mass, which is just

one example for a physical observable, remains unchanged for a fixed ratio $\bar{h}_\sigma^2/(2\bar{m}_\sigma^2)$. As in the purely fermionic formulation, this is indeed the case for $d < 4$. In $d = 4$ space-time dimensions, however, the Yukawa coupling \bar{h} is marginal. This then suggests that the partially bosonized theory in $d = 4$ depends on two input parameters in contrast to $d < 4$, see also Refs. [33, 150]. We shall come back to this issue in Sect. 5 where we discuss two examples.

In Sect. 3.1 we have discussed Fierz transformations in great detail in the context of the purely fermionic formulation of our simple NJL model. One may wonder if the ambiguity arising from the possibility of Fierz transformations is still present in the partially bosonized formulation. As we have discussed, the Fierz transformation (22) states that only two of the three four-fermion couplings are independent. Thus, one of these couplings, say $\bar{\lambda}_A$, can be chosen freely. For example, we may choose $\bar{\lambda}_A = \gamma\bar{\lambda}_V$ with $\gamma \in \mathbb{R}$, see Refs. [77, 140]. Applying then the Fierz transformation (22) to our result for the critical coupling $\lambda_\sigma^{\text{crit.}}$ we observe that this quantity is not invariant under such a transformation:

$$\lambda_\sigma^{\text{crit.}} \xrightarrow{\text{Fierz}} \lambda_\sigma^{\text{crit.}} - 2\gamma\lambda_V = 4\pi^2 - 2\gamma\lambda_V. \quad (72)$$

Thus, the critical value of the coupling depends on the arbitrary parameter γ , if λ_V is finite. As argued above, the critical couplings correspond to the value of the non-trivial fixed-point of the four-fermion interactions which are of course not universal but depend on the renormalization scheme. Therefore one might be tempted to not worry about this artificial γ -dependence. However, it is fundamentally different from a scheme dependence since the γ -dependence can be removed within any scheme. In particular, this so-called Fierz ambiguity affects not only the values of the critical couplings but also physical observables, such as the phase boundary at finite temperature or the mass spectrum of the theory. This can be readily seen from the corresponding change in the self-consistency equation (67):

$$\left(\frac{4\pi^2}{\lambda_\sigma + 2\gamma\lambda_V} - 1 \right) = \left(\frac{m_\psi^2}{\Lambda^2} \right) \ln \left(\frac{m_\psi^2}{\Lambda^2} \right). \quad (73)$$

We stress that it is *not* possible to resolve this ambiguity within a mean-field approach [140]. Due to this, mean-field results of fermionic models will always be tainted with an uncertainty.

Since mean-field studies underly many investigations of phases of strongly-interacting theories, ranging from condensed-matter physics to QCD, we briefly discuss the relevance of the Fierz ambiguity for these type of studies. Usually, the strategy for studying phases, e. g. finite-temperature phase transitions, in NJL-type models is as follows: first, one chooses a physically motivated parameter set at zero temperature. Then, one uses the *same* initial conditions for a study of the model at finite temperature. Naively, one might now argue that the Fierz ambiguity is of no relevance since it might always be possible to adjust the initial conditions such that the IR physics at zero temperature remains unchanged. However, our present analysis already suggests that, e. g., a vector-like coupling might be generated due to quantum and also thermal fluctuations, see Sects. 3.3 and 3.5.3. The finite-temperature dynamics might therefore be significantly altered for different sets of parameters even though they have been adjusted to yield the same IR physics at zero temperature.

A further comment on the present bosonization procedure is in order. In the remainder of this section, we shall follow the strategy to bosonize the four-fermion interaction at a given UV scale Λ . Below this scale, we then consider only operators in the RG flow which arise from the bosonization at $k = \Lambda$. We stress that this is an approximation, since the four-fermion interactions are generated again in the RG flow, after each infinitesimal RG step δk . This can be traced back to the existence of finite Yukawa couplings. For example, the Yukawa coupling \bar{h}_σ re-generates the four-fermion coupling $\bar{\lambda}_\sigma$ in the RG flow due to the presence of so-called box diagrams, see Fig. 6. Thus, the β functions of the four-fermion couplings are non-zero even though we have removed these couplings from the action at the initial scale Λ . The right-hand side of the RG flow equations of the four-fermion couplings then assumes the following form:

$$\partial_t \bar{\lambda}_i \sim \sum_{m,n} c_{mn}^{(i)} \bar{h}_m^2 \bar{h}_n^2, \quad (74)$$

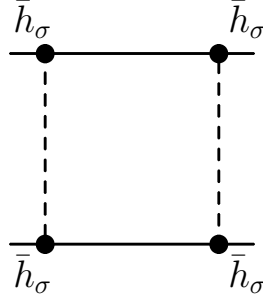


Fig. 6 Box diagram $\sim \bar{h}_\sigma^4$ which contributes to the RG flow of the four-fermion coupling. Dashed lines denote boson propagators while straight lines depict fermion propagators.

where $i, m, n \in \{\sigma, V, A\}$ and the $c_{mn}^{(i)}$'s are scale-dependent functions depending on the boson masses. The box diagrams shrink to point-like diagrams corresponding to four-fermion interactions in the case of large boson masses. Of course, the running of the four-fermion interactions generated by the Yukawa couplings is then expected to be small. However, it may become significant if the bosons become light, e. g. close to a phase boundary. In any case, the re-generation of the four-fermion couplings is problematic from a field-theoretical point of view, as one now encounters bosonic as well as purely fermionic operators at the scale $\Lambda - \delta k$. A so-called re-bosonization technique has been proposed to cure this problem by performing a bosonization of the newly generated four-fermion interactions in each RG step [28, 104, 105, 124–127], to put it sloppily. This method has been successfully applied to QED and one-flavour QCD at zero temperature [28, 124, 125] and finite temperature [32]. In addition to the phenomenological importance of this re-bosonization technique, it is of great importance from a field-theoretical point of view. In fact, the discussed Fierz ambiguity, which is present in the partially bosonized description of the NJL model, can only be removed using this technique [140].

Let us make one more point by comparing the NJL model and its bosonized version in more detail. Our analysis of the partially bosonized theory allows us to define a sufficient and necessary criterion for the detection of the onset of (chiral) symmetry breaking in the purely fermionic formulation:

- (i) Necessary condition: a four-fermion coupling must exceed its critical value to approach an IR regime with broken (chiral) symmetry.
- (ii) Sufficient criterion: a rapidly increasing (divergent) four-fermion coupling λ signals the onset of (chiral) symmetry breaking:

$$\frac{1}{\lambda} \rightarrow 0 \quad \Leftrightarrow \quad \epsilon = \frac{\bar{m}^2}{Zk^2} \rightarrow 0,$$

where ϵ and Z denote the dimensionless renormalized boson mass and the corresponding bosonic wave-function renormalization, respectively. In other words, a divergent four-fermion coupling signals a change in the sign of the coefficient of the term quadratic in the fields in the Ginzburg-Landau effective potential.

Note that the necessary criterion is equivalent to the sufficient criterion for vanishing temperature only, see Sect. 3.5.3. At finite temperature, the two criteria are no longer equivalent. This can be ultimately traced back to the fact that we only have pseudo fixed-points in the RG flow once we introduce a dimensionful (external) parameter into the theory. This so-called pseudo fixed-points then depend on, e. g., the ratio of the temperature T and the RG scale k .

Of course, the divergence of a four-fermion coupling at a finite scale k_{SB} is an artifact of the point-like approximation employed in our studies of the purely fermionic formulation. It can be resolved by

taking into account (some of) the momentum dependence of the four-fermion coupling, see also below. In any case, the scale k_{SB} at which $1/\lambda(k_{\text{SB}}) = 0$ sets the scale for the IR observables. Thus, k_{SB} can be considered as the UV cutoff of a low-energy theory describing the physics in the regime with broken chiral symmetry.

It is worth noting that, in general, the onset of (chiral) symmetry breaking is not simply indicated by a single rapidly growing four-fermion coupling. It is rather signaled by a strong RG running of various different four-fermion couplings associated with competing channels. This is due to the fact that a given rapidly increasing four-fermion coupling potentially entails a strong running of other four-fermion couplings, see, e. g., the set of flow equations (42) and (43). In a purely fermionic formulation it may therefore be a highly non-trivial task to resolve the symmetry-breaking patterns of a given theory. A partially bosonized formulation might then be more beneficial.

Our discussion shows that both the purely fermionic formulation in a point-like approximation and the partially bosonized formulation come with advantages and disadvantages from a technical as well as from a phenomenological point of view. The purely fermionic formulation is very convenient to study the phase diagram of theories in the (chirally) symmetric regime without suffering from Fierz ambiguities. From such a highly controlled study of the symmetric phase we can then determine the regimes in parameter space in which the underlying symmetries are broken in the ground state of the theory. In particular, the purely fermionic description is well-suited for analytic studies. On the other hand, the partially bosonized ansatz allows us to resolve momentum dependences of fermionic self-interactions in a simple manner and therefore permits a study of the formation of condensates and the mass spectrum of a given theory. However, the Fierz ambiguity is more difficult to resolve in this picture. A fixed-point study in the purely fermionic formulation of the theory may therefore provide important guidance for the construction of suitable low-energy models.

To further illustrate the relation (and equivalence) of the purely fermionic formulation and the partially bosonized formulation we study the RG flow of the following action:

$$\Gamma_k[\bar{\psi}, \psi, \phi_1, \phi_2] = \int d^4x \left\{ Z_\psi \bar{\psi} i \not{\partial} \psi + \frac{\bar{h}_\sigma}{\sqrt{2}} \bar{\psi} (\vec{\tau} \cdot \vec{\phi}) \psi + \frac{1}{2} Z_\sigma (\partial_\mu \vec{\phi})^2 + \frac{1}{2} \bar{m}_\sigma^2 \vec{\phi}^2 + \frac{1}{8} \bar{\omega}_\sigma \vec{\phi}^4 \right\}, \quad (75)$$

where Z_σ denotes the wave-function renormalization of the boson field. The coupling $\bar{\omega}_\sigma$ measures the strength of the four-boson interaction. The boundary conditions of the flow equations at the initial RG scale Λ read

$$\lim_{k \rightarrow \Lambda} Z_\sigma = 0, \quad (76)$$

$$\lim_{k \rightarrow \Lambda} Z_\psi = 1, \quad (77)$$

$$\lim_{k \rightarrow \Lambda} \bar{\omega}_\sigma = 0. \quad (78)$$

These conditions together with the identity

$$\bar{\lambda}_\sigma = \frac{\bar{h}_\sigma^2}{2\bar{m}_\sigma^2} \quad (79)$$

allow us to map the ansatz (75) onto the action (19) at the initial RG scale. As our study of the RG flow of the action (75) is just meant to highlight a few more aspects of the relation of purely fermionic theories and their partially bosonized formulations, we drop the vector-interaction channel as well as the axial-vector channel. We will also not make use of re-bosonization techniques. For a more complete study of the RG flow of partially bosonized theories based on the action (57), we refer the reader to Refs. [77, 140].

Let us now demonstrate that the partially bosonized formulation of our model allows us to conveniently resolve the momentum dependence of four-fermion interactions. To this end, we consider the (quantum)

equations of motion of the fields ϕ_1 and ϕ_2 in momentum space, $(\delta\Gamma/\delta\phi_1(p)) = 0$ and $(\delta\Gamma/\delta\phi_2(p)) = 0$:

$$\phi_1(-p) = -\frac{i}{Z_\sigma p^2 + \bar{m}_\sigma^2} \int \frac{d^4 q}{(2\pi)^4} \frac{\bar{h}_\sigma}{\sqrt{2}} [\bar{\psi}(q)\psi(q-p)], \quad (80)$$

$$\phi_2(-p) = -\frac{1}{Z_\sigma p^2 + \bar{m}_\sigma^2} \int \frac{d^4 q}{(2\pi)^4} \frac{\bar{h}_\sigma}{\sqrt{2}} [\bar{\psi}(q)\gamma_5\psi(q-p)], \quad (81)$$

where we have set $\omega_\sigma = 0$ for simplicity. Now we insert these solutions for the scalar fields into our ansatz (75). The Yukawa interaction term then assumes the following form in momentum space:

$$\begin{aligned} & \frac{1}{2} \int \frac{d^4 p_1}{(2\pi)^4} \int \frac{d^4 p_2}{(2\pi)^4} \int \frac{d^4 p_3}{(2\pi)^4} \left\{ [\bar{\psi}(p_1)\psi(p_2)] \frac{\bar{h}_\sigma^2}{Z_\sigma(p_1-p_2)^2 + \bar{m}_\sigma^2} [\bar{\psi}(p_3)\psi(p_1-p_2+p_3)] \right. \\ & \left. - [\bar{\psi}(p_1)\gamma_5\psi(p_2)] \frac{\bar{h}_\sigma^2}{Z_\sigma(p_1-p_2)^2 + \bar{m}_\sigma^2} [\bar{\psi}(p_3)\gamma_5\psi(p_1-p_2+p_3)] \right\}. \quad (82) \end{aligned}$$

This corresponds to an s-channel approximation of the momentum dependence of the four-fermion vertex. The expression in Eq. (82) illustrates that the interaction between the fermions is mediated by the scalar fields which act as exchange bosons (see Fig. 4). We find that this term simply reduces to the point-like four-fermion interaction term $\sim \bar{\lambda}_\sigma$ included in the action (19) for a large (renormalized) boson mass, $m_\sigma^2 = \bar{m}_\sigma^2/Z_\sigma \gg \Lambda^2 \geq p^2$, see also Eq. (28). Thus, this analysis shows that the partially bosonized formulation allows us to resolve the momentum dependence of four-fermion interactions in a simple manner and that the point-like approximation in our purely fermionic description in Sect. 3.1 is reasonable if the exchange bosons are heavy. On the other hand, the point-like approximation ultimately breaks down in the limit of vanishing boson masses, e. g. at the phase boundary and in the phase with a spontaneously broken, continuous chiral symmetry where we encounter massless bosonic excitations.

The solutions of the equation of motion of the scalar fields, Eqs. (80) and (81), show also that the term $\sim \vec{\phi}^4$ in the effective action (75) corresponds to an 8-fermion interaction term in the purely fermionic description. Due to the boundary condition (78) this term is generated dynamically and not adjusted by hand in our RG approach, see e. g. Refs. [28, 32, 33, 135, 151]. Thus, the value of the corresponding coupling at the initial RG scale Λ does not represent an additional parameter of the theory. In any case, this coupling only plays a prominent role in the (deep) IR regime with broken chiral symmetry where it accounts for the mass difference between the Nambu-Goldstone boson and the mass of the radial mode.

Of course, the discussion in this section is mainly meant to address technical issues of fermionic models. Nonetheless we would like to remind the reader at this point that, in particular, the (partially) bosonized actions (57) and (75) resemble models from various fields of physics, ranging from condensed-matter physics (e. g. Gross-Neveu-type models and ultracold atomic gases) to high-energy physics. In fact, our model is closely related to the action of the so-called *quark-meson model*, see Sect. 5. In hadron physics, the auxiliary fields play the role of the scalar meson and the pseudo-scalar Nambu-Goldstone modes, i. e. the pions, whereas the fermions are the constituent quarks. The Yukawa-coupling \bar{h}_σ then specifies the strength of the quark-meson interaction.

Let us now discuss the RG flow equations for the couplings specified in the action (75) as well as their mapping onto the RG flows of the purely fermionic formulation of this model, see Eq. (19). The partially bosonized version of our model has been studied in detail in Ref. [33] for zero and finite temperature. To simplify the comparison between the two formulations, we shall employ a so-called covariant regulator function for the bosons and the fermions which we have already used in Sect. 3.1. In the chirally symmetric regime the flow equations can be computed along the lines of Sect. 3.1: we compute the second functional derivative of the effective action (75) with respect to the boson and the fermion fields and evaluate it for homogeneous fermionic and bosonic background fields, respectively. The second functional derivative of the effective action can then be split into a background-field dependent part (fluctuation matrix) and a part which does not depend on the background fields (propagator matrix). A straightforward calculation then

yields the following flow equations for the couplings:

$$\partial_t \epsilon_\sigma = (\eta_\sigma - 2)\epsilon_\sigma - 8v_4 l_1^{(4)}(\epsilon_\sigma; \eta_\sigma) \omega_\sigma + 8v_4 l_1^{(F),(4)}(0; \eta_\psi) h_\sigma^2, \quad (83)$$

$$\partial_t \omega_\sigma = 2\eta_\sigma \omega_\sigma + 20v_4 l_2^{(4)}(\epsilon_\sigma; \eta_\sigma) \omega_\sigma^2 - 8v_4 l_2^{(F),(4)}(0; \eta_\psi) h_\sigma^4, \quad (84)$$

$$\partial_t h_\sigma^2 = (\eta_\sigma + 2\eta_\psi) h_\sigma^2, \quad (85)$$

where we have introduced the dimensionless renormalized couplings $\epsilon_\sigma = \bar{m}_\sigma^2 / (Z_\sigma k^2)$, $\omega_\sigma = \bar{\omega}_\sigma / Z_\sigma^2$ and the Yukawa coupling $h_\sigma = \bar{h}_\sigma / (Z_\sigma^{1/2} Z_\psi)$. The equations for the anomalous dimensions $\eta_\sigma = -\partial_t \ln Z_\sigma$ and $\eta_\psi = -\partial_t \ln Z_\psi$ read¹⁸

$$\eta_\sigma = 4v_4 h_\sigma^2 m_4^{(F),(4)}(0; \eta_\psi), \quad (86)$$

$$\eta_\psi = 2v_4 h_\sigma^2 m_{1,2}^{(FB),(4)}(0, \epsilon_\sigma; \eta_\psi, \eta_\sigma). \quad (87)$$

The threshold functions are defined in App. D. The functions $l_n^{(4)}$ represent purely bosonic loops. Note that the fermions are massless (ungapped) in the symmetric regime since the vacuum expectation value $\langle \vec{\phi} \rangle$ of the boson fields vanishes.

From the flow equation for the Yukawa coupling we recover the one-loop result for $\epsilon_\sigma \rightarrow 0$, see Refs. [33, 124]:

$$\partial_t h_\sigma^2 = \frac{h_\sigma^4}{4\pi^2}. \quad (88)$$

The running of the Yukawa coupling is driven only by the anomalous dimensions in the symmetric regime. This is a peculiarity of the present model with a continuous chiral symmetry but only one fermion species. In theories with more than one fermion species, such as two-flavor QCD, or in theories with a discrete chiral symmetry, the running of the Yukawa coupling receives also contributions from so-called triangle diagrams, see Sect. 5. In these types of theories, it turns out that the contributions from triangle diagrams are subleading in a systematic expansion of the flow equations in powers of the inverse number of fermion species.¹⁹

We now have a closer look at the relation between the partially bosonized and the purely fermionic formulation. To this end, we consider the RG flow of the ratio $h_\sigma^2 / (2\epsilon_\sigma) = (k^2 / Z_\psi^2) \bar{h}_\sigma^2 / (2\bar{m}_\sigma^2) = \lambda_\sigma$ which can be obtained straightforwardly from the flow equations (83) and (85):

$$\partial_t \lambda_\sigma \equiv \partial_t \left(\frac{h_\sigma^2}{2\epsilon_\sigma} \right) = (2 + 2\eta_\psi) \lambda_\sigma - 16v_4 l_1^{(F),(4)}(0; \eta_\psi) \lambda_\sigma^2 + 8v_4 l_1^{(4)}(\epsilon_\sigma; \eta_\sigma) \frac{\lambda_\sigma \omega_\sigma}{\epsilon_\sigma}. \quad (89)$$

We observe that the first two terms on the right-hand side of this flow equation are identical to the terms appearing in the flow equation (33) which we computed in the point-like approximation in the purely fermionic formulation. In particular, we find that the flows are identical in the limit $k \rightarrow \Lambda$ where we have $\omega_\sigma = 0$ and $\epsilon_\sigma \rightarrow \infty$ according to the boundary conditions (76)-(78). From this comparison we deduce that the partially bosonized description indeed allows us to go conveniently beyond the point-like approximation employed in Sect. 3.1. To be more specific, we observe that the momentum dependence of the four-fermion vertex is effectively parameterized by the wave-function renormalization Z_σ and the mass parameter $\epsilon_\sigma \sim m_\sigma^2$. As discussed above, ω_σ parameterizes fermionic self-interactions of higher order. Thus, the contribution $\sim \omega_\sigma$ on the right-hand side of Eq. (89) indicates that the RG flows of fermionic interactions of higher order, such as eight-fermion interactions, contribute to the RG flows of four-fermion interactions, if we go beyond the point-like approximation. For scales $k < \Lambda$, the purely fermionic point-like description and the partially bosonized description are then no longer identical. From

¹⁸ In order to obtain the flow equations for the wave-function renormalizations, we have to evaluate the second functional derivative of the effective action for spatially varying bosonic and fermionic background fields, see Sect. 3.1.

¹⁹ In the Gross-Neveu model the expansion parameter is the inverse number of fermion flavors, whereas it is the inverse number of colors in QCD.

the flow equation of the ratio $h_\sigma^2/(2\epsilon_\sigma)$, however, it follows that the differences are quantitatively small in the (chirally) symmetric regime since the renormalized mass of the bosons is large.

In addition, we find that the anomalous dimension η_ψ is non-zero in the partially bosonized formulation whereas it is identically zero in the point-like approximation of the purely fermionic description. Again, the running of Z_ψ is small in the symmetric regime due to the large (renormalized) boson mass.²⁰

Our analysis of the partially bosonized NJL model reveals clearly that spontaneous (chiral) symmetry breaking can be studied within a purely fermionic formulation. Some information on the symmetries of the ground-state is already encoded in the strength of the four-fermion couplings compared to their values at the non-trivial RG fixed point. These values can be viewed as critical values for the four-fermion couplings: in this framework, the system approaches a phase with broken chiral symmetry in the ground state, if the critical values are exceeded by the initial values of the four-fermion couplings at the UV scale.

Let us highlight a subtlety concerning the existence of the non-trivial RG fixed point of the four-fermion coupling. From Eqs. (83)-(85) we deduce that we can only have fixed-points with $(h_\sigma^*)^2 \equiv 0$. Considering the relation $\lambda_\sigma = h_\sigma^2/(2\epsilon_\sigma)$, this suggests that only a Gaussian fixed point exists for the four-fermion coupling beyond the point-like approximation. In fact, the non-trivial fixed point of the four-fermion coupling in the present type of fermionic models²¹ is most likely an artifact of the point-like approximation in $d = 4$. It is only present for a finite UV cutoff Λ . In the spirit of low-energy models, the UV cutoff of a fermionic model in $d = 4$ should therefore always be considered as an additional parameter of the theory.²² For any finite value of Λ , it is then still possible to define a critical value of the four-fermion coupling above which we have chiral symmetry breaking in the IR limit, also beyond the point-like approximation. In our discussion we refer to this critical coupling as a quantum critical point, even if we discuss fermionic models in $d = 4$.

The partially bosonized formulation also allows us to study the deep IR regime in which the dynamics are governed by massless Nambu-Goldstone bosons. Of course, this regime can also be studied with the aid of RG flow equations, see e. g. Refs. [28, 32, 33, 113, 135, 136, 151]. We have shown that the mass parameter $m_\sigma^2 \sim \epsilon_\sigma$ assumes negative values in this regime. This behavior signals the existence of a finite vacuum expectation value of the field $\vec{\phi}$. For an RG study, it is then convenient to parametrize the flow of the effective action in terms of the four-boson coupling ω_σ and the vacuum expectation value $\langle \vec{\phi} \rangle$ rather than the mass parameter ϵ_σ . The RG flow of $\langle \vec{\phi} \rangle$ can be derived from the following condition:

$$\frac{d}{dt} \left[\frac{\partial}{\partial \vec{\phi}^2} \left(\frac{1}{2} \bar{m}_\sigma^2 \vec{\phi}^2 + \frac{1}{8} \bar{\omega}_\sigma \vec{\phi}^4 \right) \right]_{\langle \vec{\phi} \rangle} \stackrel{!}{=} 0. \quad (90)$$

However, a discussion of the regime governed by spontaneous symmetry breaking is beyond the scope of this review. For a detailed study of the IR dynamics of this particular NJL model, we refer the reader to Refs. [33, 140]. In the following we restrict our discussions to the RG flow of four-fermion interactions in the point-like limit in the symmetric regime. As discussed, this already allows us to map the phase diagram of a given theory as a function of various couplings in a clean and very controlled way. This has been explicitly demonstrated in the context of gauge theories in Ref. [29], where the regularization-scheme independence of universal quantities has been found to hold remarkably well in the point-like limit.

3.3 Spontaneous Symmetry Breaking and Fermion Interactions

Now that we have discussed the relation between spontaneous symmetry breaking and the fixed-point structure of four-fermion interactions, we are in a position to compute the zero-temperature phase diagram of the simple NJL model with only one species. To this end, we employ the flow equations (42) and (43) as obtained from the Fierz-complete ansatz (26) for the effective action.

²⁰ This follows immediately when we replace the four-fermion vertex in the diagram on the right in Fig. 1 with two Yukawa vertices connected by a boson propagator.

²¹ This includes QCD low-energy models, see Sect. 5.2.

²² In contrast to the present NJL model in $d = 4$, the limit $\Lambda \rightarrow \infty$ is well-defined in, e. g., the Gross-Neveu model in $d = 3$, see Sect. 5.1.

In the previous section we have found that the non-trivial fixed-point of the four-fermion coupling in a single-channel approximation can be identified with the critical value which needs to be exceeded in order to have chiral symmetry breaking in the IR limit. In such a single-channel approximation this non-trivial fixed point is IR repulsive, as discussed in Sect. 3.1. Since the fermionic interactions are not induced by, e. g., fluctuations of gauge fields, we have to tune the initial value $\lambda_\sigma^{\text{UV}}$ of the four-fermion coupling such that $\lambda_\sigma^{\text{UV}} > \lambda_\sigma^*$ in order to observe chiral symmetry breaking in the IR. The four-fermion coupling then increases rapidly and diverges at a finite RG scale k_{SB} , $1/\lambda_\sigma(k_{\text{SB}}) \rightarrow 0$. The value of this scale is clearly scheme-dependent. In any case, k_{SB} sets the scale for a given (chiral) low-energy observable \mathcal{O} , e. g. the chiral condensate or the phase transition temperature:

$$\mathcal{O} \sim k_{\text{SB}}^{d_{\mathcal{O}}}, \quad (91)$$

where $d_{\mathcal{O}}$ is the canonical dimension of the observable. This observation is at the heart of our study of scaling in the subsequent section and our analysis of chiral symmetry breaking in gauge theories. On the other hand, choosing $\lambda_\sigma^{\text{UV}} < \lambda_\sigma^*$, we find that the λ_σ -coupling approaches zero in the IR limit. Thus, the non-trivial fixed point separates a trivial (non-interacting) phase from a phase with broken chiral symmetry in the ground state. The initial value for the four-fermion coupling can be considered as an external parameter which controls chiral symmetry breaking and triggers a quantum phase transition at $\lambda_\sigma^{\text{UV}} = \lambda_\sigma^*$. From a thermodynamical point of view, one can think of $\lambda_\sigma^{\text{UV}}$ as a proxy for the temperature of the system, and of λ_σ^* as the critical temperature.

At this point we would like to remind the reader that the divergence of the four-fermion coupling at a finite scale k_{SB} is an artifact of the point-like approximation. This divergence simply indicates the onset of the breaking of the chiral U(1) symmetry of our model. Hence the divergence has a physical meaning. It can be resolved by taking into account some of the momentum dependence of the coupling λ_σ , as discussed in the previous subsection. Such an improvement of the truncation is indispensable if we are interested in the IR properties of the model or the order of the phase transition. However, for a computation of the phase boundaries at zero as well as at finite temperature, it is a good approximation to simply detect the divergence in the RG flow.

Let us now turn to a discussion of symmetry breaking within our Fierz-complete ansatz for the effective action. To this end, we can indeed apply similar arguments as for the discussion of the single-channel approximation above. However, the RG flow is now governed by the existence of fixed points in the two-dimensional plane spanned by the couplings λ_σ and λ_V . As discussed in Sect. 3.1, we find three fixed points, see Eq. (46): one Gaußian fixed point with two IR attractive directions and two fixed points with both a repulsive and an attractive direction. The notion of a critical coupling becomes more complicated in the present case. The role of the critical coupling in the single-channel approximation is now essentially taken over by the so-called separatrices. In the d_c -dimensional space spanned by the d_c couplings of a given theory, separatrices can be viewed as $(d_c - 1)$ -dimensional manifolds. These manifolds separate disjunct domains of the RG flow. Fixed points are elements of the set of points defined by the separatrices. This implies that a separatrix also determines the RG flow between two fixed points. In the present case, we have $d_c = 2$ and separatrices correspond to lines in the $(\lambda_V, \lambda_\sigma)$ -plane, see Fig. 7.

In Fig. 7 we show the zero-temperature phase diagram of our model as obtained from an evaluation of the flow equations with an optimized regulator function. The fixed points \mathcal{F}_i are given by red (light gray) points. We observe that the separatrices (thick solid lines) allow us to divide the $(\lambda_\sigma, \lambda_V)$ -plane into various distinct domains which we denote by roman numbers. Choosing a set of initial conditions in the regimes Ia, Ib, IIIa and IIIb we find that the couplings increase rapidly and diverge at a finite scale k_{SB} indicating the onset of chiral symmetry breaking in the infrared. However, the four-fermion couplings in the domains Ia/b and IIIa/b approach different points for $k \rightarrow k_{\text{SB}}$. While the RG flows in the regimes Ia and Ib are attracted to the point

$$\mathcal{F}_2^\infty := \lim_{\alpha \rightarrow \infty} \alpha \cdot \mathcal{F}_2 \stackrel{(46)}{=} \lim_{\alpha \rightarrow \infty} (3\alpha\zeta, \alpha\zeta), \quad (92)$$

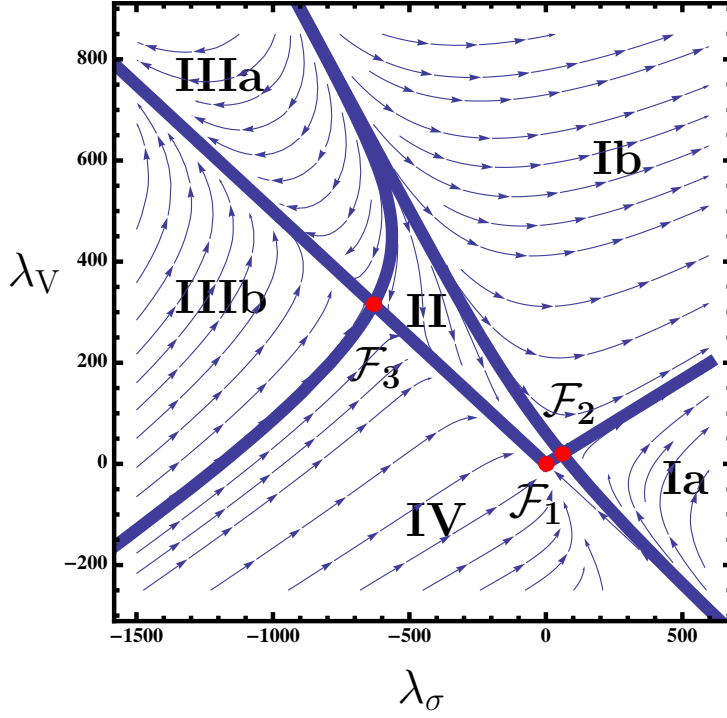


Fig. 7 Phase diagram of the NJL model with only one fermion species. The fixed points \mathcal{F}_i are given by red (light gray) dots. The separatrices (thick solid line) separate domains with different IR properties. The arrows of the various RG trajectories (thin solid lines) indicate the direction of the flow towards the infrared.

the flows approach the point

$$\mathcal{F}_3^\infty := \lim_{\alpha \rightarrow \infty} \alpha \cdot \mathcal{F}_3 \stackrel{(46)}{=} \lim_{\alpha \rightarrow \infty} (-32\alpha\zeta, \alpha\zeta) \quad (93)$$

for $k \rightarrow k_{\text{SB}}$ in the regimes IIIa and IIIb; the scheme-dependent quantity ζ is defined in Eq. (47). From a phenomenological point of view, the low-energy theories associated with the domains Ia/b might therefore be different, even though both correspond to theories with a broken chiral symmetry in the ground state. To identify the IR properties of these theories, we would need to go beyond the point-like approximation and include the momentum dependence of the fermionic interactions. However, this is beyond the scope of the present analysis.

It is worth mentioning that the RG trajectories in the regimes Ib and IIIa originate from the very same point at infinity. This point corresponds to a fixed point to which we refer as \mathcal{F}_4 . This is the fixed point which seems to be missing in our analysis in Sect. 3.1. It has two IR repulsive directions. In a study with N_f fermions it indeed turns out that the two coordinates of \mathcal{F}_4 assume finite values, see e. g. Refs. [29, 31, 152, 153].

In contrast to the regimes with a strongly-interacting IR limit, the dynamics in the regimes II and IV are governed by the Gaußian fixed point \mathcal{F}_1 . These regimes represent the basin of attraction of the Gaußian fixed point. If we choose a set of initial conditions in these two domains, both couplings are attracted to the Gaußian fixed point and therefore vanish in the IR limit. Thus such initial conditions yield trivial, i. e. non-interacting, IR theories.

From the phase diagram we can also read off that there exists no trajectory for which either of the two couplings, namely λ_σ and λ_V , remains constant under RG transformations. For example, a vector-channel interaction is always generated in the RG flow even if we set it to zero at the initial RG scale, provided

we choose a non-vanishing initial value for the λ_σ -coupling. The existence of a trajectory with $\lambda_V \equiv 0$ (NJL-like trajectory) would imply that one of the non-trivial fixed points was located on the λ_σ -axis of the phase diagram, with its IR repulsive direction pointing towards the Gaussian fixed point. In Sects. 3.5.1 and 3.5.2, we further discuss whether an NJL-like trajectory exists in the limit of many fermion flavors. Note that this question is certainly an interesting and important question for, e. g., the construction of low-energy QCD models in the limit of many colors. In a Fierz-complete study of the Thirring model in three dimensions, it has indeed been found that a pure Thirring-like trajectory exists in the limit of many fermion flavors. On this trajectory we only have a running of the four-fermion interaction that is included in standard mean-field studies of the Thirring model [75].

3.4 A First Look at Scaling Behavior close to a Quantum Critical Point

In statistical physics, one finds that completely different many-body systems show the same *quantitative* behavior near critical phase transitions, where long-range fluctuations are important. In the vicinity of these critical points, the behavior of a given theory is independent of its (microscopic) details and can be described completely by scaling relations and a small set of so-called critical exponents. This phenomenon is called *universality*. For example, finite-temperature phase transitions of the $3d$ Ising model and $SU(2)$ Yang-Mills theory belong to the same universality class. Typical scaling relations near a critical point (e. g. a second-order phase transition) are of the form

$$\xi \sim \left(\frac{T - T_{\text{cr}}}{T_{\text{cr}}} \right)^{-\nu} \quad \text{and} \quad G(x, 0) \sim |x|^{2-d-\eta}, \quad (94)$$

where ξ is the range of correlated fluctuations (correlation length) and G denotes the two-point correlation function between fluctuations at the origin and at space-time point x at $T = T_{\text{cr}}$. The universal critical exponents are ν and η , and d denotes the number of Euclidean space-time dimensions. The temperature is denoted by T and the critical temperature by T_{cr} .

The existence of universal behavior plays a very important role in modern physics. First, it allows us to classify theories according to their scaling behavior close to a phase transition which turns out to depend solely on the symmetry properties and the dimensionality of the critical system. Second, we may check numerical data from studies of more involved theories with the aid of scaling functions as obtained from an investigation of simpler models in the same universality class. Due to dimensional reduction at finite temperature we can, for example, use scaling functions from a simple three-dimensional scalar $O(4)$ model to analyze lattice QCD data for $d = 4$ close to the chiral phase transition, see e. g. Refs. [55, 154–157].

It is important to stress that such scaling laws and functions cannot be deduced from any fixed-order perturbation theory calculation, since there are inherently non-perturbative phenomena underlying these laws.

In the following we discuss scaling behavior at zero temperature rather than at finite temperature. In particular, we aim to understand the scaling behavior of fermionic theories at vanishing temperature close to a so-called *quantum critical point*. The associated quantum phase transition is driven purely by the variation of a parameter other than the temperature. For example, a variation of the number of fermion flavors may induce a quantum phase transition, as we shall discuss in detail in Sect. 6. In this section, however, we discuss only basic aspects of the scaling behavior close to quantum phase transitions. This will be helpful for our investigations in the remainder of this review.

3.4.1 Power-law Scaling

For simplicity, we start our discussion with an analysis of scaling in the single-channel approximation of the simple NJL model given in Eq. (33). As discussed above in detail, the statement about the mere existence of the fixed-point λ_σ^* , see Eq. (35), is universal, even though its actual value is clearly scheme-dependent. The control parameter for quantum critical behavior is given by the value $\lambda_\sigma^{\text{UV}}$ at the initial RG scale Λ . In fact, choosing an initial value $\lambda_\sigma^{\text{UV}} < \lambda_\sigma^*$ at the UV scale Λ , we find that the theory becomes

non-interacting in the IR regime, see Fig. 2. For $\lambda_\sigma^{\text{UV}} > \lambda_\sigma^*$, we find that the four-fermion coupling λ_σ increases rapidly and diverges eventually at a finite scale k_{SB} , so that $1/\lambda_\sigma(k_{\text{SB}}) = 0$. This indicates the onset of chiral symmetry breaking. Hence chiral symmetry breaking in the IR only occurs if we choose $\lambda_\sigma^{\text{UV}} > \lambda_\sigma^*$. Since $\lambda_\sigma^{\text{UV}}$ distinguishes between two different phases in the IR limit, i. e. in the long-range limit, we can consider λ_σ^* as a quantum critical point which divides the model into two substantially different physical regimes.

The scale k_{SB} sets the scale for a given IR observable, see Eq. (91). In the present case, this scale can be directly obtained from the solution Eq. (38) of the flow equation (33). Solving $1/\lambda_\sigma(k_{\text{SB}}) = 0$ for k_{SB} , we then find

$$k_{\text{SB}} = \Lambda \theta(\lambda_\sigma^{\text{UV}} - \lambda_\sigma^*) \left(\frac{\lambda_\sigma^{\text{UV}} - \lambda_\sigma^*}{\lambda_\sigma^{\text{UV}}} \right)^{\frac{1}{|\Theta|}} + \mathcal{O}(\eta_\psi^*), \quad (95)$$

where $\theta(\dots)$ is the unit-step function. The critical exponent Θ associated with the fixed point λ_σ^* , which governs the critical behavior, is given by

$$\Theta := - \frac{\partial(\partial_t \lambda_\sigma)}{\partial \lambda_\sigma} \Big|_{\lambda_\sigma^*} = 2 + 2\eta_\psi^* - 2\lambda_\sigma^* \frac{\partial \eta_\psi}{\partial \lambda_\sigma} \Big|_{\lambda_\sigma^*} + 16v_4 (\lambda_\sigma^*)^2 \frac{\partial l_1^{(\text{F}), (4)}(0; \eta_\psi)}{\partial \lambda_\sigma} \Big|_{\lambda_\sigma^*}, \quad (96)$$

see also Eq. (49). This reduces to

$$\Theta = 2 \quad (97)$$

for $\eta_\psi \equiv 0$, independent of the regulator function. Apparently an exact computation of the exponent Θ requires to include corrections beyond the point-like limit.

In any case, the value k_{SB} scales with the distance of the initial value $\lambda_\sigma^{\text{UV}}$ from the fixed-point value λ_σ^* . If this distance is increased, the scale k_{SB} increases and the values of physical (low-energy) observables \mathcal{O} , such as the correlation length ξ or the fermion mass, increase in turn:

$$\mathcal{O} \sim k_{\text{SB}}^{d_{\mathcal{O}}} = \Lambda^{d_{\mathcal{O}}} \theta(\lambda_\sigma^{\text{UV}} - \lambda_\sigma^*) \left(\frac{\lambda_\sigma^{\text{UV}} - \lambda_\sigma^*}{\lambda_\sigma^{\text{UV}}} \right)^{\frac{d_{\mathcal{O}}}{|\Theta|}}. \quad (98)$$

Here, $d_{\mathcal{O}}$ is the canonical mass dimension of the observable \mathcal{O} . From this expression it is clear that the absolute values of the scheme-dependent quantities $\lambda_\sigma^{\text{UV}}$ and λ_σ^* are not physically relevant, but only their relative distance is.²³ We stress again that the critical exponent Θ governs the long-range physics at the quantum critical point λ_σ^* . It is related to the standard correlation length exponent ν by $\nu = 1/\Theta$. In addition, it follows from the scaling law Eq. (98) that the quantum critical point is associated with a vanishing boson mass $m \sim k_{\text{SB}}$ and a diverging correlation length $\xi \sim 1/m$ in the long-range limit. The critical exponent η in Eq. (94) is determined by the anomalous dimension of the (bosonic) order-parameter field $\sim \bar{\psi}\psi$, and the fixed-point value λ_σ^* plays the role of the critical temperature.

One may wonder how the scaling behavior changes when we consider the Fierz-complete set of flow equations, since we then have to deal with two couplings instead of one. For illustration, let us consider a situation in which we have chosen a set of initial conditions in the domain Ib of the phase diagram given in Fig. 7. In this domain, the RG flows are attracted to the point \mathcal{F}_2^∞ :

$$\mathcal{F}_2^\infty := \lim_{\alpha \rightarrow \infty} \alpha \cdot \mathcal{F}_2. \quad (99)$$

For any initial condition $(\lambda_\sigma^{\text{UV}}, \lambda_\psi^{\text{UV}})$ in this domain we can then find a suitably chosen scale $k_0 < \Lambda$ for which the RG trajectory is close to the separatrix connecting the points \mathcal{F}_2 and \mathcal{F}_2^∞ . In other words, the point $(\lambda_\sigma(k_0), \lambda_\psi(k_0))$ lies close to this separatrix. Of course, the scale k_0 depends strongly on the initial conditions at the scale Λ . For scales $k < k_0$, the direction of the RG flow is then essentially determined by

²³ In a phenomenological application of the model, the initial condition $\lambda_\sigma^{\text{UV}}$ is fixed by the values of a given set of IR observables.

the repulsive direction, i. e. the RG relevant direction, of the fixed point \mathcal{F}_2 . Thus, our two-dimensional flow is effectively reduced to a one-dimensional flow for $k < k_0$ and we are left with the situation that we have discussed above in the single-channel approximation. Consequently, we find the following scaling behavior of physical observables:

$$\mathcal{O} \sim k_{\text{SB}}^{d_{\mathcal{O}}} \sim k_0^{d_{\mathcal{O}}} \left| \vec{\lambda}_0 \right|^{-\frac{d_{\mathcal{O}}}{|\Theta|}} \left| \vec{\lambda}_0 - \vec{\lambda}_* \right|^{\frac{d_{\mathcal{O}}}{|\Theta|}}, \quad (100)$$

where $\vec{\lambda}_0^{\text{T}} := (\lambda_{\sigma}(k_0), \lambda_{\text{V}}(k_0))$ and $\vec{\lambda}_*$ is determined by the coordinates of the fixed point \mathcal{F}_2 . The exponent Θ is given by the critical exponent associated with the RG relevant direction of \mathcal{F}_2 . Thus, the scale k_0 now plays the role of the UV scale Λ in our single-channel approximation.

From the scaling relation (100), we deduce that the scaling behavior at the quantum critical point is still universal and fully determined by the critical exponent Θ . Thus, the quantum critical behavior does *not* depend on the initial conditions, but only on the symmetries of the theory. The latter restrict the number of allowed interactions in the underlying action. However, the absolute values of physical observables depend on the scale k_0 and the distance $|\vec{\lambda}_0 - \vec{\lambda}_*|$. Both depend strongly on the choice of the initial conditions for $k \rightarrow \Lambda$. The initial conditions are therefore of utmost importance for phenomenological applications.

Our discussion is obviously not restricted to initial conditions in the domain Ib of the phase diagram in Fig. 7. It can be easily adapted to initial conditions in the domains Ia, IIIa and IIIb. Of course, the present analysis of scaling can be readily generalized to theories in d dimensions with more than two interaction terms and symmetries different from those of this model.

3.4.2 Essential Scaling

Next we discuss a very special behavior of a theory close to a quantum critical point, namely *essential* scaling. This type of scaling plays a crucial role in our study of gauge theories in Sect. 6. In the context of gauge theories, such a scaling behavior is often referred to as Miransky scaling [158, 159]. It has also been found in the context of specific 2-dimensional condensed-matter systems where it is known as Berezinskii-Kosterlitz-Thouless (BKT) scaling [160–162].

For this discussion we shall consider an extension of the presently employed NJL model. To be specific, we shall assume that an extension of this model exists such that the RG flow equation for the λ_{σ} -coupling remains unchanged, but that the one for the λ_{V} -coupling receives contributions from the extension of the model. These additional contributions will give rise to a non-trivial, i. e. interacting, IR fixed point for the λ_{V} -coupling, even in the limit $\lambda_{\sigma} \rightarrow 0$. The fixed-point value λ_{V}^* can then be controlled by the additional parameters of the extended model. This still describes a very general setup and may therefore apply to a large variety of theories. In particular, gauge theories in the limit of many fermion flavors are to some extent reminiscent of this setup. This will be discussed in Sect. 6. There, the gauge coupling associated with the gauge vector bosons plays the role of the vector-channel interaction in our study.²⁴

In the following we ignore the running of the vector-like coupling and consider it as a *scale-independent* “external” parameter. The RG flow of this coupling is then governed by

$$\partial_t \lambda_{\text{V}} \equiv 0. \quad (101)$$

This corresponds to a case in which the λ_{V} -coupling assumes a finite IR fixed point value λ_{V}^* . In the vicinity of this fixed point, Eq. (101) may still be a reasonable approximation.²⁵ The flow equation for the λ_{σ} -coupling reads

$$\partial_t \lambda_{\sigma} = 2\lambda_{\sigma} - 8v_4 l_1^{(\text{F}), (4)}(0; 0) \left[\lambda_{\sigma}^2 + 4\lambda_{\sigma} \lambda_{\text{V}} + 3\lambda_{\text{V}}^2 \right], \quad (102)$$

²⁴ The minimal coupling of the fermions and the gauge vector bosons is given by a term $\sim \bar{\psi} \gamma_{\mu} A_{\mu} \psi$. This type of interaction corresponds to the Yukawa-like interaction term $\bar{\psi} \gamma_{\mu} V_{\mu} \psi$ which is present in the partially bosonized version of our simple NJL model. $\lambda_{\text{V}} \sim h_{\text{V}}^2$.

²⁵ Note that λ_{V}^* may depend on other control parameters of the theory, such as the number of fermion flavors or an external magnetic field.

where $v_4 = 1/(32\pi^2)$ and we have set $\eta_\psi \equiv 0$ for the sake of simplicity. As illustrated in Fig. 3, a variation of λ_V allows to shift the fixed points of the λ_σ -coupling. In particular, a finite value of λ_V turns the Gaussian fixed point into an interacting fixed point. Moreover, we observe that a critical value for λ_V exists for which the two fixed points of the scalar-pseudoscalar channel merge. For $\lambda_V > \lambda_V^{\text{crit.}}$, the fixed points then annihilate each other and the RG flow is no longer governed by any (finite) real-valued fixed point. From Eq. (102) we find the following value for the critical coupling strength:

$$\lambda_V^{\text{crit.}} = \frac{(2 - \sqrt{3})}{8v_4 l_1^{(\text{F}), (4)}(0; 0)} = 8\pi^2(2 - \sqrt{3}). \quad (103)$$

Here, we have used an optimized regulator function to evaluate this expression; for this regulator, one finds $l_1^{(\text{F}), (4)}(0; 0) = \frac{1}{2}$, see App. D.2. Note that $\lambda_V^{\text{crit.}}$ is defined as the value of λ_V for which the right-hand side of Eq. (102) has exactly one zero. Strictly speaking, there exist two solutions for $\lambda_V^{\text{crit.}}$: $0 < \lambda_{V,1}^{\text{crit.}} < \lambda_{V,2}^{\text{crit.}}$. In the following we assume that we increase λ_V by hand starting from $\lambda_V = 0$. Therefore we can exclude $\lambda_{V,2}^{\text{crit.}}$ from our considerations and set $\lambda_V^{\text{crit.}} = \lambda_{V,1}^{\text{crit.}}$, where $\lambda_{V,1}^{\text{crit.}}$ is identical to the right-hand side of Eq. (103).

For $\lambda_V > \lambda_V^{\text{crit.}}$, the λ_σ -coupling becomes a relevant operator and increases rapidly towards the IR indicating the onset of chiral symmetry, even if we choose $\lambda_\sigma = 0$ as initial condition at $k = \Lambda$. Thus, λ_σ necessarily diverges at a finite RG scale k_{SB} for $\lambda_V > \lambda_V^{\text{crit.}}$. Again, this scale sets the scale for chiral low-energy observables \mathcal{O} .

In order to find the scaling behavior of the symmetry breaking scale k_{SB} when λ_V is varied by hand as a constant “external” parameter, we have to solve the RG flow equation of the coupling λ_σ . We find

$$\ln k - \ln \Lambda = - \frac{2 \arctan \left(\frac{2\lambda_V - 8\pi^2 + \lambda'_\sigma}{4\pi^2 \delta(\lambda_V)} \right)}{\delta(\lambda_V)} \Bigg|_{\lambda_\sigma^{\text{UV}}}^{\lambda_\sigma}, \quad (104)$$

where we have again used an optimized regulator function for convenience. The function $\delta(\lambda_V)$ is given by

$$\delta(\lambda_V) = \frac{1}{4\pi^2} \sqrt{3\lambda_V^2 - 4(4\pi^2 - \lambda_V)^2}. \quad (105)$$

We shall only consider values of λ_V such that $\delta(\lambda_V)$ is real-valued, e. g. $\lambda_V \geq \lambda_V^{\text{crit.}}$. From Eq. (104), we obtain k_{SB} by solving for the zero of $1/\lambda_\sigma(k)$, i. e. $1/\lambda_\sigma(k_{\text{SB}}) = 0$:

$$\ln k_{\text{SB}} - \ln \Lambda = - \frac{\pi}{\delta(\lambda_V)} + \text{const.} \quad (106)$$

Here, we have chosen the initial conditions such that $\lambda_\sigma^{\text{UV}} = \lambda_\sigma^{\text{max}}$ where $\lambda_\sigma^{\text{max}}$ denotes the position of the maximum of the β_{λ_σ} -function (102), i. e., the peak of the parabola in Fig. 3. An expansion of Eq. (106) around $\lambda_V^{\text{crit.}}$ yields

$$k_{\text{SB}} \propto \Lambda \theta(\lambda_V - \lambda_V^{\text{crit.}}) \exp \left(- \frac{\pi}{2\epsilon \sqrt{\lambda_V - \lambda_V^{\text{crit.}}}} \right), \quad (107)$$

where ϵ is simply a numerical factor,

$$\epsilon = \frac{\sqrt[4]{3}}{2\pi}, \quad (108)$$

which in general depends on the details of the theory under consideration and is scheme dependent. In any case, the exponential (essential) scaling behavior of k_{SB} is *universal* for λ_V close to $\lambda_V^{\text{crit.}}$. Since the dynamically generated scale k_{SB} sets the scale for the low-energy sector, we expect that all IR observables \mathcal{O} with canonical mass dimension $d_{\mathcal{O}}$ scale according to

$$\mathcal{O} \sim k_{\text{SB}}^{d_{\mathcal{O}}}. \quad (109)$$

A few comments on the history of the scaling law Eq. (107) are in order at this point. In the context of QCD, the scaling law in Eq. (107) has been first derived by Miransky [158, 159], but it has also been found in the context of specific 2-dimensional condensed-matter systems [160–162]. A way to derive the scaling law (107) via an analysis of the RG flow of four-fermion operators has been recently pointed out by Kaplan, Lee, Son and Stephanov [163].

The scaling behavior (107) is clearly distinguishable from the power-law behavior (95). In particular, we observe that essential scaling is not governed by the critical exponent Θ associated with the IR repulsive direction at the fixed point λ_σ^* . To find exponential (essential) scaling behavior, we have assumed that the initial condition for the four-fermion coupling λ_σ at the UV scale Λ has been chosen such that $\lambda_\sigma^{\text{UV}}$ is smaller than the value of the IR repulsive fixed point λ_σ^* , see Fig. 3. We therefore stress that essential scaling behavior can only be observed when $\lambda_\sigma^{\text{UV}}$ is chosen to be smaller than the corresponding value of the IR repulsive fixed point for a given value of the constant “external” parameter λ_V . Otherwise we expect power-law-like scaling behavior as discussed above, see Eq. (95). In our discussion of quantum critical behavior in gauge theories in Sect. 6, we shall discuss a new kind of scaling behavior which can be considered as a superposition of power-law scaling and essential scaling. In the present toy-model setup, this new type of scaling behavior emerges when we allow for an RG running of the λ_V -coupling.

3.5 Deformations of Fermionic Theories

Deformations of a theory play a crucial role in physics. For example, studies of fermionic models at finite temperature provide us with insights into the mechanisms of symmetry breaking as we expect them to have been at work in the early stage of the universe. Further examples can be found in the context of condensed-matter physics: Apparently, comprehension of so-called high- T_c superconductors requires an understanding of the finite-temperature dynamics of strongly interacting fermions, see e. g. Ref. [110]. Other important deformations are given by the inclusion of terms which break explicitly the underlying symmetries. For example, explicit mass terms for the fermions break the chiral symmetry. From the point of view of a Ginzburg-Landau effective potential, such terms effectively play the role that an external magnetic field plays for a ferromagnet, e. g. an Ising model. In the theory of the strong interaction, such terms are of particular importance since they determine the so-called current quark masses. Also, studies of fermionic theories in a finite volume are of interest and represent a valuable deformation. Depending on the theory under consideration, the study of finite-size effects may help to make better contact between theoretical results and experimental data, see e. g. Ref. [41]. On the other hand, finite-size effects are important from a field-theoretical point of view. For example, Monte-Carlo simulations are necessarily performed in a finite volume. For the extrapolation to the continuum limit a rigorous understanding of the scaling behavior of a system with its volume size is certainly required, see e. g. Refs. [51, 53–55, 57, 155] for RG studies of finite-size effects relevant for Monte-Carlo simulations. In any case, we start our discussion of deformations with a first analysis of theories with many fermion flavors. To this end, we consider two distinct extensions of our NJL model with one fermion species. In Sect. 3.5.1 we study a NJL model with N_f fermions and a chiral $SU(N_f)_L \otimes SU(N_f)_R$ symmetry. An extension with a chiral $U(1)^{\otimes N_f}$ symmetry is then discussed in Sect. 3.5.2. These studies of many-flavor physics should be considered as a warm-up for Sects. 5 and 6.

3.5.1 Many-Flavor Physics I: Chiral $SU(N_f)_L \otimes SU(N_f)_R$ Symmetry

For our first study of many-flavor physics we employ a NJL model with a (chiral) $SU(N_f)_L \otimes SU(N_f)_R$ symmetry. We will encounter this type of chiral symmetry again when we discuss QCD and, in particular, when we analyze chiral symmetry breaking in strongly-flavored gauge theories in Sect. 6. QCD is in fact symmetric under $SU(N_f)_L \otimes SU(N_f)_R$ transformations in the limit of massless quarks. Apart from its relevance for QCD phenomenology, this type of flavor symmetry appears in studies of chiral symmetry breaking in quantum gravity [153].

In direct analogy to the simple NJLmodel with one fermion species, the chiral charge Q_5 ,

$$Q_5^a = \int d^3x \bar{\psi} \gamma_0 \gamma_5 T^a \psi, \quad (110)$$

does not commute with the composite fields $\sim (\bar{\psi} i \gamma_0 \gamma_5 T^a \psi) \equiv \bar{\psi}_c i \gamma_0 \gamma_5 T_{cd}^a \psi_d$, if the vacuum expectation value $\langle \bar{\psi} \psi \rangle$ is finite. In other words, the chiral symmetry of such a model is broken dynamically when $\langle \bar{\psi} \psi \rangle$ assumes a finite value. Here, the T^a denote the $(N_f^2 - 1)$ generators of the group $SU(N_f)$ in the fundamental representation. For $SU(2)$ these generators are related to the Pauli matrices, whereas they are related to the Gell-Mann matrices for $SU(3)$. For a finite chiral condensate $\langle \bar{\psi} \psi \rangle$ it then follows from the *Nambu-Goldstone* theorem that $(N_f^2 - 1)$ massless states exist in the spectrum of the theory, the *Nambu-Goldstone* bosons. In QCD, this yields a natural explanation for the existence of three light (massless) hadrons, namely the pions, in the hadronic spectrum in the theory with two light (massless) quark flavors.

We are again interested in an analysis of the fixed-point structure of the theory. To this end, we consider the effective action in leading order in the derivative expansion:

$$\Gamma[\bar{\psi}, \psi] = \int d^4x \left\{ Z_\psi \bar{\psi} i \not{\partial} \psi + \frac{1}{2} \bar{\lambda}_- (\mathbf{V}-\mathbf{A}) + \frac{1}{2} \bar{\lambda}_+ (\mathbf{V}+\mathbf{A}) \right\}, \quad (111)$$

where

$$\begin{aligned} (\mathbf{V}-\mathbf{A}) &= [(\bar{\psi} \gamma_\mu \psi)^2 + (\bar{\psi} \gamma_\mu \gamma_5 \psi)^2], \\ (\mathbf{V}+\mathbf{A}) &= [(\bar{\psi} \gamma_\mu \psi)^2 - (\bar{\psi} \gamma_\mu \gamma_5 \psi)^2]. \end{aligned}$$

The flavor indices are contracted pairwise, $(\bar{\psi} \mathcal{O} \psi) \equiv (\bar{\psi}_i \mathcal{O} \psi_i)$. This ansatz corresponds to the matter part employed in a study of chiral symmetry breaking in quantum gravity [153].

The effective action (111) is complete with respect to Fierz transformations, i. e. all other $SU(N_f)_L \otimes SU(N_f)_R$ symmetric four-fermion interactions can be transformed into a linear combination of the terms included in our ansatz. Note that

$$[(\bar{\psi} \psi)^2 - (\bar{\psi} \gamma_5 \psi)^2]$$

is *not* invariant under $SU(N_f)_L \otimes SU(N_f)_R$ transformations. However,

$$[(\bar{\psi}_i \psi_j)(\bar{\psi}_j \psi_i) - (\bar{\psi}_i \gamma_5 \psi_j)(\bar{\psi}_j \gamma_5 \psi_i)]$$

is invariant, as can be seen from the following Fierz relation:

$$(\mathbf{V}+\mathbf{A}) \equiv [(\bar{\psi} \gamma_\mu \psi)^2 - (\bar{\psi} \gamma_\mu \gamma_5 \psi)^2] = -2[(\bar{\psi}_i \psi_j)(\bar{\psi}_j \psi_i) - (\bar{\psi}_i \gamma_5 \psi_j)(\bar{\psi}_j \gamma_5 \psi_i)]. \quad (112)$$

Of course, the effective action can be directly related to the action (26) of our simple one-flavor model. Using the Fierz identity (112), we find for $N_f = 1$ that

$$\bar{\lambda}_\sigma = 2(\bar{\lambda}_- - \bar{\lambda}_+) \quad \text{and} \quad \bar{\lambda}_\nu = -2\bar{\lambda}_-. \quad (113)$$

From the point of view of high-energy phenomenology it is instructive to relate the interaction channels in Eq. (111) to the interaction channel conventionally employed in so-called quark-meson models, namely the scalar-pseudoscalar channel, see Sect. 5.2. From the Fierz identities in App. B it follows that

$$(\mathbf{V}-\mathbf{A}) = [(\bar{\psi}_i \gamma_\mu \psi_j)(\bar{\psi}_j \gamma_\mu \psi_i) + (\bar{\psi}_i \gamma_\mu \gamma_5 \psi_j)(\bar{\psi}_j \gamma_\mu \gamma_5 \psi_i)] \quad (114)$$

and

$$\begin{aligned} (\mathbf{V}+\mathbf{A}) &= -2 [(\bar{\psi}_i \psi_j)(\bar{\psi}_j \psi_i) - (\bar{\psi}_i \gamma_5 \psi_j)(\bar{\psi}_j \gamma_5 \psi_i)] \\ &= -4[(\bar{\psi} T^\alpha \psi)^2 - (\bar{\psi} \gamma_5 T^\alpha \psi)^2] - \left(\frac{2}{N_f} - 1 \right) [(\bar{\psi} \psi)^2 - (\bar{\psi} \gamma_5 \psi)^2] \\ &\stackrel{(N_f=2)}{=} -[(\bar{\psi} \psi)^2 - (\bar{\psi} \gamma_5 \tau^a \psi)^2] - \dots, \end{aligned} \quad (115)$$

with τ^a being the Pauli matrices. Here, we have dropped terms on the right-hand side of the last line in Eq. (115). However, we have included all terms in our flow equation study. This is most conveniently achieved by working with the (V+A)-channel and (V-A)-channel. Note that $\alpha = 0, 1, \dots, (N_f^2 - 1)$ and $a = 1, 2, \dots, (N_f^2 - 1)$. To derive Eq. (115), we have used the Fierz transformation for flavor indices:²⁶

$$\mathbb{1}_{ab} \mathbb{1}_{cd} = 2 \left(\frac{2}{N_f} - 1 \right) \mathbb{1}_{ad} \mathbb{1}_{cb} + 2 \sum_{\alpha=0}^{N_f^2-1} (T_{ad}^\alpha) (T_{cb}^\alpha), \quad (116)$$

where $T^0 := (1/2)\mathbb{1}$. We observe that the first term on the right-hand side of the last line in Eq. (115) corresponds to the standard scalar-pseudoscalar channel included in low-energy models for 2-flavor QCD, see Sect. 5.2 for a detailed discussion.

Let us now discuss the RG flow equations and the associated fixed-point structure. In our point-like approximation, it follows immediately that $\eta_\psi = 0$. Thus, we set $Z_\psi \equiv 1$ from now on. The flow equations for the two four-fermion couplings specified in the action (3.5.1) read

$$\partial_t \lambda_- = 2\lambda_- + 8v_4 l_1^{(F),(4)}(0;0) [(N_f - 1)\lambda_-^2 + N_f \lambda_+^2], \quad (117)$$

$$\partial_t \lambda_+ = 2\lambda_+ + 8v_4 l_1^{(F),(4)}(0;0) [2\lambda_+^2 + 2\lambda_+ \lambda_- (N_f + 1)], \quad (118)$$

where $\lambda_i = Z_\psi^{-2} k^2 \bar{\lambda}_i$. From this set of equations it is apparent that we only have three (finite) fixed points for $N_f = 1$. For arbitrary $N_f > 1$, we find the following four fixed points $\mathcal{F}_i^{\text{SU}(N_f)} = (\lambda_+^*, \lambda_-^*)$:

$$\begin{aligned} \mathcal{F}_1^{\text{SU}(N_f)} &\equiv \mathcal{F}_{\text{GauB}} = (0, 0), \quad \mathcal{F}_2^{\text{SU}(N_f)} = \left(0, -\frac{8\zeta}{N_f - 1} \right), \\ \mathcal{F}_3^{\text{SU}(N_f)} &= \left(\frac{8\zeta}{2N_f - 1}, -\frac{8\zeta}{2N_f - 1} \right), \quad \mathcal{F}_4^{\text{SU}(N_f)} = \left(-\frac{8\zeta(N_f + 3)}{9 + 5N_f + 2N_f^2}, -\frac{8\zeta N_f}{9 + 5N_f + 2N_f^2} \right), \end{aligned}$$

where ζ is defined in Eq. (47). From the stability matrix we obtain the critical exponents which allow us to classify these fixed points. We find that the Gaußian fixed point has two infrared-attractive directions. The second fixed point has two infrared-repulsive directions whereas the third and the fourth fixed point have an infrared-attractive as well as an infrared repulsive direction. Using the relations given in Eq. (113), the fixed-point values in the limit $N_f \rightarrow 1$ can be translated into those of the NJL model with only one fermion species, see Eq. (46). This confirms that the "missing" fourth fixed point in our one-flavor study is pushed to $(\lambda_\sigma \rightarrow -\infty, \lambda_V \rightarrow \infty)$ for $N_f \rightarrow 1$ from above, as indicated in Fig. 7.

Finally we would like to analyze this model in the limit of many flavors. In leading order in an expansion in powers of $1/N_f$ we find a Gaußian fixed point $\mathcal{F}_1^{\text{SU}(N_f)} = (0, 0)$ as well as three non-Gaußian fixed points:

$$\mathcal{F}_2^{\text{SU}(N_f)} = \left(0, -\frac{8\zeta}{N_f} \right), \quad \mathcal{F}_3^{\text{SU}(N_f)} = \left(\frac{4\zeta}{N_f}, -\frac{4\zeta}{N_f} \right), \quad \mathcal{F}_4^{\text{SU}(N_f)} = \left(-\frac{4\zeta}{N_f}, -\frac{4\zeta}{N_f} \right).$$

Note that the rescaled fixed-point couplings $N_f \cdot \mathcal{F}_i^{\text{SU}(N_f)}$ approach constant values in the limit $N_f \rightarrow \infty$. The associated critical exponents in leading order in $1/N_f$ are given by

$$\begin{aligned} \Theta_1^{\text{SU}(N_f)} &= \{-2, 2\}, \quad \Theta_2^{\text{SU}(N_f)} = \left\{ 2, 2 + \frac{8}{N_f} \right\}, \\ \Theta_3^{\text{SU}(N_f)} &= \left\{ 2, -2 - \frac{4}{N_f} \right\}, \quad \Theta_4^{\text{SU}(N_f)} = \left\{ 2, -2 - \frac{4}{N_f} \right\}. \end{aligned}$$

Thus, the critical behavior of such a theory at the quantum phase transition is modified when we vary the number of fermion flavors. Our analysis for $N_f > 1$ shows that an RG trajectory exists with $\lambda_+ \equiv 0$

²⁶ This identity can in principle be obtained from the general relation (24). The complete set of basis elements is now given by $\{\frac{1}{2}\mathbb{1}, T^1, T^2, \dots\}$.

which connects the fixed point $\mathcal{F}_2^{\text{SU}(N_f)}$ with the Gaussian fixed point in the IR limit. However, the interaction channel associated with the λ_- -coupling cannot be transformed into the phenomenologically relevant scalar-pseudoscalar channel, see Eqs. (114) and (115). On the contrary, a Fierz-complete analysis of the Thirring model in three dimensions provides evidence that a pure Thirring-like trajectory indeed exists in the limit of many fermion flavors [75]. In any case, these observations show that a careful analysis of fermionic theories in the large- N_f limit can provide useful information for a controlled and systematic construction of effective theories for physically relevant systems.

3.5.2 Many-Flavor Physics II: Chiral $U(1)^{\otimes N_f}$ Symmetry

As a second example for fermionic models with many flavors we consider an NJL model with a continuous chiral $U(1)^{\otimes N_f} \equiv \otimes_{i=1}^{N_f} U(1)$ symmetry, i. e. each flavor transforms independently under the chiral transformation given in Eq. (21). As a consequence, there is only one massless excitation in the spectrum for each (spontaneously broken) $U(1)$ symmetry rather than $(N_f^2 - 1)$ massless excitations as in the case of a spontaneously broken chiral $SU(N_f)_L \otimes SU(N_f)_R$ symmetry. Thus, the number of fermions can in principle be arbitrarily increased without changing the number of the Nambu-Goldstone bosons. As we shall discuss in Sect. 5, this chiral symmetry is closely related to the one realized in the Gross-Neveu model with many flavors. Moreover, such a flavor number dependence is faintly reminiscent of the dependence of QCD on the number of colors. In fact, increasing the number of colors increases the number of fermions linearly but leaves the number of Nambu-Goldstone bosons unchanged. In Sect. 6 we shall come back to QCD in the limit of many colors.

To be specific, let us consider the following ansatz for the effective action:

$$\Gamma[\bar{\psi}, \psi] = \int d^4x \left\{ Z_\psi \bar{\psi} i \not{\partial} \psi + \frac{1}{2} \bar{\lambda}_\sigma [(\bar{\psi} \psi)^2 - (\bar{\psi} \gamma_5 \psi)^2] - \frac{1}{2} \bar{\lambda}_V [(\bar{\psi} \gamma_\mu \psi)^2] - \frac{1}{2} \bar{\lambda}_A [(\bar{\psi} \gamma_\mu \gamma_5 \psi)^2] \right\}. \quad (119)$$

This ansatz has a continuous chiral $U(1)^{\otimes N_f}$ symmetry. It is even invariant under $U(N_f)$ flavor-transformations. However, it does not form a complete basis of (point-like) four-fermion interactions with respect to the $U(N_f)$ flavor-symmetry. For the latter, it is possible to show that the corresponding complete basis includes six distinct four-fermion interaction channels [164]. Nonetheless, the ansatz (119) can be considered to be closed for our purposes in this section. By this, we mean that the RG flow of this model only generates four-fermion interactions which are included in the ansatz (119). In other words, the ansatz (119) forms an invariant subspace of operators with respect to continuous chiral $U(1)^{\otimes N_f}$ transformations.

The RG flow equations for this model can be derived along the lines of Sect. 3.1. Since we restrict ourselves to the point-like limit, the anomalous dimension vanishes, $\eta_\psi \equiv 0$, and we set $Z_\psi \equiv 1$. The flow equations for the three four-fermion couplings read:

$$\partial_t \lambda_\sigma = 2\lambda_\sigma - 16v_4 l_1^{(F),(4)}(0;0) [N_f \lambda_\sigma^2 + 2\lambda_\sigma \lambda_V - \lambda_\sigma \lambda_A], \quad (120)$$

$$\partial_t \lambda_V = 2\lambda_V + 8v_4 l_1^{(F),(4)}(0;0) [2\lambda_V \lambda_A - \lambda_\sigma \lambda_V - (N_f + 1)\lambda_V^2], \quad (121)$$

$$\partial_t \lambda_A = 2\lambda_A + 4v_4 l_1^{(F),(4)}(0;0) [3\lambda_V^2 - \lambda_\sigma^2 + (1 - 2N_f)\lambda_A^2 - 2\lambda_V \lambda_A + 2\lambda_\sigma \lambda_A]. \quad (122)$$

As discussed in Sect. 3.1, for $N_f = 1$ only two of the three couplings are independent, see also Eq. (22). Using

$$\lambda_\sigma \rightarrow \lambda_\sigma + 2\lambda_A \quad \text{and} \quad \lambda_V \rightarrow \lambda_V - \lambda_A \quad (123)$$

in the above flow equations, we indeed recover the flow equations (42) and (43) of the NJL model with one fermion species.

The fixed points and the associated critical exponents of our $U(1)^{\otimes N_f}$ -symmetric NJL model can be computed straightforwardly. We do not give the explicit expressions here, but we find eight distinct fixed points for $N_f > 1$. In leading order in an expansion in powers of $1/N_f$ the expressions simplify significantly. To be specific, we find the following eight points $\mathcal{F}_i^{U(1)} = (\lambda_\sigma^*, \lambda_V^*, \lambda_A^*)$:

$$\begin{aligned} \mathcal{F}_1^{U(1)} &= (0, 0, 0), \quad \mathcal{F}_2^{U(1)} = \left(\frac{4\zeta}{N_f}, \frac{8\zeta}{N_f}, \frac{8\zeta}{N_f} \right), \quad \mathcal{F}_3^{U(1)} = \left(\frac{4\zeta}{N_f}, \frac{8\zeta}{N_f}, 0 \right), \quad \mathcal{F}_4^{U(1)} = \left(\frac{4\zeta}{N_f}, 0, \frac{8\zeta}{N_f} \right), \\ \mathcal{F}_5^{U(1)} &= \left(0, \frac{8\zeta}{N_f}, \frac{8\zeta}{N_f} \right), \quad \mathcal{F}_6^{U(1)} = \left(0, \frac{8\zeta}{N_f}, 0 \right), \quad \mathcal{F}_7^{U(1)} = \left(0, 0, \frac{8\zeta}{N_f} \right), \quad \mathcal{F}_8^{U(1)} = \left(\frac{4\zeta}{N_f}, 0, 0 \right), \end{aligned}$$

where ζ is defined in Eq. (47).

In contrast to our study of the $SU(N_f)_L \otimes SU(N_f)_R$ symmetric NJL model, we now find an RG trajectory on which only the scalar-pseudoscalar interaction is non-vanishing. This trajectory connects the non-trivial fixed point $\mathcal{F}_8^{U(1)}$ with the Gaussian fixed point in the IR limit. This observation is of phenomenological interest. Generally speaking, we can find RG trajectories in the large- N_f limit such that condensation can only occur in one specific channel while the other channels remain trivial, i. e. non-interacting. This type of observation may be used as a field-theoretical justification for models in which only one interaction channel has been taken into account, e. g. studies of Gross-Neveu models in the large- N_f limit. This will be discussed in more detail in Sect. 5.1.

3.5.3 Finite Temperature

Let us now study the dynamics of fermions at finite temperatures T . To this end, we start with an analysis of the symmetries of our Fierz-complete NJL model with one fermion species, see Eq. (26).

For $T > 0$, the Euclidean time has a finite extent $\beta = 1/T$ and therefore Lorentz symmetry is broken explicitly.²⁷ Thus, the time direction in our $d = 4$ Euclidean space-time is distinguished due to the presence of a heat-bath. In fact, we can introduce a velocity $n_\mu = (1, \vec{0})$ which defines the velocity of the heat-bath in the rest-frame of an observer. At finite temperature the most general ansatz for the effective action Γ_{NJL} compatible with the underlying symmetries of our model then reads²⁸

$$\begin{aligned} \Gamma_{\text{NJL}}[\bar{\psi}, \psi] &= \int_0^\beta dx_0 \int d^3x \left\{ Z_\psi^\parallel \bar{\psi} i \gamma_0 \partial_0 \psi + Z_\psi^\perp \bar{\psi} i \gamma_i \partial_i \psi + \frac{1}{2} \bar{\lambda}_\sigma [(\bar{\psi} \psi)^2 - (\bar{\psi} \gamma_5 \psi)^2] \right. \\ &\quad \left. - \frac{1}{2} \bar{\lambda}_V^{(0)} [(\bar{\psi} \gamma_0 \psi)^2] - \frac{1}{2} \bar{\lambda}_V^\perp [(\bar{\psi} \gamma_\mu \psi)^2] \right. \\ &\quad \left. - \frac{1}{2} \bar{\lambda}_A^{(0)} [(\bar{\psi} \gamma_0 \gamma_5 \psi)^2] - \frac{1}{2} \bar{\lambda}_T^{(0)} [(\bar{\psi} \sigma_{0\mu} \psi)^2 - (\bar{\psi} \sigma_{0\mu} \gamma_5 \psi)^2] \right\}, \end{aligned} \quad (124)$$

where

$$\bar{\lambda}_V^{(0)} = \bar{\lambda}_V^\parallel - \bar{\lambda}_V^\perp, \quad \bar{\lambda}_V^\perp \equiv \bar{\lambda}_V, \quad \bar{\lambda}_A^{(0)} = \bar{\lambda}_A^\parallel - \bar{\lambda}_A^\perp, \quad \bar{\lambda}_T^{(0)} = \bar{\lambda}_T^\parallel - \bar{\lambda}_T^\perp. \quad (125)$$

Note that both the kinetic term as well as the interaction terms in Eq. (26) can be split up into contributions longitudinal (\parallel) and perpendicular (\perp) to the heat bath. We add that the action (124) can be deduced from the ansatz (26) with the aid of the following relation:

$$(\bar{\psi} \mathcal{O}_\mu \psi)^2 \equiv (\bar{\psi} \mathcal{O}_\mu \psi) \mathbb{1}_{\mu\nu} (\bar{\psi} \mathcal{O}_\nu \psi) = (\bar{\psi} \mathcal{O}_\mu \psi) \left[P_{\mu\nu}^\parallel + P_{\mu\nu}^\perp \right] (\bar{\psi} \mathcal{O}_\nu \psi), \quad (126)$$

where \mathcal{O}_μ stands for γ_μ and $\gamma_\mu \gamma_5$, respectively, and the heat-bath projectors are defined as follows:

$$P_{\mu\nu}^\parallel = n_\mu n_\nu \quad \text{and} \quad P_{\mu\nu}^\perp = \mathbb{1}_{\mu\nu} - P_{\mu\nu}^\parallel. \quad (127)$$

²⁷ We restrict our discussion to quantum field theories in equilibrium. For related approaches to quantum field theories away from equilibrium we refer the reader to Refs. [165–169].

²⁸ We only take into account four-fermion interactions.

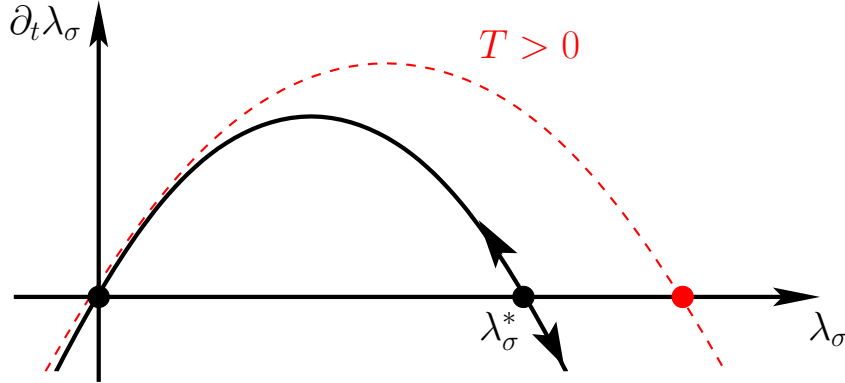


Fig. 8 Sketch of the β_{λ_σ} function of the four-fermion interaction for vanishing temperature (black/solid line) and a given finite value of the temperature T (red/dashed line). The arrows indicate the direction of the RG flow towards the infrared.

These projectors are orthogonal, $P^\parallel \cdot P^\perp = P^\perp \cdot P^\parallel = 0$, and idempotent. A further invariant at finite temperature emerges from the tensor-axialtensor channel defined in Eq. (45). This channel is chirally symmetric but vanishes identically at zero temperature, since

$$(\bar{\psi}\sigma_{\mu\nu}\psi)^2 = (\bar{\psi}\sigma_{\mu\nu}\gamma_5\psi)^2.$$

However, the chirally symmetric combination

$$[(\bar{\psi}\sigma_{0\mu}\psi)^2 - (\bar{\psi}\sigma_{0\mu}\gamma_5\psi)^2] \quad (128)$$

is not identical to zero.

For convenience, we have introduced the couplings $\bar{\lambda}_V^{(0)}$, $\bar{\lambda}_A^{(0)}$ and $\bar{\lambda}_T^{(0)}$ which effectively measure the difference between the couplings longitudinal and perpendicular to the heat bath and therefore allow for a simple mapping between the couplings of the effective actions (26) and (124). To ensure comparability of our results for zero and finite temperature, we have to fix the boundary conditions for our couplings properly. To this end, it seems natural to fix the parameters (initial conditions) of our model at zero temperature, e. g., by fitting them to a given set of low-energy observables. At finite temperature, we then use the same set of initial conditions to compute, e. g., the phase transition temperature. It is evident that such an approach requires $T/\Lambda \ll 1$. Moreover, it naturally fixes the initial conditions for the new couplings $\bar{\lambda}_V^{(0)}$, $\bar{\lambda}_A^{(0)}$ and $\bar{\lambda}_T^{(0)}$ as follows:

$$\lim_{T/\Lambda \rightarrow 0} \bar{\lambda}_V^{(0)} = \lim_{T/\Lambda \rightarrow 0} \bar{\lambda}_A^{(0)} = \lim_{T/\Lambda \rightarrow 0} \bar{\lambda}_T^{(0)} = 0. \quad (129)$$

In order to study chiral symmetry restoration at finite temperature, we now have to derive the RG flow equations for the various four-fermion couplings in our ansatz (124). To keep our discussion as simple as possible, we only take into account the $\bar{\lambda}_\sigma$ -coupling and set all other couplings to zero. This leaves us with the ansatz (19). Of course, this ansatz is not complete with respect to Fierz transformations. As in the zero-temperature case, however, the underlying mechanisms of chiral symmetry breaking can nevertheless be understood with such a simple ansatz. The Fierz-complete study will be published elsewhere [170].

The flow equation for the coupling λ_σ can in principle be derived along the lines of Sect. 3.1. Therefore we only highlight the subtleties of the derivation. For studies of quantum field theories at finite temperature, it is convenient to use a dimensionally reduced regulator function which only regularizes the spatial momenta but leaves the time-like momenta essentially unconstrained [137, 171, 172]. The (regularized)

propagator matrix \mathcal{P}_k then assumes the following form:

$$\mathcal{P}_k = \begin{pmatrix} 0 & -Z_\psi^\parallel \gamma_0^T \nu_n - Z_\psi^\perp \not{\mathbf{p}}^T (1+r_\psi) \\ -Z_\psi^\parallel \gamma_0 \nu_n - Z_\psi^\perp \not{\mathbf{p}} (1+r_\psi) & 0 \end{pmatrix} \beta \delta_{n,n'} (2\pi)^3 \delta^{(3)}(\vec{p} - \vec{p}'),$$

where the fermionic Matsubara frequencies are given by $\nu_n = (2n+1)\pi T$.

At this point we would like to add a word of caution concerning dimensionally-reduced (spatial) regulator functions, e. g. Eq. (349) in the appendix. From the propagator matrix it is apparent that such a regulator function necessarily breaks the $O(d=4)$ symmetry in the derivative terms of our truncation, i. e. $\partial_t Z_\psi^\parallel \neq \partial_t Z_\psi^\perp$ even in the zero-temperature limit. In so-called local potential approximations, this problem does not appear since the non-trivial momentum dependence of the propagators is neglected [33, 137, 138, 171, 172]. In studies beyond the point-like limit, however, we would have to deal with the broken Poincare-invariance at vanishing temperature which arises due to the choice of our dimensionally reduced regulator function.²⁹ In principle, one can solve this problem by taking care of the symmetry violating terms with the aid of the corresponding Ward identities. Equivalently, one can adjust the initial conditions for the RG flow equations such that one finds $Z_\psi^\perp = Z_\psi^\parallel$ for $k \rightarrow 0$ and $T \rightarrow 0$, see Ref. [33]. From a field-theoretical point of view the adjustment of the initial conditions for a given truncation means nothing else than adding appropriate counter-terms, such that the theory remains Poincare-invariant for $k \rightarrow 0$ and $T \rightarrow 0$. At finite temperature, the breaking of the $O(d)$ symmetry in momentum space due to the regulator function is not problematic since this symmetry is broken anyway. In any case, the choice of a dimensionally reduced regulator function offers the possibility to perform the Matsubara sums in 1PI diagrams analytically. This simplifies finite-temperature studies considerably and justifies our choice of such a regulator function.

Let us now discuss the flow equations at finite temperature. In the present approximation, the fluctuation matrix \mathcal{F}_k remains unchanged and is given by Eq. (31). To study effects of a finite temperature, it is convenient to consider the temperature T as an additional coupling and define the corresponding dimensionless coupling τ as

$$\tau = \frac{T}{k}. \quad (130)$$

Together with the propagator and the fluctuation matrix this yields the following set of flow equations:

$$\beta \lambda_\sigma \equiv \partial_t \lambda_\sigma = (2 + 2\eta_\psi^\perp) \lambda_\sigma - 16v_3 l_1^{(F),(4)}(\tau, 0, 0; \eta_\psi, \hat{z}_\psi) \lambda_\sigma^2, \quad (131)$$

$$\partial_t \tau = -\tau. \quad (132)$$

where $v_3 = 1/(8\pi^2)$. Note that the prefactor of the second term on the right-hand side of Eq. (131) differs from the corresponding one in Eq. (33) since we use a dimensionally reduced regulator function; the definition of the corresponding (thermal) threshold function can be found in App. D. The (dimensionless) renormalized coupling λ_σ is given by

$$\lambda_\sigma = (Z_\psi^\perp)^{-2} k^2 \bar{\lambda}_\sigma. \quad (133)$$

In addition, we have $\eta_\psi^{\parallel,\perp} = -\partial_t \ln Z_\psi^{\parallel,\perp}$ and $\hat{z}_\psi = Z_\psi^\parallel / Z_\psi^\perp$. The flow of the latter reads

$$\hat{\eta}_\psi = -\frac{\partial_t \hat{z}_\psi}{\hat{z}_\psi} = \eta_\psi^\parallel - \eta_\psi^\perp. \quad (134)$$

Recall that at vanishing temperature the wave-function renormalizations have to satisfy the boundary condition $\hat{z}_\psi = 1$ for $k \rightarrow 0$ to render the IR limit Poincare-invariant.

²⁹ This issue does not occur if one applies a $4d$ regulator function.

Next, we turn to a discussion of the fixed-point structure at finite temperature in the point-like limit, i. e. $\eta_\psi^{\parallel, \perp} \equiv 0$. Apart from a Gaussian fixed point, we find a pseudo fixed-point $\lambda_\sigma^*(\tau)$ at which the right-hand side of the flow equation is zero:³⁰

$$\lambda_\sigma^*(\tau) = \frac{1}{8v_3 l_1^{(F),(4)}(\tau, 0, 0; 0, 1)}. \quad (135)$$

For high temperatures the fermions are screened due to the absence of a thermal zero mode. This is encoded in the large- τ behavior of the (fermionic) threshold function. Independent of the regularization scheme,³¹ we have $l_1^{(F),(4)} \sim (k/T)^{-3}$. As an immediate consequence we find $\lambda_\sigma^* \sim (T/k)^3$. In other words, the value of the pseudo fixed-point is pushed to larger values for increasing $\tau = T/k$, see also Fig. 8.

Let us now assume that we have fixed the physical IR observables at zero temperature by choosing $\lambda_\sigma^{\text{UV}} > \lambda_\sigma^*(\tau = 0)$. This implies that we have chosen the initial condition for the four-fermion interaction such that chiral symmetry is broken in the IR limit. Recall that the fixed point $\lambda_\sigma^*(\tau = 0)$ can be viewed as a quantum critical point. Since the value of the (pseudo) fixed-point increases with increasing $\tau = T/k$, the rapid increase of the four-fermion coupling towards the IR is effectively slowed down and the RG flow may even change its direction in the (λ_σ, τ) -plane, see Fig. 9 for an illustration. Due to this behavior of the pseudo fixed-point $\lambda_\sigma^*(\tau)$, it is already clear that for a fixed initial value $\lambda_\sigma^{\text{UV}}$ a critical temperature T_χ exists above which the λ_σ -coupling does not diverge but tends to zero for $k \rightarrow 0$. From a phenomenological point of view, such a behavior is indeed expected for high temperatures: The fermions become effectively stiff degrees of freedom due to their 'Matsubara' mass $\sim T$ and chiral symmetry is restored.

With the aid of the pseudo fixed-point $\lambda_\sigma^*(\tau)$ we can formulate a *sufficient* criterion for chiral symmetry breaking at finite temperature. First, we note that for a given initial condition $\lambda_\sigma^{\text{UV}} > \lambda_\sigma^*(\tau = 0)$ the pseudo fixed-point $\lambda_\sigma^*(\tau)$ determines a dimensionless temperature τ_* through

$$\lambda_\sigma^*(\tau_*) = \lambda_\sigma^{\text{UV}}. \quad (136)$$

Since the β_{λ_σ} -function is strictly positive for $\lambda_\sigma < \lambda_\sigma^*(\tau)$, it follows immediately that it is *sufficient* to choose $\tau > \tau_*$ to restore chiral symmetry for a given fixed value of $\lambda_\sigma^{\text{UV}}$. Thus, $T_* = \Lambda\tau_*$ defines a strict upper bound for the chiral phase transition temperature T_χ .

It is important to stress that $\lambda_\sigma^*(\tau)$ does not define a separatrix in the space spanned by the coupling λ_σ and τ . From the above discussion it is clear that $\lambda_\sigma^*(\tau)$ only represents a strict upper bound for the separatrix $\lambda_\sigma^{\text{sep.}}(\tau)$, see also Fig. 9:

$$\lambda_\sigma^*(\tau) \geq \lambda_\sigma^{\text{sep.}}(\tau). \quad (137)$$

For a given initial condition $\lambda_\sigma^{\text{UV}} > \lambda_\sigma^*(\tau = 0)$, we can now define a second (dimensionless) temperature $\tau_{\text{sep.}}$ via

$$\lambda_\sigma^{\text{sep.}}(\tau_{\text{sep.}}) = \lambda_\sigma^{\text{UV}}. \quad (138)$$

Due to the very definition of a separatrix in coupling space, this allows us to define a *necessary* criterion for chiral symmetry breaking (restoration) at finite temperature: choosing $\tau < \tau_{\text{sep.}}$ ($\tau > \tau_{\text{sep.}}$) for a given fixed UV coupling $\lambda_\sigma^{\text{UV}}$, the theory approaches necessarily a regime with broken (restored) chiral symmetry in the IR limit. For a given value of the UV cutoff Λ , the quantity $\tau_{\text{sep.}}$ can then be translated into a physical temperature $T_{\text{sep.}} = \Lambda\tau_{\text{sep.}}$. Moreover, we have $\tau_{\text{sep.}} \leq \tau_*$.

Strictly speaking, even the temperature $T_{\text{sep.}}$ defines only an upper bound for the actual chiral phase transition temperature T_χ since it is only sensitive to an emergence of a condensate on intermediate momentum scales, but insensitive to the fate of the condensate in the deep IR due to fluctuations of the bosonic

³⁰ At finite temperature T , the fixed-point value depends on the dimensionless temperature $\tau = T/k$. We shall refer to it as a pseudo fixed point since its value has an intrinsic dependence on the RG scale k .

³¹ The associated perturbative Feynman diagram (diagram on the left in Fig. 1) has two internal fermion lines, yielding a factor τ^{-2} . The regulator insertion splits one of the two internal lines apart and provides an extra factor τ^{-1} .

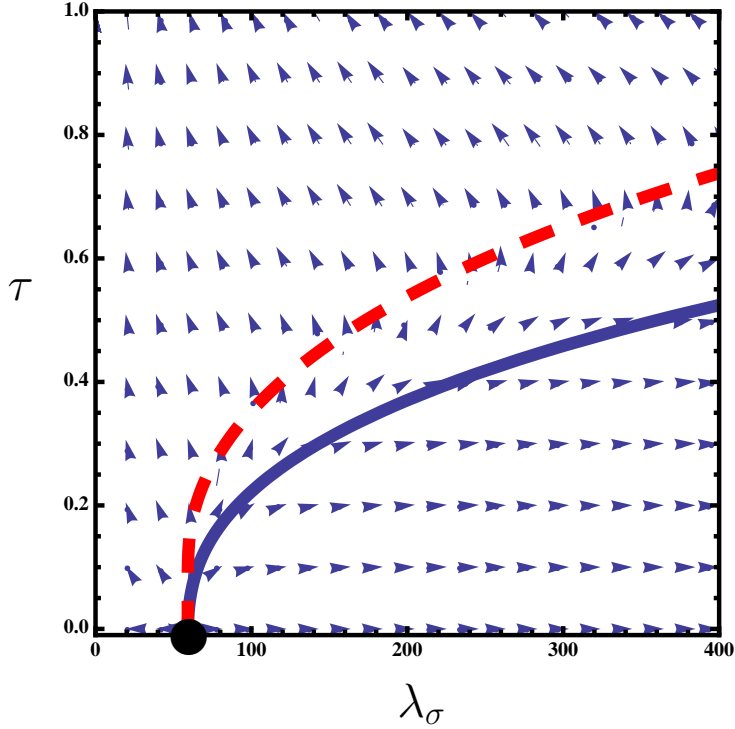


Fig. 9 RG flow in the plane spanned by the four-fermion coupling λ_σ and the dimensionless temperature $\tau = T/k$. The blue (straight) line depicts the separatrix $\lambda_\sigma^{\text{sep}}(\tau)$, whereas the red (dashed) line represents the line of pseudo fixed-points $\lambda_\sigma^*(\tau)$. Here, the separatrix has been obtained by solving the flow equations (131) and (132) with suitably fine-tuned initial conditions. For a given value of τ , the theory approaches a non-interacting IR limit for initial conditions $\lambda_\sigma^{\text{UV}} > \lambda_\sigma^{\text{sep}}(\tau)$, whereas the system flows into an IR limit with broken chiral symmetry in the ground state for $\lambda_\sigma^{\text{UV}} < \lambda_\sigma^{\text{sep}}(\tau)$. The dot represents the quantum critical point $(\lambda_\sigma^*(0), 0)$. The arrows indicate the direction of the RG flow towards the infrared.

modes, e. g. Nambu-Goldstone modes. In fact, the phase transition temperature decreases when one goes beyond the point-like limit, e. g., by taking into account bosonic loops in the RG flow to resolve the momentum dependence of the fermionic vertices [33]. In particular, the Nambu-Goldstone bosons play a prominent role at a thermal phase transition, since they tend to restore the chiral symmetry, while fermions tend to build up a condensate and thereby break the symmetry of the ground state. In contrast to the bosonic fields, however, the anti-periodic boundary conditions of the fermion fields in Euclidean time direction lead to a suppression of the associated modes in the vicinity of the phase transition and above. We shall come back to this in Sect. 5.2.2, where we discuss the thermal phase transition in QCD low-energy models.

In Fig. 9 we show the RG flow of our theory in the plane spanned by the coupling λ_σ and the dimensionless temperature τ . It is instructive to analyze the RG flow in this plane with the aid of the matrix \tilde{B} :

$$\tilde{B} = \begin{pmatrix} \frac{\partial(\partial_t \lambda_\sigma)}{\partial \lambda_\sigma} & \frac{\partial(\partial_t \lambda_\sigma)}{\partial \tau} \\ \frac{\partial(\partial_t \tau)}{\partial \lambda_\sigma} & \frac{\partial(\partial_t \tau)}{\partial \tau} \end{pmatrix}.$$

Evaluated at the non-Gaussian zero-temperature fixed point $(\lambda_\sigma^*(\tau = 0), \tau = 0)$, the matrix \tilde{B} corresponds to the stability matrix B defined in Eq. (48). Following our discussion in Sect. 3.1, we find that we have two IR repulsive (RG relevant) directions at the non-Gaussian fixed point. The eigenvectors of B are simply given by $\vec{v}_1 = (1, 0)$ and $\vec{v}_2 = (0, 1)$. The associated critical exponents of B are given by $\Theta_1 = 2$ and $\Theta_2 = 1$, respectively. Note that the functional form of the separatrix in the (λ_σ, τ) -plane is determined

by the largest critical exponent, namely Θ_1 , see Fig. 9. Close to the quantum critical point $(\lambda_\sigma^*(0), \tau=0)$, we therefore expect that the phase transition temperature T_χ scales according to

$$T_\chi \sim \Lambda \theta (\lambda_\sigma^{\text{UV}} - \lambda_\sigma^*) \left(\frac{\lambda_\sigma^{\text{UV}} - \lambda_\sigma^*}{\lambda_\sigma^{\text{UV}}} \right)^{\frac{1}{|\Theta_1|}}, \quad (139)$$

see also Eq. (98) and Sect. 5.2.2. Corrections to this scaling behavior then arise from the subleading exponent Θ_2 .

Away from the fixed point, we can use the eigenvectors of the matrix \tilde{B} to study the direction of the RG flow towards the IR. Let us first consider the eigenvectors of \tilde{B} for increasing λ_σ but fixed (dimensionless) temperature $\tau > 0$. For $\lambda_\sigma \gg \lambda_\sigma^*(\tau)$, the eigenvectors become independent of τ : $\vec{v}_1 = (1, 0)$ and $\vec{v}_2 = (c\lambda_\sigma, 1)$ with a constant $c > 0$. Thus, the angle between the two directions shrinks to zero and we are effectively left with a one-dimensional RG flow pointing into λ_σ -direction, i. e. $(1, 0)$ -direction. At the Gaussian fixed-point we find that the eigenvectors are given by $\vec{v}_1 = (1, 0)$ and $\vec{v}_2 = (0, 1)$ with exponents $\Theta_1 = -2$ and $\Theta_2 = 1$, respectively. Thus, the flow is driven by the $(0, 1)$ -direction close to the Gaussian fixed point. In accordance with this observation, we find that the flow is pushed into the $(0, 1)$ -direction (τ -direction) for fixed λ_σ and increasing τ . For sufficiently large values of τ , the RG flows are therefore attracted by the 'thermal' fixed-point $\mathcal{F}_T^\infty := \lim_{\alpha \rightarrow \infty} (0, \alpha)$. On the other hand, the RG flows are attracted by the line of fixed points $\mathcal{F}_\lambda^\infty := \lim_{\alpha \rightarrow \infty} (\alpha, \tau)$ for a given $\lambda_\sigma^{\text{UV}} < \lambda_\sigma^{\text{sep.}}(\tau)$. Overall, this is simply another way of saying that a finite temperature tends to restore chiral symmetry, whereas increasing the coupling tends to break the chiral symmetry of the ground state.

Finally we would like to comment on the effect of other four-fermion interaction channels compatible with the underlying symmetries of our model. Qualitatively, the effect of a finite temperature is the same in a Fierz-complete ansatz. To be specific, we have shown that the (modulus) of the pseudo fixed-point value increases with increasing τ . For the Fierz-complete phase diagram³² in Fig. 7 this means that the fixed-points \mathcal{F}_2 and \mathcal{F}_3 are pushed away from the Gaussian fixed point \mathcal{F}_1 for increasing τ . Hence the domain II increases for increasing τ while the domains Ia/b and IIIa/b effectively shrink. Since the domains II and IV represent the basin of attraction of the Gaussian fixed point, we conclude that a chiral phase transition temperature T_χ must exist for any initial condition lying in the domains Ia/b and IIIa/b. Thus, the very general mechanisms of dynamical chiral symmetry breaking remain unchanged. However, we expect that the prediction for the actual value of the (chiral) phase transition temperature changes when a Fierz-complete ansatz is considered.

3.5.4 Mass-like Explicit Symmetry Breaking

Let us now study another phenomenologically highly important deformation of fermionic theories, namely the inclusion of an explicit mass term $\sim \bar{\psi} m_\psi \psi$. For example, in QCD such terms correspond to the so-called current quark masses. From a field-theoretical point of view, the deformation of a theory with an explicit mass term is also of great importance since it can be used as a control parameter to study systematically the scaling behavior of physical observables in finite volumes and at finite temperatures, see e. g. Refs. [154, 173–176]. From this scaling behavior the critical exponents at the phase transition can be read off, which then allows to assign the theory under consideration to a certain universality class. Such an approach is indeed applied in the context of Monte-Carlo simulations to determine the QCD universality class, see e. g. Ref. [177].

In the following we shall discuss only general aspects of RG flows of fermionic theories with an explicit mass term. In our discussion we leave aside other possible deformations such as finite temperature and finite volume. As in our study of finite-temperature effects in the previous section, we shall consider only

³² Note that the study of the phase diagram in Fig. 7 is only Fierz-complete for $T = 0$. We only use it here to illustrate our point concerning the effect of a Fierz-complete basis of four-fermion interactions. This is justified since the difference between couplings longitudinal and transversal to the heat bath is parametrically suppressed for $T/k < 1$ anyway. Note also that $T_\chi/k_{\text{SB}} \lesssim 1$ in our present study.

a scalar-pseudoscalar interaction channel to keep our discussion of the physical mechanisms as simple as possible. However, a more quantitative study would again require the consideration of a Fierz-complete set of four-fermion interactions. To be specific, we consider a theory with only one fermion species and employ the following effective action:³³

$$\Gamma[\bar{\psi}, \psi] = \int d^4x \left\{ \bar{\psi} (Z_\psi i \not{\partial} + i\bar{m}_\psi) \psi + \frac{1}{2} \bar{\lambda}_\sigma (\bar{\psi} \psi)^2 - \frac{1}{2} \bar{\lambda}_{\text{PS}} (\bar{\psi} \gamma_5 \psi)^2 \right\}. \quad (140)$$

This ansatz represents a straightforward generalization of the effective action (19). Since we allow for an explicit fermion mass term in our ansatz, the chiral symmetry is broken explicitly and the couplings $\bar{\lambda}_\sigma$ and $\bar{\lambda}_{\text{PS}}$ will in general be different. We assume that the UV cutoff Λ has been chosen such that $\bar{m}_\psi^{\text{UV}}/\Lambda \ll 1$ and fix the initial conditions for the various couplings at the UV scale Λ as follows:

$$\lim_{\bar{m}_\psi^{\text{UV}}/\Lambda \rightarrow 0} \bar{\lambda}_\sigma = \lim_{\bar{m}_\psi^{\text{UV}}/\Lambda \rightarrow 0} \bar{\lambda}_{\text{PS}} = \lambda_\sigma^{\text{UV}} \quad \text{and} \quad \lim_{\bar{m}_\psi^{\text{UV}}/\Lambda \rightarrow 0} \bar{m}_\psi = \bar{m}_\psi^{\text{UV}}. \quad (141)$$

Thus, we are left with only two input parameters for our simple model, namely $\bar{\lambda}_\sigma^{\text{UV}}$ and \bar{m}_ψ^{UV} . In QCD, the latter parameter plays the role of the current quark mass.

It is also possible to consider a partially bosonized version of the fermionic action (140). This yields two different Yukawa couplings and corresponding mass terms, and a linear term for the composite field $\phi_1 \sim \bar{\psi} \psi$ appears. The net effect of this term is to stretch and tilt the order-parameter potential shown in Fig. 5 into the direction associated with the field ϕ_1 . As a result, we have a finite vacuum expectation value $\langle \phi_1 \rangle$ on all scales and the ground state is no longer degenerate. Of course, it is also possible to deal with such an order-parameter potential in RG flows. As is well known, a linear symmetry breaking term remains unchanged in the RG flow [176]. Therefore the usual strategy is to evolve the potential without a symmetry breaking term. Explicit symmetry breaking is then taken into account after the quantum fluctuations have been integrated out on all scales [113, 135, 136]. Alternatively, it is also possible to include the explicit symmetry breaking in the (partially) bosonized RG flows which is particularly convenient for studies of finite-volume effects in quantum field theories [51, 53, 54, 57, 154, 155].

Returning to the purely fermionic formulation, we first note that the propagator matrix now includes a mass term \bar{m}_ψ :

$$\mathcal{P}_k = \begin{pmatrix} 0 & -Z_\psi \not{p}^T (1 + r_\psi) - i\bar{m}_\psi \\ -Z_\psi \not{p} (1 + r_\psi) + i\bar{m}_\psi & 0 \end{pmatrix} (2\pi)^4 \delta^{(4)}(p - p').$$

In the following we shall employ a covariant regulator function (d -dimensional regulator) for convenience. The fluctuation matrix in Eq. (32) remains unchanged except for the fact that the coupling $\bar{\lambda}_{\text{PS}}$ is attached to the terms depending on γ_5 , whereas the coupling $\bar{\lambda}_\sigma$ is attached to the terms independent of γ_5 . Since we allow for a term $\sim \bar{\psi} \psi$ in our ansatz for the effective action, the Feynman diagram shown on the right in Fig. 1 also contributes to the RG flow of the effective action on all scales and yields a mass renormalization.³⁴ Within the present truncation of the effective action there are nevertheless no contributions to the RG flow of the wave-function renormalization Z_ψ in the point-like limit, which we shall consider from now on. For $Z_\psi \equiv 1$ and $\eta_\psi = 0$, the flow equations then read

$$\partial_t \epsilon_\psi = -2\epsilon_\psi - 8 [3\lambda_\sigma - \lambda_{\text{PS}}] v_4 b_1^{(\text{F}), (4)}(\epsilon_\psi; 0), \quad (142)$$

$$\partial_t \lambda_\sigma = 2\lambda_\sigma - 8 [\lambda_\sigma^2 + \lambda_\sigma \lambda_{\text{PS}}] v_4 \tilde{l}_1^{(\text{F}), (4)}(\epsilon_\psi; 0) - 8 [\lambda_{\text{PS}}^2 - \lambda_\sigma \lambda_{\text{PS}}] v_4 \tilde{l}_1^{(\text{F}), (4)}(\epsilon_\psi; 0), \quad (143)$$

$$\partial_t \lambda_{\text{PS}} = 2\lambda_{\text{PS}} - 8 [\lambda_{\text{PS}}^2 + \lambda_\sigma \lambda_{\text{PS}}] v_4 \tilde{l}_1^{(\text{F}), (4)}(\epsilon_\psi; 0) - 8 [\lambda_{\text{PS}}^2 + 3\lambda_\sigma \lambda_{\text{PS}}] v_4 \tilde{l}_1^{(\text{F}), (4)}(\epsilon_\psi; 0), \quad (144)$$

³³ The imaginary unit factor "i" in front of the mass term \bar{m}_ψ appears due to our conventions in Euclidean space-time.

³⁴ Strictly speaking, our RG approach includes resummations of both diagrams in Fig. 1 as well as combinations thereof.

where the renormalized dimensionless fermion mass is given by

$$\epsilon_\psi = \frac{\bar{m}_\psi^2}{k^2}, \quad (145)$$

and the renormalized dimensionless four-fermion couplings are defined as $\lambda_\sigma = k^2 \bar{\lambda}_\sigma$ and $\lambda_{\text{PS}} = k^2 \bar{\lambda}_{\text{PS}}$. The various threshold functions are defined in App. D. Here we only note that

$$l_1^{(\text{F}), (4)}(\epsilon_\psi; \eta_\psi) = \hat{l}_1^{(\text{F}), (4)}(\epsilon_\psi; \eta_\psi) + \tilde{l}_1^{(\text{F}), (4)}(\epsilon_\psi; \eta_\psi) \quad (146)$$

and $l_1^{(\text{F}), (4)}(0; 0) = \hat{l}_1^{(\text{F}), (4)}(0; 0)$. This implies $\tilde{l}_1^{(\text{F}), (4)}(0; 0) = 0$. The function $b_1^{(\text{F}), (4)}$ behaves as

$$b_1^{(\text{F}), (4)}(\epsilon_\psi; 0) \sim \epsilon_\psi \quad (147)$$

for $\epsilon_\psi \ll 1$, whereas $\hat{l}_1^{(\text{F}), (4)}$ and $\tilde{l}_1^{(\text{F}), (4)}$ are constant for small ϵ_ψ . Moreover, we have

$$b_1^{(\text{F}), (4)}(\epsilon_\psi; 0) \sim \frac{1}{\epsilon_\psi}, \quad \hat{l}_1^{(\text{F}), (4)} \sim -\frac{1}{\epsilon_\psi^2} \quad \text{and} \quad \tilde{l}_1^{(\text{F}), (4)} \sim \frac{1}{\epsilon_\psi^2} \quad (148)$$

for $\epsilon_\psi \gg 1$. With the aid of these identities it is straightforward to show that the flow equations for λ_σ and λ_{PS} are identical in the limit $\epsilon_\psi \rightarrow 0$. Thus, we have $\lambda_\sigma \equiv \lambda_{\text{PS}}$ in the chirally symmetric limit, as it should be. Moreover, the flow equations of these coupling reduce to the flow equation (33) in this limit.

From our RG equations (142)-(144) we read off that a strong four-fermion interaction induces a strong increase in the fermion mass. This is in accordance with our expectations, since strong fermion self-interactions signal the onset of chiral symmetry breaking which is associated with a finite fermion mass (gap). From the 1PI Feynman diagrams and the associated threshold functions, it is clear that a large fermion mass suppresses quantum corrections and therefore prevents the couplings and the mass from growing further. Nevertheless it is in general not possible to “stabilize” the RG flows in the point-like approximation with the aid of the evolving fermion mass term, such that the four-fermion interactions remain finite on all scales. We only find that for a given value of $\lambda_\sigma^{\text{UV}}$ a critical initial value $\epsilon_\psi^{\text{cr.}} = (m_\psi^{\text{cr.}}/\Lambda)^2$ exists, such that the four-fermion interactions remain finite on all scales for $\epsilon_\psi^{\text{UV}} > \epsilon_\psi^{\text{cr.}}$. For $\epsilon_\psi^{\text{UV}} < \epsilon_\psi^{\text{cr.}}$ the four-fermion couplings still diverge at a finite scale k_{SB} , provided we choose the initial conditions $\lambda_\sigma^{\text{UV}}$ to be larger than the fixed-point λ_σ^* of the chirally symmetric theory ($\epsilon_\psi^{\text{UV}} \rightarrow 0$), see Eq. (35). To put it sloppily, the critical value $\epsilon_\psi^{\text{cr.}}$ plays a role roughly similar to that of the critical (dimensionless) temperature. More precisely, the functional dependence of $\epsilon_\psi^{\text{cr.}}$ on $\lambda_\sigma^{\text{UV}}$ can be viewed as a critical line similar to the separatrix discussed in our finite-temperature studies in the previous section. We indeed find that $\epsilon_\psi^{\text{cr.}}$ increases monotonously with increasing $\lambda_\sigma^{\text{UV}}$. In other words, larger masses are required to screen strong self-interactions.

From a phenomenological point of view, $\epsilon_\psi^{\text{cr.}}$ distinguishes between a phase with a trivial explicit chiral symmetry breaking in the IR limit and a phase with spontaneous chiral symmetry breaking associated with a non-trivial momentum dependence of the fermionic self-interactions. In fact, a large initial value $\epsilon_\psi^{\text{UV}} > \epsilon_\psi^{\text{cr.}}$ suppresses the fermion self-interactions and therefore keeps the theory from approaching criticality. From a field-theoretical point of view, the deformation of a fermionic theory with an explicit mass term might be still useful to guide lattice studies of conformal phases in gauge theories [178–180], see also Sect. 6. Whereas functional approaches (RG and Dyson-Schwinger equations) allow to study explicitly the chiral limit ($\epsilon_\psi^{\text{UV}} \rightarrow 0$) of such theories, lattice simulations usually involve explicit mass terms for the fermions and therefore require a controlled extrapolation to the chiral limit.

Finally we remark that once one has resolved the momentum-dependence of the fermionic vertices, the explicit mass term can indeed be used to “stabilize” the RG flows to study IR observables, even for (arbitrarily) small values of $\epsilon_\psi^{\text{UV}}$. This was found in the context of condensed-matter physics [110, 181], where it was shown explicitly that the point-like limit and the limit $\epsilon_\psi^{\text{UV}} \rightarrow 0$ do not commute in general.

4 Non-relativistic Quantum Field Theories

As first examples of strongly interacting fermionic field theories we consider non-relativistic many-body systems. However, we do not aim at a quantitative study of these systems. We only present very general arguments concerning universality in non-relativistic Fermi gases and the existence of inhomogeneous phases in such systems. This allows us to apply our field-theoretical discussion in the previous section to phenomenologically relevant systems, such as ultracold atomic gases and nuclear physics. In Sect. 4.1, we show that the non-Gaussian fixed-point of the four-fermion coupling plays a decisive role in ultracold atomic gases. In fact, the coupling strength of fermions in two different hyperfine states can be tuned in experiments by means of an external magnetic field [2]. This strong experimental control opens up the possibility to gain deep insights into the mechanisms of quantum many-body phenomena, such as *Bose-Einstein* (BEC) condensation and *Bardeen-Cooper-Schrieffer* (BCS) superfluidity, and to benchmark different approaches to strongly interacting field theories.

In principle, non-relativistic many-body problems can be studied by simply solving the *Schrödinger* equation. However, exact solutions of the *Schrödinger* equation are difficult (or even impossible) to find for most of the problems, making approximations necessary. Therefore a path-integral approach to many-body problems might be promising since it allows us to employ complementary approximation schemes and gain insights into the dynamics of the system from a different perspective. In the spirit of this review, we shall restrict our discussion to path-integral approaches in what follows.

Before we actually discuss RG flows of non-relativistic systems, it is instructive to compare actions which describe the dynamics of relativistic and non-relativistic theories, respectively. For non-relativistic fermions with spin $1/2$, we consider an action consisting of only a one-body part (kinetic term) and a two-body part (interaction term). Whether it is justified to neglect higher n -body interactions depends on the system under consideration and needs to be carefully analyzed. For example, this might be a reasonable approximation for the description of a dilute gas of ultracold atoms. In nuclear physics, on the other hand, it has been found that three-body interactions have to be taken into account to compute accurately ground-state properties of nuclei, see e. g. Refs. [182–184]. In any case, it is sufficient for our purposes to consider the following ansatz for the action in $d + 1$ Euclidean space-time dimensions:

$$\begin{aligned} S[\psi^\dagger, \psi] &= \sum_{\sigma} \int d\tau \int d^d x \psi_{\sigma}^{\dagger}(\tau, \vec{x}) (\partial_{\tau} - \Delta) \psi_{\sigma}(\tau, \vec{x}) \\ &+ \frac{1}{2} \sum_{\sigma, \sigma'} \int d\tau \int d^d x \int d^d y \psi_{\sigma}^{\dagger}(\tau, \vec{x}) \psi_{\sigma'}^{\dagger}(\tau, \vec{y}) U(\vec{x}, \vec{y}) \psi_{\sigma'}(\tau, \vec{y}) \psi_{\sigma}(\tau, \vec{x}), \end{aligned} \quad (149)$$

where Δ denotes the Laplace operator and the indices σ, σ' refer to the spin components of the two-component Grassmann-valued spinor $\psi^T = (\psi_{\uparrow}, \psi_{\downarrow})$. For example, we can think of these two components as two different hyperfine-states of the atoms in ultracold gases. As usual, Hermitian conjugation is defined as $\psi^{\dagger} = (\psi^*)^T$. For convenience, we have set $\hbar = 1$ and $2m = 1$, where m denotes the mass (parameter) of the fermions. The interaction potential is given by the function U . Prominent examples are the Coulomb potential or a contact interaction potential.

Comparing the non-relativistic action (149) with a simple action describing relativistic fermions, see e. g. Eq. (19), we immediately observe that we have an $O(d)$ symmetry in the kinetic term in Eq. (19) owing to Poincaré invariance. In non-relativistic theories, on the other hand, we have Galilei invariance and the (canonical) mass dimension of space- and time-like coordinates is different, see App. A.1 for our conventions. This implies that the dimension of the interaction potential U and the four-fermion coupling in Eq. (19) is also different. On the other hand, both the relativistic as well as the non-relativistic theory are invariant under continuous $U(1)$ transformations. For the non-relativistic case, the symmetry transformations are given by

$$\psi_{\uparrow} \mapsto e^{i\alpha} \psi_{\uparrow}, \quad \psi_{\uparrow}^* \mapsto e^{-i\alpha} \psi_{\uparrow}^*, \quad \psi_{\downarrow} \mapsto e^{i\alpha} \psi_{\downarrow}, \quad \psi_{\downarrow}^* \mapsto e^{-i\alpha} \psi_{\downarrow}^*. \quad (150)$$

This symmetry reflects particle number conservation. The corresponding transformation for the relativistic case is given in Eq. (20).

In the subsequent section we study universality in non-relativistic Fermi gases. To this end, we consider a special choice for the interaction potential, namely a contact interaction. In Sect. 4.2 we then discuss an RG approach to density functional theory (DFT) which gives direct access to the density and opens up the possibility to conveniently resolve inhomogeneities of the ground state of (self-bound) many-body systems, such as nuclei.

4.1 Cold Atomic Quantum Gases

While particles approach the classical limit for high temperatures, their quantum nature becomes important for low temperatures T , where the thermal wavelength $\sim 1/\sqrt{T}$ becomes much larger than the interparticle distance. In the past fifteen years it has become possible to achieve low temperatures in ultracold Fermi gases and study quantum many-body phenomena, such as Bose-Einstein condensation and BCS superfluidity in great detail [185–188]. Different experimental setups can be used to study quantum effects of atomic gases at low temperatures. Here, we shall consider a dilute gas consisting of fermions in two different hyperfine states which interact resonantly. For example, such a situation can be achieved in experiments with ${}^6\text{Li}$ atoms. From now on, we refer to the fermions in the two different hyperfine states as spin-up and spin-down fermions. For simplicity, we shall assume that the number of fermions in these two spin states is identical which implies that the corresponding chemical potentials are identical. However, we would like to point out that spin-polarized Fermi gases have also attracted a lot of attention in the past few years, both from the experimental [3, 4] as well as from the theoretical side, see e. g. Refs. [15, 18, 23, 41].

Let us now discuss the interaction of the fermions in such experiments in more detail. The two-body interaction potential U of two fermions at position \vec{x} and \vec{y} is short-range repulsive and long-range attractive. A prominent and simple example for such a potential is a hard-core square-well potential with range R :

$$U(\vec{x}, \vec{y}) \rightarrow \infty \quad \text{for} \quad 0 \leq |\vec{x} - \vec{y}| \leq R_a, \quad U(\vec{x}, \vec{y}) = -U_0 \quad \text{for} \quad R_a < |\vec{x} - \vec{y}| \leq R,$$

and

$$U(\vec{x}, \vec{y}) = 0 \quad \text{for} \quad |\vec{x} - \vec{y}| > R,$$

where U_0 and R_a are positive constants characterizing the specific type of the atoms. In a situation where the interparticle distance r is much larger than the range R of the interaction (limit of a dilute gas; atom density $n \sim 1/r^3$), the details of the interaction potential U are of no importance and we may simply approximate it by a δ -function:

$$U(\vec{x}, \vec{y}) \approx \bar{\lambda}_\psi \delta^{(d)}(\vec{x} - \vec{y}), \tag{151}$$

where $\bar{\lambda}_\psi$ defines the (bare) four-fermion coupling. Note that only fermions in different hyperfine states can interact via such a potential due to the Pauli exclusion principle. It should be also stressed that our approximation of using a contact interaction potential causes UV divergences. To obtain the "true" effective interaction potential in the limit of a dilute Fermi gas, these divergences have to be removed by, e. g., introducing a UV cutoff $\Lambda \gg n^{1/3} \sim 1/r$. From a phenomenological point of view, this UV cutoff acquires a physical meaning and can be viewed as the *Bohr* radius of the atoms in cold gases. As we shall discuss below, the dynamics of the system can become effectively independent of this parameter, i. e. it is possible to remove this parameter by taking the limit $\Lambda \rightarrow \infty$.

The (dimensionless) renormalized four-fermion coupling λ_ψ can be directly related to an experimentally accessible control parameter, namely the s-wave scattering length a_s of the atoms. This can be readily seen from a study of the $2 \rightarrow 2$ scattering process. To be more specific, one needs to compute the contributions to the T-matrix arising from the $2 \rightarrow 2$ scattering process. These contributions can be summed up analytically and then be related to the s-wave scattering amplitude [189]. The leading order of an expansion of the scattering amplitude in the external momentum (i. e. the relative momentum of the atoms) is constant and defines minus the s-wave scattering length a_s . In the limit of low temperatures $1/\sqrt{T} \gg r$ and low densities $n \sim 1/r^3$, the typical momenta of the atoms are indeed small (low-energy limit) and the wavefunction describing the scattered atoms is therefore mainly dominated by s-wave states. Overall, such

an analysis yields a relation between the dimensionless renormalized four-fermion coupling λ_ψ and the s-wave scattering length a_s :

$$\lambda_\psi = \frac{8\pi\Lambda}{\frac{1}{a_s} - c_s\Lambda}, \quad (152)$$

where Λ denotes the UV cutoff. The constant $c_s > 0$ depends on the employed regularization scheme. For example, we have $c_s = 2/\pi$ for the sharp UV cutoff.

At this point a comment is in order concerning the expansion of the scattering amplitude in the (external) momentum. The coefficient of the quadratic term in this expansion determines the so-called effective range r_e of the interaction potential which allows us to distinguish between narrow and broad Feshbach resonances. While the effective range $|r_e|$ is much larger than R in the vicinity of *narrow* Feshbach resonance,³⁵ we have $r_e \sim R$ close to a *broad* Feshbach resonance. However, we have $a_s \rightarrow \infty$ in both cases. As we shall see below, these two types of Feshbach resonances are associated with two distinct fixed points of the theory.

In experiments, it is possible to tune the scattering length a_s by hand to arbitrarily large values with the aid of an external magnetic field B . In fact, one finds the following relation between a_s and a magnetic field B that couples to the magnetic moment of the fermions [2]:

$$a_s \simeq a_{\text{bg}} \left(1 - \frac{\Delta_W}{B - B_0} \right), \quad (153)$$

where a_{bg} is the (background) scattering length away from the resonance limit and Δ_W defines the width of the resonance; B_0 is the value of the magnetic field at which the resonance occurs. From Eqs. (152) and (153) it follows that the (effective) interaction strength can be tuned to arbitrarily large values by varying the external magnetic field B . The limit of large scattering length $|a_s|$ defines a *universal* regime (unitary regime), provided the range R of the interaction potential as well as the effective range r_e are much smaller than the interparticle distance r :

$$0 \leftarrow \frac{1}{|a_s|} \ll \frac{1}{r} \sim n^{\frac{1}{3}} \ll \frac{1}{r_e} \sim \frac{1}{R}. \quad (154)$$

Here, n is the atom density. Since $r/R \gg 1$ and $r/r_e \gg 1$, the theory depends on only a single parameter, namely the density.³⁶ Thus, the dynamics of the theory is independent of the details of the interaction (potential). For a narrow Feshbach resonance ($r_e > R$), the details of the interaction potential become important and the theory depends on more than one parameter. We shall return to the case of a narrow Feshbach resonance at the end of this section.

From our discussion it becomes already apparent that the s-wave scattering length a_s plays a prominent role in ultracold Fermi gases. Away from the Feshbach resonance for $B > B_0$, where a_s is positive and small, the interaction between the fermions is strongly attractive. Two fermions can form a tight bosonic bound state (bosonic molecule) with a binding energy $E_b \sim 1/a_s^2$. For sufficiently low temperatures and $a_s > 0$, we therefore expect Bose-Einstein condensation which is associated with a spontaneous breakdown of the U(1) symmetry of the theory.³⁷ We shall therefore refer to this regime as the BEC regime.

In the regime where $|a_s|$ is small but $a_s < 0$, the interaction of atoms with opposite spin is weakly attractive. Therefore it is not possible to form tightly bound bosonic molecules. However, pairs of fermions with opposite spin and opposite momenta can form bound states, so-called Cooper pairs, since the Fermi surface is unstable to pairing in this case [34]. These pairs can be viewed as bosonic bound states with a large spatial extent, i. e. they are highly-localized in momentum space. These bound states can also condense at sufficiently low temperatures and form a superfluid macroscopic state. The existence of this superfluid

³⁵ Near a narrow Feshbach resonance we have $r_e < 0$ and $|r_e| > R$.

³⁶ In this case, the scattering amplitude is proportional to i/q , where q denotes the external momenta. Therefore this limit is also known as the *unitary* limit.

³⁷ Note that the interaction between the tightly bound bosonic molecules is effectively repulsive.

state is associated with a broken U(1) symmetry in the ground state of the theory. In the following we refer to this regime as the BCS regime.

At the Feshbach resonance $B = B_0$, i. e. $|a_s| \rightarrow \infty$, we encounter resonant Cooper pairs. The binding energy of these states becomes arbitrarily small and we are left with spatially delocalized bound-states.

Let us now discuss the fixed-point structure of an ultracold Fermi gas in $d = 3$ space dimensions close to a broad Feshbach resonance. To be specific, we consider the following ansatz for the effective action:³⁸

$$\Gamma[\psi^\dagger, \psi] = \int d\tau \int d^3x \left\{ \psi^\dagger \left(Z_\psi^\parallel \partial_\tau - Z_\psi^\perp \Delta - \mu \right) \psi + \frac{1}{2} \bar{\lambda}_\psi (\psi^\dagger \psi) (\psi^\dagger \psi) \right\}, \quad (155)$$

where μ denotes the chemical potential of the fermions. The wave-function renormalizations Z_ψ^\parallel and Z_ψ^\perp are in general different. We would like to stress that we solely consider the continuum limit in this section. This implies that we study the system in the infinite-volume limit. The particle number is then not well-defined but only the (fermion) density.

Ultracold Fermi gases have been studied extensively within the functional RG approach. The phase diagram of symmetric Fermi gases at zero and finite temperature has been studied in Refs. [21, 190–193]; for reviews, see Refs. [27, 194]. The phase transition in a non-relativistic Bose gas (regime with a small positive s-wave scattering length) has been studied in great detail in Refs. [39, 195, 196]. Note that the latter studies have triggered the development of novel techniques to resolve the momentum dependence of correlation functions in non-perturbative RG flows [197–199]. Moreover, spin-polarized Fermi gases have also been studied with Wilsonian-type RG flows [23, 40]. Here, we do not aim at a quantitative study of the phase diagram of ultracold gases. In the spirit of this review, we are rather interested in a simple analysis of the fixed-point structure of the four-fermion coupling λ_ψ . As it will turn out, such an analysis is already sufficient to understand the experimentally observed universality in these systems.

The flow equation for the λ_ψ -coupling can be derived along the same lines as the flow equations for the four-fermion couplings of the NJL model in Sect. 3.1. We only add that in the present case it is convenient to define a generalized field vector $\Phi^T = (\psi^T, \psi^*)$. The regularized propagator matrix (in Φ -space) then reads³⁹

$$\mathcal{P}_k = \begin{pmatrix} 0 & ip_0 - (\vec{p}^2 - \mu) - k^2 r_\psi(\mathcal{Z}) \\ ip_0 + (\vec{p}^2 - \mu) + k^2 r_\psi(\mathcal{Z}) & 0 \end{pmatrix} (2\pi)^4 \delta(p_0 - p'_0) \delta^{(3)}(\vec{p} - \vec{p}')$$

with $\mathcal{Z} = (\vec{p}^2 - \mu)/k^2$. Here, we have chosen a spatial regulator for convenience. A possible choice for the shape function r_ψ is given in Eq. (353). Since it suffices to consider the point-like limit for our purposes, we can set the wave-function renormalizations equal to one. The fluctuation matrix \mathcal{F} can be derived straightforwardly from the action (155). Using the regulator shape function (353), we find the following set of flow equations:

$$\partial_t \lambda_\psi = \lambda_\psi + \frac{8}{6} v_3 l(\tilde{\mu}) \lambda_\psi^2, \quad (156)$$

$$\partial_t \tilde{\mu} = -2\tilde{\mu}, \quad (157)$$

where $v_3 = 1/(8\pi^2)$. The dimensionless four-fermion coupling is defined as $\lambda_\psi = k \bar{\lambda}_\psi$. The dimensionless chemical potential is given by $\tilde{\mu} = \mu/k^2$. Moreover, we have

$$l(\tilde{\mu}) = (1 + \tilde{\mu})^{\frac{3}{2}} \theta(1 + \tilde{\mu}) - (\tilde{\mu} - 1)^{\frac{3}{2}} \theta(\tilde{\mu} - 1). \quad (158)$$

Analogous to our studies of spontaneous symmetry breaking in the NJL model in Sect. 3, the onset of U(1) symmetry breaking in the present case is signaled by the fact that the four-fermion coupling diverges at a finite scale k_{SB} , i. e. $1/\lambda_\psi(k_{\text{SB}}) = 0$. Recall that in experiments the spontaneous breakdown of the U(1) symmetry is associated with a superfluid behavior of the system.

³⁸ Our ansatz follows directly from the action (149) by employing the interaction potential given in Eq. (151).

³⁹ Recall that the mass-dimension of time-like and space-like momenta are different.

Let us now analyze the fixed-point structure of an ultracold Fermi gas. We begin with a study of the UV limit of the theory, i. e. we first consider $k^2 \gg |\mu|$. This limit can be viewed as the "vacuum" limit associated with the two-body scattering problem [21]. The flow equation for the λ_ψ coupling simplifies considerably for $k^2 \gg |\mu|$:

$$\partial_t \lambda_\psi = \lambda_\psi + \frac{8}{6} v_3 \lambda_\psi^2. \quad (159)$$

For the sharp cutoff, this flow equation reads

$$\partial_t \lambda_\psi = \lambda_\psi + 2v_3 \lambda_\psi^2. \quad (160)$$

Independent of the regularization scheme, we find two fixed points. The Gaussian fixed point is IR attractive (UV repulsive), whereas the non-Gaussian fixed point $\lambda_\psi^* < 0$ is IR repulsive (UV attractive). For the regulator function (353), the non-Gaussian fixed point is given by

$$\lambda_\psi^* = -6\pi^2. \quad (161)$$

For the sharp cutoff, on the other hand, we find

$$\lambda_\psi^* = -4\pi^2. \quad (162)$$

From a comparison of these fixed-point values with the relation (152), we conclude that the non-Gaussian fixed point can be identified with the renormalized four-fermion coupling in the limit $a_s \rightarrow \infty$ (for a broad Feshbach resonance). In other words, the *experimentally* observed universal behavior of ultracold Fermi gases in the limit $a_s \rightarrow \infty$ is tightly linked to the existence of the non-Gaussian fixed point λ_ψ^* . This fixed point can be viewed as a quantum critical point since the choice for the initial value λ_ψ^{UV} relative to λ_ψ^* distinguishes between two distinct regimes in the IR limit, namely a strongly interacting superfluid phase and a weakly interacting phase with restored U(1) symmetry. The Gaussian fixed point, on the other hand, can be associated with the limit of a narrow Feshbach resonance, as we shall see below.

In Fig. 10 we show the RG flow of an ultracold Fermi gas in the plane spanned by the dimensionless four-fermion coupling λ_ψ and the dimensionless chemical potential $\tilde{\mu} = \mu/k^2$. The red line depicts the separatrix $\lambda_\psi^{\text{sep.}}(\tilde{\mu})$, which separates a weakly interacting IR regime from a strongly interacting regime associated with spontaneous U(1)-symmetry breaking. By definition, we have $\lambda_\psi^{\text{sep.}}(\tilde{\mu} = 0) = \lambda_\psi^*$. For large positive values of $\tilde{\mu}$, the separatrix tends to zero, $\lambda_\psi^{\text{sep.}}(\tilde{\mu}) \sim \tilde{\mu}^{-1/2}$. On the other hand, it approaches the asymptote $\tilde{\mu} = -1$ for large negative values of λ_ψ .

Let us now discuss the (physical) meaning of the initial value λ_ψ^{UV} at the scale Λ . Choosing $\lambda_\psi^{\text{UV}} < \lambda_\psi^{\text{sep.}}(\tilde{\mu})$, we find that the four-fermion coupling increases rapidly and diverges eventually at a finite scale k_{SB} . This indicates the breakdown of the U(1) symmetry of the ground state, see Fig. 10. From Eq. (152), on the other hand, it follows that

$$\Delta_\psi := \frac{1}{\lambda_\psi^*} - \frac{1}{\lambda_\psi^{\text{UV}}} \sim -\frac{1}{a_s \Lambda}, \quad (163)$$

where we have tacitly assumed that λ_ψ^{UV} is of the order of the fixed-point value λ_ψ^* . Since the s-wave scattering length a_s is directly related to the applied (external) magnetic field B , see Eq. (153), it follows that a variation of λ_ψ^{UV} corresponds to a variation of B . Recall that the latter is an experimentally controllable parameter.

From the action (155) we deduce that a negative chemical potential has a similar effect as a fermion mass. In other words, a negative chemical potential suppresses the fermion propagation and the dynamics of the system is rather governed by bosonic bound states of two fermions. The binding energy of these bosons is twice the chemical potential of the fermions [200]. We conclude that the low-energy limit for $\lambda_\psi^{\text{UV}} < \lambda_\psi^{\text{sep.}}(\tilde{\mu}_{\text{UV}})$ (i. e. positive s-wave scattering length) and $\tilde{\mu}_{\text{UV}} = \mu/\Lambda^2 < 0$ defines a superfluid

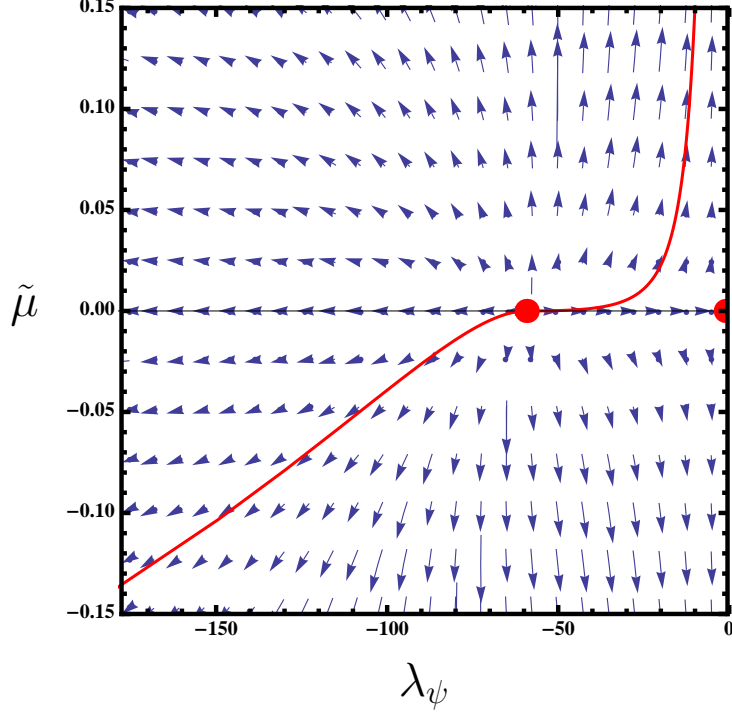


Fig. 10 RG flow of an ultracold Fermi gas in the plane spanned by the four-fermion coupling λ_ψ and the dimensionless chemical potential $\tilde{\mu}$. The red (straight) line depicts the separatrix which separates the regime with a dynamically broken U(1) symmetry in the IR from a weakly interacting IR regime. The dots represent the Gaußian and the non-Gaußian fixed point, respectively. The latter can be viewed as quantum critical point, see main text. The arrows indicate the direction of the RG flow towards the infrared.

phase of bosonic bound states: these bosons macroscopically occupy the ground-state and form a Bose-Einstein condensate.⁴⁰

Now we turn to the limit of infinite s-wave scattering length. Here, the initial condition for the four-fermion coupling is given $\lambda_\psi^{\text{UV}} = \lambda_\psi^*$. From Fig. 10 it follows immediately that condensation can then only occur for $\tilde{\mu} > 0$. For $\mu/\Lambda^2 \ll 1$, we can approximate $l(\tilde{\mu})$ by $l(\tilde{\mu}) \approx 1 + \frac{3}{2}\tilde{\mu}$. This allows us to solve the flow equation for the four-fermion coupling (156) analytically. For $\lambda_\psi^{\text{UV}} = \lambda_\psi^*$ we then find that the symmetry breaking scale k_{SB} is solely determined by the density, as it should be in the universal regime:

$$k_{\text{SB}} \sim \sqrt{\tilde{\mu}} \sim n^{\frac{1}{3}}. \quad (164)$$

Here, we have dropped a scheme-dependent constant of proportionality. As discussed in detail for the NJL model in Sect. 3.2, the scale k_{SB} sets the scale for all low-energy observables, e. g. the fermion gap or the critical temperature. We conclude that all physical low-energy observables are fully determined by our choice for the density n .

Finally we discuss the regime defined by a positive chemical potential and $\lambda_\psi^{\text{UV}} \neq \lambda_\psi^*$. The flow equation for the λ_ψ -coupling can again be solved analytically and assumes a simple form, provided we approximate the function $l(\tilde{\mu})$ by $l(\tilde{\mu}) \approx 1 + 3\sqrt{\tilde{\mu}}$; the limit $\tilde{\mu} = 0$ as well as the limit $\tilde{\mu} \gg 1$ are correctly reproduced by this approximation. The solution for λ_ψ then reads

$$\frac{1}{\lambda_\psi(k)} = \frac{1}{\lambda_\psi^*} - \left(\frac{\Lambda}{k}\right) \Delta_\psi - \frac{1}{2\pi^2} \sqrt{\frac{\mu}{k^2}} \ln\left(\frac{k}{\Lambda}\right). \quad (165)$$

⁴⁰ This is signaled by a finite expectation value of the order-parameter potential.

From this expression we can derive the symmetry breaking scale k_{SB} . For $k_{\text{SB}}/\Lambda \ll 1$, we find

$$k_{\text{SB}} = \Lambda \exp\left(-\frac{2\pi^2 \Lambda \Delta_\psi}{\sqrt{\mu}}\right) \sim \Lambda \exp\left(-\frac{c_{\text{BCS}}}{|a_s| n^{1/3}}\right), \quad (166)$$

where we have used Eq. (163) and $a_s < 0$; c_{BCS} is a positive constant. Thus, k_{SB} scales exponentially in the BCS regime. Moreover, we observe that k_{SB} depends only on the dimensionless quantity $a_s n^{1/3}$. With decreasing $a_s n^{1/3}$, the scale k_{SB} decreases exponentially. As an immediate consequence, we expect that all low-energy observables (fermion gap, phase transition temperature, ...) depend only on the value of $a_s n^{1/3}$ for $a_s < 0$ and change exponentially when $a_s n^{1/3}$ is varied. This was first observed by Bardeen, Cooper and Schrieffer [34] and then further investigated by Gorkov and Melik-Barkhudarov [35]. We stress that k_{SB} does not scale exponentially on the BEC side for increasing $1/(a_s n^{1/3})$. In fact, it is well known that the phase transition temperature of a Bose gas is finite, even in the non-interacting limit.

We would like to point out that the transition from a BCS-type superfluid to a BEC-type superfluid at $1/|a_s| \rightarrow 0$ should not be confused with a quantum phase transition. On the contrary, the U(1) symmetry of the ground state is spontaneously broken in the (deep) IR on both sides of the Feshbach resonance. Thus, the transition from positive to negative s -wave scattering length rather corresponds to a smooth crossover between two phenomenologically different superfluid regimes.

We have seen that the analysis of the fixed point structure and the RG flows in the U(1) symmetric regime already allows us to understand many aspects of ultracold Fermi gases in the limit of a broad Feshbach resonance. Moreover, such an analysis provides insights into the dynamics away from the Feshbach resonance. Let us close this section by discussing the limit of a *narrow* Feshbach resonance. To this end, it is convenient to consider the partially bosonized form of the effective action (155). Following our discussion in Sect. 3.2, this form can be obtained by introducing a complex scalar field $\varphi \sim (\bar{h}_\varphi/\bar{m}_\varphi^2)(\psi_\uparrow\psi_\downarrow)$ into the path integral by means of a Hubbard-Stratonovich transformation. The complex field φ describes the dynamics of the bound states; the prefactors \bar{h}_φ and \bar{m}_φ are *a priori* constants at our disposal and are chosen such that the four-fermion interaction term is canceled, $\bar{\lambda}_\psi = -\bar{h}_\varphi^2/\bar{m}_\varphi^2$, see also Sect. 3.2. Due to the Hubbard-Stratonovich transformation, the (classical) action now includes a Yukawa-type interaction term $\sim \bar{h}_\varphi$ and a mass term \bar{m}_φ for the composite field φ :

$$S = \int d\tau \int d^3x \left\{ \psi^\dagger (\partial_\tau - \Delta - \mu) \psi + \bar{m}_\varphi^2 \varphi^* \varphi - \bar{h}_\varphi [\varphi^* \psi_\uparrow \psi_\downarrow - \varphi \psi_\uparrow^* \psi_\downarrow^*] \right\}. \quad (167)$$

Due to quantum corrections, the Yukawa interaction generates kinetic terms for the bosonic fields in the RG flow,

$$Z_\varphi^{\parallel} \varphi^* \partial_\tau \varphi \quad \text{and} \quad Z_\varphi^\perp \varphi^* \Delta \varphi, \quad (168)$$

even if these terms have been set to zero at the initial RG scale Λ . The (non-trivial) momentum-dependence of the four-fermion vertex is to some extent encoded in these kinetic terms. Close to a narrow Feshbach resonance, the details of the interaction (potential) of the atoms matter. The wave-function renormalizations $Z_\varphi^{\parallel, \perp}$ should then be rather considered as parameters of the theory, which in general assume finite values even at the initial scale Λ , see also below.

In leading order in a derivative expansion, the anomalous dimensions associated with the wave-function renormalizations $Z_\varphi^{\parallel, \perp}$ are essentially given by a purely fermionic 1PI diagram in the U(1) symmetric regime. Thus, we have

$$\eta_\varphi^{\parallel, \perp} = c_\varphi \bar{h}_\varphi^2, \quad (169)$$

where c_φ is a positive constant [27]. Contributions from 1PI diagrams with one internal fermion line and one internal boson line are suppressed in the symmetric regime due to the large (renormalized) boson mass, at least in the limit of a broad Feshbach resonance. For the same reason, the running of the fermionic wave-function renormalizations is subleading. Finally, the RG flow equation of the Yukawa coupling also

assumes a simple form in the symmetric regime, since it is only driven by the anomalous dimensions of the bosonic fields:

$$\partial_t h_\varphi^2 = (\eta_\varphi^\perp - 1) h_\varphi^2, \quad (170)$$

where $h_\varphi^2 = \bar{h}_\varphi^2 / (Z_\varphi^\perp k)$, see Ref. [27]. Note that we are free to choose either Z_φ^\parallel or Z_φ^\perp to renormalize the Yukawa coupling. Since we have $\lambda_\psi \equiv -h_\varphi^2/m_\varphi^2$, we conclude that a non-trivial fixed-point of the four-fermion coupling λ_ψ requires that $\eta_\varphi^\perp = 1$. From Eq. (169) it is then clear that $(h_\varphi^*)^2 > 0$.

In our study of the NJL model with one species in Sect. 3.2, we have also found that the Yukawa coupling is only driven by the anomalous dimensions of the bosonic fields.⁴¹ However, the Yukawa coupling is marginal in the NJL model in $d = 4$ space-time dimensions. Strictly speaking, the non-trivial fixed-point of the four-fermion coupling in the NJL model in $d = 4$ is an artifact of our point-like approximation and is only there for a finite UV cutoff Λ . In the present case of a non-relativistic theory, the non-trivial four-fermion fixed-point also exists in the limit $\Lambda \rightarrow \infty$ beyond the point-like approximation. In this respect, our non-relativistic model should be rather compared to an NJL model with one fermion species in $d = 3$ space-time dimensions, where the Yukawa coupling is also a relevant coupling. We shall come back to this when we discuss the partially bosonized form of the Gross-Neveu model in $d = 3$ space-time dimensions in Sect. 5.1.3.

For the NJL model we have shown in Eq. (82) that the partially bosonized form of the action allows us to conveniently resolve momentum dependences of four-fermion vertices. A corresponding expression can be derived for the present non-relativistic theory. In any case, we conclude that the Gaussian fixed point of the four-fermion coupling $\lambda_\psi \sim h_\varphi^2/m_\varphi^2$ is associated with the Gaussian fixed-point of the Yukawa coupling h_φ . Since $\bar{\lambda}_\psi \sim a_s$, it also follows that the width of the resonance is directly related to the value of the Yukawa coupling at the initial RG scale, see Eq. (153). The narrow resonance limit is therefore approached with $\bar{h}_\varphi^2 \rightarrow 0$, corresponding to the Gaussian fixed-point of the four-fermion coupling.

As discussed above, *universality* in the limit of a broad Feshbach resonance means that the RG flow is governed by the non-trivial fixed-point. In the partially bosonized formulation of the action (155), this is the case, if the initial Yukawa coupling $(\bar{h}_\varphi^{\text{UV}})^2$ is chosen to be reasonably close to the fixed-point $(h_\varphi^*)^2 \Lambda$. Close to the Gaussian fixed-point, the theory can be treated perturbatively [200]. However, the details of the underlying interaction potential (e. g. the effective range r_e) now become important. These are encoded in the momentum dependence of the four-fermion vertex. Therefore we expect that a description of an ultracold Fermi gas close to the narrow Feshbach resonance in general depends on more than one parameter. For a detailed discussion of this fixed point, we refer the reader to Ref. [21].

Up to this point, we have mainly discussed the (UV) fixed-point structure of a non-relativistic Fermi gas. Although such a study already provides us with important information about the properties of the theory, the phenomenologically relevant IR observables are not accessible. For a consideration in the continuum limit, a derivative expansion of the partially bosonized action allows us to conveniently gain access to IR observables [21, 27, 190, 192–194]. However, a derivative expansion becomes inefficient when we are interested in, e. g., density profiles of finite systems. In the next section, we discuss an RG approach which treats the density as an effective degree of freedom and therefore provides an alternative approach for a study of inhomogeneities of the ground state of strongly interacting fermionic theories.

⁴¹ Recall that the partially bosonized version of our NJL model with one fermion species can be rewritten in terms of a complex scalar field $\varphi = (\phi_1 + i\phi_2)/\sqrt{2}$. The associated Yukawa interaction term in Eq. (57) is then given by $\sim \bar{h}_\sigma [\varphi \bar{\psi}_R \psi_L - \varphi^* \bar{\psi}_L \psi_R]$, where the left- and right-handed fermions are defined as $\psi_{L,R} = (\mathbb{1} \pm \gamma_5)\psi$. This reformulation of the Yukawa interaction term in the NJL model with one fermion species is clearly reminiscent of the Yukawa interaction given in Eq. (167). Note that the mass dimension of the Yukawa coupling in relativistic and non-relativistic theories in $d = 4$ space-time dimension is different, see also App. A.1.

4.2 Excursion: Density Functional Theory and the Renormalization Group

In general, the ground-state density of a given finite many-body problem is inhomogeneous, even in the case of a non-interacting system. For example, the ground-state density $n_{\text{gs}}(\vec{x})$ of N fermions in a harmonic oscillator potential is clearly not uniform: it varies rapidly for $|\vec{x}| \lesssim \ell_{\text{HO}} \sim 1/\sqrt{\omega}$ and approaches zero exponentially for $|\vec{x}| \gg \ell_{\text{HO}}$, where ω is the oscillator frequency and ℓ_{HO} denotes the length scale set by the oscillator potential. For increasing N the effective extent of the ground-state wave-function increases and inhomogeneities of the ground-state density are washed out. In the limit $N \rightarrow \infty$, we effectively approach the continuum limit and the density becomes uniform.

We emphasize that it depends on the details of the theory under consideration, whether the continuum limit is approached rapidly for increasing particle number N , see e. g. Refs. [41, 201–203] for explicit studies of this issue. However, the ground-state of a theory might also be inhomogeneous in the continuum limit. For example, this can be the case in a (weakly) interacting theory if the chemical potentials of the spin-up and the spin-down fermions are different. It was shown by Fulde and Ferrell and independently by Larkin and Ovchinnikov that only Cooper pairs with a finite center-of-mass momentum can be formed if the difference in the chemical potentials is large [204]. The finite center-of-mass momentum then renders the ground state inhomogeneous. We would like to point out that the existence of inhomogeneous phases is not bound to non-relativistic systems, a stable inhomogeneous ground state can also occur in relativistic theories. This has been explicitly shown for the high-density phase of the Gross-Neveu model in $d = 1+1$ space-time dimensions [42].

In the following we are particularly interested in strongly-interacting many-body systems away from the continuum limit. In particular, we aim at a study of a finite system of fermions interacting via a non-local interaction which is repulsive at short range and attractive at long range. Prominent examples for such systems are nuclei, but also ultracold trapped Fermi gases fall into this class of systems. Indeed, the density profiles of protons and neutrons in (heavy) nuclei are reminiscent of the density profiles of the spin-up and spin-down fermions in spin-polarized Fermi gases. In order to study the ground-state properties of such systems, density functional theory (DFT) has proven to be useful.

Let us begin with a brief discussion of the underlying principles of DFT. To this end, we consider the following action:

$$S[\psi^\dagger, \psi] = \sum_{\sigma} \int d\tau \int d^d x \psi_{\sigma}^{\dagger}(\tau, \vec{x}) [\partial_{\tau} - \Delta + V(\vec{x})] \psi_{\sigma}(\tau, \vec{x}) + \frac{1}{2} \sum_{\sigma, \sigma'} \int d\tau \int d^d x \int d^d y \psi_{\sigma}^{\dagger}(\tau, \vec{x}) \psi_{\sigma'}^{\dagger}(\tau, \vec{y}) U(\vec{x}, \vec{y}) \psi_{\sigma'}(\tau, \vec{y}) \psi_{\sigma}(\tau, \vec{x}), \quad (171)$$

where $V(\vec{x})$ is a (background) potential. DFT is based on the famous *Hohenberg-Kohn theorem* [205]. For a given interaction potential U , this theorem states that there exists a one-to-one correspondence between the ground-state density and the potential $V(\vec{x})$ (up to an additive constant), at least for non-degenerate ground states. This implies that the ground-state density (uniquely) determines the ground-state wave-function of the N -body problem under consideration. The latter can therefore be considered as a functional of the ground-state density. Moreover, the expectation value of any physical observable is determined by a unique functional of the ground-state density. In particular, this is true for the ground-state energy of the system and implies the existence of an energy density functional $E[n]$. Following the *Rayleigh-Ritz theorem*, the ground-state energy $n_{\text{gs}}(\vec{x})$ can then be obtained by minimizing $E[n]$ with respect to the density:

$$E_{\text{gs}} = \min_n E[n]. \quad (172)$$

Moreover, it can be shown that the energy density functional in the limit of vanishing external potential V , the so-called *Hohenberg-Kohn functional* E_{HK} , is *universal* for a given interaction potential U :

$$E_{\text{HK}}[n] = E[n] - \int d^d x n(\vec{x}) V(\vec{x}). \quad (173)$$

These considerations can be generalized to the case of degenerate ground states.⁴²

Originally, DFT has been invented to compute efficiently ground-state energies of atoms. In recent years, however, DFT has also been successfully employed in condensed-matter physics and for studies of ground-state properties of (heavy) nuclei [63–65]. For reviews and introductions to DFT approaches in nuclear physics, we refer the reader to Refs. [206, 207]. At this point we would like to highlight an important difference between DFT studies of atoms and nuclei. In studies of the ground-state energy of atoms, the center-of-mass momentum of the system is essentially carried by the nucleus. This allows us to easily subtract the center-of-mass energy of the system. The electrons in the atomic shell can then essentially be considered as an electron gas with vanishing center-of-mass motion in an external Coulomb potential. In studies of ground-state properties of nuclei, however, the center-of-mass energy cannot be simply subtracted since the constituents, namely the protons and neutrons, have almost identical masses. Therefore an accurate computation of ground-state energies (binding energies) of nuclei is generically spoiled by the finite center-of-mass energy of the system. Fortunately, these contributions become smaller when the number of nucleons increases. Nonetheless, a systematic computation of the corrections to the ground-state energies of nuclei due to the center-of-mass motion of the system is inherently difficult [208, 209].

The Hohenberg-Kohn theorem can be viewed as a starting point for an efficient description of many-body problems. However, the theorem does not provide a recipe for the computation of the Hohenberg-Kohn functional. Similar to the effective action in conventional quantum field theory, the Hohenberg-Kohn functional consists of infinitely many terms.⁴³ Therefore it is in general not possible to write down the exact Hohenberg-Kohn functional for a given many-body problem. This implies that an ansatz for this functional is required in order to compute the ground-state energy of a given many-body problem. The simplest approximation to the energy density functional is the so-called local density approximation (LDA). This approximation can be obtained straightforwardly from the density dependence of the ground-state energy $E_{\text{gs}}(n)$ of the associated uniform many-body problem,⁴⁴ where $E_{\text{gs}}(n) = V\epsilon_{\text{gs}}(n)$ ($n = \text{const.}$). The energy-density functional in LDA then corresponds to the coordinate-space integral of $\epsilon_{\text{gs}}(n(\vec{x}))$. It is possible to show that LDA represents the lowest order in a derivative expansion of the exact energy-density functional [210]. Such an approximation might be justified in systems with weakly varying densities,⁴⁵ such as ultracold Fermi gases with a large number of atoms in an isotropic trap [61].

Let us now make contact to the effective action approach to quantum field theories which underlies most of our studies in the present review.⁴⁶ To this end, we consider the following path integral

$$Z[J] = \int \mathcal{D}\psi^\dagger \mathcal{D}\psi e^{-S[\psi^\dagger, \psi] + \sum_\sigma \int_0^\beta d\tau \int d^d x J_\sigma(\tau, \vec{x})(\psi_\sigma^\dagger(\tau, \vec{x})\psi_\sigma(\tau, \vec{x}))} \equiv e^{W[J]}, \quad (174)$$

where the action S is defined in Eq. (171) and, for convenience, we assume that the Euclidean-time direction is compactified. In order to fix the particle number in a study of a finite many-body problem, we have essentially two options: First, one can introduce chemical potentials into the path integral to fix the numbers of the various particle species. Second, one does not include chemical potentials into the path integral but fixes the particle numbers by choosing appropriate boundary conditions for the equations of motion [212]. In the following we shall follow the latter approach to fix the particle number since it turns out to be more convenient for studies of finite many-body problems.

In contrast to the conventional textbook approach to quantum field theories, we have coupled the external source J in Eq. (174) to a term which is bilinear in the fermion fields and can be viewed as a composite

⁴² Here, we leave aside a discussion of the issue of V -representability.

⁴³ As we shall see below, the Hohenberg-Kohn functional is indeed closely related to the effective action.

⁴⁴ For example, LDA requires the knowledge of the ground-state energy of a uniform electron gas when we are interested in a computation of the ground-state energies of atoms. We add that the computation of ground-state energies of uniform systems is already a highly non-trivial problem.

⁴⁵ We stress that LDA should by no means be confused with the so-called local potential approximation (LPA) which represents the lowest order in an expansion of the effective action in derivatives of the fields.

⁴⁶ For conciseness, we shall skip many details in the following. For reviews and introductions on this subject matter, we refer the reader to, e. g., Refs. [206, 207, 211].

bosonic degree of freedom. As usual, we may define the classical field $\rho_\sigma(\tau, \vec{x})$ as the (functional) derivative of $W[J]$ with respect to the corresponding source $J_\sigma(\tau, \vec{x})$:

$$\rho_\sigma(\tau, \vec{x}) = \frac{\delta W[J]}{\delta J_\sigma(\tau, \vec{x})}. \quad (175)$$

Apparently, these classical fields are related to the particle densities. Similar to the derivation of the 1PI effective action, we can now define a 2PPI effective action as follows:⁴⁷

$$\Gamma[\rho] = \sup_{\{J_\sigma\}} \left\{ -W[J] + \sum_\sigma \int_0^\beta d\tau \int d^d x J_\sigma(\tau, \vec{x}) \rho_\sigma(\tau, \vec{x}) \right\}. \quad (176)$$

The effective action $\Gamma[\rho]$ determines the dynamics of the many-body problem under consideration and should be compared with the energy-density functional mentioned above in the context of the standard Hohenberg-Kohn DFT formalism. The exact equivalent of the energy density functional as introduced by Hohenberg and Kohn can be derived along these lines by employing time-independent sources $J_\sigma(\vec{x})$, see Refs. [212–215].

As in the conventional 1PI formalism, the effective action $\Gamma[\rho]$ does not depend on the sources J_σ , i. e. $(\delta\Gamma[\rho]/\delta J_\sigma) = 0$. Let us now consider the first functional derivative of $\Gamma[\rho]$ with respect to the classical field ρ_σ :

$$\frac{\delta\Gamma[\rho]}{\delta\rho_\sigma(\tau, \vec{x})} = J_\sigma(\tau, \vec{x}). \quad (177)$$

The ground-state configuration $\rho_{\sigma, \text{gs}}$ is determined by this equation in the limit $J_\sigma \rightarrow 0$. We add that this equation can be also viewed as the equation of motion of the composite degree of freedom ρ_σ . From the solutions $\rho_{\sigma, \text{gs}}(\tau, \vec{x})$ of Eq. (177), we obtain the (time-independent) ground-state density $n_{\text{gs}}(\vec{x})$:

$$n_{\text{gs}}(\vec{x}) = \frac{1}{\beta} \int_0^\beta d\tau \rho_{\text{gs}}(\tau, \vec{x}). \quad (178)$$

The ground-state energy E_{gs} can be obtained from an evaluation of the effective action $\Gamma[\rho]$ at the ground-state ρ_{gs} :

$$E_{\text{gs}} = \lim_{\beta \rightarrow \infty} \frac{1}{\beta} \Gamma[\rho_{\text{gs}}]. \quad (179)$$

We would like to add that the *universality* of the Hohenberg-Kohn functional E_{HK} can be easily proven in the effective action approach [216]. It follows from the fact that background potential can be absorbed into source term J_σ by a simple shift, $J_\sigma \rightarrow J_\sigma + V$. Exploiting this observation, we find

$$\Gamma[\rho] = \Gamma_{\text{HK}}[\rho] + \sum_\sigma \int_0^\beta d\tau \int d^d x V(\vec{x}) \rho_\sigma(\tau, \vec{x}), \quad (180)$$

where $\Gamma_{\text{HK}}[\rho] = \Gamma_{V=0}[\rho]$. Thus, the functional $\Gamma_{\text{HK}}[\rho]$ depends only on our choice for the interaction potential but not on the background potential V .

As mentioned above, the computation of the effective action $\Gamma[\rho]$ for a given theory can be inherently difficult. Following Refs. [215–217], we now present an RG flow equation which allows for a systematic computation of the density functional $\Gamma[\rho]$. Since this equation can be essentially derived along the lines of the Wetterich equation (see Sect. 2), we shall be brief here. To keep our discussion as simple as possible, we consider a system of N spinless fermions. However, the derivation of the flow equation is not bound

⁴⁷ Here, “2PPI” stands for “two-particle point-irreducible”. A 2PPI diagram is a 1PI diagram that cannot be split into two by cutting two internal lines attached to the same vertex. To put it sloppily, this type of effective actions arises generically from the path-integral when one couples a local source term to a term bilinear in the fields. For a more general discussion of the properties of 2PPI effective actions and RG flow equations thereof, we refer the reader to Ref. [104].

to such a theory but can be straightforwardly generalized to other non-relativistic theories [216]. To be specific, we consider an action of the following form:

$$S_\gamma[\psi^*, \psi] = \int_0^\beta d\tau \int d^d x \psi^*(\tau, \vec{x}) [\partial_\tau - \Delta + V_\gamma(\vec{x})] \psi(\tau, \vec{x}) \\ + \frac{\gamma}{2} \int_0^\beta d\tau \int d^d x \int_0^\beta d\tau' \int d^d x' \psi^*(\tau, \vec{x}) \psi(\tau, \vec{x}) U(\tau, \tau'; \vec{x}, \vec{x}') \psi^*(\tau', \vec{x}') \psi(\tau', \vec{x}').$$

For convenience, we have reordered the fermion fields in the second term compared to Eq. (171). The parameter $\gamma \in [0, 1]$ denotes a dimensionless control parameter. For $\gamma = 0$, the two-body interaction potential U is turned off and we are left with an exactly soluble problem. For $\gamma = 1$, the potential U is fully turned on. We shall assume that the interaction potential U is attractive at long range and repulsive at short range, such that the system can potentially be self-bound for $V_\gamma \rightarrow 0$. In particular, we shall assume that the Fourier transform of the interaction potential U falls off sufficiently rapidly for large momenta to avoid the occurrence of UV divergences. Examples for such a two-body potential are nucleon-nucleon interaction potentials. The one-body potential V_γ is at our disposal. However, it needs to be chosen such that the N -body system has a finite extent ℓ_V for $\gamma = 0$, where the interaction term vanishes identically. This length scale ℓ_V sets a momentum scale $1/\ell_V$ which screens (potentially existing) IR divergences. Moreover, our choice for V_γ partially defines the many-body problem under consideration. For a study of ground-state properties of nuclei, one may choose $V_\gamma = \frac{1}{4}(1-\gamma)\omega^2 \vec{x}^2$ where ω is the oscillator frequency, see Ref. [216]. For a study of trapped Fermi gases, on the other hand, one may choose a γ -independent potential $V_\gamma = \frac{1}{4}\omega^2 \vec{x}^2$. (Note that we have set $2m = 1$ in our conventions.)

Now it is straightforward to derive the effective action $\Gamma_\gamma[n]$ associated with the (classical) action S_γ . By taking the derivative of $\Gamma_\gamma[\rho]$ with respect to γ we find the following flow equation [216, 217]:

$$\partial_\gamma \Gamma_\gamma[\rho] = (\partial_\gamma V_\gamma) \cdot \rho + \frac{1}{2} \rho \cdot U \cdot \rho + \frac{1}{2} \text{Tr} U \cdot \left(\frac{\delta^2 \Gamma[\rho]}{\delta \rho \delta \rho} \right)^{-1}, \quad (181)$$

where the dot indicates a product in Euclidean space-time, i. e.

$$A \cdot B \equiv \int_0^\beta d\tau \int d^d x A(\tau, \vec{x}) B(\tau, \vec{x}). \quad (182)$$

This flow equation governs the flow from the non-interacting system at $\gamma = 0$ to the (strongly) interacting system at $\gamma = 1$. In the terminology of many-body physics, the second term can be identified as the so-called Hartree term. The third term on the right-hand side depends on the density-density correlator $\delta^2 \Gamma[\rho]/(\delta \rho \delta \rho)$ and includes all higher order corrections to the effective action, e. g. the so-called Fock term.

Note that the derivation of the flow equation (181) does not require that the (effective) interaction strength is small. Moreover, this flow equation does not rely on an approximation scheme, such as a gradient expansion. In fact, the flow equation (181) is exact, if we only allow for a two-body interaction potential in the underlying action S_γ . A generalization of this flow equation to include the effects of higher n -body operators is straightforward. In any case, it is in general not possible to solve the flow equation (181) exactly. Therefore, a systematic approximation scheme is required, such as an expansion of the effective action $\Gamma_\gamma[\rho]$ about the ground state ρ_{gs} . This would correspond to a vertex expansion in the terminology of quantum field theory.

In order to obtain the initial condition of the flow equation (181) at $\gamma = 0$ for a given many-body problem, we need to solve the non-interacting N -body problem defined by the action S_γ evaluated at $\gamma = 0$. The effective action $\Gamma_{\gamma=0}[\rho]$ associated with this exactly soluble N -body problem then determines the initial condition of the RG flow. For illustration, let us assume that we would like to compute the ground-state energies of so-called Alexandrou-Negele nuclei [218], i. e. self-bound systems in $d = 1+1$ Euclidean space-time dimensions consisting of N spinless fermions interacting via a specific choice for a

long-range attractive and short-range repulsive potential U . A convenient and appropriate choice for the background potential V is then a harmonic oscillator potential [216]: $V_\gamma(\vec{x}) = (1/4)(1 - \gamma)\omega^2 x^2$. Thus, the initial condition at $\gamma = 0$ corresponds to a simple oscillator potential in which the N lowest lying states are filled. In other words, the initial condition is simply given by a one-dimensional shell model (“mean-field” approximation). By lowering the control parameter γ , i. e. by solving the flow equation (181), we gradually remove the background potential V and turn on the interaction potential U . In the spirit of the RG, removing the background potential corresponds to lowering the RG scale which is given by the inverse of the γ -dependent oscillator length $\ell_{\text{HO}} \sim ((1-\gamma)^{\frac{1}{4}}\omega^{\frac{1}{2}})^{-1}$. For $\gamma \rightarrow 1$, the background-potential is removed and we are left with the fully interacting system. A quantitative study of Alexandrou-Negele nuclei with the presented RG approach to DFT is on its way [217]; preliminary results have been presented in Refs. [219, 220].

Let us close this section by stating that the presented RG approach to DFT is promising for a study of finite many-body problems since an expansion of the theory in terms of the density scales favorably to large systems, i. e. systems with many constituents. Since the presented RG-inspired approach allows for an ab-initio calculation of ground-state properties of strongly interacting many-body systems, it might be promising tool for studies of ground-state properties of (heavy) nuclei from microscopic interactions.

5 Gross-Neveu and Nambu-Jona-Lasinio-type Models

In this section we apply the techniques discussed and developed in Sect. 3 to specific examples of relativistic quantum field theories, namely the Gross-Neveu model and QCD low-energy models. While Gross-Neveu-type models play a prominent role in the description of (ferromagnetic) superconductors, QCD low-energy models aim to describe the equation of state of hadronic matter under extreme conditions. Recently, the Gross-Neveu model in two space-time dimensions has attracted a lot of attention in the high-energy physics community, since its finite-temperature phase diagram can be computed analytically in the limit of many fermion flavors and shows an intriguing phase structure exhibiting inhomogeneous phases at high densities [42]. Whether such phases also exist as stable ground states beyond this limit is still not clear. Since relatives of the Gross-Neveu model, namely Nambu-Jona-Lasinio-type models, underlie the construction of QCD low-energy models, it is tempting to speculate whether such inhomogeneous phases are also present in the phase diagram of 3+1-dimensional field theories, such as QCD [44, 45]. Even though these are certainly interesting questions, we shall restrict ourselves in the following to much simpler issues which arise in studies of Gross-Neveu models and QCD low-energy models.

After a brief discussion of the Gross-Neveu model and its symmetries in Sect. 5.1.1, we study the fixed-point structure of its purely fermionic formulation in Sect. 5.1.2. The partially bosonized formulation and quantum critical behavior are then analyzed in detail in Sect. 5.1.3 in the large- N_f limit and in Sect. 5.1.4 in next-to-leading order in the $1/N_f$ -expansion. In addition to a discussion of quantum criticality, we highlight the differences between the derivative expansion and the $1/N_f$ -expansion of the effective action. We shall keep our discussion as general as possible. However, explicit numerical solutions are presented only for the 2+1-dimensional case, if not stated otherwise. As a bonus, we relate quantum criticality to the issue of non-perturbative renormalizability of quantum field theories in Sect. 5.1.5.

In Sect. 5.2 we study aspects of QCD low-energy models in $d = 3 + 1$ space-time dimensions. To this end, we begin in Sect. 5.2.1 with a discussion of the Fierz ambiguity in QCD low-energy models and study the fixed-point structure of a Fierz-complete low-energy model in the limit of many colors, the so-called large- N_c limit. This limit corresponds to the limit of many-flavors in the Gross-Neveu model. Quantum and thermal phase transitions in low-energy QCD models are then discussed in Sect. 5.2.2, where we mainly focus on the large- N_c limit. In addition, we comment on the widely used so-called local potential approximation (LPA) and its relation to the $1/N_c$ -expansion. This includes a discussion of the effects of the next-to-leading order corrections in a $1/N_c$ -expansion.

In addition to the discussion of physical aspects of the Gross-Neveu model and QCD low-energy models, our goal is to highlight the field-theoretical differences and the similarities in the description of these models. The latter allow for a cross-fertilization of QCD and condensed-matter physics.

5.1 Gross-Neveu Model and Quantum Criticality

5.1.1 Gross-Neveu Model

The Gross-Neveu model represents a quantum field theory of N_f massless (relativistic) fermion flavors in d space-time dimensions which allows to study dynamical chiral symmetry breaking. This model is related to the Peierls-Froehlich model and models for ferromagnetic (relativistic) superconductors, see e. g. Refs. [72, 73]. Moreover, the Gross-Neveu model has attracted a lot of attention in high-energy physics, since the finite-temperature phase boundary in $d = 2$ can be studied analytically, at least in the limit of many flavors, see e. g. Ref. [42].

The classical action of the Gross-Neveu model reads

$$S_{\text{GN}}[\bar{\psi}, \psi] = \int d^d x \left\{ \bar{\psi} i \not{\partial} \psi + \frac{1}{2} \bar{\lambda}_\sigma (\bar{\psi} \psi)^2 \right\}, \quad (183)$$

where $(\bar{\psi} \psi) \equiv \bar{\psi}_i \psi_i$ and $i = 1, \dots, N_f$. The model depends on a single parameter which is the coupling constant $\bar{\lambda}_\sigma$ with mass dimension $2 - d$. In $d = 2$, the model is asymptotically free and perturbatively renormalizable, as the Gaußian fixed point is UV attractive. In this respect the Gross-Neveu model is reminiscent of QCD. On the other hand, $d = 4$ turns out to be a marginal case, see our discussion of the NJL model in Sect. 3.2. In the following we shall restrict ourselves mainly to the case $d = 3$ for which we shall employ a four-component (reducible) representation for the Dirac γ -matrices, $\gamma_\mu = \{\gamma_0, \gamma_1, \gamma_2\}$, see App. B for our conventions.

The action of the Gross-Neveu model is invariant under global $U(N_f)$ transformations of the fermion fields. This implies that the model is invariant under $U(1)^{\otimes N_f}$ transformations, i.e. the associated $U(1)$ -charge is conserved in each flavor-sector separately. The matrix $\gamma_{35} = i\gamma_3\gamma_5$ further realizes a $U^{35}(1)$ symmetry in each flavor sector:

$$\bar{\psi}_j \mapsto \bar{\psi}_j e^{-i\alpha\gamma_{35}}, \quad \psi_j \mapsto e^{i\alpha\gamma_{35}} \psi_j, \quad (184)$$

where α denotes the ‘‘rotation’’ angle. In addition to these two symmetries, the Gross-Neveu model is invariant under discrete $\mathbb{Z}_2^5 = \{\mathbb{1}_4, \gamma_5\}$ chiral transformations acting on all flavors simultaneously:

$$\bar{\psi} \mapsto -\bar{\psi}\gamma_5, \quad \psi \mapsto \gamma_5\psi. \quad (185)$$

Note that a similar symmetry transformation involving γ_3 can be understood as a combination of \mathbb{Z}_2^5 and $U^{35}(1)$ transformations.

In Sect. 5.1.3 we shall see that the chiral symmetry of the Gross-Neveu model can be associated with a \mathbb{Z}_2 symmetry for the order parameter. As we shall also discuss below, the infrared regime of the theory is governed by dynamical chiral symmetry breaking, provided the *only* parameter of the model, namely $\bar{\lambda}_\sigma$, is adjusted accordingly.

5.1.2 Fermionic Formulation

Let us start with an analysis of the fermionic fixed-point structure of the Gross-Neveu model. To this end, we consider only a point-like four-fermion interaction. Our ansatz for the effective action then reads

$$\Gamma_{\text{GN}}[\bar{\psi}, \psi] = \int d^d x \left\{ Z_\psi \bar{\psi} i \not{\partial} \psi + \frac{1}{2} \bar{\lambda}_\sigma (\bar{\psi} \psi)^2 \right\}. \quad (186)$$

As we have discussed in detail in Sect. 3, this ansatz can be viewed as a derivative expansion of the effective action, with the leading-order defined by a constant Z_ψ . A running wave-function renormalization then

corresponds to the next-to-leading order approximation. Aside from derivatives, further fermion interaction channels and higher-order interactions compatible with the symmetries can be taken into account. Recall that Z_ψ is indeed constant when we treat the four-fermion interaction in the point-like limit, see discussion of Eq. (41). Thus, we set $Z_\psi \equiv 1$ in the following.

The RG flow equation for the four-fermion coupling can be derived along the lines of Sect. 3.1. We find

$$\partial_t \lambda_\sigma = (d-2)\lambda_\sigma - 4(N_f d_\gamma - 2)v_d l_1^{(F),(d)}(0;0) \lambda_\sigma^2, \quad (187)$$

where

$$\lambda_\sigma = k^{d-2} \bar{\lambda}_\sigma, \quad (188)$$

and $d_\gamma = 4$ denotes the dimension of the Dirac algebra. For the sake of simplicity, we have dropped contributions from further (possibly fluctuation-induced) interaction channels as well as dependences on the Fierz basis, see discussion in Sect. 3.1 and Refs. [76, 77, 140]. Nevertheless, we expect this to be a reasonable approximation for two reasons: first, we find that the considered scalar interaction channel does not generate other interaction channels.⁴⁸ Second, we are particularly interested in a study of the Gross-Neveu model in the large- N_f limit which we consider as a controlled starting point for the construction of an effective (low-energy) theory for this model. This means we assume that a pure Gross-Neveu-type RG trajectory exists in the large- N_f limit, i. e. a trajectory on which only the λ_σ -coupling is finite but all other four-fermion couplings are identical to zero. In Sect. 3.5.2 we have shown that a fermionic model with similar symmetry properties as the Gross-Neveu model indeed exhibits a trajectory which corresponds to a pure Gross-Neveu-type trajectory in our present study. However, further studies are needed to confirm the existence of such a trajectory in the Gross-Neveu model.

Apart from a Gaussian fixed point, we find a second non-trivial fixed point for the coupling λ_σ which is given by

$$\lambda_\sigma^* = \frac{d-2}{4(N_f d_\gamma - 2)v_d l_1^{(F),(d)}(0;0)}. \quad (189)$$

For the optimized regulator function defined in Eq. (349) we find

$$\lambda_\sigma^* = \frac{d(d-2)}{8(N_f d_\gamma - 2)v_d} \stackrel{(d=3)}{=} \frac{3\pi^2}{(4N_f - 2)}.$$

Recall that the fixed-point value is a non-universal quantity as indicated by the regulator dependence. Nevertheless, the mere existence of the fixed point is a universal statement.

For a sketch of $\partial_t \lambda_\sigma$ as a function of λ_σ we refer to Fig. 2. As discussed in detail in Sect. 3, the choice for the initial condition $\lambda_\sigma^{\text{UV}}$ relative to the fixed-point λ_σ^* distinguishes between two different phases in the long-range limit: for $\lambda_\sigma^{\text{UV}} < \lambda_\sigma^*$, we approach a trivial phase in the IR limit, whereas we run into a phase with broken chiral symmetry in the ground state for $\lambda_\sigma^{\text{UV}} > \lambda_\sigma^*$. Thus, the fixed-point λ_σ^* can be considered as a quantum critical point which divides the model into two physically different regimes.

The scale for a given IR observable \mathcal{O} is set by the scale k_{SB} at which $1/\lambda_\sigma(k_{\text{SB}}) \rightarrow 0$. In our study of power-law scaling in Sect. 3.4.1, we have discussed how this scale can be obtained from the flow equation of the four-fermion coupling. We proceed along these lines to compute k_{SB} . From the flow equation (187) we then find

$$k_{\text{SB}} = \Lambda \theta (\lambda_\sigma^{\text{UV}} - \lambda_\sigma^*) \left(\frac{\lambda_\sigma^{\text{UV}} - \lambda_\sigma^*}{\lambda_\sigma^{\text{UV}}} \right)^{\frac{1}{|\Theta|}}, \quad (190)$$

where the critical exponent Θ is given by

$$\Theta = - \left. \frac{\partial(\partial_t \lambda_\sigma)}{\partial \lambda_\sigma} \right|_{\lambda_\sigma^*} = d-2. \quad (191)$$

⁴⁸ Note that this does not mean that the ansatz (186) is closed with respect to Fierz transformations. In fact, other four-fermion interactions compatible with the symmetries may generate contributions to the flow of the coupling λ_σ .

Thus, relation (190) determines how a given physical IR observable scales when $\lambda_\sigma^{\text{UV}}$ is varied. In particular, we observe that the exponent Θ governing the scaling behavior does not depend on N_f in the present approximation.

Let us conclude with a word of caution concerning the derivative expansion in the fermionic truncation. In this simple approximation, the fixed point seems to exist with similar properties in any dimension $d > 2$, in particular also in $d = 4$ and beyond. This conclusion changes when composite bosonic degrees of freedom are taken into account in the subsequent section. In the purely fermionic description, the bosonic degrees of freedom correspond to specific nonlocal interactions or momentum-structures in the fermionic vertices. These are not properly resolved in a derivative expansion. As $d = 4$ is a marginal case, the conclusions for fermionic theories in $d = 4$ may depend on the details of the interaction and the algebraic structure of a given model.

5.1.3 Partial Bosonization and the Large- N_f Limit

We now study the fixed-point structure of the Gross-Neveu model by employing its (partially) bosonized version. We follow closely our discussion of (partial) bosonization in Sect. 3.2 We relate our findings to the purely fermionic description, study the large- N_f limit analytically and show how corrections beyond the mean-field approximation can be systematically taken into account. In particular, we demonstrate how the quantum critical behavior of the model is affected by the inclusion of momentum dependences and corrections beyond the large- N_f limit. Note that the partially bosonized formulation has been used to study various aspects of the Gross-Neveu model, such as the phase structure at zero and finite temperature and density [42, 221, 222].

A partially bosonized description of the Gross-Neveu model is appealing from a field-theoretical point of view as it also forms the basis for an expansion in powers of $1/N_f$. In addition, it allows us to systematically resolve parts of the momentum dependence of the vertices by means of a derivative expansion. As we shall see below, these two expansion schemes are *not* identical and should therefore not be confused with each other. For our study we use the following ansatz for the effective action:

$$\Gamma[\bar{\psi}, \psi, \sigma] = \int d^d x \left\{ \frac{1}{2} Z_\sigma (\partial_\mu \sigma)^2 + Z_\psi \bar{\psi} i \not{\partial} \psi + i \bar{h}_\sigma \bar{\psi} \sigma \psi + \frac{1}{2} \bar{m}_\sigma^2 \sigma^2 + \frac{1}{8} \bar{\omega}_\sigma \sigma^4 \right\}, \quad (192)$$

where we allow all couplings and wave-function renormalizations to be scale dependent. Note that we drop possibly generated higher-order bosonic self-interaction terms for the sake of simplicity. As we have discussed in Sect. 3.2, cf. Eq. (75), the kinetic term of the boson field allows us to go beyond the local approximation of simple mean-field theory. In terms of the fermionic language, this kinetic term corresponds to a specific momentum dependence in the scalar interaction channel of the four-fermion coupling. Thus, it allows us to conveniently resolve (part of) the momentum dependence of the associated four-point function. As we shall see below, this term and the associated wave-function renormalization receive contributions to leading order in the large- N_f approximation. Therefore the large- N_f approximation corresponds to the following choice for the initial conditions of Z_σ and Z_ψ :

$$\lim_{k \rightarrow \Lambda} Z_\sigma = 0, \quad \partial_t Z_\sigma \neq 0, \quad \lim_{k \rightarrow \Lambda} Z_\psi = 1, \quad \partial_t Z_\psi \equiv 0. \quad (193)$$

This choice for the initial conditions exemplifies nicely the difference between large- N_f and derivative expansions, as we include next-to-leading order corrections in terms of a derivative expansion in the bosonic sector but treat the fermionic sector in the leading-order approximation.

As detailed in Sect. 3.2, the choice for the initial conditions allows us to map the partially bosonized action (192) exactly onto the purely fermionic ansatz (186) at the initial RG scale Λ . In fact, we fix the bosonized Yukawa-type model to the fermionic Gross-Neveu model by a suitable choice of initial conditions for Γ at the scale Λ :

$$\lim_{k \rightarrow \Lambda} Z_\sigma = 0, \quad \lim_{k \rightarrow \Lambda} Z_\psi = 1, \quad \lim_{k \rightarrow \Lambda} \bar{\omega}_\sigma = 0. \quad (194)$$

Thus, the renormalized boson mass $m_\sigma = \bar{m}_\sigma/Z_\sigma^{1/2}$ at the UV cutoff Λ becomes much larger than Λ and renders the boson propagator essentially momentum independent. This so-called compositeness condition for the bosonic formulation can be considered as a locality condition at the UV scale for the four-fermion coupling λ_σ in the purely fermionic formulation of the model.

Since we are interested in the quantum critical behavior associated with the fixed-point structure⁴⁹ of the partially bosonized Gross-Neveu model, we anticipate that a possible non-Gaussian fixed point occurs in the symmetric regime. Therefore, we only need to study the RG flow in the symmetric regime with vanishing vacuum expectation value for the σ field. The flow equations for the Yukawa coupling h as well as the anomalous dimensions $\eta_\sigma = -\partial_t \ln Z_\sigma$ and $\eta_\psi = -\partial_t \ln Z_\psi$ read⁵⁰

$$\partial_t h_\sigma^2 = (d - 4 + 2\eta_\psi + \eta_\sigma)h_\sigma^2 + 8v_d h_\sigma^4 l_{1,1}^{(\text{FB}),(\text{d})}(0, \epsilon_\sigma; \eta_\psi, \eta_\sigma), \quad (195)$$

$$\eta_\sigma = 8N_f \frac{d_\gamma v_d}{d} h_\sigma^2 m_4^{(\text{F}),(\text{d})}(0; \eta_\psi), \quad (196)$$

$$\eta_\psi = 8 \frac{v_d}{d} h_\sigma^2 m_{1,2}^{(\text{FB}),(\text{d})}(0, \epsilon_\sigma; \eta_\psi, \eta_\sigma), \quad (197)$$

where $\epsilon_\sigma = \bar{m}_\sigma^2/(Z_\sigma k^2)$, $\omega_\sigma = \bar{\omega}_\sigma/(Z_\sigma^2 k^{(d-4)})$ and $h_\sigma^2 = \bar{h}_\sigma^2/(Z_\sigma Z_\psi^2 k^{(d-4)})$. The definition of the threshold functions can be found in App. D. The RG flow equations of the bosonic self-interactions are given by

$$\partial_t \epsilon_\sigma = (\eta_\sigma - 2)\epsilon_\sigma - 6v_d l_1^{(d)}(\epsilon_\sigma; \eta_\sigma)\omega_\sigma + 4N_f d_\gamma v_d l_1^{(\text{F}),(\text{d})}(0; \eta_\psi)h_\sigma^2, \quad (198)$$

$$\partial_t \omega_\sigma = (d - 4 + 2\eta_\sigma)\omega_\sigma + 18v_d l_2^{(d)}(\epsilon_\sigma; \eta_\sigma)\omega_\sigma^2 - 8N_f d_\gamma v_d l_2^{(\text{F}),(\text{d})}(0; \eta_\psi)h_\sigma^4. \quad (199)$$

From these flow equations we deduce that 1PI diagrams with at least one inner bosonic line do not contribute to the flow of the couplings in the large- N_f limit. As a consequence, η_σ is non-vanishing in leading order in the $1/N_f$ expansion, whereas the fermionic anomalous dimension is zero. We emphasize that the large- N_f counting is very different from that in scalar $O(N)$ models, where the anomalous dimensions are zero to leading order at large N , see e. g. Ref. [225]. This already makes clear that such a large- N expansion should not be confused with the large- N_f expansion in the Gross-Neveu model. In fact, we always have to deal with an $O(1) \simeq Z(2)$ symmetric order-parameter potential in the Gross-Neveu model due to its underlying symmetries.

At this point it is instructive to make contact to expansion schemes employed in the context of high-energy physics. The parameter N_f counting the number of flavors in the Gross-Neveu model should then be compared to the number of colors in QCD. Thus, a large- N_c expansion in QCD (models) corresponds to a large- N_f expansion in the Gross-Neveu model.⁵¹ On the other hand, the number of fermion flavors in QCD is directly related to the number of Nambu-Goldstone modes and therefore to the symmetry properties of the order-parameter potential. In fact, we expect⁵² that QCD falls into the $O(N_f^2)$ universality class [226].

⁴⁹ More precisely, quantum critical behavior in the Gross-Neveu model is associated with the UV fixed-point structure, see also Sect. 5.1.5.

⁵⁰ These flow equations agree with those derived in Refs. [223, 224].

⁵¹ For an analysis of the role of corrections beyond the large- N_c approximation for the thermodynamics of QCD low-energy models we refer to Sect. 5.2 and Ref. [33].

⁵² Note that QCD exhibits a (continuous) chiral $SU(N_f)_L \otimes SU(N_f)_R$ symmetry, in contrast to the Gross-Neveu model, see also Sect. 5.2 and Sect. 6.

Let us now begin with an analysis of the Gross-Neveu model in the large- N_f limit. In this limit, the flow equations simplify considerably:

$$\partial_t \epsilon_\sigma = (\eta_\sigma - 2)\epsilon_\sigma + 4N_f d_\gamma v_d l_1^{(F),(d)}(0; \eta_\psi) h_\sigma^2, \quad (200)$$

$$\partial_t \omega_\sigma = (d - 4 + 2\eta_\sigma)\omega_\sigma - 8N_f d_\gamma v_d l_2^{(F),(d)}(0; \eta_\psi) h_\sigma^4, \quad (201)$$

$$\partial_t h_\sigma^2 = (d - 4 + 2\eta_\psi + \eta_\sigma) h_\sigma^2, \quad (202)$$

$$\eta_\sigma = 8N_f \frac{d_\gamma v_d}{d} h_\sigma^2 m_4^{(F),(d)}(0; \eta_\psi), \quad (203)$$

$$\eta_\psi = 0. \quad (204)$$

Fixed points of the theory can be identified as the zeroes of these β functions. Of course, we have a Gaussian fixed point with all couplings vanishing. As the RG flows for the bosonic couplings decouple in the large- N_f limit, a non-trivial fixed point requires $h_{\sigma,*} \neq 0$. From this it follows that

$$\eta_\sigma^* = 4 - d, \quad (205)$$

independent of the RG scheme. While this close relation between the dimensionality and the bosonic anomalous dimension here is an artifact of the large- N_f expansion, a similar relation exists in gravity for the graviton anomalous dimension at the (interacting) fixed point as a consequence of background gauge invariance [227]. Similar sum rules are known for Yukawa theories with chiral symmetries [76]. Such a sum rule for a corresponding fixed point is also responsible for the universality of the BCS-BEC crossover in the broad resonance limit of ultracold Fermi gases, see Sect. 4.1 and Ref. [190]. In the present case, this rule simply determines the value of the Yukawa fixed-point coupling:

$$(h_\sigma^*)^2 = \frac{1}{N_f} \left(\frac{d}{8d_\gamma v_d} \right) \frac{(4-d)}{m_4^{(F),(d)}(0;0)} = \frac{1}{N_f} \left(\frac{d}{d_\gamma v_d} \right) \frac{(d-4)(d-2)}{(8-6d)}, \quad (206)$$

where we have used the optimized regulator function defined in Eq. (349) to evaluate the threshold function $m_4^{(F),(d)}(0;0)$. Note that the fixed point is interacting for $2 < d < 4$ and merges with the Gaussian fixed point of the Yukawa coupling in $d = 4$, see also Fig. 11. Also the fixed-point values for the bosonic mass parameter and couplings can be given analytically. For the optimized regulator we find

$$\epsilon_\sigma^* = -\frac{8d(d-4)(d-2)}{d_\gamma(8-6d)(2-d)}, \quad \omega_\sigma^* = \frac{1}{N_f} \frac{8d^2(d-4)^2(d-2)^2}{d_\gamma(8-6d)^2(4-d)v_d}. \quad (207)$$

Thus, the fixed-point values for the bosonic mass parameter as well as the four-boson self-interaction are non-vanishing. In a purely fermionic formulation of the model, higher bosonic self-interactions, such as the four-boson interaction, correspond to higher (non-local) fermionic self-interactions. In any case, we find that the fixed-point structure in $2 < d < 4$ for $N_f \rightarrow \infty$ is not identical to the effective action (186) at the initial RG scale Λ but involves operators of higher order. Recall our discussion in Sect. 3.2 where we have shown that bosonic self-interaction terms $\sim \sigma^{2n}$ can be viewed as momentum-dependent (non-local) fermionic self-interaction terms $\sim (\bar{\psi}\psi)^{2n}$.

We add that the fixed-point values of all bosonic self-interactions of the form σ^{2n} can be computed analytically in the limit $N_f \rightarrow \infty$ and that they are non-vanishing with their sign determined by $(-1)^n$. It turns out that the resulting alternating series for the full fixed-point (effective) potential,

$$u^*(\sigma^2) = \text{const.} + \frac{1}{2}\epsilon_\sigma^* \sigma^2 + \frac{1}{8}\omega_\sigma^* \sigma^4 + \dots,$$

can be resummed analytically, yielding $u^*(\sigma^2) \sim (\sigma)^{3/2}$ for large σ , see Ref. [150].

From a phenomenological point of view the scale-invariant fixed-point action describes a theory of massless fermions interacting via the exchange of scalar bosons. On the other hand, we have seen that the purely fermionic formulation of the Gross-Neveu model depends only on a single input parameter, namely

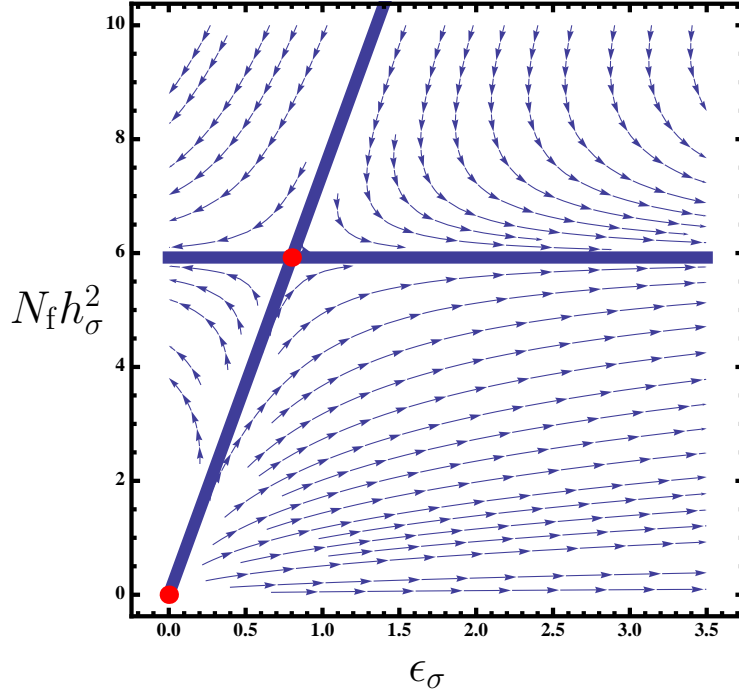


Fig. 11 RG flow of the partially bosonized Gross-Neveu model in leading order in the $1/N_f$ -expansion in the plane spanned by $N_f h_\sigma^2$ and ϵ_σ , see Ref. [150]. The arrows indicate the direction of flow towards the infrared.

the four-fermion coupling at the initial RG scale. In the following we show that the partially bosonized theory still has predictive power. It will turn out that the deviations of the partially bosonized fixed-point theory from the classical GN action are only due to IR irrelevant operators which neither modify the predictive power of the Gross-Neveu model nor the leading-order scaling behavior at the quantum critical point.

The number of physical parameters is determined by the number of RG relevant directions corresponding to the number of positive critical exponents. As discussed in Sect. 3.1, the latter can be computed from the stability matrix:

$$B = \begin{pmatrix} \frac{\partial(\partial_t h_\sigma^2)}{\partial h_\sigma^2} & \frac{\partial(\partial_t h_\sigma^2)}{\partial \epsilon_\sigma} & \frac{\partial(\partial_t h_\sigma^2)}{\partial \omega_\sigma} \\ \frac{\partial(\partial_t \epsilon_\sigma)}{\partial h_\sigma^2} & \frac{\partial(\partial_t \epsilon_\sigma)}{\partial \epsilon_\sigma} & \frac{\partial(\partial_t \epsilon_\sigma)}{\partial \omega_\sigma} \\ \frac{\partial(\partial_t \omega_\sigma)}{\partial h_\sigma^2} & \frac{\partial(\partial_t \omega_\sigma)}{\partial \epsilon_\sigma} & \frac{\partial(\partial_t \omega_\sigma)}{\partial \omega_\sigma} \end{pmatrix}_{h_\sigma^*, \epsilon_\sigma^*, \omega_\sigma^*}. \quad (208)$$

More precisely, the zeroes of the (characteristic) polynomial $\det(B + \Theta \mathbb{1})$ of the stability matrix B represent the critical exponents at the non-Gaussian fixed point. In the present case the polynomial reads

$$\det(B + \Theta \mathbb{1}) = (4 - d + \Theta)(2 - d + \Theta)(4 - d + \Theta). \quad (209)$$

In $d = 3$ we thus have one positive critical exponent associated with an RG relevant direction and two negative critical exponents associated with RG irrelevant directions. As it should be, the exponent of the RG relevant direction is identical to the one found in the purely fermionic formulation, see Eq. (191). In $d = 4$ the situation is substantially different. There, we have two marginal directions and one relevant parameter. This suggests that the Gross-Neveu model in $d = 4$ may depend on more than one input parameter. In any case, we observe that the critical exponents are independent of N_f .

Even if we take into account bosonic self-interactions σ^{2n} of arbitrarily high order, we still have only a single RG relevant direction at the non-Gaussian fixed point. All additional directions are RG irrelevant,

see Ref. [150]. Thus, the IR physics of the model depends on only a single parameter as stated above in the case of the purely fermionic formulation.

At the Gaussian fixed point the critical exponents coincide with the mass dimension of the Yukawa coupling and the bosonic couplings, reproducing simple perturbative power counting. In total, one finds three relevant RG directions and one marginal RG direction in $d = 3$. Note that the Gaussian fixed point in the purely fermionic flow in Sect. 5.1.2 translates into a diverging dimensionless renormalized boson mass, $\epsilon_\sigma^{1/2} \sim \lambda_\sigma^{-1/2}$.

At this point it is instructive to make the contact with the purely fermionic description more explicit and deduce the fixed point of the four-fermion coupling from the fixed point values of the Yukawa coupling and the bosonic mass parameter ϵ_σ . We find

$$\lambda_\sigma^* = \frac{(h_\sigma^*)^2}{\epsilon_\sigma^*} = \frac{1}{N_f} \left(\frac{d}{d_\gamma v_d} \right) \frac{d-2}{8} \stackrel{(d=3)}{=} \frac{3\pi^2}{4N_f} \quad (210)$$

for the optimized regulator, which agrees with our findings in Sect. 5.1.2. As we have discussed in Sect. 3.2, the flow equation of the four-fermion interaction λ_σ can be reconstructed from the flow of $h_\sigma^2/\epsilon_\sigma$:

$$\begin{aligned} \partial_t \left(\frac{h_\sigma^2}{\epsilon_\sigma} \right) &= (2 + 2\eta_\psi) \left(\frac{h_\sigma^2}{\epsilon_\sigma} \right) - 4N_f d_\gamma v_d l_1^{(F),(d)}(0; \eta_\psi) \left(\frac{h_\sigma^2}{\epsilon_\sigma} \right)^2 \\ &\quad + 6v_d l_1^{(d)}(\epsilon_\sigma; \eta_\sigma) \omega_\sigma \left(\frac{h_\sigma^2}{\epsilon_\sigma^2} \right) + 8v_d l_{1,1}^{(FB),(d)}(0, \epsilon_\sigma; \eta_\psi, \eta_\sigma) \left(\frac{h_\sigma^4}{\epsilon_\sigma} \right). \end{aligned} \quad (211)$$

Using Eq. (194) and $\lambda_\sigma = h_\sigma^2/\epsilon_\sigma$ as well as

$$l_{1,1}^{(FB),(d)}(0, \epsilon_\sigma; \eta_\psi, \eta_\sigma) \stackrel{(\epsilon_\sigma \gg 1)}{\rightarrow} \frac{1}{\epsilon_\sigma} l_1^{(F),(d)}(0; \eta_\psi), \quad (212)$$

we recover the flow equation (187) found in the purely fermionic formulation. In the large- N_f limit, the flow equation (211) simplifies considerably. We find

$$\partial_t \left(\frac{h_\sigma^2}{\epsilon_\sigma} \right) = (d-2) \left(\frac{h_\sigma^2}{\epsilon_\sigma} \right) - 4N_f d_\gamma v_d l_1^{(F),(d)}(0; 0) \left(\frac{h_\sigma^2}{\epsilon_\sigma} \right)^2. \quad (213)$$

We observe that the flow equations for λ_σ and $h_\sigma^2/\epsilon_\sigma$ are indeed identical. In turn, also the scale k_{SB} , which sets the scale for low-energy observables, must be the same in both cases. Recall that $\eta_\psi = 0$ in this limit.

Due to the equivalence of λ_σ and $h_\sigma^2/\epsilon_\sigma$, the quantum critical point found in the purely fermionic formulation is also present in the partially bosonized theory for $N_f \rightarrow \infty$, as it should be the case. As can be seen from the scaling law (190), this quantum critical point is associated with a vanishing boson mass, i.e. a diverging correlation length, in the long-range limit. The scaling behavior of physical observables close to this point is governed by the critical exponent associated with the RG relevant direction.

Let us conclude our large- N_f analysis with a word of caution on the widely used LPA in which the running of the wave-function renormalizations are neglected. If we ignored the running of the wave-function renormalization of the bosonic field in the present case, the model would depend on more than one physical parameter and this additional dependence would be artificial. To be more specific, let us consider the mass spectrum of the theory in the regime with broken chiral symmetry and assume that we have already fixed the mass of the fermions. Using the definition of the masses and the flow equations of the couplings, we find that the (dimensionless) renormalized boson mass m_σ in the broken regime can be written in terms of the (renormalized) fermion mass m_ψ :

$$m_\sigma^2 = \omega_\sigma \sigma_0^2 \sim Z_\sigma^{-1} \bar{h}_\sigma^2 (\bar{h}_\sigma^2 \bar{\sigma}_0^2) \sim Z_\sigma^{-1} \bar{h}_\sigma^2 m_\psi^2, \quad (214)$$

where σ_0 is the expectation value of the bosonic field in the regime with broken chiral symmetry in the ground state,⁵³ see also Fig. 5 for illustration. Neglecting the running of Z_σ , i. e. setting $Z_\sigma = \text{const.}$ as

⁵³ Note that our conventions are such that $\epsilon_\sigma = m_\sigma^2/k^2$ and $\epsilon_\psi = m_\psi^2/k^2$.

done in the LPA, we observe that the boson mass does not only depend on a single physical parameter, but on two parameters independently, namely the fermion mass and the (bare) Yukawa coupling. In contrast, taking the running of $Z_\sigma \sim \bar{h}_\sigma^2$ into account, the value of the boson mass is fixed solely in terms of the fermion mass, in agreement with the fixed-point analysis.

While this argument might be altered in $d = 4$ space-time dimensions, where the Yukawa coupling is marginal, it is true for the Gross-Neveu model (as well as the Nambu-Jona-Lasinio model) in any dimension d in which the flow equation for Z_σ is non-vanishing even at leading order in an expansion in $1/N_f$. Therefore the flow of Z_σ has to be taken into account in a systematic and consistent expansion of the flow equations in powers of $1/N_f$. To be specific, the flow of the bosonic self-interactions Eqs. (198) and (199) incorporates fluctuations at next-to-leading order in $1/N_f$ due to the presence of the bosonic loop. However, for a systematic and consistent study of the effects of corrections beyond the large- N_f expansion, the flow of Z_σ , Z_ψ as well as of the Yukawa coupling needs to be taken into account.

5.1.4 Quantum Critical Behavior Beyond the Large- N_f Limit

Let us now discuss quantum critical behavior beyond the large- N_f limit. Beyond the large- N_f approximation, bosonic fluctuations play an important role. As an immediate consequence, a new fixed point for $h_\sigma \equiv 0$ arises for the flow of the effective potential in $2 < d < 4$. In the limit $N_f \rightarrow 0$ we are left with a scalar \mathbb{Z}_2 theory. This limit is equivalent to the limit $h_\sigma \rightarrow 0$ and therefore this fixed point of the purely bosonic theory is nothing but the Wilson-Fisher fixed point which describes critical phenomena in the Ising universality class.

The non-Gaussian fixed point of the full Gross-Neveu system can now be understood as stemming from the leading large- N_f terms discussed above and the bosonic fluctuations inducing a Wilson-Fisher fixed point. Depending on the value of N_f , the non-Gaussian Gross-Neveu fixed point interpolates between the large- N_f fixed point for $N_f \rightarrow \infty$ and the Wilson-Fisher fixed point in the (formal) limit $N_f \rightarrow 0$. For the latter, the functional RG has proven to be a useful quantitative tool for describing non-perturbative critical phenomena, see e. g. Refs. [100, 143–146, 228, 229].

In the following we repeat the large- N_f analysis with the full set of flow equations for $d = 3$ at next-to-leading order of the derivative expansion, see Eqs. (195)–(199). In particular for our numerical study of the critical behavior in $d = 3$, we restrict ourselves to this set of flow equations evaluated for the linear regulator. This implies that we only consider the RG flows of bosonic self-interaction terms up to order σ^4 . We do not take into account corrections arising from higher bosonic self-interactions terms. However, we expect that our analysis is sufficient to analyze the effect of corrections beyond the large- N_f limit as well as of the next-to-leading order terms in the derivative expansion. For a more quantitative study of the critical exponents including, effects of bosonic self-interactions up to 22nd order in σ , we refer the reader to Refs. [150, 223].

In the chirally symmetric regime, a nontrivial fixed point in the Yukawa coupling requires that the following inequality is satisfied:

$$d - 4 + 2\eta_\psi^* + \eta_\sigma^* < 0, \quad (215)$$

for $N_f < \infty$. This holds because the second term of the Yukawa flow Eq. (195) is strictly positive for all admissible values of the anomalous dimensions $\eta_\sigma, \eta_\psi \lesssim \mathcal{O}(1)$. For instance, in $d = 3$, the sum of the anomalous-dimension terms is always slightly smaller than one, see Tab. 1. The inequality becomes an equality in the large- N_f limit, see Eq. (205).

In the following we use the optimized regulator functions given in Eqs. (350) and (351) to evaluate the flow equations. The fixed point values for the Yukawa coupling in $d = 3$ are given in Tab. 1. For increasing N_f , the fixed point quickly approaches its large- N_f limit (206), whereas it decreases and (slowly) tends to zero for small N_f , leaving us with the pure Wilson-Fisher fixed point of a pure scalar model [150, 223]. As the latter is known to exhibit a fixed-point potential in the broken regime [100, 143–146, 228] with a non-vanishing expectation value of the scalar field σ , we expect such a fixed-point potential to appear for small N_f . For all integer values of $N_f \geq 1$ Dirac (four-component) fermions, we still find fixed-point actions in

N_f	η_σ^*	η_ψ^*	$N_f (h_\sigma^*)^2$	ϵ_σ^*
2	0.7598	0.0320	4.5576	0.3966
4	0.8869	0.0138	5.2812	0.5831
6	0.9267	0.0087	5.5068	0.6534
8	0.9458	0.0063	5.6152	0.6894
10	0.9571	0.0050	5.6788	0.7113
12	0.9644	0.0041	5.7205	0.7260
50	0.9917	0.0009	5.8746	0.7821
100	0.9958	0.0004	5.8983	0.7911
∞	1	0	5.9218	0.8

Table 1 Non-Gaussian fixed-point values of the *universal* anomalous dimensions and the (non-universal) fixed-point values of the couplings h_σ^* and ϵ_σ^* for various flavor numbers N_f in $d = 3$. The results have been obtained using the flow equations (195)-(199) evaluated for the linear regulator. In Monte-Carlo simulations [230], $\eta_{\sigma,*} = 0.754(8)$ has been found for $N_f = 4$ two-component fermions (corresponding to $N_f = 2$ in our setting).

the chirally symmetric regime, see also Ref. [223]. As has also been pointed out in Ref. [223], the fixed point seems to occur in the broken regime for the Gross-Neveu model with one two-component fermion.⁵⁴ This would correspond to $N_f = 1/2$ in our setting.

Let us now turn our discussion to the universal critical exponents $\Theta^{(i)}$. In our conventions, $\Theta^{(1)}$ denotes the leading, i. e. the largest, critical exponent. The critical exponents for $N_f = 2$ read

$$\Theta^{(1)} = 0.9928, \quad \Theta^{(2)} = -0.8687, \quad \Theta^{(3)} = -1.5743.$$

Our result for the critical exponent $\Theta^{(1)}$ agrees within errors with the result from corresponding Monte-Carlo (MC) simulations [230], $1/\Theta_{\text{MC}}^{(1)} = \nu_{\text{MC}} \approx 1.00(4)$. For $N_f = 12$, we find the following values for the critical exponents:

$$\Theta^{(1)} = 0.9898, \quad \Theta^{(2)} = -0.9735, \quad \Theta^{(3)} = -1.0701.$$

From this we conclude that the critical exponents do depend on N_f but converge rapidly to their values in the large- N_f limit, namely $\Theta^{(1)} = 1$, $\Theta^{(2)} = -1$ and $\Theta^{(3)} = -1$. This is also visible in the values of the anomalous dimensions and of the fixed points for the couplings, see Tab. 1. Whereas the values of the fixed-point couplings are non-universal, the anomalous dimensions are universal and illustrate the inequality (215).

As we have discussed above, the critical exponent $\Theta^{(1)}$ governs the long-range physics at the quantum critical point associated with the fixed-point $\lambda_\sigma^* \sim (h_\sigma^*)^2/\epsilon_\sigma^*$ of the four-fermion coupling. The exponent $\Theta^{(1)}$ is related to the correlation length exponent ν by $\nu = 1/\Theta^{(1)}$. Together with the scalar anomalous dimension and the corresponding scaling and hyperscaling relations, all thermodynamic exponents of the (quantum) phase transition are determined. The results presented here are in quantitative agreement with the functional RG study of Höfling et al. [223]. The agreement with results from other methods such as $1/N_f$ expansions [231] and Monte Carlo simulations is also satisfactory [230, 232]. Discrepancies are mainly visible in the anomalous dimensions for small N_f , a feature familiar from scalar models.

To summarize, the non-perturbative features of the Gross-Neveu model near the quantum critical point can be described well by our functional RG approach, as the model interpolates between two well-accessible limits within this framework: the large- N_f limit and the Wilson-Fisher fixed point in the Ising universality class for $N_f \rightarrow 0$. The ansatz for the effective action employed in our study is still incomplete in the sense that it does not exhibit all possible four-fermion terms compatible with the underlying symmetries of the model. However, we have argued that a Gross-Neveu-type RG trajectory might exist in the large- N_f limit, similar to the corresponding NJL-type trajectory in our study in Sect. 3.5.2. In any case, our results

⁵⁴ Note that two-component fermions have been used in Ref. [223].

suggest that the Gross-Neveu model depends only on a single parameter, even when we take into account corrections beyond the large- N_f limit. This might provide helpful information for a systematic study of the finite-temperature phase diagram of the Gross-Neveu model beyond the large- N_f approximation.

5.1.5 Excursion: Quantum Criticality and Asymptotic Safety

Let us finally exploit our results for the Gross-Neveu model to discuss aspects of renormalizability in quantum field theories. In the context of our model, this question can be related to the question of quantum criticality. In fact, the Gross-Neveu model allows us to discuss the issue of renormalizability in quantum gravity in a very pedagogic way, as pointed out in Ref. [150].

Renormalizability is often described as a technical cornerstone for the construction of admissible models in particle physics. Renormalization fixes physical parameters of a model to measured values of observable quantities. A main physical meaning of renormalizability is the capability of a model to provide an accurate description of a physical system over a wide range of scales at which measurements can be performed. The set of physical parameters, e. g. mass parameters, measured at different scales then defines the renormalized trajectory in parameter space. We have already introduced this idea in our basic discussion of the RG in Sect. 2. If we demand for a specific model to provide a *fundamental* description of nature, the model must be valid on all scales, in particular down to arbitrary short-distance scales, i. e. large momentum scales. In turn, the renormalized trajectory must exist on all scales without developing singularities.

The requirement of renormalizability can formally be verified and realized in perturbatively renormalizable theories in a weak coupling expansion. Here, all free parameters of a model can be fixed to physical values and the renormalized trajectory can be constructed order-by-order in a perturbative expansion. This strategy can be applied successfully to theories that exist over a wide range of scales, such as QED. However, the perturbative construction can even be applied on all scales if a theory is asymptotically free, i. e. if the Gaussian fixed point is UV attractive. Prominent examples are $SU(N_c)$ Yang-Mills theories in $d = 4$ and the theory of the strong interaction, namely QCD.

However, renormalizability is by no means tied to a perturbative construction. Even though reliable non-perturbative information might be difficult to obtain, the concept of renormalizability and the existence of a renormalized trajectory on all scales can be formulated rather generally within *Weinberg's asymptotic safety scenario* [233]. To put it sloppily, asymptotic safety is the generalization of asymptotic freedom at the Gaussian fixed point to the case of a non-Gaussian fixed point. By construction, a fixed point of the RG defines a point in parameter space where the system becomes scale invariant, RG trajectories that hit the fixed point towards the UV can be extended to arbitrarily high energy scales, thereby defining a fundamental theory; for reviews we refer to Refs. [108, 234]. On the other hand, we have shown that non-Gaussian fixed-points can be viewed as quantum critical points governing long-range physics.

While quantum criticality plays a crucial role in fermionic models of, e. g., condensed-matter systems, the asymptotic safety scenario has recently become an important ansatz for quantizing gravity. In contrast to other approaches, this scenario is based on the standard gravitational degrees of freedom and also the quantization procedure proceeds in a rather standard fashion; for recent developments we refer to Refs. [153, 227, 235–243]

In our study of the purely fermionic formulation of the Gross-Neveu model, we have found that the critical exponent Θ is positive for $d > 2$ and determines the scaling behavior of physical IR observables. From a field-theoretical point of view this means that the Gross-Neveu coupling λ_σ corresponds to an RG relevant coupling being repulsed by the non-Gaussian fixed point λ_σ^* towards the IR. However, we can also think of λ_σ as a coupling which is in the RG flow attracted by the non-Gaussian fixed point λ_σ^* towards the UV. In our simplified study, this suggests that the Gross-Neveu model can be renormalized and extended as a fundamental theory over all scales on RG trajectories that emanate from the non-Gaussian fixed point. As there is only one relevant direction, only one physical parameter has to be fixed (say, the value of the coupling at a UV scale Λ) in order to predict all physical quantities in the long-range limit. Thus, the Gross-Neveu model is asymptotically safe, i. e. non-perturbatively renormalizable. This observation has also been confirmed by our study of the partially bosonized Gross-Neveu model in Sect. 5.1.4 where we

have systematically included corrections beyond the large- N_f limit. Our results indeed suggest that the Gross-Neveu model in $d = 3$ is asymptotically safe for all $N_f > 0$. In any case, the present discussion illustrates the tight connection between quantum criticality and asymptotic safety.

Let us make one more point concerning the asymptotic safety scenario by considering the Gross-Neveu model at the Gaussian fixed point. At the Gaussian fixed point the critical exponent associated with the coupling λ_σ is given by $\Theta_{\text{Gau\ss}} = 2 - d$. Thus, the Gaussian fixed point is IR attractive. In this case, the limit $\Lambda \rightarrow \infty$ can only be taken if the RG trajectory emanates from the fixed point, but then the theory would be noninteracting on all scales and therefore “trivial”. Within perturbation theory, one therefore concludes that the Gross-Neveu model is perturbatively *non-renormalizable*. Note that this conclusion remains unchanged also if the anomalous dimension is taken into account. In fact, we have $\eta_\psi = 0$ at the Gaussian fixed point, implying that standard power-counting can only be modified logarithmically.

In quantum gravity, there is strong evidence that an IR repulsive non-Gaussian fixed point exists. It has been found that this fixed point indeed exists in (simple) truncations based on derivative expansions in all $d > 2$, see Refs. [237, 244]. The (upper) critical dimension for the existence of this non-Gaussian fixed point is $d = 2$ as in the Gross-Neveu model. It is interesting to speculate about a possible destabilization of the fixed point above another so far unknown critical dimension due to strong-coupling phenomena such as bound-state formation. A similar phenomenon has been observed in extra-dimensional Yang-Mills theories [245], where a non-Gaussian fixed point exists in $d = 4 + \epsilon$ but is non-perturbatively destabilized for $\epsilon \gtrsim \mathcal{O}(1)$.

We would like to add that the underlying ideas of the asymptotic safety scenario allow to construct UV-complete scenarios for the matter sector of the standard model (as well as for toy models of the Higgs sector), see Refs. [152, 224, 246], and Ref. [247] for a study of the non-linear sigma model.

Our comparison of the Gross-Neveu model and quantum gravity shows that the property of asymptotic safety in the Gross-Neveu model is closely related to the occurrence of a quantum phase transition of second order separating a disordered phase from a phase with broken chiral symmetry in the ground state. More generally, models with such quantum phase transitions of second order are guaranteed to be asymptotically safe. Whether the converse is true, i.e., whether asymptotically safe models always exhibit a physically relevant order-disorder quantum phase transition, is an interesting question for future studies.

5.2 Nambu-Jona-Lasinio Models and QCD at Low Energies

The Gross-Neveu model represents an effective theory for systems relevant in the context of condensed-matter physics. However, we have already hinted that the Gross-Neveu model also shares certain aspects with the theory of the strong interaction, namely QCD. In this section we now discuss aspects of strongly interacting fermions in the context of QCD low-energy models. As we shall see below, such models can be viewed as an extension of the simple NJL model discussed in Sect. 3. Of course, the construction of the NJL model has been originally inspired by the mechanisms of superconductivity in condensed-matter physics [132, 133]. The application of these type of models to QCD exemplifies once more that the action itself does not completely specify a physical system. Only the (quantum) equations of motion together with their boundary conditions fully determine the physical system under consideration. The “universality” of the equations of motion resulting from a given action allows for a cross-fertilization of seemingly different fields of physics, e. g. QCD and condensed-matter physics.

In Sect. 5.2.1 we discuss some facets of QCD and related low-energy models. Quantum and thermal phase transitions are then discussed in Sect. 5.2.2 with the aid of a particular low-energy model, the so-called *quark-meson model*. The corresponding RG flow equations can be derived along the lines of Sect. 3. In particular, we shall see that QCD low-energy models are closely related to the NJL model with a continuous chiral $SU(N_f)_L \otimes SU(N_f)_R$ symmetry as discussed in Sect. 3.5.1.

5.2.1 Low-energy QCD Models and the Fierz Ambiguity

As a prelude to Sect. 6 we briefly outline how QCD low-energy models can in principle be derived from the QCD action functional. One of the “ancestors” of QCD is the Gell-Mann-Zweig quark model for hadrons [248, 249] which is based on the observation that hadrons can be classified according to the structure of the (flavor) $SU(N_f = 3)$ gauge group. Even though this model was able to explain the existence of some particles, it was not possible to explain the existence of all hadronic resonances in a simple manner. For example, it was not possible to reconcile the existence of the baryonic resonance $\Delta^{++}(\frac{3}{2}^+)$, which is made up of three up-quarks in a spin-up state, with the Pauli Principle. In the 1970s, it was then shown that the shortcomings of the original quark model could be resolved by assigning a so-called color charge to the quarks [250–253]. Considering the problems of the original quark model with the resonance $\Delta^{++}(\frac{3}{2}^+)$, this was a reasonable assumption. Starting from the principle of gauge invariance, the existence of gauge bosons, the gluons, which carry combinations of color and anti-color, was postulated as well. The gluons are massless and mediate the interaction between the quarks, as the photons do in QED. In contradistinction to QED, however, the gauge bosons of the strong interaction interact with each other, which explains the short range of the strong force. As a consequence, photons are represented by Abelian gauge fields while gluons are described by non-Abelian gauge fields.

The action functional of QCD is approximately symmetric under continuous chiral flavor $SU(N_f)_L \otimes SU(N_f)_R$ transformations. As motivated above, the quarks also carry a color charge resulting in a local $SU(N_c)$ gauge symmetry, where N_c denotes the number of colors. The simplest action compatible with these symmetry constraints reads

$$S_{\text{QCD}} = \int d^4x \left\{ \frac{1}{4} F_{\mu\nu}^a F_{\mu\nu}^a + \bar{\psi} (i\not{\partial} + \bar{g}A) \psi \right\}, \quad (216)$$

where $A_\mu \equiv A_\mu^a T_{ij}^a$ denotes the gauge fields and \bar{g} is the (bare) coupling constant; the T_{ij}^a are the generators of the $SU(N_c)$ gauge group. Note that the fermions transform under the fundamental representation of the $SU(N_c)$ color group, whereas the gluons transform under the adjoint representation. The parameters N_c and N_f can in principle be chosen freely. For low-energy QCD phenomenology, we have $N_f = 2$ (and $N_c = 3$). In nature the flavor symmetry is broken explicitly by so-called current quark mass terms for the fermions, see also Sect. 3.5.4. For a study of the thermal phase transition of QCD, however, we expect that the dynamics is essentially driven by the two lightest quark flavors, which we shall assume to be massless in the following. The masses of the other quarks are large compared to the relevant scale of the theory,⁵⁵ e. g. the (chiral) phase transition temperature or the condensate $|\langle \bar{\psi}\psi \rangle|^{1/3}$ (associated with the light quarks).

The QCD action functional possesses also a conformal symmetry which is broken in the quantum theory due to the generation of a mass gap, even in the limit $N_f \rightarrow 0$. Moreover, the axial $U_A(1)$ symmetry of the flavor group, which is present on the classical level, is broken explicitly due to topologically non-trivial gauge configurations. This is known as the chiral anomaly. We shall comment on this anomaly below.

We now discuss how the basic structure of QCD low-energy models emerges from the QCD action functional. The local gauge symmetry gives rise to an interaction between the quarks and the gluons. The details of the momentum-scale dependence of the associated (renormalized) quark-gluon coupling g is of no relevance for the subsequent discussion. We only state that it increases towards the IR for $N_f < \frac{11}{2}N_c$. In Sect. 6 we shall then discuss this issue in more detail. In any case, the interaction between the quarks and the gluons induces quark self-interactions, e. g. by two-gluon exchange, of the following form:

$$\int d^4x \bar{\lambda}_{\alpha\beta\gamma\delta} \bar{\psi}_\alpha \psi_\beta \bar{\psi}_\gamma \psi_\delta, \quad (217)$$

where $\alpha, \beta \dots$ denote a specific set of collective indices including, e. g., flavor and/or color indices. Thus, quark self-interactions are gluon-induced in QCD, and the associated couplings are not fundamental

⁵⁵ Strange quarks with mass $m_s \approx 200$ MeV might still affect the dynamics close to the chiral phase boundary. Here, we do not take these effects into account for the sake of simplicity.

parameters. In fact, QCD in the chiral limit (i. e. limit of vanishing current quark masses) does depend only on a single parameter, e. g. the value of the (renormalized) coupling g at a given scale. Once we have fixed the coupling, all physical observables are fixed. This is reminiscent of the situation in the Gross-Neveu model in $2 \leq d < 4$ which also depends on only a single input parameter, see Sect. 5.1.

Let us assume for the moment that it would be possible to integrate out the gauge degrees of freedom completely. The dynamics associated with the gauge fields would then be encoded in highly non-local fermionic self-interactions of arbitrarily high order.⁵⁶ We assume further that the strength of these dynamically generated fermionic self-interactions can be related to a set of initial conditions for this purely fermionic theory at a given (UV) scale Λ_H by means of an RG trajectory. These initial conditions are in principle fixed by the gauge dynamics at scales $k \gtrsim \Lambda_H$. The scale Λ_H can then be viewed as a UV cutoff for this (purely) fermionic effective low-energy theory. For (momentum) scales $k \lesssim \Lambda_H$ we may expect a description of QCD in terms of a purely fermionic effective field theory to be valid and convenient, at least for a study of some aspects of QCD, such as dynamical chiral symmetry breaking.

We add a comment on the scale Λ_H : This scale essentially divides QCD into two regimes, namely a perturbative high-energy regime and a low-energy regime governed by dynamical mass generation. We therefore expect Λ_H to be at least of the order of the scale k_{SB} associated with chiral symmetry breaking, $\Lambda_H \gtrsim k_{SB}$, see also Sects. 6.4 and 6.5.1. Of course, the scale k_{SB} is a scheme-dependent quantity. In the context of QCD low-energy models, however, Λ_H should be considered as an additional (input) parameter which needs to be fixed by comparison to physical observables.

Based on these considerations effective low-energy QCD models are usually constructed from a given set of four-fermion interactions, see e. g. Refs. [134] for a review. Fermionic operators of higher order are usually dropped for the sake of simplicity. A commonly used ansatz for a low-energy effective theory for QCD with two massless quark flavors is given by⁵⁷

$$\Gamma_{N_f=2}[\bar{\psi}, \psi] = \int d^4x \left\{ \bar{\psi} i \not{\partial} \psi + \frac{1}{2} \bar{\lambda}_\sigma \left[(\bar{\psi} \psi)^2 - (\bar{\psi} \tau^\chi \gamma_5 \psi)^2 \right] \right\}, \quad (218)$$

with τ^χ being the Pauli matrices ($\chi = 1, 2, 3$), see e. g. Refs. [33, 53, 55, 100, 113, 134–139, 254–260]. For three light (massless) quark flavors one may use [134, 254, 261–266]

$$\Gamma_{N_f=3}[\bar{\psi}, \psi] = \int d^4x \left\{ \bar{\psi} i \not{\partial} \psi + \frac{1}{2} \bar{\lambda}_\sigma \left[(\bar{\psi} T^X \psi)^2 - (\bar{\psi} T^X \gamma_5 \psi)^2 \right] \right\}, \quad (219)$$

where the T^X denote the generators of the $SU(N_f)$ flavor group. In the three flavor case the generators are related to the so-called Gell-Mann matrices. In Eqs. (218) and (219) color indices (a, b, \dots) are contracted pairwise, e. g. $(\bar{\psi} \psi) \equiv \bar{\psi}_a \psi_a$. Moreover, we employ the following convention for the flavor indices (α, β, \dots): $(\bar{\psi} T^X \gamma_5 \psi)^2 \equiv (\bar{\psi}_\alpha T_{\alpha\beta}^X \gamma_5 \psi_\beta) (\bar{\psi}_\gamma T_{\gamma\delta}^X \gamma_5 \psi_\delta)$. From a phenomenological point of view this ansatz is obvious since it incorporates pions $\pi^\chi \sim (\bar{\psi} \tau^\chi \gamma_5 \psi)$ as composite degrees of freedom. This can be seen most easily from the partially bosonized formulation of this ansatz.⁵⁸ The pions arise as effective degrees of freedom in the low-energy limit of QCD due to the spontaneous breakdown of the chiral flavor symmetry. Since they are the massless Nambu-Goldstone bosons of QCD, they dominate the long-range physics and are of utmost importance for an accurate description of, e. g., the dynamics close to the finite-temperature phase boundary.

The ansatz (218) represents an effective two-flavor model for dynamical chiral symmetry breaking at intermediate scales of $k \lesssim \Lambda_H$. It is important to stress that this model cannot predict the temperature

⁵⁶ In studies of the Gross-Neveu model in the large- N_f limit the fermions are often integrated out explicitly, yielding a highly non-local but purely bosonic action, as discussed in Sect. 3.2.

⁵⁷ Note that this ansatz does not possess a $U_A(1)$ symmetry, see discussion below. On the other hand, the ansatz (219) has a $U_A(1)$ symmetry.

⁵⁸ In the literature the partially bosonized versions of the purely fermionic actions (218) and (219) are often referred to as the *quark-meson model*. We refer the reader to Sect. 3.2 for a detailed discussion of bosonization and to Sect. 3.5.1 for a discussion of symmetry breaking in theories with a chiral $SU(N_f)_L \otimes SU(N_f)_R$ symmetry.

dependence of physical observables exactly. By construction, it has neither gluons nor quark confinement. At moderate energy scales, below the hadronic mass scale Λ_H , unconfined *constituent quarks* appear instead of baryonic degrees of freedom. However, the low-energy couplings as derived from the partially bosonized version of this model are compatible with those of chiral perturbation theory [267, 268].

From a phenomenological point of view the ansatz (218) is well-justified for a description of two-flavor QCD at low energies. However, it is not complete with respect to Fierz transformations. The most general ansatz for the effective action compatible with the underlying symmetries of QCD reads [152]

$$\Gamma_k[\bar{\psi}, \psi] = \int d^4x \left\{ \bar{\psi} i \not{\partial} \psi + \frac{1}{2} \left[\bar{\lambda}_- (\mathbf{V}-\mathbf{A}) + \bar{\lambda}_+ (\mathbf{V}+\mathbf{A}) + \bar{\lambda}_\sigma (\mathbf{S}-\mathbf{P}) + \bar{\lambda}_{\text{VA}} [2(\mathbf{V}-\mathbf{A})^{\text{adj}} + (1/N_c)(\mathbf{V}-\mathbf{A})] \right] \right\}. \quad (220)$$

The four-fermion interactions appearing here have been classified according to their color and flavor structure. Color and flavor singlets are

$$(\mathbf{V}-\mathbf{A}) = (\bar{\psi} \gamma_\mu \psi)^2 + (\bar{\psi} \gamma_\mu \gamma_5 \psi)^2, \quad (221)$$

$$(\mathbf{V}+\mathbf{A}) = (\bar{\psi} \gamma_\mu \psi)^2 - (\bar{\psi} \gamma_\mu \gamma_5 \psi)^2, \quad (222)$$

where (fundamental) color (i, j, \dots) and flavor (χ, ξ, \dots) indices are contracted pairwise, e.g., $(\bar{\psi} \psi) \equiv (\bar{\psi}_i^X \psi_i^X)$. The remaining operators have non-singlet color or flavor structure,

$$\begin{aligned} (\mathbf{S}-\mathbf{P}) &= (\bar{\psi}^X \psi^\xi)^2 - (\bar{\psi}^X \gamma_5 \psi^\xi)^2 \equiv (\bar{\psi}_i^X \psi_i^\xi)^2 - (\bar{\psi}_i^X \gamma_5 \psi_i^\xi)^2, \\ (\mathbf{V}-\mathbf{A})^{\text{adj}} &= (\bar{\psi} \gamma_\mu T^a \psi)^2 + (\bar{\psi} \gamma_\mu \gamma_5 T^a \psi)^2, \end{aligned} \quad (223)$$

where $(\bar{\psi}^X \psi^\xi)^2 \equiv \bar{\psi}^X \psi^\xi \bar{\psi}^\xi \psi^X$, etc., and $(T^a)_{ij}$ denote the generators of the gauge group in the fundamental representation. We stress that the set of fermionic self-interactions introduced in Eq. (220) forms a complete basis. This means that any other pointlike four-fermion interaction which is invariant under $SU(N_c)$ gauge symmetry and $SU(N_f)_L \otimes SU(N_f)_R$ flavor symmetry can be related to those in (220) by means of Fierz transformations. Here, we have dropped $U_A(1)$ -violating interactions induced by topologically non-trivial gauge configurations. These interactions can in principle be parametrized by fermionic self-interactions of the form $\sim (\bar{\psi} \psi)^{N_f}$ and then be included straightforwardly in effective low-energy models [269–273].

The action (220) represents a very general ansatz for an effective low-energy model. The strategy for employing such a model is usually as follows: First, one uses a set of parameters and the UV cutoff Λ_H to fit the values of low-energy observables at vanishing temperature and chemical potential, e. g. the pion decay constant and the meson masses.⁵⁹ Second, one then computes the phase boundary while keeping the parameters at the UV cutoff fixed. A shortcoming of these models is apparent: The set of parameters used to fit a given set of low-energy observables is not necessarily unique. Even worse, two sets of parameters, which both give the same results for the low-energy observables, do not necessarily lead to the same results for the chiral phase boundary, see e. g. Ref. [274]. Strictly speaking, the initial conditions for the four-fermion couplings are fixed by gluodynamics at high momentum scales $p \sim k \gtrsim \Lambda_H$. However, this information is usually not available. Here, RG approaches may provide a systematic and consistent framework to derive these initial conditions from first principles QCD, see Sect. 6.

The effective action (220) naturally encompasses the ansatz (218). One may wonder whether the action (218) represents an "exact" limit of the action (220), e. g. in the limit $N_c \rightarrow \infty$. This would be indicated by, e. g., the existence of an RG trajectory on which only the coupling included in Eq. (218) is finite and all other interaction channels vanish identically. In order to investigate this question we study the fixed-point structure of the Fierz-complete ansatz (220). The RG flow equations for the couplings

⁵⁹ We stress that the limit $\Lambda_H \rightarrow \infty$ is not meaningful here, in contrast to the Gross-Neveu model in $2 \leq d < 4$ where the limit $\Lambda \rightarrow \infty$ is well-defined.

can be derived straightforwardly along the lines of Sect. 3.1. In the point-like limit we then find (see Refs. [29, 152])

$$\begin{aligned} \partial_t \lambda_- &= 2\lambda_- - 8v_4 l_1^{(F),(4)} \left\{ -N_f N_c (\lambda_-^2 + \lambda_+^2) + \lambda_-^2 \right. \\ &\quad \left. - 2(N_c + N_f) \lambda_- \lambda_{VA} + N_f \lambda_+ \lambda_\sigma + 2\lambda_{VA}^2 \right\}, \end{aligned} \quad (224)$$

$$\begin{aligned} \partial_t \lambda_+ &= 2\lambda_+ - 8v_4 l_1^{(F),(4)} \left\{ -3\lambda_+^2 - 2N_c N_f \lambda_- \lambda_+ - 2\lambda_+ (\lambda_- + (N_c + N_f) \lambda_{VA}) \right. \\ &\quad \left. + N_f \lambda_- \lambda_\sigma + \lambda_{VA} \lambda_\sigma + \frac{1}{4} \lambda_\sigma^2 \right\}, \end{aligned} \quad (225)$$

$$\partial_t \lambda_\sigma = 2\lambda_\sigma - 8v_4 l_1^{(F),(4)} \left\{ 2N_c \lambda_\sigma^2 - 2\lambda_- \lambda_\sigma - 2N_f \lambda_\sigma \lambda_{VA} - 6\lambda_+ \lambda_\sigma \right\}, \quad (226)$$

$$\partial_t \lambda_{VA} = 2\lambda_{VA} - 8v_4 l_1^{(F),(4)} \left\{ -(N_c + N_f) \lambda_{VA}^2 + 4\lambda_- \lambda_{VA} - \frac{1}{4} N_f \lambda_\sigma^2 \right\}, \quad (227)$$

where $l_1^{(F),(4)} = l_1^{(F),(4)}(0; 0)$ and the dimensionless couplings λ_i are defined as $\lambda_i = k^2 \bar{\lambda}_i$ with $i \in \{+, -, \sigma, VA\}$. Apart from a Gaussian fixed point, this set of equations possesses 15 non-trivial fixed points. The values of these can be computed straightforwardly from the flow equations. In the following, however, we restrict our analysis to the limit $N_c \rightarrow \infty$. Loosely speaking, this limit corresponds to the large- N_f limit in the Gross-Neveu model discussed in Sect. 5.1.

From the (Dirac) Fierz transformations given in App. B we deduce that the channels associated with the couplings λ_- and λ_{VA} cannot be directly transformed into a channel with a scalar-pseudoscalar Dirac structure as included in the commonly employed action (218). On the other hand, the (V+A)-channel can be transformed into a channel with a scalar-pseudoscalar structure. Thus, we are left with the (V+A)-channel and the (S-P)-channel. In the large- N_c limit it then turns out that no non-trivial fixed point exists at which only the λ_+ -coupling assumes a finite value. Moreover, no non-trivial fixed point exists at which only the λ_- - and λ_{VA} -coupling are zero. However, a non-Gaussian fixed point exists at which only the λ_σ -coupling assumes a finite value. In fact, the set of flow equations for the couplings λ_- , λ_+ , λ_σ and λ_{VA} simplifies considerably in the limit $N_c \rightarrow \infty$ for $\lambda_- = \lambda_+ = \lambda_\sigma = 0$:

$$\partial_t \lambda_\sigma = 2\lambda_\sigma - 16N_c v_4 l_1^{(F),(4)} \lambda_\sigma^2. \quad (228)$$

The associated fixed point $\mathcal{F}_{(S-P)}^\infty = (\lambda_-^*, \lambda_+^*, \lambda_\sigma^*, \lambda_{VA}^*)$ of the full set of equations in this limit reads

$$\mathcal{F}_{(S-P)}^\infty = \left(0, 0, \frac{8\pi^2}{N_c}, 0 \right), \quad (229)$$

where we have used the optimized regulator function for illustration, $l_1^{(F),(4)}(0; 0) = \frac{1}{2}$.

Let us have closer look at the (S-P)-channel and its relation to the the interaction channel included in the simplified action (218). Similar to our study in Sect. 3.5.1, we may use the Fierz transformation for flavor indices Eq. (116) to obtain

$$(S-P) = \left(\frac{1}{2N_f} - \frac{1}{4} \right) [(\bar{\psi}\psi)^2 - (\bar{\psi}\gamma_5\psi)^2] + [(\bar{\psi}T^\chi\psi)^2 - (\bar{\psi}T^\chi\gamma_5\psi)^2], \quad (230)$$

where $\chi = 0, 1, \dots, N_f^2 - 1$. For convenience, we have defined $T^0 = \frac{1}{2} \mathbb{1}$ and the T^χ for $\chi \geq 1$ denote the generators of the $SU(N_f)$ flavor group in the fundamental representation. Note that the second term in Eq. (230) is invariant even under $U(N_f)$ transformations. For the phenomenologically important case $N_f = 2$ we are left with

$$\begin{aligned} (S-P) &= \frac{1}{4} [(\bar{\psi}\tau^\chi\psi)^2 - (\bar{\psi}\tau^\chi\gamma_5\psi)^2] \\ &= \frac{1}{2} [(\bar{\psi}\psi)^2 - (\bar{\psi}\tau^\chi\gamma_5\psi)^2] - [\det \bar{\psi}(1 + \gamma_5)\psi + \det \bar{\psi}(1 - \gamma_5)\psi], \end{aligned} \quad (231)$$

with τ^x being the Pauli matrices, $T^x = \frac{1}{2}\tau^x$, see also Ref. [134]. The determinant is performed in flavor space.

Apparently, the (S–P)-channel includes the standard scalar-pseudoscalar interaction channel of commonly used effective low-energy models for QCD with two massless flavors, see Eq. (218). The second term in Eq. (231) has the same structure as a term associated with topologically non-trivial gauge configurations that break the $U_A(1)$ symmetry of the theory [269–273]. In our case, we have attached the same coupling to the first and the second term in Eq. (231). This keeps the $U_A(1)$ symmetry intact. In an even more general approach we could allow for an explicit $U_A(1)$ breaking term by, e. g., replacing the (S–P)-channel in Eq. (220) as follows:

$$\bar{\lambda}_\sigma (\text{S–P}) \longrightarrow \bar{\lambda}_\sigma (\text{S–P}) - (\bar{\lambda}_\sigma - \bar{\lambda}_{\text{top.}}) [\det \bar{\psi}(1 + \gamma_5)\psi + \det \bar{\psi}(1 - \gamma_5)\psi]. \quad (232)$$

In any case, our analysis suggests that in the large- N_c limit a separatrix in coupling-constant space exists on which only the coupling included in Eq. (218) assumes a finite value. The fixed point on this separatrix can be considered as a quantum critical point in analogy to our study of the Gross-Neveu model. The initial condition for the scalar-pseudoscalar coupling being smaller or larger than the value of the fixed point then distinguishes between two different phases in the long-range limit (IR limit): a non-interacting phase and a strongly-interacting phase in which the dynamics is governed by the pions. In practice, the initial condition for the scalar-pseudoscalar coupling is adjusted to fit the values of low-energy observables. In the subsequent section we shall now employ the effective action (218) to study quantum and thermal phase transitions.

5.2.2 Phase Transitions in QCD Low-energy Models

We now study quantum⁶⁰ and thermal phase transitions with the effective action (218). According to our analysis in the previous section this ansatz can be considered as a controlled starting point for an analysis of the QCD matter sector in the large- N_c limit.⁶¹ As mentioned above, the partially bosonized action corresponding to the purely fermionic action (218) is widely known as the *quark-meson model*.

Despite the shortcomings of this low-energy model, we believe that its study can shed some light on the mechanisms underlying chiral symmetry breaking in QCD. While the actual mechanism in (full) QCD may be different due to the presence of color interactions, the approach employed here gives a possible explanation for the scaling behavior observed in the low-energy observables, as far as they relate to the mechanisms of chiral symmetry breaking in an effective low-energy description of QCD by means of light Nambu-Goldstone particles.

We start our discussion of chiral symmetry breaking at zero and finite temperature with an analysis of the fixed-point structure of the purely fermionic formulation of the quark-meson model, see Eq. (218). In this two-flavor model, the spontaneous breakdown of chiral symmetry gives rise to the existence of three massless Nambu-Goldstone bosons. In the following, we restrict ourselves to the case $N_f = 2$ but keep the number of colors N_c as an arbitrary (control) parameter. Of course, the ansatz (218) is not complete with respect to Fierz transformations. In particular, we do not take into account additional four-fermion operators which arise at finite temperature due to the broken Poincare invariance, see Sect. 3.5.3. In the large- N_c limit, however, the scalar-pseudoscalar channel defines an RG trajectory on which all other four-fermion couplings are identical to zero, see Sect. 5.2.1.

In our study we follow closely the steps detailed in Sects. 3.1 and 3.5.3. This means that we drop a possible momentum dependence of the four-fermion coupling, $\lambda_\sigma(|p| \ll k)$ which implies $\eta_\psi = 0$. This approximation does not permit a study of properties of the system, such as the meson mass spectrum, in

⁶⁰ Concerning the issue of the existence of a non-trivial fixed-point of the four-fermion coupling associated with a quantum critical point in $d = 4$ space-time dimensions, we refer the reader to our discussion in Sects. 3.2 and 4.1.

⁶¹ In (full) QCD, we have a $U_A(1)$ symmetry. However, this symmetry is anomalously broken due to the presence of topologically non-trivial gauge configurations. The widely-used definition of the two-flavor quark-meson model, see Eq. (218), does not have such a $U_A(1)$ symmetry. This becomes apparent from the fact that the interaction term in the ansatz (218) essentially arises from the $U_A(1)$ -invariant expression Eq. (231) by simply dropping the contributions from the determinants.

the chirally broken regime; for example, mesons manifest themselves as momentum singularities in the four-fermion couplings. As discussed in detail in Sect. 3.2, the point-like limit can still be a reasonable approximation in the chirally symmetric regime above the chiral phase transition. It allows us to gain some insight into the question how the theory approaches the regime with broken chiral symmetry in the ground state [30–32]. Since we are simply interested in mapping the phase diagram in the plane spanned by the temperature and the initial condition for the coupling λ_σ , the point-like limit still represents a reasonable approximation.

At this point we would also like to remind the reader that in the point-like limit the RG flow of the four-fermion coupling, which signals the onset of chiral symmetry breaking, is completely decoupled from the RG flow of fermionic n -point functions of higher order. For example, 8-fermion interactions do not contribute to the RG flow of the coupling $\bar{\lambda}_\sigma$ in this limit.

Using the ansatz (218) we obtain the RG flow equation for the dimensionless renormalized four-fermion coupling $\lambda_\sigma = k^2 \bar{\lambda}_\sigma$ in the point-like limit:⁶²

$$\beta_{\lambda_\sigma} \equiv \partial_t \lambda_\sigma = 2\lambda_\sigma - 16(2N_c + 1)v_3 l_1^{(F),(4)}(\tau, 0) \lambda_\sigma^2, \quad (233)$$

where $v_3 = 1/(8\pi^2)$. Note that the coupling λ_σ depends on the dimensionless temperature $\tau = T/k$. Here, we have used a $3d$ (optimized) regulator function which is convenient for an analysis of chiral symmetry breaking at finite temperature. The definition of the regulator and the temperature-dependent threshold function $l_1^{(F),(4)}$ can be found in App. D. Recall that the wave-function renormalizations longitudinal and transversal to the heat bath are constant in leading order in the derivative expansion, i. e. $\eta_\psi^{\parallel, \perp} = 0$.

Let us now discuss the fixed-point structure of the coupling λ_σ . Apart from a Gaussian fixed point we have a second non-trivial fixed point. The value of this fixed point depends on the dimensionless temperature τ , see also Fig. 8. At vanishing temperature we find

$$\lambda_\sigma^* = \frac{1}{8(2N_c + 1)v_3 l_1^{(F),(4)}(0, 0, 0)} = \frac{6\pi^2}{(2N_c + 1)} \quad (234)$$

for the non-Gaussian fixed point. For illustration we have evaluated the threshold function $l_1^{(F),(4)}$ for the $3d$ optimized regulator, see Eq. (349). Note that the rescaled fixed-point coupling $N_c \lambda_\sigma^*$ approaches a constant value for $N_c \rightarrow \infty$: $N_c \lambda_\sigma^* \rightarrow 3\pi^2$.

Let us briefly recall the physical observations of Sect. 3 which are of relevance here: First of all, we stress that the fixed-point value λ_σ^* is not a universal quantity, as its dependence on the threshold function indicates. However, the statement about the mere existence of the fixed point is universal. Choosing an initial value $\lambda_\sigma^{\text{UV}} < \lambda_\sigma^*$ at the initial UV scale Λ_H , we find that the theory becomes non-interacting in the infrared regime ($\lambda_\sigma \rightarrow 0$ for $k \rightarrow 0$), see Fig. 8. For $\lambda_\sigma^{\text{UV}} > \lambda_\sigma^*$ we find that the four-fermion coupling λ_σ increases rapidly and diverges eventually at a finite scale k_{SB} . This behavior indicates the onset of chiral symmetry breaking associated with the formation of a quark condensate and the emergence of massless Nambu-Goldstone bosons, namely the pions. Hence chiral symmetry breaking in the IR only occurs if we choose $\lambda_\sigma^{\text{UV}} > \lambda_\sigma^*$ and λ_σ^* can be viewed as a quantum critical point.

The scale k_{SB} at which $1/\lambda_\sigma(k_{\text{SB}}) = 0$ sets the scale for a given IR observable \mathcal{O} :

$$\mathcal{O} \sim k_{\text{SB}}^{d_{\mathcal{O}}}, \quad (235)$$

where $d_{\mathcal{O}}$ is the canonical mass dimension of the observable \mathcal{O} . At vanishing temperature the scale k_{SB} can be computed analytically from Eq. (233). Analogously to our derivation of Eq. (95), we find

$$k_{\text{SB}} = \Lambda_H \theta \left(\lambda_\sigma^{\text{UV}} - \lambda_\sigma^* \right)^{\frac{1}{\Theta}}, \quad (236)$$

⁶² Note that the factor in front of λ_σ^2 differs from the one in Eq. (228) for two reasons: first, we have used a $3d$ regulator function. Second, we started from the action (218) to derive Eq. (233). This action is not complete with respect to Fierz transformations. However, this only changes the (non-universal) fixed-point value but not the (universal) critical exponents in the large- N_c limit.

where the critical exponent Θ is independent of N_c in the present approximation:

$$\Theta = - \left. \frac{\partial(\partial_t \lambda_\sigma)}{\partial \lambda_\sigma} \right|_{\lambda_\sigma^*} = 2. \quad (237)$$

Thus, the critical value k_{SB} scales with the distance of the initial value $\lambda_\sigma^{\text{UV}}$ from the fixed-point value λ_σ^* . For increasing $\lambda_\sigma^{\text{UV}}$ the scale k_{SB} increases and, in turn, the values of low-energy observables, such as the pion decay constant f_π and the chiral phase transition temperature T_χ , increase.

From now on, let us assume that we have fixed $\lambda_\sigma^{\text{UV}} > \lambda_\sigma^*$ at $T = 0$. The value of $\lambda_\sigma^{\text{UV}}$ then determines the scale $k_{\text{SB}} \equiv k_{\text{SB}}(\lambda_\sigma^{\text{UV}})$ which is related to the values of the low-energy values. For a study of the effects of a finite temperature we then leave our choice for $\lambda_\sigma^{\text{UV}}$ unchanged. This ensures comparability of the results at zero and finite temperature for a given theory defined by the choice for $\lambda_\sigma^{\text{UV}}$ at zero temperature.

At finite temperature we still have a Gaussian fixed point. Moreover, we find a pseudo fixed-point $\lambda_\sigma^*(\tau)$ for arbitrary values of $\tau = T/k$ at which the right-hand side of the flow equation is zero:

$$\lambda_\sigma^*(\tau) = \frac{1}{8(2N_c + 1)v_3 l_1^{(F),(4)}(\tau, 0, 0)}. \quad (238)$$

We would like to remind the reader that the pseudo fixed-point $\lambda_\sigma^*(\tau)$ is not necessarily an element of the separatrix in the plane spanned by the coupling λ_σ and the dimensionless temperature τ . However, we have $\lambda_\sigma^*(\tau) \geq \lambda_\sigma^{\text{sep.}}(\tau)$ for a given value of τ , where $\lambda_\sigma^{\text{sep.}}(\tau)$ defines the separatrix in (λ_σ, τ) -space, see our detailed discussion in Sect. 3.5.3. Therefore the analytically accessible value of the pseudo fixed-point $\lambda_\sigma^*(\tau)$ is well-suited for a discussion of the basic mechanisms of chiral symmetry breaking at finite temperature.

For high temperatures $T \gg k$ we find $\lambda_\sigma^* \sim (T/k)^3$. Since the value of the (pseudo) fixed-point increases with increasing $\tau = T/k$, the rapid increase of the four-fermion coupling towards the IR ($k \rightarrow 0$) is effectively slowed down and may even change its direction in the plane spanned by the coupling λ_σ and τ , see Figs. 8 and 9. This behavior of the pseudo fixed-point $\lambda_\sigma^*(\tau)$ already suggests that for a fixed initial value $\lambda_\sigma^{\text{UV}}$ a critical temperature T_χ exists above which the four-fermion coupling does not diverge but approaches zero in the IR. Such a behavior is indeed expected for high temperatures since the quarks become effectively stiff degrees of freedom due to their thermal mass $\sim T$ and chiral symmetry is restored. As discussed in Sect. 3.5.3, the equation $\lambda_\sigma^*(\tau_*) = \lambda_\sigma^{\text{UV}}$ defines a strict upper bound for the critical temperature T_χ for a given value of $\lambda_\sigma^{\text{UV}}$ and Λ_H , i. e. $T_\chi \leq T_* = \tau_* \Lambda_H$. Moreover, the equation $\lambda_\sigma^{\text{sep.}}(\tau_{\text{sep.}}) = \lambda_\sigma^{\text{UV}}$ defines an even stronger upper bound for the critical temperature: $T_\chi \leq T_{\text{sep.}} \leq T_*$. The actual phase transition temperature T_χ might be smaller than $T_{\text{sep.}}$ due to fluctuations of the Nambu-Goldstone bosons in the IR close to the phase boundary. However, we have $T_\chi \equiv T_{\text{sep.}}$ for $N_c \rightarrow \infty$ since bosonic fluctuations are parametrically suppressed in this limit.

To illustrate our analytic results we have studied the RG flow of the four-fermion coupling λ_σ for finite N_c numerically. Following the discussion in the previous paragraph, the phase transition temperature T_χ is defined to be the smallest temperature for which λ_σ remains finite in the infrared limit $k \rightarrow 0$. In Fig. 12 we present the phase diagram for two massless quark flavors and various values of N_c in the plane spanned by the temperature and the UV coupling $\lambda_\sigma^{\text{UV}}(N_c)$. For the UV cutoff Λ_H defining the range of validity of our model, we have chosen $\Lambda_H = 1 \text{ GeV}$. In accordance with our analytic findings we observe that there is only a chirally symmetric phase for $\lambda_\sigma^{\text{UV}} < \lambda_\sigma^*$. Increasing $\lambda_\sigma^{\text{UV}}$ above λ_σ^* , the system undergoes a quantum phase transition at λ_σ^* . We expect that the chiral phase transition temperature T_χ increases monotonously with $\lambda_\sigma^{\text{UV}} > \lambda_\sigma^*$ according to

$$T_\chi \sim k_{\text{SB}}. \quad (239)$$

Therefore we expect that the scaling behavior of this chiral observable is determined by the exponent $\Theta = 2$, see Eq. (236). In fact, the numerical data can be fitted to this analytic estimate:

$$\frac{T_\chi}{\Lambda_H} \approx 0.316 \left(\frac{\lambda_\sigma^{\text{UV}} - \lambda_\sigma^*}{\lambda_\sigma^{\text{UV}}} \right)^{0.498}, \quad (240)$$

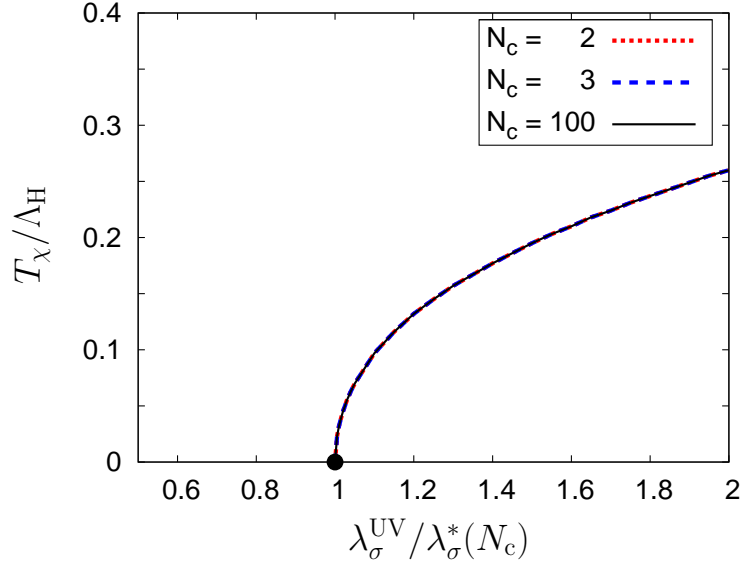


Fig. 12 Phase diagram for two massless quark flavors and $N_c = 2, 3, 100$ colors in the plane spanned by the temperature and the rescaled coupling $\lambda_\sigma^{\text{UV}}/\lambda_\sigma^*(N_c)$. The lines depict our results for the phase boundary for various values of N_c . For $T > T_\chi$ the theory remains in the chirally symmetric phase on all scales $k \leq \Lambda_H$. For $T = 0$ and increasing $\lambda_\sigma^{\text{UV}}$ the system undergoes a quantum phase transition at $\lambda_\sigma^{\text{UV}}/\lambda_\sigma^*(N_c) = 1$. Note that T_χ as a function of $\lambda_\sigma^{\text{UV}}/\lambda_\sigma^*(N_c)$ does not depend on N_c in the present approximation.

which is in good agreement with the expected behavior. For the fit we have used the results for T_χ/Λ_H for 11 equidistant values of $\lambda_\sigma^{\text{UV}}/\lambda_\sigma^*$ between $\lambda_\sigma^{\text{UV}}/\lambda_\sigma^* = 1.0$ and $\lambda_\sigma^{\text{UV}}/\lambda_\sigma^* = 1.01$. Note that our estimate for the phase transition temperature does not depend on N_c if we keep the initial condition $\lambda_\sigma^{\text{UV}}/\lambda_\sigma^*(N_c)$ fixed. This illustrates that the values of (chiral) observables in the large- N_c limit depend only on the relative distance of the initial condition $\lambda_\sigma^{\text{UV}}$ from the fixed-point value $\lambda_\sigma^*(N_c)$, as indicated by the scaling behavior of the critical scale k_{SB} in Eq. (236).

Let us now relate our model study of the phase diagram in the $(T, \lambda_\sigma^{\text{UV}})$ -plane to QCD. First of all, the initial condition $\lambda_\sigma^{\text{UV}}$ is not a free parameter in QCD but originally generated by quark-gluon interactions at high (momentum) scales. In a given regularization scheme, the value of $\lambda_\sigma^{\text{UV}}$ can therefore in principle be related to the value of the gauge coupling at some scale (e. g. the τ mass scale), see Sect. 6 and Refs. [29–32]. We would like to point out that neither the value of the gauge coupling at some scale nor the value of $\lambda_\sigma^{\text{UV}}$ on a given RG trajectory are physical observables. Nevertheless, their values can be related to physical low-energy observables, e. g. the pion decay constant or the quark condensate. For example, this has been explicitly illustrated in Ref. [275] by means of partial bosonization. In fact, the value of $\lambda_\sigma^{\text{UV}}$ determines the scale for IR observables, as explicitly demonstrated for the phase transition temperature T_χ . Since we expect that the (constituent) quark mass m_ψ also scales as $m_\psi \sim k_{\text{SB}}$ in leading order, it follows that $T_\chi \sim m_\psi$. In the following, however, we are not interested in a quantitative analysis of the relation of $\lambda_\sigma^{\text{UV}}$ to low-energy observables but rather in very general aspects of QCD low-energy models.

Within our point-like approximation of the fermionic vertices it is not possible to predict the order of the finite-temperature phase transition. In particular, our present approximation does not allow to determine the associated critical exponents. However, we expect our model to fall into the $O(N_f^2)$ universality class at the critical temperature. This can be understood most easily in terms of the partially bosonized version

of our model:⁶³

$$\Gamma_k[\bar{\psi}, \psi, \sigma, \{\pi^\chi\}] = \int d^4x \left\{ Z_\psi \bar{\psi} i \not{\partial} \psi + \frac{1}{2} Z_\sigma (\partial_\mu \sigma)^2 + \frac{1}{2} Z_\sigma (\partial_\mu \pi^\chi)^2 \right. \\ \left. + i \bar{h}_\sigma \bar{\psi} (\sigma + i \tau^\chi \pi^\chi \gamma_5) \psi + \frac{1}{2} \bar{m}_\sigma^2 (\sigma^2 + \vec{\pi}^2) + \frac{1}{8} \bar{\omega}_\sigma (\sigma^2 + \vec{\pi}^2)^2 \right\}, \quad (241)$$

with $\chi = 1, \dots, N_f^2 - 1$, $\vec{\pi}^2 := \pi^\chi \pi^\chi$, a Yukawa coupling $\bar{h}_\sigma \in \mathbb{R}$ and the boundary conditions

$$\lim_{k \rightarrow \Lambda_H} Z_\sigma = 0, \quad \lim_{k \rightarrow \Lambda_H} Z_\psi = 1, \quad \lim_{k \rightarrow \Lambda_H} \bar{\omega}_\sigma = 0. \quad (242)$$

These boundary conditions together with the identity

$$\bar{\lambda}_\sigma = \frac{\bar{h}_\sigma^2}{\bar{m}_\sigma^2} \quad (243)$$

allow us to map the ansatz (241) onto the fermionic action (218) at the initial UV scale Λ . In this picture, we assume that the bosons are composites of fermions and do not carry an internal charge, e. g. color or flavor: $\sigma \sim (\bar{\psi} \psi)$ and $\pi^\chi \sim (\bar{\psi} \tau^\chi \gamma_5 \psi)$. The interaction between the fermions is mediated by the Nambu-Goldstone bosons, namely the pion fields π^χ . The expectation value of the σ -field is proportional to the pion decay constant f_π . This is a consequence of the *Goldberger-Treiman relation*, which results from a detailed study of the axial-vector currents of the bosonized action [276].

At this point we mention a subtlety concerning the mapping of the partially bosonized formulation onto the purely fermionic formulation of our model. First of all, the identity (243) suggests that we have only one input parameter in the present study, namely the value of the ratio $(\bar{h}_\sigma^{\text{UV}} / \bar{m}_\sigma^{\text{UV}})$ at the UV scale Λ_H . In $d = 4$ space-time dimensions, however, the Yukawa coupling \bar{h}_σ is marginal. This suggests that the partially bosonized theory in $d = 4$ depends on two input parameters in contrast to $d = 3$, see also our discussion of the Gross-Neveu model in $d = 3$ in Sect. 5.1. Nonetheless the critical scale k_{SB} depends only on the ratio $(\bar{h}_\sigma^{\text{UV}} / \bar{m}_\sigma^{\text{UV}})$ in leading order in an expansion in powers of $1/N_c$ and receives only small corrections from the next-to-leading order, see also below. On the other hand, the ratio of IR observables, such as the ratio of the σ -mass and the constituent quark mass, depends on both parameters, see Eq. (214). In practice, this means that the ratio $(\bar{h}_\sigma^{\text{UV}} / \bar{m}_\sigma^{\text{UV}})$ and the Yukawa coupling $\bar{h}_\sigma^{\text{UV}}$ should be considered as independent input parameters at the UV scale Λ .

As we have seen in Sect. 3.2, the partially bosonized formulation of a fermionic model allows us to conveniently compute the order parameter, i. e. the chiral condensate, and in principle also its temperature dependence. The latter can be used to determine the order of the phase transition and to relate the initial condition $\lambda_\sigma^{\text{UV}}$ to physical observables. The gap equation for the expectation value of the σ -field in the mean-field approximation can be obtained along the lines of the derivation of Eq. (66). From the effective action (241) with $Z_\sigma = 0$ and $\bar{\omega}_\sigma = 0$, we find

$$\langle \sigma \rangle = 8N_c \left(\frac{\bar{h}_\sigma^2}{\bar{m}_\sigma^2} \right) T \sum_{n=-\infty}^{\infty} \int \frac{d^3p}{(2\pi)^3} \left[\frac{\langle \sigma \rangle}{\nu_n^2 + \vec{p}^2 + \langle \sigma \rangle^2} - \frac{\langle \sigma \rangle}{\nu_n^2 + \Lambda_H^2 + \langle \sigma \rangle^2} \right] \theta(\Lambda_H^2 - \vec{p}^2), \quad (244)$$

where we have used Eq. (15) and the optimized 3d regulator function given in Eq. (349). We have chosen this regulator since it allows us to directly relate the initial conditions $\lambda_\sigma^{\text{UV}}$ in Fig. 12 to the expectation value $\langle \sigma \rangle$. The Yukawa coupling has been absorbed into a redefinition of the bosonic field which is possible in the mean-field approximation. Using Eq. (244) we find that $(\Lambda_H^2 \bar{h}_\sigma^2 / \bar{m}_\sigma^2) \approx 14.1$ yields a (constituent)

⁶³ Recall that at finite temperature the Poincare invariance of the theory is broken explicitly. Therefore the wave-function renormalizations longitudinal and transversal to the heat-bath obey a different RG running. We neglect this difference for our general discussion in this section. In general, this is at least a reasonable approximation since it has indeed been found in Ref. [33] that the difference is small at low temperatures and only yields mild corrections to, e. g., the thermal mass of the bosonic degrees of freedom for intermediate temperatures $T \gtrsim T_\chi$. Moreover, we identify the wave-function renormalizations and the couplings of the Nambu-Goldstone modes and the so-called radial σ -mode. This is justified for our general discussion concerning universality at finite temperature.

quark mass $m_\psi \approx 0.3 \text{ GeV}$ for $T = 0$, $N_c = 3$ and $\Lambda_H = 1 \text{ GeV}$. Now we can either read off the corresponding phase transition temperature T_χ from Fig. 12 or we can compute T_χ with the gap equation (244). It is reassuring that we find $T_\chi \approx 0.183 \text{ GeV}$ either way. Moreover, the phase transition turns out to be of second order in this simple large- N_c approximation.

Concerning the phase diagram in the $(T, \lambda_\sigma^{\text{UV}})$ -plane, we expect that corrections to the large- N_c approximation arising from boson fluctuations will lower the phase transition temperature. This implies that the N_c -independence of the phase boundary is lifted. To be specific, we expect that the exact phase boundary approaches the large- N_c phase boundary from below. Since fluctuations of the bosons are parametrically suppressed for $N_c \rightarrow \infty$, the phase boundary shown in Fig. 12 simply represents the large- N_c phase boundary. Note that $1/N_c$ -corrections to the gap equation (244) can be conveniently taken into account within our RG framework, see e. g. Refs. [135–137, 275]. However, a detailed analysis of such corrections is beyond the scope of the present work. We only state that the results of these studies agree qualitatively with the simple estimates presented here.

Returning to the universal critical behavior of the theory at the thermal phase transition, we find that the Nambu-Goldstone bosons, namely the pions, tend to restore the chiral symmetry while the fermions tend to build up a condensate and thereby break the symmetry of the ground state. However, the anti-periodic boundary conditions for the fermions in Euclidean time direction lead to a suppression of the fermionic modes in the vicinity and above the phase transition due to the absence of a zero mode.

The critical temperature T_χ of our model can be viewed to be the temperature at which all N_f^2 bosonic modes are exactly massless in the limit $k \rightarrow 0$. In this limit the (dimensionless) extent $1/\tau = k/T$ of the Euclidean time direction becomes arbitrarily small. This means that the wave-length of these bosonic modes becomes much larger than the extent of the Euclidean time direction. Thus, the dynamics close to the thermal phase transition is effectively described by an $O(N_f^2)$ scalar theory in $d = 3$ dimensions:

$$\Gamma_k[\sigma, \{\pi^x\}] = \int d^3x \left\{ \frac{1}{2} Z_\sigma^\perp (\partial_i \sigma)^2 + \frac{1}{2} Z_\sigma^\perp (\partial_i \pi^x)^2 + \frac{1}{2} \bar{m}_\sigma^2 (\sigma^2 + \vec{\pi}^2) + \dots \right\}, \quad (245)$$

where $i = 1, 2, 3$. This three-dimensional scalar field theory possesses a quantum critical point similar to the one in our fermionic theories at vanishing temperature. This critical point divides the theory into two physically distinct regimes in the IR limit, namely one with a spontaneously broken $O(N_f^2)$ symmetry in the ground-state and one with a restored $O(N_f^2)$ symmetry. The critical exponents associated with this quantum critical point govern the scaling behavior of physical observables at the thermal phase transition of the quark-meson model. The computation of these (thermal) critical exponents is beyond the scope of this review. However, we stress that the Wetterich equation can indeed be used to determine these exponents accurately, see e. g. Refs. [106, 143–146, 229].

In the present work we have essentially restricted ourselves to an analysis of QCD low-energy effective models in the large- N_c limit. In this limit we expect the effective action (218) to be a controlled starting point according to our fixed-point analysis in the previous section. In principle, we have to take into account the Fierz-complete basis of four-fermion interactions given in Eq. (220) when we intend to go beyond the large- N_c limit. Moreover, we would have to take into account further four-fermion operators at finite temperature due to the broken Poincare invariance, see our discussion in Sect. 3.5.3. In a partially bosonized language this means that we have to take into account the associated bosonic degrees of freedom, e. g. vector bosons and axial-vector bosons. This already indicates that the determination of the order of the chiral phase transition in QCD and, in particular, the determination of the location of a possibly existing critical point at finite temperature and density is an inherently complicated task. Note that in our considerations we have not even taken into account effects of topologically non-trivial gauge configurations which break the $U_A(1)$ symmetry.

We would also like to add that our simple model description breaks down above the phase transition. In fact, we expect gluonic degrees of freedom to become relevant at high temperatures. In order to cure this shortcoming, extensions of the presently studied low-energy model have been put forward in Refs. [137, 255–260, 277–284].

Despite all these shortcomings of this simple model, our study already reveals the basic mechanism of dynamical chiral symmetry breaking. Moreover, we have shown in this and the previous section that a detailed analysis of the fixed-point structure is extremely useful since it provides us with important insights for a reliable construction of effective models.

Let us conclude our discussion of QCD low-energy models with a few words of caution concerning the LPA which is often used to include corrections beyond the large- N_c limit in studies of the partially bosonized action Eq. (241). To this end, we consider the mapping of the fermionic and partially bosonized theory in more detail. In the chirally symmetric regime the flow equations for the dimensionless renormalized couplings $\epsilon_\sigma = \bar{m}_\sigma^2/(Z_\sigma k^2)$, $\omega_\sigma = \bar{\omega}_\sigma/Z_\sigma^2$ and the Yukawa coupling $h_\sigma = \bar{h}_\sigma/(Z_\sigma^{1/2}Z_\psi)$ are given by⁶⁴

$$\partial_t \epsilon_\sigma = (\eta_\sigma - 2)\epsilon_\sigma - 12v_3 l_1^{(4)}(\tau, \epsilon_\sigma; \eta_\sigma)\omega_\sigma + 32N_c v_3 l_1^{(F),(d)}(\tau, 0, 0; \eta_\psi)h_\sigma^2, \quad (246)$$

$$\partial_t \omega_\sigma = 2\eta_\sigma \omega_\sigma + 24v_3 l_2^{(4)}(\tau, \epsilon_\sigma; \eta_\sigma)\omega_\sigma^2 - 64N_c v_3 l_2^{(F),(4)}(\tau, 0, 0; \eta_\psi)h_\sigma^4, \quad (247)$$

$$\partial_t h_\sigma^2 = (\eta_\sigma + 2\eta_\psi)h_\sigma^2 - 16v_3 l_{1,1}^{(FB),(4)}(\tau, 0, \epsilon_\sigma; \eta_\psi, \eta_\sigma)h_\sigma^4, \quad (248)$$

where $v_3 = 1/(8\pi^2)$. Again, we have employed 3d regulator functions to derive these equations. The threshold functions are defined in App. D. Note that the sign in front of the term $\sim h_\sigma^4$ in Eq. (248) differs from the one in Eq. (195). This change in the sign is due to the existence of the Nambu-Goldstone bosons in our QCD model; the latter enter this equation with the opposite sign compared to the radial mode (σ -mode). Moreover, we would like to point out that the term $\sim h_\sigma^4$ is not present in the NJL model with one fermion species and a continuous chiral symmetry. In this case, we have one Nambu-Goldstone mode and one radial mode which cancel each other identically, see Eq. (88).

As in our study of the Gross-Neveu model we can now study the RG flow of the ratio $h_\sigma^2/\epsilon_\sigma$ which can be obtained straightforwardly from the flow equations (246) and (248). We obtain

$$\begin{aligned} \partial_t \left(\frac{h_\sigma^2}{\epsilon_\sigma} \right) &= (2 + 2\eta_\psi) \left(\frac{h_\sigma^2}{\epsilon_\sigma} \right) - 32N_c v_3 l_1^{(F),(4)}(\tau, 0, 0; \eta_\psi) \left(\frac{h_\sigma^2}{\epsilon_\sigma} \right)^2 \\ &\quad + 12v_3 l_1^{(4)}(\tau, \epsilon_\sigma; \eta_\sigma)\omega_\sigma \left(\frac{h_\sigma^2}{\epsilon_\sigma^2} \right) - 16v_3 l_{1,1}^{(FB),(4)}(\tau, 0, \epsilon_\sigma; \eta_\psi, \eta_\sigma) \left(\frac{h_\sigma^4}{\epsilon_\sigma} \right). \end{aligned} \quad (249)$$

Using Eqs. (212), (242) and (243), we recover the RG flow equation (233) of the four-fermion coupling λ_σ . Thus, the partially bosonized and the purely fermionic description are indeed identical at the UV scale Λ_H . Note that the prefactor of the term $\sim h_\sigma^2/\epsilon_\sigma$ would turn out to be incorrect if we did not include the RG running of the Yukawa coupling, as done in the standard LPA. In other words, a standard LPA does not incorporate all terms associated with a systematic expansion of the flow equations in powers of $1/N_c$. This observation agrees with our analysis of the Gross-Neveu model in Sect. 5.1.

6 Gauge Theories

6.1 Gauge Theories with Few and Many Fermion Flavors - A Motivation

Chiral gauge theories are of utmost importance for our understanding of the fundamental forces in nature. For example, the strong interaction is mediated by the exchange of gluons, the gauge bosons of the theory of the strong interaction (QCD). To obtain a quantitatively and qualitatively consistent description of the generation of hadron masses in the early universe, a comprehensive understanding of chiral symmetry breaking in gauge theories is therefore mandatory.

Strongly-flavored asymptotically free gauge theories, i. e. gauge theories with many flavors, are currently very actively researched. Two prominent examples are QCD with many (light) flavors and QED₃, i. e. QED in $d = 2+1$ dimension. While there is a long-standing interest in QED₃ as an effective theory for

⁶⁴ We have set $Z_\psi^\parallel = Z_\psi^\perp$ and $Z_\sigma^\parallel = Z_\sigma^\perp$ for simplicity. This implies $\eta_\psi^\parallel = \eta_\psi^\perp$ and $\eta_\sigma^\parallel = \eta_\sigma^\perp$.

graphene [285–287], QCD with many quark flavors has drawn a lot of attention in recent years. The reasons for this great interest in strongly-flavored gauge theories are manifold. First, the number of (massless) fermions can be considered as an external parameter. Such gauge theories are then expected to exhibit a quantum phase transition from a chirally broken to a *conformal phase* when the number of fermion flavors is increased. Second, the understanding of strongly-flavored gauge theories underlies (walking) technicolor-like scenarios for the Higgs sector, see e. g. Refs. [80–88]. Returning to the dynamics underlying the generation of hadron masses, a controllable deformation of real QCD (with two light flavors) can teach us important lessons about the underlying principles of chiral symmetry breaking in nature.

The phase structure of gauge theories with N_f fermions can indeed be rich, as simple considerations may already suggest. Due to the screening property of fermionic fluctuations in gauge theories, asymptotic freedom is lost for large N_f . For instance, an $SU(N_c)$ gauge theory with N_f fermions is no longer asymptotically free (a.f.) for $N_f > N_f^{\text{a.f.}} := \frac{11}{2}N_c$. Another prominent fermion number, N_f^{CBZ} , potentially exists and denotes the smallest flavor number for which an infrared fixed point g_*^2 of the running gauge coupling in QCD still occurs. Consider the universal⁶⁵ two-loop β_{g^2} function of the gauge coupling g^2 :

$$\beta_{g^2} \equiv \partial_t g^2 = - \left(\beta_0 + \beta_1 \left(\frac{g^2}{16\pi^2} \right) + \dots \right) \frac{g^4}{8\pi^2} \quad (250)$$

with

$$\beta_0 = \frac{11}{3}N_c - \frac{2}{3}N_f \quad \text{and} \quad \beta_1 = \frac{34N_c^3 + 3N_f - 13N_c^2N_f}{3N_c}. \quad (251)$$

One readily observes that this β -function exhibits a non-trivial fixed point for $N_f > N_f^{\text{CBZ}}$, the so-called Caswell-Banks-Zaks (CBZ) fixed point [288]. For $SU(3)$, we have $N_f^{\text{CBZ}} \simeq 8.05$ in the two-loop approximation, marking a sign change of the coefficient β_1 . With increasing $N_f > N_f^{\text{CBZ}}$, the fixed-point value g_*^2 decreases and a perturbative treatment of the theory therefore seems possible near $N_f \lesssim N_f^{\text{a.f.}}$. Moreover, the existence of this fixed point suggests the existence of a conformally invariant limit in the deep infrared [289]. For decreasing N_f , g_*^2 becomes larger, suggesting the onset of chiral symmetry breaking.⁶⁶ The fermions then acquire a mass and decouple from the dynamics of the theory. This effect destabilizes the CBZ fixed point g_*^2 in the gauge sector of the theory. In this case, the IR limit of the theory is dominated by massless bosonic excitations, the Nambu-Goldstone modes, and the spectrum of the theory is characterized by a dynamically generated mass gap. A similar reasoning also applies to QED_3 , see e. g. Refs. [290, 291].

Our considerations suggest the existence of a critical value g_{cr}^2 of the gauge coupling which needs to be exceeded to trigger chiral symmetry breaking. As a direct consequence, we expect the existence of a *quantum critical point* associated with a critical flavor number $N_f^{\text{CBZ}} \leq N_{f,\text{cr}} < N_f^{\text{a.f.}}$ above which gauge theories approach a conformally invariant IR limit, see Fig. 13. Thus, N_f serves as a control parameter for a quantum phase transition. Note the difference to our studies of quantum critical behavior in the Gross-Neveu model and NJL-type models, where we have varied the initial values of the fermionic couplings directly to force the system to undergo a quantum phase transition.

Studies of the phase structure of strongly-flavored gauge theories have been performed with continuum methods as well as lattice simulations. In QED_3 many studies have provided estimates for $N_{f,\text{cr}}$ using Dyson-Schwinger equations and resummation techniques [290–300]. Since the dynamically generated mass is substantially smaller than the scale set by the gauge coupling, lattice simulations of QED_3 with many flavors are inherently challenging [301–304]. The phase structure of many-flavor QCD has also been studied with continuum methods [29–31, 159, 272, 288, 289, 305–317] and lattice simulations [318–333]. Recent results suggest in this case that a conformal phase indeed exists, with a quantum phase transition occurring around $9 \lesssim N_f^{\text{cr}} \lesssim 13$.

⁶⁵ While the one-loop coefficient is independent of the scheme, the two-loop coefficient is only universal in mass-independent regularization schemes, e. g. the $\overline{\text{MS}}$ scheme.

⁶⁶ Of course, it is well-known that the phenomenologically important case of two massless flavors exhibits chiral symmetry breaking in the IR limit.

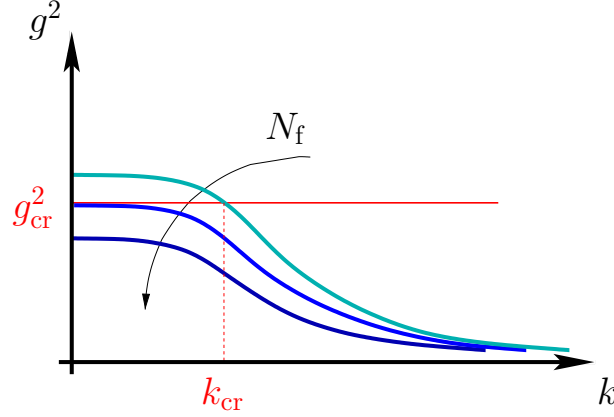


Fig. 13 Illustration of the IR running of the gauge coupling in comparison to the critical value of the gauge coupling g_{cr}^2 . The figure has been taken from Ref. [79]. Below the conformal window, $N_f < N_{f,\text{cr}}$, the gauge coupling g^2 exceeds its critical value g_{cr}^2 at the scale $k = k_{\text{cr}}$, triggering chiral symmetry breaking. For increasing flavor number, the IR fixed-point value g_*^2 becomes smaller than the critical value, indicating that the theory is inside of the conformal window. Note that k_{cr} should not be confused with the chiral symmetry breaking scale k_{SB} . In fact, we have $k_{\text{cr}} \geq k_{\text{SB}}$, see discussion below.

Given the existence of such a quantum critical point in an asymptotically free gauge theory with N_f flavors, the question arises how the spectrum of the theory behaves when we approach this point from below. This question is tightly bound to the N_f -dependence of the dynamically generated chiral symmetry breaking scale k_{SB} . It is well-known from studies of Dyson-Schwinger equations in the rainbow-ladder approximation that physical observables, e. g. the fermion condensate or the fermion mass, exhibit an exponential scaling close to $N_{f,\text{cr}}$, *provided that* the (momentum) scale dependence of the gauge coupling can be neglected [158, 306, 334–337]:

$$m_\psi \propto \Lambda \theta(N_{f,\text{cr}} - N_f) \exp\left(-\frac{\pi}{2\epsilon\sqrt{|\alpha_1|}|N_{f,\text{cr}} - N_f|}\right). \quad (252)$$

This type of scaling behavior has already been introduced in Sect. 3.4.2. Here, m_ψ denotes the dynamically generated fermion mass, and Λ denotes a suitably chosen UV scale. The quantities ϵ and α_1 in Eq. (252) are constants arising from the details of the theory and will be defined in Sect. 6.3.1. This scaling behavior can be viewed as a generalization of essential Berezinskii-Kosterlitz-Thouless (BKT) scaling [160–162] to higher-dimensional systems [163]. We rush to add that the spectra of the different theories below and above $N_{f,\text{cr}}$ are substantially different. In particular, a construction of an effective low-energy theory in terms of light scalar fields may no longer be possible above $N_{f,\text{cr}}$. In any case, the fact that essential scaling behavior may occur in various different systems, ranging from specific 2-dimensional condensed-matter systems over QED₃ to QCD, exemplifies once more that a phenomenological and technical exchange between these seemingly different research fields offers great potential to gain deep insights into the mechanisms of symmetry breaking in fermionic theories.

One may wonder how the essential scaling behavior (252) close to the quantum phase transition is altered when the running of the gauge coupling is taken into account. We shall derive the corresponding modified scaling laws for physical observables in this case, following the discussion in Ref. [79]. Our main arguments are based on very general considerations and involve only few assumptions about the fixed-point structure of the theory. The resulting scaling laws can be tested in QCD and QED₃, for example with the aid of Monte-Carlo simulations. In Sect. 6.2 we begin our discussion of chiral symmetry breaking in gauge theories with the simple few-flavor case using the example of QCD. We explain the issue of scale fixing in gauge theories which arises when one is interested in a meaningful comparison of theories with a different number of flavors. These ideas have been put forward in Refs. [31, 78] and have been used to

improve the parameter fixing in QCD model studies [281]. In Sect. 6.3 we analyze the scaling behavior in gauge theories close to a quantum critical point on general grounds. In Sect. 6.3.1, we briefly repeat the arguments given in Sect. 3.4.2 which lead to an exponential scaling behavior at a quantum phase transition. In addition, we give the leading-order correction to the exponential scaling behavior in gauge theories. In Sect. 6.3.2, we discuss power-law-like scaling behavior in gauge theories, which provides a strict upper bound for the N_f -scaling of chiral low-energy observables. In Sect. 6.3.3, we present the *universal* corrections to the exponential scaling behavior (252) which arise due to the running of the gauge coupling. Moreover, we show that power-law scaling and exponential scaling arise as two different limits of one and the same RG flow. The consequences for low-energy observables from the existence of a nearby quantum critical point are explained in Sect. 6.4 with the aid of a simple low-energy model. To illustrate our analytic findings, we review numerical results from non-perturbative RG studies of the scaling behavior in many-flavor QCD in Sect. 6.5.

For our discussion of many-flavor QCD in Sect. 6.5, we focus on the chiral phase transition, even though we also expect an impact of the confining nature of the theory on the properties of the system near criticality. However, since we work in the chiral limit, there is no good order parameter for confinement, in particular for many quark flavors. This implies that for large N_f nonanalyticities in the correlation functions are rather dominated by the chiral degrees of freedom. For few-flavor QCD, on the other hand, we may indeed expect that the fixed-point structure of the matter sector is significantly affected by the confining dynamics of the theory. In Sect. 6.6, we show that at finite temperature an interrelation of the confinement and chiral order parameter exists, at least for small N_f . This can be simply understood in terms of the fixed-point structure of the matter sector.

An outlook is given in Sect. 6.7, including a discussion of the implications of our findings for other gauge theories, e. g., with fermions in the adjoint representation.

6.2 The Issue of Scale Fixing in Gauge Theories

To illustrate the issue associated with scale fixing in gauge theories, let us consider few-flavor QCD. In the limit of zero current quark masses (chiral limit), QCD depends only on one parameter, namely the gauge coupling g , see Eq. (216). In the quantum theory, the gauge coupling has to be fixed at a certain momentum scale in terms of a renormalization condition. The RG finally trades the gauge coupling fixed at an arbitrary scale in for one single parameter Λ_{QCD} of mass dimension one. The latter sets the mass scale for all physical observables of the theory. In other words, all physical observables respond trivially to a variation of Λ_{QCD} according to their canonical mass dimension. In units of Λ_{QCD} , the theory is completely fixed.

In order to discuss the dependence on quantities such as the flavor number, it is important to emphasize that a variation of the flavor number does not correspond to a change of a parameter of the theory. It rather corresponds to changing the theory itself. In particular, there is no unique way to unambiguously compare theories of different flavor number with each other, as different theories may have different scales Λ_{QCD} .

For example, it may seem natural to compare theories with different flavor numbers at fixed Λ_{QCD} with each other. However, Λ_{QCD} itself is not a direct observable. Hence, such a comparison is generically spoiled with theoretical uncertainties. Moreover, Λ_{QCD} is regularization-scheme dependent which can affect comparisons between different theoretical methods, say, lattice and functional approaches. Another option could be a scale fixing in the deep perturbative region, say, at the Z-boson mass scale by fixing $g^2(M_Z)$. However, theories with different flavor numbers then exhibit a different perturbative running, such that IR observables vary because of both high-scale perturbative as well as non-perturbative (RG) evolution.

Following Ref. [78], we propose to choose a mid-momentum scale for the scale fixing, as the high-scale perturbative running is then separated from the more interesting non-perturbative dynamics. For example, we may fix the theories at any N_f by keeping the running coupling at the τ mass scale fixed to $g^2(m_\tau)/(4\pi) = 0.322$. Even though also this choice is scheme dependent, these dependences should be subdominant, as they follow a perturbative ordering. In general, fixing the scale via the coupling is a prescription which is well accessible by many non-perturbative methods. As an alternative of the described

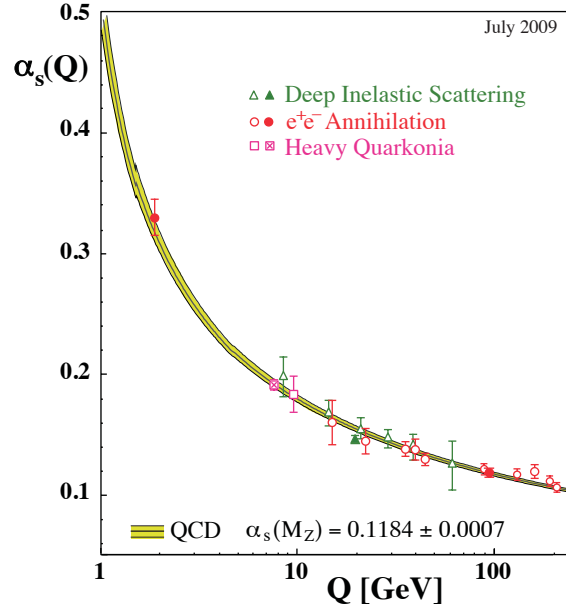


Fig. 14 Strong coupling $\alpha_s = g^2/(4\pi)$ as a function of the momentum (transfer) Q . The figure has been taken from Ref. [338].

scale-fixing prescription, however, one might think of keeping the value of an IR observable fixed for theories with different N_f , e. g. the pion decay constant or the critical temperature. Of course, this is also possible, e. g. in lattice QCD simulations. We shall comment on possible difficulties arising from such a procedure in Sect. 6.3.2.

Let us now present a simple argument that illustrates how the N_f -dependence of physical observables can be understood in the limit of small N_f . As already stated above, all IR observables such as the chiral phase transition temperature T_χ , the pion decay constant f_π , the chiral condensate $\langle\psi\psi\rangle$, and model-dependent concepts such as the constituent quark mass, are proportional to Λ_{QCD} . On the one hand, the latter can be read off from the UV behavior of the running coupling, $g^2(k) \sim 1/\ln(k/\Lambda_{\text{QCD}})$ for large $k \sim Q$, see also Fig. 14. On the other hand, the value of Λ_{QCD} can be associated with the position of the Landau pole in perturbation theory.⁶⁷ In this simple reasoning, the artificial Landau pole in the one-loop β_{g^2} function can be taken as an estimate for the scaling of physical observables. To be specific, we have

$$\beta_{g^2}^{1\text{-loop}} \equiv \partial_t g^2 = -\beta_0 \left(\frac{g^4}{8\pi^2} \right), \quad (253)$$

where β_0 is defined in Eq. (251). The position of the Landau pole can then be read off from

$$0 = \frac{1}{g^2(\Lambda_{\text{QCD}})} = \frac{1}{g^2(\mu_0)} + \beta_0 \ln \left(\frac{\Lambda_{\text{QCD}}}{\mu_0} \right), \quad (254)$$

where μ_0 denotes a perturbative scale, such as the τ -mass scale m_τ or the Z-boson mass M_Z . Solving this equation for Λ_{QCD} and expanding the result for small N_f leads us to

$$\Lambda_{\text{QCD}} \simeq \mu_0 e^{-\frac{1}{b_0 g^2(\mu_0)}} \simeq \mu_0 e^{-\frac{24\pi^2}{11N_f g^2(\mu_0)}} (1 - xN_f + \mathcal{O}((xN_f)^2)). \quad (255)$$

⁶⁷ Of course, this statement has to be taken with care, since Λ_{QCD} is a meaningful scale, whereas the Landau pole is simply an artifact of perturbation theory.

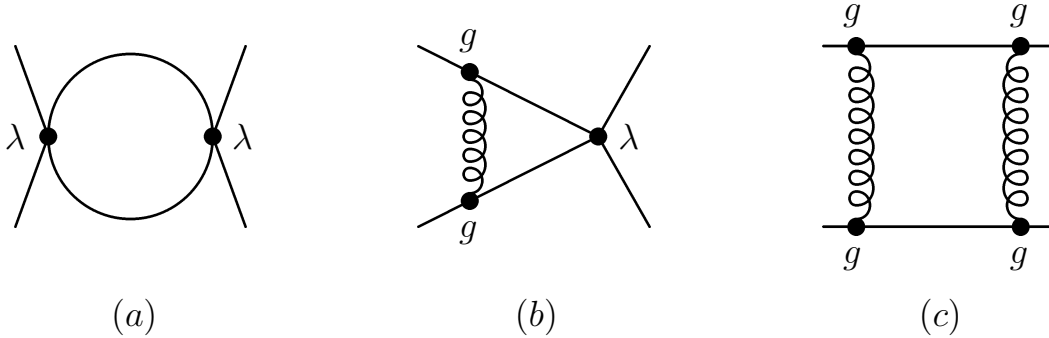


Fig. 15 Representation of the terms on the right-hand side of the RG flow equation (258) by means of 1PI Feynman diagrams, see Refs. [79, 341]. Our functional RG approach, see e. g. Sect. 6.5, includes resummations of all diagram types including ladder-diagrams generated by type (b) and (c) as well as the corresponding crossed-ladder diagrams.

Choosing $\mu_0 = m_\tau$, we find $x = \frac{48\pi^2}{121N_c^2g^2(\mu_0)} \simeq 0.107$ for $N_c = 3$. Two conclusions can immediately be deduced from this expression: first, Λ_{QCD} can be expanded in N_f and has a generically nonvanishing linear term. Second, for the present way of scale fixing the linear behavior should be a reasonable approximation for $N_f \lesssim 4$, as the (dimensionless) expansion parameter x is small in this regime.

Since Λ_{QCD} sets the scale for all dimensionful IR observables, we are tempted to conclude that all IR observables scale linearly with N_f for small N_f with the same proportionality constant x . Of course, this would be too simple since the dynamics which establishes the value of the IR observables generically carries an N_f dependence as well. For example, the chiral symmetry-breaking dynamics depends on the number of light mesonic degrees of freedom, which is an N_f -dependent quantity. Nonetheless, it is reasonable to expect that in leading order (chiral) low-energy observables \mathcal{O} indeed scale according to

$$\mathcal{O} = \mathcal{O}_0 (1 - xN_f + \dots), \quad (256)$$

where \mathcal{O}_0 is a dimensionful proportionality constant. For example, a linear dependence of the chiral phase transition temperature $\mathcal{O} = T_\chi$ on N_f has been found in lattice simulations [339] and in studies with functional RG methods [30, 31], see also Sect. 6.5.2. Note that Eq. (255), which underlies Eq. (256), has led to a significant improvement of the parameter fixing in studies of so-called Polyakov-loop extended low-energy models [259, 281, 340].

Let us finally generalize our discussion to gauge theories other than QCD. Our scale-fixing prescription indeed also applies to other theories in which dynamical chiral symmetry breaking is triggered by a running coupling that approaches a non-trivial IR fixed point. To be more specific, we shall focus our discussion on strongly-flavored asymptotically free gauge theories, such as QCD with many flavors and QED_3 . By asymptotic freedom, we refer here to the vanishing of the dimensionless renormalized coupling in the UV. In such theories, it seems natural to expect that the dependence of the coupling on the (momentum) scale modifies the exponential scaling behavior (252). We will discuss this in detail in Sect. 6.3.3.

6.3 General Aspects of Quantum Critical Behavior in Gauge Theories

6.3.1 Miransky Scaling

In Sect. 3.4.2 we have discussed essential/exponential scaling behavior in a simple NJL-type model. These considerations can be straightforwardly generalized to gauge theories. The role of the vector-coupling in our simple model is now played by the squared gauge coupling g^2 . In gauge theories, exponential scaling behavior near a *quantum critical point* is also known as Miransky scaling [158, 159].

The following analysis is by no means bound to QCD. To make this explicit, we shall keep our discussion as general as possible and consider a very general class of theories where symmetry breaking and

condensate formation is driven by fermionic self-interactions. Independently of whether these interactions may be fluctuation-induced (as in QCD) or fundamental (as in beyond standard-model applications) This class of theories can be parameterized by the following action:

$$S_M = \int d^d x \left\{ \bar{\psi}(\mathbf{i}\not{\partial} + \bar{g}\mathbf{A})\psi + \bar{\lambda}_{\alpha\beta\gamma\delta}\bar{\psi}_\alpha\psi_\beta\bar{\psi}_\gamma\psi_\delta \right\}, \quad (257)$$

where $\alpha, \beta \dots$ denote a specific set of collective indices including, e. g., flavor and/or color indices. In general, we expect to have more than just one four-fermion interaction channel as it is indeed the case in QCD, see Eq. (220).

From the action (257) we can derive the β function of the dimensionless four-fermion coupling λ in the point-like limit. It assumes the following simple form:

$$\beta_\lambda \equiv \partial_t \lambda = (d-2)\lambda - a\lambda^2 - b\lambda g^2 - cg^4. \quad (258)$$

The couplings $\lambda \sim \bar{\lambda}/k^{(d-2)}$ and $g \sim \bar{g}/k^{4-d}$ denote dimensionless and suitably renormalized couplings. The quantities a, b and c do not depend on the RG scale but may depend on control parameters, such as the number of fermion flavors N_f or the number of colors N_c in QCD. This β_λ function can be directly compared to the flow equation (102) of our toy model, where the role of g^2 is played by the vector coupling. Note that the coefficients a, b and c can depend implicitly on the RG scale as soon as we introduce a dimensionful external parameter, e. g., temperature T . However, the coefficients remain dimensionless since they depend only on the ratio T/k , see e. g. Refs. [30, 31].

The various terms on the right-hand side of Eq. (258) can be understood in terms of perturbative Feynman diagrams [341], see Fig. 15. Note that we have dropped terms in Eq. (258) which are proportional to the anomalous dimension η_ψ of the fermion fields. In contrast to purely fermionic theories, η_ψ can be finite in gauge theories even in the point-like limit. This is due to the existence of 1PI diagrams proportional to g^2 with one internal fermion line and one internal gauge boson line.⁶⁸ In the following we assume that these contributions are small. This is indeed true in the chirally symmetric regime where these contributions are proportional to the gauge-fixing parameter and therefore vanish at least in the Landau gauge [152].

As we have not specified the running of the vector coupling in our toy model study of essential scaling in Sect. 3.4.2, we have not further specified the details of the gauge sector in Eq. (257). In fact, let us ignore the running of the gauge coupling in this section, and consider the gauge coupling as a *scale-independent* “external” parameter. The RG flow of the gauge coupling is then trivially governed by

$$\partial_t g^2 \equiv 0. \quad (259)$$

This might be an acceptable approximation in the vicinity of an IR fixed point g_*^2 . Nonetheless, the value of g_*^2 may still depend on other control parameters such as N_f or N_c , see our discussion of QCD with many flavors in Sect. 6.5.

In Fig. 16 we show a sketch for the β_λ function, implicitly assuming that $a > 0, b > 0$ and $c > 0$ in Eq. (258). For a vanishing gauge coupling g^2 we find two fixed points, an IR attractive Gaussian fixed point at $\lambda = 0$ and an IR repulsive fixed point at $\lambda > 0$. For increasing g^2 these fixed points approach each other and eventually merge for a *critical* value g_{cr}^2 ,

$$g_{\text{cr}}^2 = \frac{d-2}{b+2\sqrt{ac}}. \quad (260)$$

For $g^2 > g_{\text{cr}}^2$ we strictly have $\partial_t \lambda < 0$ and the four-fermion coupling then becomes a relevant operator and increases rapidly towards the IR, indicating the onset of (chiral) symmetry breaking. Thus, the four-fermion coupling λ necessarily diverges for $g^2 > g_{\text{cr}}^2$ at a finite RG scale $k_{\text{SB}} = k_{\text{SB}}(g^2)$. Here, we assume that the initial conditions at the UV scale $k = \Lambda$ for the four-fermion coupling λ are chosen such

⁶⁸ This is in close analogy to the partially bosonized formulations of purely fermionic models where η_ψ is finite due to the existence of a 1PI diagram with one internal fermion line and one internal boson line, see e. g. Eqs. (87) and (197).

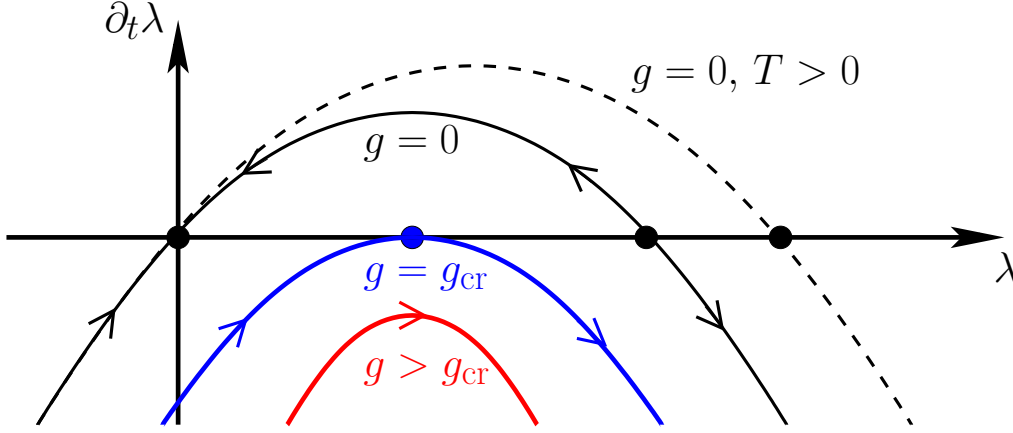


Fig. 16 Sketch of a typical β function for the fermionic self-interactions λ , see Refs. [29, 79] and also [31] for the generalization to finite temperature): at vanishing gauge coupling, $g^2 = 0$, the Gaussian fixed point $\lambda = 0$ is IR attractive. For $g^2 = g_{\text{cr}}^2$, the fixed-points merge due to a shift of the parabola induced by the gauge-field fluctuations $\sim g^4$. For gauge couplings larger than the critical coupling $g^2 > g_{\text{cr}}^2$, no fixed points remain and the strength of the self-interactions increases rapidly, signaling the onset of chiral symmetry breaking. The arrows indicate the direction of the flow towards the infrared. For increasing temperature, the parabolas become broader and higher. This is indicated by the dashed line.

that λ^{UV} is smaller than the value of the IR repulsive fixed point, see Fig. 16. In beyond-standard model applications λ^{UV} is sometimes considered to be a finite parameter, see e. g. Ref. [342]. We therefore add that the exponential scaling behavior discussed below can only be observed when λ^{UV} is chosen to be smaller than the value of its repulsive fixed point for a given g^2 . Otherwise, we expect a power-law-like scaling behavior as discussed in Sect. 3.4.1.

This picture of the emergence of chiral symmetry in gauge theories is not new but has been put forward in [29–31, 78] and successfully employed for an analysis of the phase structure of QCD with various numbers of flavors and colors at zero and finite temperature [29–31, 78]. Moreover, this picture has also been employed to study conformal scaling in quantum field theories, see e. g. Ref. [163].

Even though the symmetry breaking scale k_{SB} is not a direct observable, it sets the scale for (chiral) observables \mathcal{O} such as condensates, decay constants, critical temperatures, etc.:

$$\mathcal{O} = f_{\mathcal{O}} k_{\text{SB}}^{d_{\mathcal{O}}}, \quad (261)$$

where $d_{\mathcal{O}}$ is the canonical mass dimension of the observable \mathcal{O} and $f_{\mathcal{O}}$ is a function which does not depend on g_{cr}^2 but may depend on g^2 and other external parameters, e. g., N_f and/or N_c . The function $f_{\mathcal{O}}$ can be computed systematically within certain approximations schemes such as large- N_c expansions or chiral perturbation theory, see Sect. 6.4 and Refs. [78, 343].

Let us now briefly discuss the scaling behavior of the symmetry-breaking scale k_{SB} when g^2 is varied by hand as a constant “external” parameter. To this end, we have to solve the RG flow equation (258). In close analogy to our study in Sect. 3.4.2, we obtain the following result for the scale k_{SB} :⁶⁹

$$k_{\text{SB}} \propto \Lambda \theta (g^2 - g_{\text{cr}}^2) \exp \left(- \frac{\pi}{2\epsilon \sqrt{g^2 - g_{\text{cr}}^2}} \right). \quad (262)$$

⁶⁹ We have chosen the initial conditions such that $\lambda^{\text{UV}} = \lambda_{\text{max}}$, where λ_{max} denotes the position of the maximum of the β_{λ} function, i. e., the peak of the parabola in Fig. 16.

Here, ϵ is a numerical factor,

$$\epsilon = \sqrt{\frac{(d-2)(2ac + b\sqrt{ac})}{b + 2\sqrt{ac}}}, \quad (263)$$

which in general depends on the details of the theory under consideration, e. g. the number of colors and flavors in QCD. In any case, we find an exponential scaling behavior of k_{SB} for g^2 close to g_{cr}^2 . Due to Eq. (261) it is reasonable to expect that physical chiral observables \mathcal{O} inherit this scaling behavior from the symmetry breaking scale k_{SB} .

Let us now discuss the consequences of the scaling law (262) when we apply our considerations to strongly-flavored gauge theories, such as QED₃ or QCD with many fermion flavors. In these cases we may choose the IR fixed-point of the gauge coupling as an external parameter, i. e. $g^2 = g_*^2(N_f)$ in Eq. (262). Depending on the N_f dependence of the coefficients a , b and c in the β_λ function, the critical value for the gauge coupling may depend on the number of flavors as well, $g_{\text{cr}}^2 = g_{\text{cr}}^2(N_f)$. The critical number of fermion flavors $N_{f,\text{cr}}$ can then be obtained from the *criticality condition*

$$g_{\text{cr}}^2(N_{f,\text{cr}}) = g_*^2(N_{f,\text{cr}}). \quad (264)$$

This corresponds to the coupling value for which the two fixed points of the four-fermion coupling λ merge and then annihilate each other for $g^2 > g_{\text{cr}}^2$. Expanding $g_*^2(N_f) - g_{\text{cr}}^2(N_{f,\text{cr}})$ around $N_{f,\text{cr}}$,

$$g_*^2(N_f) - g_{\text{cr}}^2(N_{f,\text{cr}}) = \alpha_1(N_f - N_{f,\text{cr}}) + \alpha_2(N_f - N_{f,\text{cr}})^2 + \dots, \quad (265)$$

and plugging Eq. (265) into Eq. (262), we find the exponential N_f -scaling of k_{SB} :

$$k_{\text{SB}} \propto \Lambda \theta(N_{f,\text{cr}} - N_f) \exp\left(-\frac{\pi(1 - \frac{\alpha_2}{|\alpha_1|}|N_{f,\text{cr}} - N_f| + \dots)}{2\epsilon\sqrt{|\alpha_1||N_{f,\text{cr}} - N_f|}}\right). \quad (266)$$

We observe that the size of the regime for exponential scaling depends on the ratio $|\alpha_2/\alpha_1|$ which in turn depends on the theory under consideration. Thus, the size of the scaling regime may presumably be different in, e. g., QCD and QED₃. In Sect. 6.5 we compare these analytic findings with results from a numerical analysis of QCD with many quark flavors.

6.3.2 Power-law Scaling

In this section we discuss how the running of the gauge coupling affects the RG flow of four-fermion couplings. In particular, we argue that (chiral) symmetry breaking in strongly-flavored gauge theories is a multi-scale problem, in contrast to the scenario associated with Miransky scaling. In other words, the (chiral) symmetry breaking scale k_{SB} and its scaling with the control parameters, e. g. the number of flavors N_f , depends on the scale fixing and its potential flavor dependence.

In the following, we include the running of the gauge coupling which goes beyond standard rainbow-ladder approaches employed in the context of strongly-flavored gauge theories, see e. g. Ref. [309].

As we have argued in detail in Sect. 6.2, fixing the scale of theories with, say, different flavor numbers N_f by keeping the running coupling at some scale Λ (e. g. τ mass) fixed to a certain value, seems to be a well accessible prescription for many non-perturbative methods. In general, it is important to take care that this scale-fixing procedure is not (or as little as possible) spoiled by scheme dependences. The latter constraint then essentially rules out Λ_{QCD} as a proper scale in QCD to be kept fixed in theories with different flavor numbers. For what follows, we shall choose a mid-momentum scale for the scale fixing, lying in between the high-scale perturbative running and the more interesting non-perturbative dynamics. Thus, we fix the theories at any N_f by keeping the running coupling at some intermediate scale Λ fixed to a certain value, say $g_\Lambda^2 \equiv g^2(\Lambda)$.

For a monotonically increasing coupling flow, the value of the non-trivial IR fixed point g_*^2 of the gauge coupling corresponds to the largest possible coupling strength of the system in the conformal window, i. e.

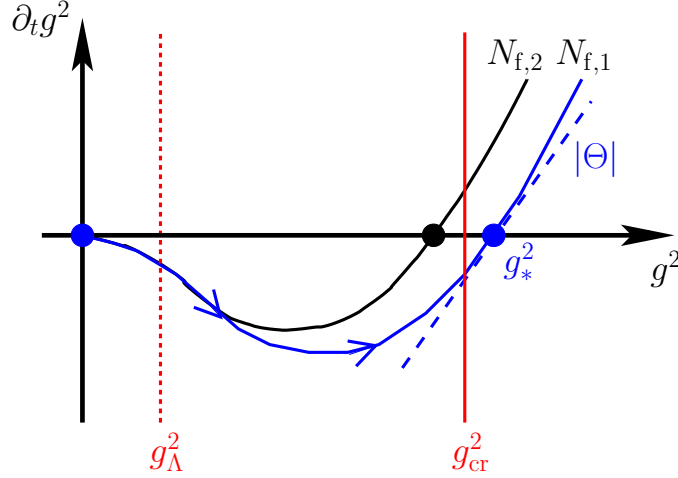


Fig. 17 Sketch of the β_{g^2} -function for $N_{f,1} < N_{f,cr}$ and $N_{f,2} > N_{f,cr}$. The slope of the β_{g^2} -function at the IR fixed-point corresponds to minus the critical exponent Θ , see Eq. (267) and Eq. (49) for a general discussion. The vertical line to the right gives the value of g_{cr}^2 . The dotted vertical line to the left gives the value of the gauge coupling at the UV scale Λ which we keep fixed for all N_f . However, the value of g_{cr}^2 may depend on N_f . The critical number of fermion flavors $N_{f,cr}$ is determined by $g_{cr}^2(N_{f,cr}) = g_*^2(N_{f,cr})$, see Eq. (264). The arrows indicate the direction of the flow towards the infrared.

for $N_{f,cr} < N_f < N_f^{a.f.}$. As both g_*^2 and g_{cr}^2 depend on the number of flavors, the criticality condition $g_*^2(N_{f,cr}) = g_{cr}^2(N_{f,cr})$ defines the lower end of the conformal window and thus the critical flavor number, see Sect. 6.3.1 and Fig. 13 for an illustration.

For $g_*^2 > g_{cr}^2$, our model (257) is below the conformal window and runs into the broken phase. Slightly below the conformal window, the running coupling g^2 exceeds the critical value while it is in the attractive domain of the IR fixed point g_*^2 . The flow in this fixed-point regime can approximately be described by the β -function expanded around the fixed point g_*^2 :

$$\beta_{g^2} \equiv \partial_t g^2 = -\Theta (g^2 - g_*^2) + \mathcal{O}((g^2 - g_*^2)^2). \quad (267)$$

The universal ‘‘critical exponent’’ Θ denotes (minus) the first expansion coefficient and depends on N_f . We know that $\Theta < 0$ for $N_f \gtrsim N_{f,cr}$, since the fixed point is IR attractive, see Fig. 17. The flow equation (267) for the running coupling can then be solved analytically:

$$g^2(k) = g_*^2 - \left(\frac{k}{k_0}\right)^{-\Theta}. \quad (268)$$

The scale k_0 corresponds to a scale where the system is already in the fixed-point regime. For the present fixed-point considerations, k_0 provides for all dimensionful scales. However, from the knowledge of the full RG trajectory, k_0 can be related to the initial scale Λ , say the τ mass scale in QCD, by RG evolution. In the following we keep the scale k_0 fixed, as we keep the UV scale Λ fixed.

As already discussed, a necessary condition for (chiral) symmetry breaking is that $g_*^2 > g_{cr}^2$. This implies that $g^2(k)$ exceeds g_{cr}^2 at some scale k_{cr} which is implicitly defined by the criticality condition, $g_*^2(N_{f,cr}) = g_{cr}^2(N_{f,cr})$, and therefore we have

$$k_{cr} \geq k_{SB}, \quad (269)$$

where k_{SB} is the scale at which the four-fermion coupling λ diverges. Thus, k_{cr} is an upper bound for the symmetry breaking scale k_{SB} . From Eq. (268) and the criticality condition $g^2(k_{cr}) = g_{cr}^2$, we derive an estimate for k_{cr} valid in the fixed-point regime

$$k_{cr} \simeq k_0 (g_*^2 - g_{cr}^2)^{-\frac{1}{\Theta}}. \quad (270)$$

The scale k_{cr} is dynamically generated. Note that $k_{\text{cr}}/k_0 \rightarrow 0$ for $g_*^2 \rightarrow g_{\text{cr}}^2$ from above. Due to our scale-fixing procedure, this scale depends on N_f and $N_{f,\text{cr}}$ in a non-trivial way. Note that it is, in principle, possible to adjust the initial value of the coupling at the initial scale Λ such that the scale k_{cr} is independent of N_f and $N_{f,\text{cr}}$. This procedure would be similar to keeping the Λ_{QCD} fixed for different values of N_f . As indicated in Sect. 6.2, we expect that such a scale-fixing procedure would, however, be strongly affected by scheme dependences, at least in our truncation. Using Eq. (265) and a Taylor expansion of the critical exponent near the quantum phase transition,

$$\Theta(N_f) = \Theta_0 + \Theta_1(N_f - N_{f,\text{cr}}) + \mathcal{O}((N_f - N_{f,\text{cr}})^2), \quad (271)$$

we find the following N_f dependence of k_{cr} for $N_f \leq N_{f,\text{cr}}$:

$$k_{\text{cr}} \simeq k_0 |N_{f,\text{cr}} - N_f|^{-\frac{1}{\Theta_0}} \left(1 - \frac{|N_{f,\text{cr}} - N_f|}{\Theta_0} \left(\frac{\alpha_2}{|\alpha_1|} - \frac{\Theta_1}{\Theta_0} \ln(|\alpha_1| |N_{f,\text{cr}} - N_f|) \right) \right) + \dots, \quad (272)$$

where $\Theta_0 := \Theta(N_{f,\text{cr}})$. Since k_{cr} defines the scale at which the fixed-points in the β function of the four-fermion coupling merge, the existence of a finite k_{cr} can be considered as a necessary condition for (chiral) symmetry breaking. Thus, we expect that the scale for a given IR observables \mathcal{O} for $N_f \leq N_{f,\text{cr}}$ is set by k_{cr} :

$$\mathcal{O} = f_{\mathcal{O}} k_{\text{cr}}^{d_{\mathcal{O}}}, \quad (273)$$

where $d_{\mathcal{O}}$ is again the canonical mass dimension and $f_{\mathcal{O}}$ depends on N_f but not on $N_{f,\text{cr}}$, see also Eq. (261). However, we stress that k_{cr} does not include the full dependence of k_{SB} on $(N_f - N_{f,\text{cr}})$, i. e. $k_{\text{cr}}/k_{\text{SB}}$ is still a function of the control parameter, as we shall discuss in the subsequent section.

Finally we would like to point out that the power-law scaling behavior discussed in this section is different from the power-law scaling behavior discussed in purely fermionic models, such as the Gross-Neveu model. In the latter, the scaling behavior at the quantum phase transition is governed by the critical exponent of the (relevant) four-fermion coupling. The scaling behavior in gauge theories, on the other hand, is governed by the critical exponent of the gauge coupling which drives the fermions to criticality. The four-fermion couplings at the UV scale are not considered to be free parameters in the present setup, as we have set them to zero at the UV scale.⁷⁰

6.3.3 Beyond Miransky Scaling

Let us now discuss how the symmetry breaking scale $k_{\text{SB}} \leq k_{\text{cr}}$ depends on $(N_f - N_{f,\text{cr}})$. We consider again an action of the form (257), and assume that $N_f \lesssim N_{f,\text{cr}}$. The crucial new ingredient compared to the derivation of Miransky scaling is the RG flow of the coupling. We also assume that the system has already evolved from the initial UV scale Λ to the scale k_{cr} at which the fixed points of the β function of the four-fermion coupling have merged. Sufficiently close to $N_{f,\text{cr}}$, the flow of the gauge coupling is governed by the fixed point regime for $g^2 > g_{\text{cr}}^2$. The running of the gauge coupling is then given by

$$g^2(k) = g_*^2 - (g_*^2 - g_{\text{cr}}^2) \left(\frac{k}{k_{\text{cr}}} \right)^{-\Theta} = g_*^2 - (\Delta g^2) \left(\frac{k}{k_{\text{cr}}} \right)^{-\Theta}, \quad (274)$$

where $\Delta g^2 = g_*^2 - g_{\text{cr}}^2$, see Eq. (268). Recall that $g_*^2 \sim N_f$ and $\Delta g^2 \sim |N_{f,\text{cr}} - N_f|$. Plugging Eq. (274) into Eq. (258), we find

$$\begin{aligned} \beta_\lambda &\equiv \partial_t \lambda = \beta_\lambda \Big|_{g_*^2} - \frac{\partial \beta_\lambda}{\partial g^2} \Big|_{g_*^2} (\Delta g^2) \left(\frac{k}{k_{\text{cr}}} \right)^{-\Theta} + \dots \\ &= (d-2)\lambda - a\lambda^2 - b\lambda g_*^2 - c g_*^4 - \frac{\partial \beta_\lambda}{\partial g^2} \Big|_{g_*^2} \left(\frac{k}{k_0} \right)^{-\Theta} + \dots, \end{aligned} \quad (275)$$

⁷⁰ Strictly speaking, we only require that the initial values of the four-fermion couplings are smaller than the values of their IR repulsive fixed points.

where we have used Eq. (270). Recall that $k \leq k_{\text{cr}} \ll k_0$ and $\Theta < 0$. We observe that the zeroth order in Δg^2 coincides with the β_λ function for which we have found an (implicit) analytic solution for constant g^2 in Sect. 6.3.1, yielding Miransky scaling. We refer to this analytic solution as $\lambda_{g_*^2}$. The solution of the β -function (275) can then be found by an expansion around the solution $\lambda_{g_*^2}$:

$$\lambda = \lambda_{g_*^2} + (\Delta g^2)\delta\lambda + \dots = \lambda_{g_*^2} + \left(\frac{k_{\text{cr}}}{k_0}\right)^{-\Theta} \delta\lambda + \dots, \quad (276)$$

where $\delta\lambda = -(\partial\lambda/\partial g^2)|_{g_*^2}$. This expression allows us to systematically compute the scaling behavior for $N_f \lesssim N_{f,\text{cr}}$. Since we are interested in the (chiral) symmetry breaking scale k_{SB} we have to solve $1/\lambda(k_{\text{SB}}) = 0$ for k_{SB} . In zeroth order, the scale k_{SB} can be computed along the lines of our analysis in Sect. 6.3.1. We find

$$\begin{aligned} k_{\text{SB}} &\propto k_{\text{cr}}\theta(N_{f,\text{cr}} - N_f) \exp\left(-\frac{\pi}{2\epsilon\sqrt{|\alpha_1|}|N_{f,\text{cr}} - N_f|}\right) \\ &\simeq k_0\theta(N_{f,\text{cr}} - N_f)|N_{f,\text{cr}} - N_f|^{-\frac{1}{\Theta_0}} \exp\left(-\frac{\pi}{2\epsilon\sqrt{|\alpha_1|}|N_{f,\text{cr}} - N_f|}\right), \end{aligned} \quad (277)$$

where we have used Eq. (272) in leading order. Higher order corrections to Eq. (277) can be computed systematically as outlined above and in the previous sections. Thus, we have found a *universal* correction to the exponential scaling behavior which is uniquely determined by the universal ‘‘critical’’ exponent Θ . A similar result has been suggested by Jarvinen and Sannino using a standard rainbow-ladder approach with a constant gauge coupling but a properly adjusted scale [343]. The presented RG analysis demonstrates in a simple and systematic way that such a rainbow-ladder approach is indeed justified and yields the correct leading-order scaling behavior. In the context of the RG the scaling law (277) has been first derived in Ref. [79].

Let us now turn to the scaling behavior of physical observables. The scale of all (chiral) low-energy observables is set by k_{SB} . In other words, k_{SB} represents the UV cutoff of an effective theory at low energies, such as chiral perturbation theory and NJL-type models in case of QCD. At zero temperature we therefore expect that a given IR observable \mathcal{O} with mass dimension $d_{\mathcal{O}}$ scales according to

$$\mathcal{O} = f_{\mathcal{O}}(N_f) k_{\text{SB}}^{d_{\mathcal{O}}}, \quad (278)$$

where $f_{\mathcal{O}}(N_f)$ is a function which depends on N_f but not on $N_{f,\text{cr}}$; in principle, it can be computed systematically in QCD using, e. g., chiral perturbation theory or a large- N_c expansion, see Sect. 6.4.

The scaling law (278) can be used as an ansatz to fit, e. g., data from lattice simulations. This scaling law is remarkable for a number of reasons: first, it relates two universal quantities with each other: quantitative values of observables and the IR critical exponent Θ . Second, it establishes a quantitative connection between the (chiral) phase structure and the IR gauge dynamics which is encoded in Θ . Third, it is a parameter-free prediction following essentially from scaling arguments. Last but not least, it shows that Miransky scaling and power-law scaling are simply two limits of the very same set of RG flows: in the limit $|\Theta| \rightarrow \infty$ we find pure Miransky-scaling behavior, while we have pure power-law scaling in the limit $\Theta \rightarrow 0$.

At this point, we would like to emphasize again that the scaling behavior of any IR observable near $N_{f,\text{cr}}$ depends crucially on the scale-fixing procedure applied in the first place. Still, the universal scaling will always show up at one or the other place and thus cannot be removed, as stressed in Ref. [78]. Our choice to fix the scale at, e. g., the τ -mass scale which is large enough not to be affected by chiral symmetry breaking is certainly not unique. In principle, the point where to fix the scale can be chosen as a free function of N_f . In Eq. (268), this would correspond to the choice of an arbitrary function $k_0 = k_0(N_f)$ for the global scale, which then appears also in the scaling relations (272) and (277). Indeed, an extreme choice would be given by measuring all dimensionful scales in units of a scale induced by chiral symmetry breaking (such as T_χ or f_π). In this case, all chiral observables would jump non-analytically across $N_f = N_f^{\text{cr}}$.

The scaling relations would then translate into scaling relations for other external scales. For example, the scale k_{g^2} at which the running coupling acquires a specific value would diverge with $N_f \rightarrow N_f^{\text{cr}}$ according to $k_{g^2} \sim |N_f - N_f^{\text{cr}}|^{-\frac{1}{|\Theta_0|}} \exp(c_M/\sqrt{|N_{f,\text{cr}} - N_f|})$, where $c_M = \pi/(2\epsilon\sqrt{|\alpha_1|})$. This point of view establishes a different way of verifying the above scaling relations on the lattice.

Let us conclude this section with a discussion of the importance of the corrections to the exponential scaling behavior due to the running of the gauge coupling. To this end, it is convenient to consider the logarithm of the (chiral) symmetry breaking scale k_{SB} ,

$$\ln k_{\text{SB}} = \text{const.} - \frac{1}{\Theta_0} \ln |N_{f,\text{cr}} - N_f| - \frac{\pi}{2\epsilon\sqrt{|\alpha_1||N_{f,\text{cr}} - N_f|}}. \quad (279)$$

This expression can be used to estimate the regime in which the corrections to the exponential scaling become subdominant. For this, we compute the minimum of the function

$$\frac{1}{|\Theta_0|} \ln |N_{f,\text{cr}} - N_f| + \frac{\pi}{2\epsilon\sqrt{|\alpha_1||N_{f,\text{cr}} - N_f|}} \quad (280)$$

with respect to $|N_{f,\text{cr}} - N_f|$. In accordance with Eq. (271), we assume $|N_{f,\text{cr}} - N_f| < 1$ here. From Eq. (280), we can then estimate that corrections to the exponential scaling behavior are subdominant as long as

$$|N_f - N_{f,\text{cr}}| \lesssim \frac{\pi^2 |\Theta_0|^2}{16\epsilon^2 |\alpha_1|}, \quad (281)$$

with ϵ being defined in Eq. (263). Thus, corrections to Miransky scaling due to the running of the gauge coupling are small when $|\Theta_0| \gg 1$ and large when $|\Theta_0| \ll 1$. In Sect. 6.5.4 we apply Eq. (281) to QCD to estimate the size of the regime in which the exponential scaling behavior dominates. We will see that the exponential scaling behavior is dominantly visible only very close to $N_{f,\text{cr}}$, provided that $N_{f,\text{cr}} \approx 12$. This implies that the Θ -dependent universal corrections are more significant in QCD.

The role of $|\Theta|$ for the scaling behavior close to $N_{f,\text{cr}}$ can also be understood by simply looking at the β_{g^2} function of the gauge coupling, see Fig. 17. For $|\Theta| \gg 1$, the gauge coupling runs very fast into its IR fixed point once it has passed g_{cr}^2 . Thus, the situation for $g^2 > g_{\text{cr}}^2$ is as close as possible to the situation studied in Sect. 6.3.1 where the coupling has been simply approximated by a constant. For $|\Theta| \ll 1$ the gauge coupling runs very slowly (“walks”) into its IR fixed point once it has passed g_{cr}^2 . This walking behavior for $g^2 \gtrsim g_{\text{cr}}^2$ then gives rise to sizable corrections to the exponential scaling behavior.

6.4 Scaling in Low-energy Models

In the previous sections we have stated that the dimensionless function $f_{\mathcal{O}}$ in the scaling law (278) can be computed explicitly with the aid of effective low-energy models. In the following we use the example of low-energy models of QCD to demonstrate that this is indeed the case. However, the subsequent analysis is by no means restricted to QCD. It can also be applied straightforwardly to other gauge theories, such as QED₃.

Let us now be explicit and compute the function $f_{\mathcal{O}}$ for the pion decay constant f_{π} . To this end, we employ a straightforward generalization of the simple ansatz (241) to QCD with N_f flavors. For the sake of the argument, it suffices to consider the large- N_c limit. Along the lines of our study in Sect. 5.2.2, it is then possible to derive a gap equation for the vacuum expectation value of the order parameter $\langle \sigma \rangle \equiv f_{\pi}$, see Ref. [78]. Here, we skip the details and only state that the resulting expression for $\langle \sigma \rangle$ is proportional to the square of the Yukawa coupling times a purely fermionic loop which yields a factor of $N_f N_c$, see also Eq. (244). This loop integral is UV divergent and needs to be regularized at an effective (regulator) scale Λ_H .

For momentum scales $p \lesssim \Lambda_H$, we expect a description in terms of such a hadronic low-energy model to be reasonable. We choose $\Lambda_H = c_{\text{reg}} k_{\text{SB}}$, where $c_{\text{reg}} \gtrsim 1$ is a numerical factor independent of N_f

and N_c . The gap equation for $\langle\sigma\rangle$ can then be solved straightforwardly and yields⁷¹

$$\langle\sigma\rangle \propto \sqrt{N_f N_c} k_0 \theta(N_{f,\text{cr}} - N_f) |N_{f,\text{cr}} - N_f|^{-\frac{1}{\Theta_0}} \exp\left(-\frac{\pi}{2\epsilon\sqrt{|\alpha_1||N_{f,\text{cr}} - N_f|}}\right), \quad (282)$$

where the last step holds near the conformal window, using the relation (277). Since $f_\pi \equiv \langle\sigma\rangle$, we have

$$f_{f_\pi}(N_f) = \sqrt{N_f}. \quad (283)$$

In the large- N_c approximation the N_f -scaling behavior of f_π and of the constituent quark mass m_ψ is identical. Following our discussion in Sect. 5.2.2, we also expect that m_ψ has a N_f -scaling behavior near $N_{f,\text{cr}}$ which is identical to that of the critical temperature $T_\chi \sim m_\psi$. The scaling behavior of other observables can be computed along these lines.

We would like to stress that the prefactor $\sqrt{N_f N_c}$ in the present example is an outcome of our large- N_c approximation of the low-energy sector. In general, we expect that any observable \mathcal{O} comes along with a complicated prefactor function $f_{\mathcal{O}}$ depending on the number of flavors N_f and N_c . The determination of this function, e. g. for the constituent mass, may become complicated, depending on the truncations made in the low-energy sector. However, we emphasize that the prefactor function is independent of $N_{f,\text{cr}}$ and therefore the N_f dependence coming from this function does not modify the $|N_f - N_{f,\text{cr}}|$ -scaling.

Finally we would like to add that the current quark mass is expected to modify the scaling relations away from the chiral limit. In order to study these modifications, a generalized Gell-Mann-Oakes-Renner relation based on the fixed-point scenario in many-flavor QCD has been advocated in Ref. [344]. Note that the scaling behavior of observables with the current quark mass in the (quasi-)conformal⁷² phase of strongly-flavored gauge theories is of particular interest for lattice simulations and currently under investigation, see Refs. [179, 180, 345].

6.5 Chiral $SU(N_c)$ Gauge Theories

In this section we review numerical RG studies of strongly-flavored $SU(N_c)$ gauge theories from first principles. In Ref. [29] the zero-temperature phase diagram in the (N_f, N_c) -plane has been computed using the functional RG. The phase diagram in the plane spanned by the temperature and N_f has first been computed in Refs. [30, 31]. In Sect. 6.5.1 we briefly review the RG setup. The various phase diagrams are then discussed in Sect. 6.5.2. In Sects. 6.5.3 and 6.5.4 we present a quantitative study of scaling close to the quantum critical point $N_{f,\text{cr}}$. This comprehensive analysis of scaling has first been performed in Ref. [79].

Before we begin with our discussion of strongly-flavored gauge theories, we would like to add a few words on the application of the Wetterich equation to gauge theories and, in particular, to QCD. The Wetterich equation has been employed for first-principles studies of QCD since the mid 1990s, where it started out with non-perturbative studies of the running of the gauge coupling [346], gluon condensation [118, 347] and the momentum dependence of Yang-Mills propagators [115, 116]. Since then these studies have been refined and further developed from a technical point of view (see Refs. [97, 104, 105, 108] for reviews) but also for the application to QCD phenomenology. Let us name a few examples. The running of the strong coupling has been computed on all scales at zero [348–350] and at finite temperature [30, 31]. The approach to chiral symmetry breaking, which we mainly review here, has been studied from first principles in Refs. [28–31]. Confinement has been investigated at zero [349, 350] as well as at finite temperature [151, 351–353]. In particular, the results for the deconfinement phase transition in Yang-Mills theories are in very good agreement with lattice simulations. Moreover, the interrelation of quark confinement and chiral symmetry breaking has been analyzed in Refs. [151, 275], and the question of gluon condensation has been recently revisited in Ref. [354]. Last but not least, the emergence of hadronic states in the IR limit

⁷¹ This can be most easily seen from a rescaling of the Yukawa coupling by a factor $\sqrt{N_f N_c}$.

⁷² Of course, conformal invariance is broken explicitly when we allow for a finite current quark mass. In this case, the theory never reaches the IR fixed point of the gauge coupling. However, the theory can still get close to the IR fixed-point of the gauge coupling for small quark masses and remain in its vicinity for a long RG time.

has been studied with so-called re-bosonization techniques in Refs. [28, 32]. These studies include a detailed discussion of how to bridge the gap between the fundamental degrees of freedom, namely quarks and gluons, and hadronic degrees of freedom as, e. g., described by low-energy QCD models. These studies have recently motivated further studies in this direction for QCD with two colors [355].

6.5.1 Renormalization Group Approach to Gauge Theories

In Refs. [29–31] the RG flow of QCD starting from quarks and gluons has been studied employing a covariant derivative expansion. A crucial ingredient for chiral symmetry breaking are the scale-dependent gluon-induced quark self-interactions of the type included in Eq. (257). We note that dynamical quarks influence the RG flow of QCD by qualitatively different mechanisms. First, quark fluctuations directly modify the running of the gauge coupling due to the screening nature of these fluctuations. On the other hand, gluon exchange between quarks induces quark self-interactions which can become relevant operators in the IR, as we have already discussed in the previous sections. These two mechanisms strongly influence each other as well. As we have seen, however, it is possible to disentangle the system once we accept that these fluctuations can be associated with different scales in the problem.

In the following we shall restrict ourselves to $d = 4$ Euclidean space-time dimensions at vanishing temperature and work solely in the Landau gauge which is known to be a fixed point of the RG flow [115, 356]. Our strategy to study phases of strongly-interacting gauge theories is now the same as applied before in the context of fermionic models: we consider the point-like limit and restrict our discussion to the RG flow in the chirally symmetric regime. This does not provide us with a direct access to the hadronic mass spectrum at low energies. However, it already allows us to map various phase diagrams in a clean and very controlled way. In fact, it has been explicitly shown in Ref. [29] that the point-like limit is a reasonable approximation in the chirally symmetric regime, where the regularization-scheme independence of universal quantities has been found to hold remarkably well in this limit.

For our study, we employ the following ansatz for the effective action which represents the lowest nontrivial order in a consistent and systematic operator expansion, see Ref. [152] and also Refs. [29–31]:

$$\Gamma_k = \int d^4x \left\{ \frac{1}{4} F_{\mu\nu}^a F_{\mu\nu}^a + \bar{\psi}(i\partial + \bar{g}A)\psi + \frac{1}{2} [\bar{\lambda}_-(V-A) + \bar{\lambda}_+(V+A) + \bar{\lambda}_\sigma(S-P) + \bar{\lambda}_{VA}[2(V-A)^{\text{adj}} + (1/N_c)(V-A)]] \right\} + \Gamma_k^{\text{gauge}}. \quad (284)$$

We do not further specify Γ_k^{gauge} since it is of no relevance of what follows. We only state that Γ_k^{gauge} contains the gauge-fixing term and the ghost terms as well as it may also contain higher gluonic operators, e. g., of the type $\sim (F_{\mu\nu}^a F_{\mu\nu}^a)^n$, see e. g. Refs. [30, 31, 118, 347, 348]. For details and reviews on gauge theories we refer the reader to Refs. [97, 104, 105, 108].

The ansatz (284) for the effective action represents a straightforward generalization of the Fierz-complete ansatz (220) for the matter sector, see Sect. 5.2.1 for a detailed discussion. The definition of the four-fermion interaction channels can be found in Eqs. (221)–(223). This ansatz falls into the QCD universality class when we set the various four-fermion interactions to zero at the initial RG scale, e. g. at the Z-boson mass scale.

In our analysis, we neglect $U_A(1)$ -violating interactions induced by topologically non-trivial gauge configurations since we expect them to become relevant only inside the χ SB regime or for small N_f . In addition, the lowest-order $U_A(1)$ -violating term schematically is $\sim (\bar{\psi}\psi)^{N_f}$, see e. g. Refs. [269–273]. Thus, larger N_f correspond to larger RG “irrelevance” by naive power-counting. Moreover, interactions of the type $\sim (\bar{\psi}\psi)^{N_f}$ for $N_f > 3$ do not contribute directly to the flow of the four-fermion interactions due to the one-loop structure of the underlying RG equation for the effective action, as discussed in Sect. 3.

Using the truncated effective action (284), we obtain the following β functions for the dimensionless couplings $\lambda_i = \bar{\lambda}_i/k^2$, see Refs. [29, 152]:

$$\begin{aligned} \partial_t \lambda_- &= 2\lambda_- - 4v_4 l_{1,1}^{(\text{FB}), (4)} \left[\frac{3}{N_c} g^2 \lambda_- - 3g^2 \lambda_{\text{VA}} \right] - \frac{1}{8} v_4 l_{1,2}^{(\text{FB}), (4)} \left[\frac{12 + 9N_c^2}{N_c^2} g^4 \right] \\ &\quad - 8v_4 l_1^{(\text{F}), (4)} \left\{ -N_f N_c (\lambda_-^2 + \lambda_+^2) + \lambda_-^2 - 2(N_c + N_f) \lambda_- \lambda_{\text{VA}} + N_f \lambda_+ \lambda_\sigma + 2\lambda_{\text{VA}}^2 \right\}, \end{aligned} \quad (285)$$

$$\begin{aligned} \partial_t \lambda_+ &= 2\lambda_+ - 4v_4 l_{1,1}^{(\text{FB}), (4)} \left[-\frac{3}{N_c} g^2 \lambda_+ \right] - \frac{1}{8} v_4 l_{1,2}^{(\text{FB}), (4)} \left[-\frac{12 + 3N_c^2}{N_c^2} g^4 \right] \\ &\quad - 8v_4 l_1^{(\text{F}), (4)} \left\{ -3\lambda_+^2 - 2N_c N_f \lambda_- \lambda_+ - 2\lambda_+ (\lambda_- + (N_c + N_f) \lambda_{\text{VA}}) \right. \\ &\quad \left. + N_f \lambda_- \lambda_\sigma + \lambda_{\text{VA}} \lambda_\sigma + \frac{1}{4} \lambda_\sigma^2 \right\}, \end{aligned} \quad (286)$$

$$\begin{aligned} \partial_t \lambda_\sigma &= 2\lambda_\sigma - 4v_4 l_{1,1}^{(\text{FB}), (4)} [6C_2(N_c) g^2 \lambda_\sigma - 6g^2 \lambda_+] - \frac{1}{4} v_4 l_{1,2}^{(\text{FB}), (4)} \left[-\frac{24 - 9N_c^2}{N_c} g^4 \right] \\ &\quad - 8v_4 l_1^{(\text{F}), (4)} \left\{ 2N_c \lambda_\sigma^2 - 2\lambda_- \lambda_\sigma - 2N_f \lambda_\sigma \lambda_{\text{VA}} - 6\lambda_+ \lambda_\sigma \right\}, \end{aligned} \quad (287)$$

$$\begin{aligned} \partial_t \lambda_{\text{VA}} &= 2\lambda_{\text{VA}} - 4v_4 l_{1,1}^{(\text{FB}), (4)} \left[\frac{3}{N_c} g^2 \lambda_{\text{VA}} - 3g^2 \lambda_- \right] - \frac{1}{8} v_4 l_{1,2}^{(\text{FB}), (4)} \left[-\frac{24 - 3N_c^2}{N_c} g^4 \right] \\ &\quad - 8v_4 l_1^{(\text{F}), (4)} \left\{ -(N_c + N_f) \lambda_{\text{VA}}^2 + 4\lambda_- \lambda_{\text{VA}} - \frac{1}{4} N_f \lambda_\sigma^2 \right\}. \end{aligned} \quad (288)$$

Here, $C_2(N_c) = (N_c^2 - 1)/(2N_c)$ is a Casimir operator of the gauge group, and $v_4 = 1/(32\pi^2)$. The definition of the threshold functions $l_1^{(\text{F}), (4)} = l_1^{(\text{F}), (4)}(0; 0)$, $l_{1,2}^{(\text{FB}), (4)} = l_{1,2}^{(\text{FB}), (4)}(0, 0; 0, \eta_A)$ and $l_{1,1}^{(\text{FB}), (4)} = l_{1,1}^{(\text{FB}), (4)}(0, 0; 0, \eta_A)$ can be found in App. D. Recall that η_ψ vanishes in the point-like limit in Landau gauge. In the numerical analysis of these flow equations, which we present below, we have dropped the contributions from the anomalous dimensions of the gauge coupling $\eta_A = \beta_{g^2}/g^2$. This is justified since it has been found in Ref. [79] that the contributions $\propto \eta_A$ in the threshold functions do not strongly affect the results for $N_{f,\text{cr}}$. This can be also understood from an analytic point of view: we have $\eta_A \rightarrow 0$ for $N_f \rightarrow N_f^{\text{a.f.}}$ and $g^2 < g_*^2$. Moreover, we can estimate η_A with the aid of the β_{g^2} function in the $\overline{\text{MS}}$ scheme. We find for $g^2 < g_*^2$ that $|\eta_A^{2\text{-loop}}| \lesssim 1$ for $N_f \gtrsim 11$ and $|\eta_A^{4\text{-loop}}| \lesssim 0.5$ for $N_f \gtrsim 8$. For our purposes, we therefore expect that these contributions may lead to quantitative corrections at most on the percent level. However, these terms may become relevant for small N_f and in the regime with broken chiral symmetry where we have $\eta_A \sim \mathcal{O}(1)$.

Let us now further discuss the running of the gauge coupling. As mentioned above, the running coupling has been computed within the functional RG approach [30, 31, 346, 348, 349]. However, we will closely follow the analysis in Ref. [79] and employ for simplicity the two- and four-loop result obtained in the $\overline{\text{MS}}$ scheme [357, 358]. This is justified since our results for the phase boundary show a satisfactory convergence in the large- N_f regime. In the following we will often restrict ourselves to the two-loop β_{g^2} function, see Eq. (250), as it already shows all qualitative features and can be dealt with analytically.

At this point a critical comment on the scheme dependence is in order: The chosen regularization scheme in the matter sector and the $\overline{\text{MS}}$ scheme do not coincide. This inconsistency results in an error for the estimate for the critical number of quark flavors, i. e. for the location of the quantum critical point. Since we are interested in the scaling behavior which is related to the universal critical exponent Θ rather than in a high-precision determination of $N_{f,\text{cr}}$, our results are only influenced indirectly by this approximation.⁷³ Therefore the results using the four-loop running may not necessarily be considered as a more precise calculation. Instead, the difference between two-loop and four-loop $\overline{\text{MS}}$ results should be

⁷³ Of course, the actual value of $\Theta_0 = \Theta(N_{f,\text{cr}})$ depends on the actual value of $N_{f,\text{cr}}$ which itself, as a universal quantity, depends on the difference of the scheme-dependent quantities g_{cr}^2 and g_*^2 .

viewed as an estimate of the dependence of our results on the quantitative details of the running gauge sector.

We close this section with a comment on gauge symmetry. Here, a subtlety becomes important. Naively, one may expect that the running of the gauge coupling is modified due to the presence of finite four-fermion couplings. In fact, it is possible to construct a 1PI diagram $\sim g\lambda_i$ with one external gluon line and two external fermion lines which potentially contributes to the running of the quark-gluon vertex $\sim g\bar{\psi}A\psi$. Now a detailed analysis shows that the question of gauge invariance is intimately linked to the existence of such contributions $\sim g\lambda_i$ to the running of the gauge coupling: To render the RG flow gauge invariant we have to take into account regulator-dependent Ward-Takahashi identities [346, 359]. In the present case, these symmetry constraints yield contributions to the running of the gauge coupling which depend on the quark self-interactions:

$$\partial_t g^2 = \beta_{g^2} - 4v_4 l_1^{(F),(4)} \frac{g^2}{1 - 2v_4 l_1^{(F),(4)} \sum c_i \lambda_i} \sum c_i \partial_t \lambda_i, \quad (289)$$

where $i \in \{\sigma, +, -, \text{VA}\}$ and β_{g^2} denotes the standard β_{g^2} function, e. g. in the two-loop approximation. The dimensionless factors c_i are given by

$$c_\sigma = 1 + N_f, \quad c_+ = 0, \quad c_- = -2, \quad c_{\text{VA}} = -2N_f. \quad (290)$$

Apparently, the additional contributions on the right-hand side of Eq. (289) are proportional to the β -functions of the four-fermion couplings and therefore vanish as long as the four-fermion couplings are at their fixed points, i. e. as long as $g^2 \leq g_{\text{cr}}^2$; this has first been pointed out in Refs. [29, 152]. We conclude that these contributions $\propto \lambda_i$ do not alter the scaling law (277) in leading order.⁷⁴ In particular, the power-law behavior is unaffected by these corrections arising due to symmetry constraints. In the following we ignore these corrections in our numerical analysis.

In the regime with broken chiral symmetry in the ground state, the λ_i -dependent contributions may alter the running of the gauge coupling. However, the fermions acquire a finite mass and diagrams with at least one internal fermion line are expected to be suppressed compared to diagrams with no internal fermion lines: $l_1^{(F),(4)}(\epsilon_\psi; \eta_\psi) \rightarrow 0$ in the limit of a large dimensionless fermion mass ϵ_ψ . In any case, we are not aiming at a study of the properties of QCD inside the broken regime but rather intend to map the phases of strongly-interacting gauge theories by determining the parameter sets (N_f, N_c) for which the system remains in the chirally symmetric regime.

6.5.2 Phases of Strongly-flavored $\text{SU}(N_c)$ Gauge Theories

Now we discuss phases of strongly-flavored gauge theories at zero and finite temperature. To simply determine the size of the conformal window at zero temperature, it suffices to consider the approximation of a constant gauge coupling:

$$\partial_t g^2 = 0.$$

As discussed in Sect. 6.3.1, the gauge coupling can then be considered as an “external” N_f -dependent parameter of the theory. To estimate the error of our truncation in the gauge sector, we choose the fixed-point value of the gauge-coupling at two-loop and four-loop level as the external parameter. This value corresponds to the largest possible IR value of the coupling inside of the conformal window. For illustration, we give the fixed-point value at two-loop level which assumes a simple form:

$$g_{*,2\text{-loop}}^2(N_f) = \frac{16(11N_c^2 - 2N_c N_f)\pi^2}{13N_c^2 N_f - 34N_c^3 - 3N_f}. \quad (291)$$

⁷⁴ In addition to the discussed next-to-leading order corrections to Eq. (277), these symmetry constraints may shift the fixed-point value g_*^2 of the gauge coupling and therefore cause additional higher-order corrections to the scaling law (277).

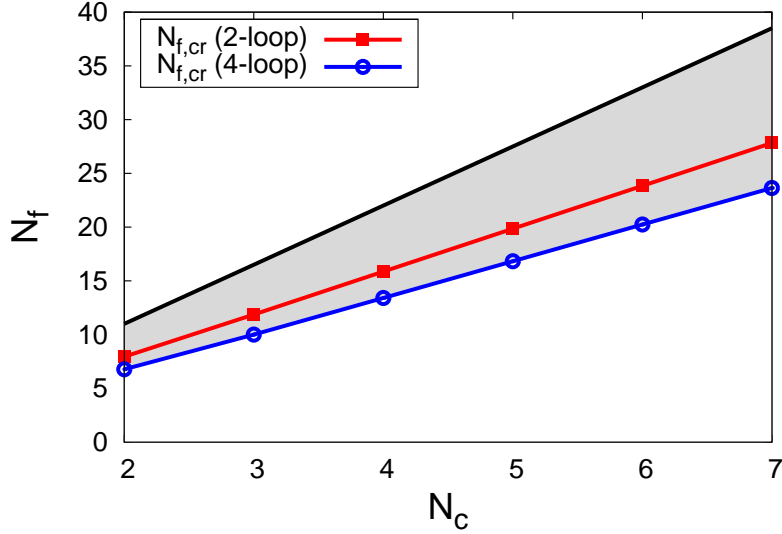


Fig. 18 Phase diagram of strongly-flavored $SU(N_c)$ gauge theories in the (N_f, N_c) -plane, see also Ref. [29]. The upper solid (black) line gives the value of N_f at which asymptotic freedom is lost, $N_f^{\text{af.}} = \frac{11}{2}N_c$. The shaded area depicts the conformal window in the approximation with a running gauge coupling at four-loop level. The result for $N_{f,\text{cr}}$ as obtained from a running coupling at two-loop level is given by the red line. We observe that the conformal window is increased when we employ the gauge coupling in the four-loop approximation instead of the two-loop approximation.

In the matter sector we employ two different truncations to which we refer as *one-channel* and *all-channels* approximation. The latter one is Fierz complete, i. e. we take into account the full set of flow equations (285)-(288). In the one-channel approximation, on the other hand, we only take into account the RG flow of the scalar-pseudoscalar channel λ_σ and set all other four-fermion couplings to zero:

$$\partial_t \lambda_\sigma = 2\lambda_\sigma - \frac{N_c}{4\pi^2} \lambda_\sigma^2 - \frac{3}{4\pi^2} C_2(N_c) \lambda_\sigma g^2 - \frac{3}{256\pi^2} \left(\frac{9N_c^2 - 24}{N_c} \right) g^4. \quad (292)$$

While the all-channels approximation can only be dealt with numerically, the one-channel approximation together with the two-loop gauge-coupling fixed-point allows for analytic estimates for $N_{f,\text{cr}}$ and the scaling behavior close to the (quantum) phase transition. It is worth mentioning that the RG flow of the λ_σ -coupling decouples from the other channels in the large- N_c limit, see Sect. 5.2.1. Recall that the associated (S-P)-channel is Fierz-equivalent to the interaction channel included in widely used QCD low-energy models, e. g. the quark-meson model.

For illustration, we first compute the critical value of the gauge coupling in the one-channel approximation using the value of the IR fixed point of the two-loop gauge-coupling. We find

$$g_{\text{cr,one}}^2 = \frac{32\pi^2 \left(2N_c^3 - 2N_c - \sqrt{3N_c^6 - 8N_c^4} \right)}{3(4 + N_c^4)} \Big|_{(N_c=3)} \approx 10.86, \quad (293)$$

which does not depend on N_f . In the all-channels approximation the critical value has to be computed numerically. As found in Ref. [29], the resulting critical value $g_{\text{cr,all}}^2$ of the gauge coupling then depends on N_f : for a given number of colors, $g_{\text{cr,all}}^2$ decreases slightly with increasing N_f .

The fixed-point value $g_{*,2\text{-loop}}^2$ together with the critical value of the gauge coupling can be used to estimate the critical number of quark flavors above which there is no chiral symmetry breaking in the IR.

N_c	2	3	4	5	6	7
$N_{f,cr}^{one}$	7.6	11.7	15.7	19.7	23.6	27.6
$N_{f,cr}^{all}$	7.9	11.9	15.9	19.9	23.8	27.8
$N_{f,cr}^{4-loop}$	6.8	10.0	13.4	16.8	20.2	23.6
ΔN_f^{2-loop}	0.36	0.27	0.31	0.36	0.42	0.48

Table 2 Critical number of flavors $N_{f,cr}$ for various values of N_c as obtained from different approximations: one-channel approximation with two-loop running gauge coupling ($N_{f,cr}^{one}$), all-channels approximation with two-loop running gauge coupling ($N_{f,cr}^{all}$), and all-channels approximation with four-loop running gauge coupling ($N_{f,cr}^{4-loop}$). The difference between $N_{f,cr}^{all}$ and $N_{f,cr}^{4-loop}$ can be considered as an error estimate for the uncertainty arising due to the truncated gauge sector in our study. In the bottom row, we give estimates for the size of the regime in which the exponential scaling behavior dominates. These estimates have been obtained from Eq. (281) by using the one-channel approximation together with a two-loop running gauge coupling. We observe that ΔN_f^{2-loop} increases only slightly with N_c , i. e. $(\Delta N_f^{2-loop})/N_c \ll 1$.

In accordance with the numerical results given in Ref. [29], we find [79]

$$N_{f,cr}^{one} = \frac{169N_c^6 - 136N_c^4 + 132N_c^2 - 68\sqrt{N_c^4(3N_c^2 - 8)}N_c^3}{58N_c^5 - 64N_c^3 - 26\sqrt{N_c^4(3N_c^2 - 8)}N_c^2 + 6\sqrt{N_c^4(3N_c^2 - 8)} + 36N_c} \stackrel{(N_c=3)}{\approx} 11.7 \quad (294)$$

for the one-channel approximation. In the all-channels approximation we obtain

$$N_{f,cr}^{all} \approx 11.9 \quad (295)$$

for $N_c = 3$. We may use our analytic estimate for $N_{f,cr}$ from the one-channel approximation to estimate $N_{f,cr}$ in the limit $N_c \rightarrow \infty$:

$$\frac{N_{f,cr}^{one}}{N_c} = \frac{68\sqrt{3} - 169}{2(13\sqrt{3} - 29)} \approx 4.0. \quad (296)$$

For the all-channels approximation with a running coupling in the two-loop and four-loop approximation, we find numerically that $N_{f,cr}^{all}/N_c \approx 4.0$ and $N_{f,cr}/N_c \approx 3.4$ for large values of N_c , respectively, see Tab. 2. These results for $N_{f,cr}$ are in accordance with the results from Dyson-Schwinger equations in the rainbow-ladder approximation, see e. g. Refs. [85, 309, 342], as well as with those from current lattice simulations [318–331].

In Fig. 18 we show the zero-temperature phase diagram of strongly-flavored $SU(N_c)$ gauge theories in the (N_f, N_c) -plane, see also Tab. 2. Within the RG framework this phase diagram has first been computed in Ref. [29]. The upper solid (black) line represents the boundary at which asymptotic freedom is lost. The shaded area depicts the conformal window. We observe that the absolute size of the conformal window increases with N_c . However, the relative size $(N_f^{a.f.} - N_{f,cr})/N_f^{a.f.} \approx 3/11$ is approximately independent of N_c . In addition, we find that the size of the conformal window is increased when we employ a running coupling in the four-loop approximation instead of the two-loop approximation. To be specific, we obtain

$$N_{f,cr}^{4-loop} \approx 10.0 \quad (297)$$

for $N_c = 3$ in the all-channels approximation and $N_{f,cr}^{4-loop} \approx 9.8$ in the one-channel approximation, in agreement with Ref. [29]. The difference between the two-loop and four-loop result can be viewed as an error estimate for the uncertainty arising due to the truncated gauge sector in our study. In addition to a test of the uncertainty in the gauge sector, the regularization scheme in the matter sector has been varied in Ref. [29]. Such a variation leaves its imprint in the estimate for the critical value g_{cr}^2 . It turns out that the present truncation is remarkably stable under a variation of the scheme which instills further confidence in our present approach. To be specific, one finds $N_f^{cr} = 10.0_{-0.7}^{+1.6}$ for $N_c = 3$ from a variation of the

β -function of the gauge coupling and the regularization scheme.⁷⁵ This is in accordance with another RG study of the conformal phase transition in which the running gauge coupling has not been treated as an “external” input but computed within the exactly same scheme as the matter sector [30, 31].

We would like to add that the phase diagram shown in Fig. 18 is also in accordance with the phase diagram found by Dietrich and Sannino with Dyson-Schwinger equations in the rainbow-ladder approximation [85]. On the present level of accuracy of lattice simulations, the results for this phase diagram go well together with those from functional RG approaches [29–31] and Dyson-Schwinger approaches, see e. g. Refs. [85, 342].

Finally, we would like to discuss the finite-temperature many-flavor phase boundary in QCD. In Fig. 19 we show the chiral phase transition temperature T_χ as a function of the number of massless quark flavors N_f . This phase diagram has been computed for the first time in Refs. [30, 31]. The results are in accordance with those obtained more recently with the aid of Dyson-Schwinger equations in the rainbow-ladder approximation [343]. We do not discuss the details related to these computations here but only name the basic ingredients which have entered the RG study. First of all, the truncation in the matter sector is identical to the one discussed in Sect. 6.5.1. The resulting flow equations (286)-(288) have been straightforwardly generalized to finite temperature. Further four-fermion operators, which may arise at finite temperature due to the broken Poincare invariance, have been neglected for the sake of simplicity. This appears to be a reasonable approximation for large N_f where T_χ becomes small and eventually approaches zero at the quantum critical point $N_{f,cr}$. Moreover, the chiral symmetry breaking scale was found to be larger than the phase transition temperature for small N_f . Therefore these additional four-fermion operators are expected to be parametrically suppressed in the chirally symmetric regime.⁷⁶ The second important ingredient is the running of the gauge coupling at finite temperature which has been computed self-consistently within the functional RG framework in Refs. [30, 31]. It was found that the running coupling (in Landau-DeWitt gauge) remains finite on all scales at finite temperature and approaches the fixed point of the underlying $3d$ Yang-Mills theory in the IR limit. We stress that a naive generalization of the *perturbative* zero-temperature running of the gauge coupling is bound to fail since the quarks decouple in the IR limit due their antiperiodic boundary conditions in Euclidean time direction. Thus, we have effectively $N_f \rightarrow 0$ at finite temperature for $k \rightarrow 0$ and we are left with the pure gauge coupling, even in the (quasi) conformal phase.⁷⁷

Let us now discuss the phase diagram in Fig. 19 from a physical point of view. In order to compute this diagram, the scale has been fixed at the τ -mass scale to the same value for all N_f , see discussion in Sect. 6.2. Due to the finite temperature of the system, the critical coupling g_{cr}^2 inherits a T -dependence from the quark modes which acquire a thermal (Matsubara) mass. This leads to a quark decoupling, requiring stronger interactions for critical quark dynamics. In Fig. 16 this is indicated by the λ_i -parabolas becoming broader with a higher maximum. Hence, the annihilation of the Gaussian fixed point by pushing the parabola below the λ_i axis requires a larger gauge coupling. It follows that $g_{cr}^2(T/k) \geq g_{cr}^2(0)$.

At zero temperature and for small N_f , the IR fixed point g_*^2 is far larger than g_{cr}^2 . Hence QCD is in the phase with broken chiral symmetry. For increasing T , the temperature dependence of the coupling and that of g_{cr}^2 compete with each other. In accordance with our analytic estimate in Sect. 6.2 we observe an almost linear decrease of the critical temperature for small but increasing N_f with a slope of $\Delta T_\chi = T_\chi(N_f) - T_\chi(N_f + 1) \approx 25 \text{ MeV}$ at small N_f . The predicted relative difference for T_χ for $N_f = 2$ and 3 flavors of $2\Delta T_\chi / (T_\chi(N_f = 2) + T_\chi(N_f = 3)) \simeq 0.146$ is in good agreement with lattice studies [339]. We conclude that the shape of the phase boundary for small N_f is basically dominated by fermionic screening.

For the case of large flavor numbers, which is of particular interest here, the critical temperature decreases further and the phase transition line terminates at the zero-temperature quantum phase transition at

⁷⁵ Note that a variation of the β function of the gauge coupling can be effectively considered as a variation of the truncation in the gauge sector.

⁷⁶ Note that $T/k \gtrsim 1$ corresponds to large temperatures in the RG flow, whereas $T/k < 1$ corresponds to low temperatures.

⁷⁷ At finite temperature conformality is broken.

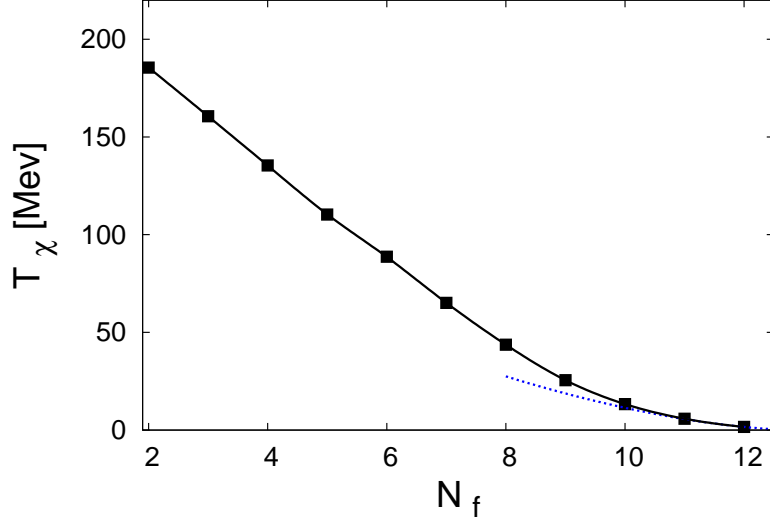


Fig. 19 Chiral phase transition temperature T_χ as a function of the number of massless quark flavors N_f for $N_f \geq 2$, as obtained in Ref. [31]. Strictly speaking, the shown results for T_χ only represent an upper bound for the (exact) chiral phase transition temperature due to the presence of potentially strong fluctuations of the Nambu-Goldstone modes in the (deep) IR sector of the theory, see main text for a detailed discussion. The flattening at $N_f \gtrsim 10$ is a consequence of the IR fixed-point structure. The dotted line depicts the power-law scaling behavior near $N_{f,\text{cr}}$, see Eq. (298).

$N_{f,\text{cr}}$, representing the lower end of the conformal window. Within the approximations in Refs. [30,31] one finds that $N_{f,\text{cr}} \approx 12.9$ and $|\Theta_0| \approx 0.71$ for $N_f = N_{f,\text{cr}}$; the discrepancy to the above given zero-temperature study can be essentially traced back to the differences in the running of the gauge coupling.

In Refs. [30, 31] it was found that the scaling of the phase boundary for large N_f is consistent with the pure power-law scaling behavior (272), as depicted by the dotted line in Fig. 19:

$$T_\chi \sim k_0 |N_{f,\text{cr}} - N_f|^{\frac{1}{|\Theta_0|}}. \quad (298)$$

From our discussion of scaling behavior this result is understandable, since the exponential scaling behavior sets in only very close to $N_{f,\text{cr}}$ and thus remains invisible in numerical fits over a wider N_f -range, see Eq. (281). Of course, our analytic estimate for the scaling behavior of T_χ still remains an upper bound, even if we took into account the exponential factor in Eq. (278). This is due to the fact that strong fluctuations of Nambu-Goldstone modes in the IR may yield further corrections and lower the phase transition temperature, see e. g. Ref. [33]. Whether these corrections at finite temperature yield additional corrections to the scaling behavior cannot be answered within the scaling analysis presented here.⁷⁸ However, it may very well be that such corrections depend only on N_f but not on $N_{f,\text{cr}}$.

We emphasize that further investigations of the finite-temperature scaling behavior close to the *quantum critical point*, $N_f = N_{f,\text{cr}}$, is worthwhile. In particular, a study of the order of the nature of the finite-temperature phase transition seems to be rewarding since it may provide us with deep insights into the underlying chiral dynamics. An analysis in this direction based on RG arguments has been performed by Wilczek and Pisarski [226]. In Fig. 20 we show a sketch of the many-flavor phase diagram which is inspired by our RG results depicted in Fig. 19. For our discussion we shall assume that the number of massless quark flavors can be indeed considered as a continuous control parameter. In the limit $N_f \rightarrow 0$ we are left with a pure $SU(N_c)$ gauge theory. In this regime we do not have any chiral quark dynamics but only a deconfinement phase transition. For $0 < N_f \lesssim 2$, we then expect a crossover rather than an actual chiral

⁷⁸ We would naively expect that corrections to Eq. (298) can be only resolved in lattice simulations with very small masses for the pseudo Nambu-Goldstone modes and on very large lattice sizes.

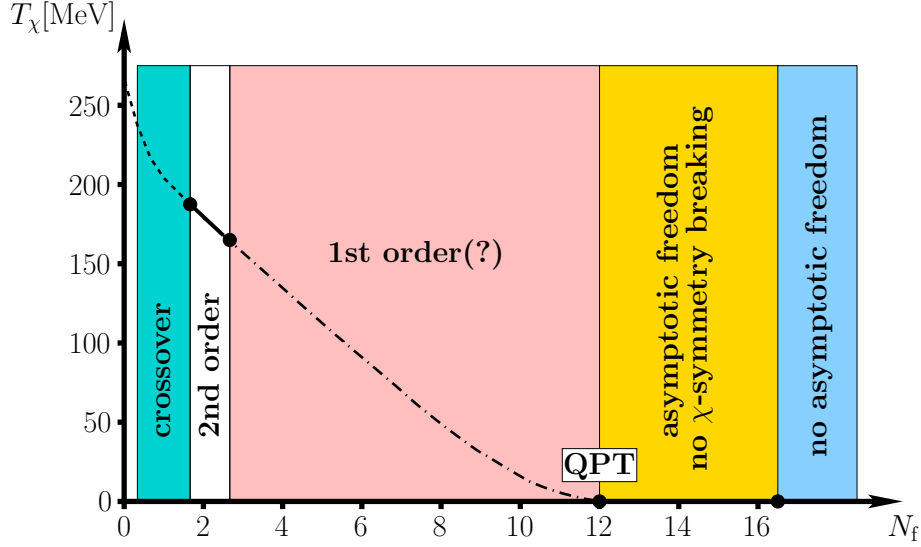


Fig. 20 Sketch of the many-flavor QCD phase diagram (for massless quark flavors). For $N_f < N_{f,\text{cr}} (\sim 12)$, we have different regimes which are distinguished by the nature of the chiral phase transition. At $N_f = N_{f,\text{cr}}$, the system undergoes a quantum phase transition (QPT). For $N_{f,\text{cr}} \leq N_f \leq (11/2)N_c = 16.5$ (conformal window), there is no chiral symmetry breaking in the IR limit but the theory is still asymptotically free.

phase transition.⁷⁹ This can be understood from a consideration of the lowest-order $U_A(1)$ -violating term(s) which are schematically given by $\sim (\bar{\psi}\psi)^{N_f}$, see e. g. Refs. [269–272]. For $N_f = 1$, such terms associated with topologically non-trivial gauge transformations act as a mass term for the quark fields which explicitly breaks the chiral symmetry. The associated crossover line (dashed line in Fig. 20) is expected to end at some point below $N_f = 2$. For $N_f = 2$, QCD is assumed to fall in the $O(4)$ universality class [226]. Recent lattice QCD data seem to be compatible with a second-order chiral phase transition for two massless quark flavors and $O(4)$ scaling behavior at the phase boundary [360–363]. The second-order phase transition line then most likely terminates in a “critical endpoint” close to $N_f \lesssim 3$. For $N_f = 3$, evidence for a chiral first-order phase transition has been found in lattice QCD simulations, see e. g. Refs. [364–367]. For larger values of N_f , only little is known about the nature of the phase transition. As discussed above, the role of $U_A(1)$ -violating terms $\sim (\bar{\psi}\psi)^{N_f}$ is probably subleading for $N_f \gtrsim 3$. From a simple “entropy” argument, it seems reasonable to expect that the chiral phase transition is also of first order: The order of the phase transition is (strongly) sensitive to the mismatch in the number of dynamical degrees of freedom below and above the chiral phase transition. Once the number of massless flavors N_f exceeds some “critical” value for a given N_c , this mismatch potentially triggers a discontinuous behavior in the associated order parameter. This type of argument is similar to arguments which seem to hold in studies of, e. g., the nature of the deconfinement transition in pure gauge theories [353, 368, 369]. In these studies it has been found that the order of the deconfinement phase transition changes from second to first order when the dimension of the gauge group is increased. In any case, the line of first-order phase transitions hits the quantum critical point at $T = 0$ for $N_f \rightarrow N_{f,\text{cr}}$ ($N_{f,\text{cr}} \approx 12$ in Fig. 20). We stress that the phase transition in N_f -direction at $T = 0$ is expected to be continuous, whereas the phase transition in temperature direction for $N_f \lesssim N_{f,\text{cr}}$ is presumably of first order. For $N_{f,\text{cr}} \leq N_f \leq (11/2)N_c = 16.5$, we are then in the conformal phase (regime) in which the theories are asymptotically free but we do not have chiral symmetry breaking in the IR limit.

⁷⁹ We add that a generalization of ’t Hooft vertices to non-integer values of N_f may not be unique.

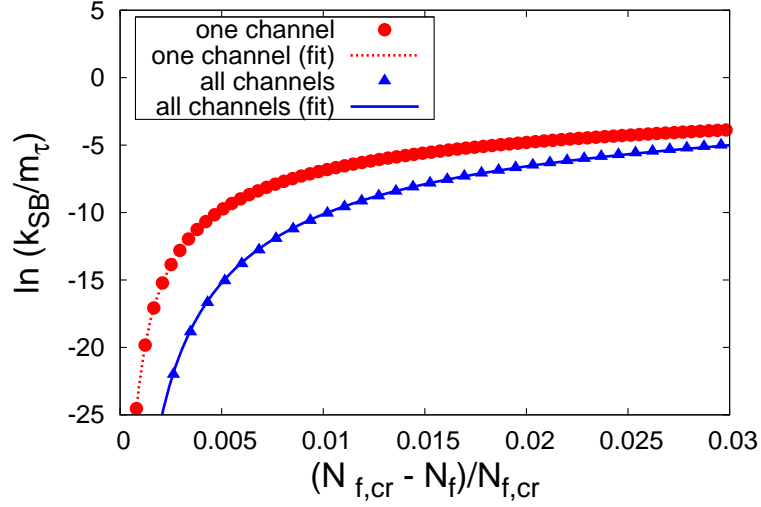


Fig. 21 Logarithm of the (chiral) symmetry-breaking scale $\ln(k_{\text{SB}}/m_\tau)$ as a function of the relative distance $(N_{f,\text{cr}} - N_f)/N_{f,\text{cr}}$ from the quantum critical point for an N_f -dependent but scale-independent, i.e. constant gauge coupling. The corresponding fits are given in Eq. (300). The figure has been taken from Ref. [79].

At vanishing temperature, the analysis of the scaling behavior of IR observables is simplified compared to a scaling analysis at finite temperature since dimensional reduction does not set in in the deep IR enhancing the Nambu-Goldstone modes. In the next two sections we shall therefore restrict ourselves to a quantitative analysis of scaling at vanishing temperature.

6.5.3 Miransky Scaling

In the previous section we have computed the critical number of quark flavors $N_{f,\text{cr}}$ as a function of N_c . To this end, it was not necessary to know the details of the running of the strong coupling g^2 . In the following we are interested in a quantitative study of the N_f -scaling behavior of the symmetry breaking scale k_{SB} close to the quantum critical point as encountered when the running of the gauge coupling is ignored,

$$\partial_t g^2 = 0.$$

To be precise, we shall consider a scenario in which the gauge coupling has assumed its IR fixed point value g_*^2 for some N_f with $N_f < N_f^{\text{a.f.}}$ but $N_f \gtrsim N_{f,\text{cr}}$. The fixed-point coupling then plays the role of an “external” parameter of the theory which can be changed by varying N_f and/or N_c . This allows us to increase the fixed-point coupling above the critical value g_{cr}^2 required for chiral symmetry breaking. In Sect. 6.3.1 we have analyzed analytically the scaling behavior of physical observables for such a setup. For our quantitative study below, we employ the fixed-point value of the gauge-coupling at two-loop level. Moreover, we restrict our quantitative analysis of exponential scaling behavior to the specific case $N_c = 3$.

In Fig. 21 we show the results for $\ln(k_{\text{SB}}/\Lambda)$ as function of $(N_{f,\text{cr}} - N_f)/N_f$ as obtained from the one-channel (dots) and from the all-channels (triangles) approximation using $g_{*,2\text{-loop}}^2$ as a fixed input parameter.⁸⁰ As initial conditions for the λ_i 's for a given $g_{*,2\text{-loop}}^2(N_f)$ we have used the solution of the coupled set of linear equations

$$\frac{\partial(\partial_t \lambda_i)}{\partial \lambda_i} = 0, \quad (299)$$

⁸⁰ Recall that the all-channels approximation is Fierz complete, while we only take into account the RG flow of the scalar-pseudoscalar channel λ_σ in the one-channel approximation and set all other four-fermion couplings to zero.

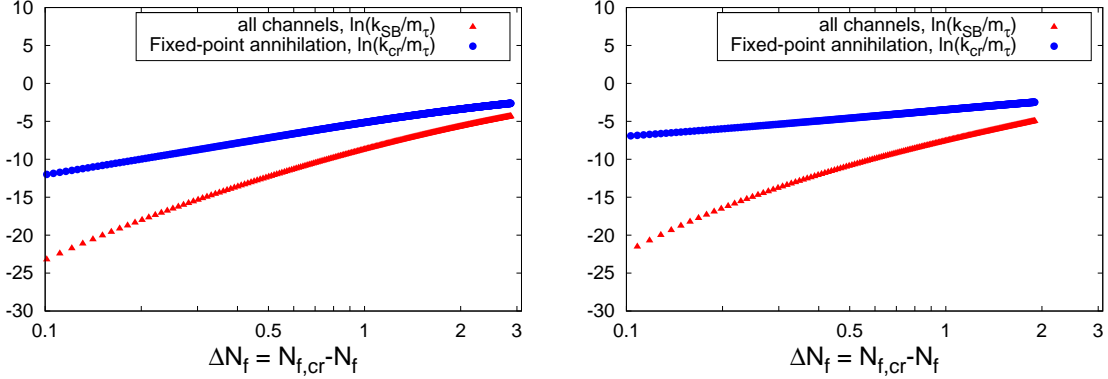


Fig. 22 Left panel: Double-logarithmic plot of N_f dependence of k_{cr} and k_{SB} as obtained from a study with a running coupling in the two-loop approximation. The criticality scale k_{cr} (blue circles) is dominated by power-law scaling (straight line with slope $\sim |\Theta_0|^{-1}$ in this double-log plot), and clearly serves as an upper bound for the symmetry breaking scale k_{SB} (red triangles), being a superposition of power-law and Miransky scaling. If the theories are probed at integer N_f , i.e., $\Delta N_f \gtrsim \mathcal{O}(1)$, the contribution due to Miransky scaling may not be visible. Right panel: Double-logarithmic plot of N_f dependence of k_{cr} and k_{SB} as obtained from a study with a running gauge coupling in the four-loop approximation. The contributions due to Miransky scaling, roughly parameterized by the difference between k_{cr} (blue circles) and k_{SB} (red triangles), extend to larger values of $\Delta N_f = N_{f,cr} - N_f$, as the estimate for the critical exponent $\Theta_0 = \Theta(N_{f,cr})$ at four-loop level is larger than at two-loop level. In this perturbative estimate for the running coupling, the curves cannot be extended to larger values of ΔN_f , see main text. The figures have been taken from Ref. [79].

where $i \in \{+, -, \sigma, VA\}$. This corresponds to starting the flow at the maxima (extrema) of the parabolas.

We observe that for a given value of N_f the symmetry breaking scale k_{SB} is smaller in the all-channels approximation compared to the one-channel approximation. The fits to the data points are also shown in Fig. 21. In agreement with the analytic results presented in Sect. 6.3.1 we find:

$$\ln k_{SB}^{\text{one}} \approx \text{const.} - \frac{2.481}{|N_{f,cr} - N_f|^{0.494}}, \quad \ln k_{SB}^{\text{all}} \approx \text{const.} - \frac{3.932}{|N_{f,cr} - N_f|^{0.516}}. \quad (300)$$

Thus, we clearly observe the expected exponential scaling behavior in the one-channel and in the all-channels approximation for $N_f \rightarrow N_{f,cr}$.

The result from the one-channel approximation is in reasonable agreement with the analytic leading-order (LO) result found in Sect. 6.3.1:

$$\ln k_{SB}^{\text{LO}} = \text{const.} - \frac{\pi}{2\epsilon\sqrt{|\alpha_1||N_{f,cr} - N_f|}} \approx \text{const.} - \frac{2.386}{\sqrt{|N_{f,cr} - N_f|}}. \quad (301)$$

Note that $|\alpha_2/\alpha_1| \approx 0.273$. Differences to the analytic results are due to numerical errors of the fit and higher-order corrections which we have derived in Sect. 6.3.1.

6.5.4 Power-law Scaling and Beyond

We now study scaling in a setup in which we take into account the (momentum) scale-dependence of the running gauge coupling. In order to compare the theories with different flavor numbers we fix the scales by keeping the running coupling at the τ -mass scale $\Lambda = m_\tau$ fixed to $g^2(m_\tau)/(4\pi) \approx 0.322$. Since we apply the truncation (284) to QCD, we do not consider the four-fermion couplings λ as independent external parameters as, e.g., in NJL-type low-energy QCD models, see Sect. 5.2.1. More precisely, we impose the boundary condition $\lambda_i \rightarrow 0$ for $k \rightarrow \infty$ which guarantees that the λ_i 's at finite k are solely generated by quark-gluon dynamics, e.g., by 1PI “box” diagrams with 2-gluon exchange, see Fig. 15(c).

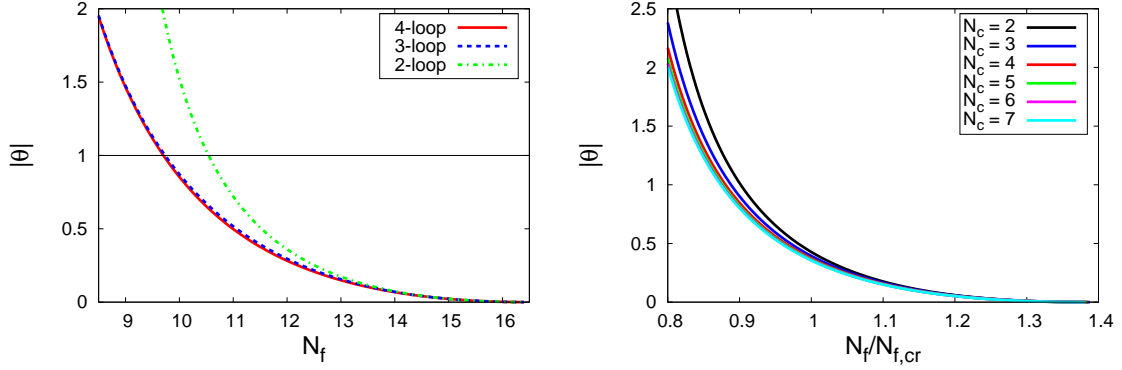


Fig. 23 Left panel: Critical exponent Θ of the running gauge coupling at the CBZ fixed point for $N_c = 3$ as a function of the number of flavors N_f as obtained from two-, three- and four-loop perturbation theory in the $\overline{\text{MS}}$ scheme. Right panel: Critical exponent Θ of the two-loop running gauge coupling at the CBZ fixed point as a function of $N_f/N_{f,\text{cr}}$ for $N_c = 2, 3, \dots, 7$ (from top to bottom). Recall that $N_{f,\text{cr}}$ depends on N_c , see Sect. 6.5.

In Fig. 22 we show the results for the N_f dependence of the scales k_{cr} and k_{SB} for $N_c = 3$ as obtained from a study with a running gauge coupling in the two-loop and the four-loop approximation, respectively. The data points can be fitted to the analytic results for the scaling behavior of k_{SB} and k_{cr} . For the all-channels approximation, we find

$$\ln k_{\text{cr}}^{2\text{-loop}} \approx \text{const.} + 2.566 \ln |N_f - N_{f,\text{cr}}|, \quad (302)$$

$$\ln k_{\text{SB}}^{2\text{-loop}} \approx \text{const.} - \frac{3.401}{|N_f - N_{f,\text{cr}}|^{0.54}} + 2.540 \ln |N_f - N_{f,\text{cr}}|, \quad (303)$$

and

$$\ln k_{\text{cr}}^{4\text{-loop}} \approx \text{const.} + 1.180 \ln |N_f - N_{f,\text{cr}}|, \quad (304)$$

$$\ln k_{\text{SB}}^{4\text{-loop}} \approx \text{const.} - \frac{5.196}{|N_f - N_{f,\text{cr}}|^{0.52}} + 1.171 \ln |N_f - N_{f,\text{cr}}|. \quad (305)$$

Thus, the fits are in reasonable agreement with our analytic predictions. For the multi-parameter fits (303) and (305), we have fixed the coefficient of the \ln -term which is the inverse critical exponent $\Theta_0 = \Theta(N_{f,\text{cr}})$. We emphasize that the predicted values for the critical exponent $\Theta(N_{f,\text{cr}})$ are substantially different for the running coupling in the two- and four-loop approximation, see left panel of Fig. 23:

$$\frac{1}{|\Theta(N_{f,\text{cr}})|} \approx 2.540 \quad (\text{two-loop}), \quad \frac{1}{|\Theta(N_{f,\text{cr}})|} \approx 1.171 \quad (\text{four-loop}). \quad (306)$$

In Fig. 22 we observe that the critical exponent Θ clearly influences the scaling behavior close to the quantum critical point $N_{f,\text{cr}}$. In agreement with the analytic findings presented in Sect. 6.3, the size of the regime with exponential scaling increases with increasing $|\Theta|$. Using Eq. (281) we can give a quantitative estimate for the size of the regime in which the exponential scaling behavior dominates. For the one-channel approximation, see Eq. (294), we find

$$\Delta N_f^{2\text{-loop}} := |N_f - N_{f,\text{cr}}| \lesssim 0.27, \quad (307)$$

where we have used the running coupling at two-loop level, see also Tab. 2. Using a running coupling in the four-loop approximation ($N_{f,\text{cr}}^{4\text{-loop}} \approx 10.0$), the size of this Miransky scaling regime can be estimated to be larger than one flavor. This is in agreement with the numerical results shown in Fig. 22. Since our studies rely on a perturbative estimate for the running coupling, the curves in Fig. 22 cannot be extended

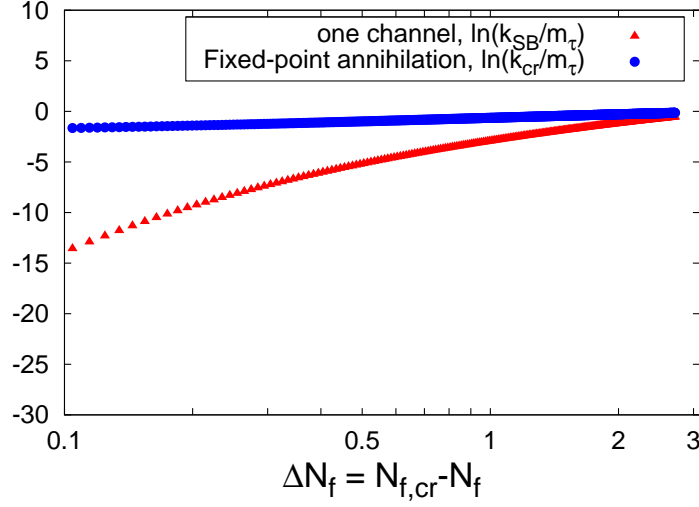


Fig. 24 N_f dependence of k_{cr} (blue circles) and k_{SB} (red triangles) as obtained from a study with a specifically designed running gauge coupling for $N_c = 3$, cf. Eq. (309). The associated β function allows us to vary the critical exponent Θ by hand. Here, we show the results for $\Theta_0 = |\Theta(N_{f,cr})| \approx 4.3$ which can be compared to the results from the “real” two-loop running coupling in the left panel of Fig. 22. Contributions due to Miransky scaling are visible as deviations from a straight-line behavior (power law) in this double-logarithmic plot. These results confirm our estimate that the Miransky-scaling window is larger for larger $|\Theta_0|$, whereas power-law scaling dominates for small $|\Theta_0|$, see left panel of Fig. 22. The figure has been taken from Ref. [79].

to larger values of $\Delta N_f = N_{f,cr} - N_f$. For instance, in the four-loop case, we have $N_{f,cr} \simeq 9.8$. However, the CBZ fixed-point vanishes for $N_f \lesssim 8$. Our RG arguments based on expansions about an IR fixed point thus only extend to $\Delta N_f^{\max} \simeq 1.8$, see right panel of Fig. 22. In non-perturbative functional studies in the Landau gauge, an IR fixed point appears to exist already in the pure gauge sector and thus also for $N_f < N_f^{\text{CBZ}}$, see Refs. [30, 31, 348, 350, 370–377]. In this case, no restriction on ΔN_f arises.

Let us now discuss our results in the light of lattice simulations. Since it is found that $N_{f,cr} \gtrsim 9$ in current lattice simulations [318–331], we expect that the pure exponential scaling behavior is difficult to resolve and the corrections due to the running of the gauge coupling might be more relevant for a scaling analysis in lattice simulations. From the viewpoint of such simulations, one might be interested in keeping the power of the “Miransky” term fixed to $1/2$ and use the scaling law (278) to fit $N_{f,cr}$ and the critical exponent $\Theta_0 = \Theta(N_{f,cr})$. Recall that all chiral low-energy observables, such as the pion decay constant, are expected to scale according to Eq. (278).

In QCD, it appears to be a general feature that $\Theta_0 \equiv \Theta(N_{f,cr})$ decreases with $N_{f,cr}$. Estimates of $\Theta(N_f)$ within two- and higher-loop approximations in the $\overline{\text{MS}}$ scheme are shown in the left panel of Fig. 23. Therefore, power-law scaling is more prominent for larger $N_{f,cr}$. In particular, power-law scaling should be visible if theories are probed only for integer values of N_f as, e.g., on the lattice.

Up to this point, we have restricted our scaling analysis to the case $N_c = 3$. One may wonder whether the size of the Miransky scaling regime changes significantly when we vary the number of colors N_c . As discussed above, this question can be essentially answered by looking at the value of the critical exponent Θ . In the right panel of Fig. 23 we show Θ as a function of $N_f/N_{f,cr}$ for $N_c = 2, 3, \dots, 7$, where $N_{f,cr} = N_{f,cr}(N_c)$ and Θ has been extracted from the running coupling in the two-loop approximation. Interestingly, we observe that Θ at $N_f = N_{f,cr}$ is approximately independent of N_c . This observation is in accordance with the result from a $1/N_c$ expansion of $\Theta_0 \equiv \Theta(N_{f,cr})$, which yields

$$\Theta_0 \equiv \Theta(N_{f,cr}) \approx -\frac{1}{3} - \frac{2}{9N_c^2} + \mathcal{O}(1/N_c^4). \quad (308)$$

In order to obtain this simple form, we have used the estimate $N_{f,cr} = 4N_c$, see Eq. (296). The large- N_c expansion of Θ_0 suggests that the exponential scaling behavior is only visible close to $N_{f,cr}$, even for $N_c > 3$. Using Eq. (281) we can even give a direct estimate of the size of the regime in which the exponential scaling behavior dominates. The results are listed in Tab. 2. From this analysis we conclude that pure exponential scaling behavior seems to be difficult to resolve in, e. g., lattice simulations, even for larger values of N_c . Therefore the corrections due to the running of the gauge coupling (power-law scaling) might be more relevant from a practical point of view in QCD.

To further illustrate the important influence of the critical exponent Θ it is instructive to compute the scaling behavior of the scales k_{cr} and k_{SB} using a specifically designed running gauge coupling. This coupling is inspired by the two-loop approximation modified by an artificial higher-order term. The latter is constructed such that the critical exponent Θ can be changed by hand but the two-loop fixed point remains unchanged:

$$\partial_t g^2 \equiv \beta_{g^2} = \beta_{g^2}^{2-loop} + \phi g^6 (g^2 - g_{*,2-loop}^2), \quad (309)$$

where the parameter ϕ allows us to change Θ without changing $N_{f,cr}$. In Fig. 24 we present our results for k_{SB} and k_{cr} for $\phi = 0.003$ (i. e. $|\Theta(N_{f,cr})| \approx 4.3$) as obtained from the one-channel approximation for $N_c = 3$. The comparison of these results with the results from the "real" two-loop running coupling with $\Theta_0 \approx 0.39$ (left panel of Fig. 22) clearly confirms that the size of the exponential-scaling regime depends strongly on Θ .

In our scaling analysis we have mainly studied the behavior of the symmetry breaking scale k_{SB} which sets the scale for low-energy observables, see e. g. Eq. (278) and Sect. 6.4. Although we expect that chiral observables scale according to the behavior of k_{SB} , an explicit computation with the aid of functional methods and lattice simulations is still appealing. In Ref. [378], the quark mass, the chiral condensate and the pion decay constant have been computed within a truncated set of Dyson-Schwinger equations for many-flavor QCD. Signatures of the quantum critical point have been identified and the critical exponents have been extracted from a pure power-law fit to the numerical data available for $N_f < N_f^{cr}$. In the light of our scaling relations Eqs. (273) and (278), the results of Ref. [378] unfortunately remain somewhat inconclusive for two reasons: First, the exponential factor in Eq. (278) has not been taken into account in the fit. Second, $N_{f,cr}$ has been fitted for each chiral IR observable separately yielding slightly different values. While neglecting the exponential scaling factor might be reasonable due to the fact that the Miransky scaling window is expected to be small in QCD, the uncertainty in $N_{f,cr}$ arising from the fitting procedure is likely to spoil the fit for the critical exponent. We expect that a more careful analysis in the vicinity of the quantum critical point can easily put our scaling relation to test.

6.6 Excursion: Confinement and Chiral Symmetry Breaking

Up to this point we have restricted our discussion to chiral symmetry breaking in gauge theories, such as QCD. We have totally left aside effects arising from the confining dynamics in QCD. However, we were mainly interested in phase transitions in the limit of many massless quark flavors. In this case, there is no good order parameter for confinement available anyway and it seems reasonable to expect that nonanalyticities in the correlation functions are mainly dominated by the chiral degrees of freedom. Now we shall discuss QCD with a small number of quark flavors. There, we may expect that the confining dynamics significantly affects the chiral dynamics at the finite-temperature phase transition.

In order to gain some insight into the interrelation of quark confinement and chiral symmetry breaking we analyze how the order parameter for confinement influences the chiral fixed-point structure of the theory. The relation of both has been studied in detail in Ref. [275]. Here, we only review the main arguments and restrict ourselves to the large- N_c limit. Before we start with our analysis, however, we would like to discuss some issues arising in studies of the relation of quark confinement and chiral symmetry breaking.

The deconfinement phase transition has been studied in pure $SU(N_c)$ gauge theories ($N_f \rightarrow 0$) and QCD with both lattice simulations, see e. g. Refs. [360–363, 379–384], and functional continuum methods [151,

351–353, 385–388]. Concerning chiral symmetry breaking, we have seen that the (chiral) condensate $\langle \bar{\psi}\psi \rangle$ serves as an order parameter. A finite chiral condensate implies that the chiral $SU(N_f)_L \otimes SU(N_f)_R$ flavor symmetry of QCD is broken. Concerning the confinement phase transition, on the other hand, an order parameter can be constructed from the so-called Polyakov-loop variable:

$$L[A_0] = \frac{1}{N_c} \mathcal{P} \exp \left(i\bar{g} \int_0^\beta dx_0 A_0(x_0, \vec{x}) \right), \quad (310)$$

where $\beta = 1/T$ is the inverse temperature and \bar{g} denotes the bare gauge coupling; \mathcal{P} stands for path ordering. In QCD with N_c colors and infinitely heavy quarks this quantity is related to the operator that generates a static quark, i. e. an infinitely heavy quark [389]. Loosely speaking, the logarithm of the expectation value $\langle \text{tr}_F L[A_0] \rangle$ can be related to the free energy F_q of a static quark. To be more specific, we can interpret it as half of the free energy $F_{q\bar{q}}$ of a static quark–anti-quark pair at infinite distance. Here, the trace tr_F is evaluated in the fundamental representation. Moreover, the expectation value $\langle \text{tr}_F L \rangle$ is an order parameter for center symmetry breaking of the underlying gauge group [390]. To see this, we consider gauge transformations $U_z(x_0, x)$ with $U_z^{-1}(0, \vec{x})U_z(\beta, \vec{x}) = z$, where $z \in \mathcal{Z}$ is an element of the center \mathcal{Z} of the gauge group. Under such a transformation the Polyakov loop is multiplied with a center element z , $\langle \text{tr}_F L \rangle \rightarrow z \langle \text{tr}_F L \rangle$. Thus, a center-symmetric confining disordered ground state with $F_q \rightarrow \infty$ is ensured by $\langle \text{tr}_F L \rangle = 0$. In turn, deconfinement with $F_q < \infty$ is signaled by $\langle \text{tr}_F L \rangle \neq 0$. This consideration implies center-symmetry breaking in the ordered phase.

The relation of quark confinement and chiral symmetry breaking in QCD is indeed not yet fully understood. As the chiral and the deconfinement phase transition are related to different symmetries of the theory, it is difficult to establish a simple (analytic) relation between both. Even worse, the deconfinement phase transition turns into a crossover in the presence of dynamical quarks since the latter break explicitly the underlying center symmetry.⁸¹ As there is no unique way to define the critical temperature associated with a crossover, a proof of an exact coincidence of the two transitions seems to be impossible in any case. On the other hand, both phase transitions are driven by the gauge degrees of freedom in QCD. This is readily apparent for the deconfinement phase transition. For the chiral phase transition the relation to the gauge degrees is more indirect.⁸² However, we have seen in the previous sections that the quark self-interactions are dynamically generated and driven to criticality by the gauge degrees of freedom: once the gauge coupling exceeds a critical value, the quark sector is driven to criticality without requiring any fine-tuning. This observation may suggest that there might be a deeper relation between the chiral dynamics in the matter sector and the confining dynamics in the gauge sector and serves as a motivation for the subsequent analysis.

In Polyakov-loop extended low-energy models a background field $\langle A_0 \rangle$ is introduced to study some aspects of quark confinement and the associated phase transition [255–260, 277–284]. This background field can be related to the Polyakov variable $L[A_0]$. In fact, it has been shown that $\text{tr}_F L[\langle A_0 \rangle]$ serves as an order parameter for quark confinement in Polyakov-Landau-DeWitt gauge [351, 352], where $\langle A_0 \rangle$ is an element of the Cartan subalgebra and denotes the ground state of the associated order-parameter potential in the adjoint gauge algebra.⁸³ This potential can be computed, e. g., from the knowledge of gauge correlation functions, as first demonstrated in a first-principles RG study [351, 353]. In any case, the order parameter $\text{tr}_F L[\langle A_0 \rangle]$ is related to the standard Polyakov loop $\langle \text{tr}_F L[A_0] \rangle$ via the Jensen inequality,

$$\text{tr}_F L[\langle A_0 \rangle] \geq \langle \text{tr}_F L[A_0] \rangle. \quad (311)$$

⁸¹ The explicit symmetry breaking becomes stronger the smaller the current quark masses are.

⁸² As a matter fact, the chiral phase transition in QCD can be investigated with NJL-type models (and in Polyakov-loop extended versions thereof). In these models the quark interactions are considered as parameters which are tuned by hand to fit low-energy observables, see our discussion in Sect. 5.2.

⁸³ Strictly speaking, we have to distinguish between the background temporal gauge field in Landau-DeWitt gauge and its expectation value associated with the order parameter for confinement, see Refs. [351, 353]. We skip this subtlety here since it is of no importance for our present analysis and refer to $\langle A_0 \rangle$ as the position of the ground-state of the order-parameter potential.

We would like to add that one of the underlying approximations in (Polyakov-loop extended) low-energy model studies is to set $\text{tr}_F L[\langle A_0 \rangle] = \langle \text{tr}_F L[A_0] \rangle$. This opens up the possibility to incorporate results for the Polyakov loop $\langle \text{tr}_F L[A_0] \rangle$ as obtained from lattice simulations in these studies. It is then found that the chiral and the deconfinement phase transition lie indeed close to each other at small values of the quark chemical potential, as it is found to be the case in lattice QCD simulations [360–363, 379, 382–384].

Recently, so-called dual observables arising from a variation of the boundary conditions of the fermions in time-like direction have been introduced [391] and employed for a study of the relation of quark confinement and chiral symmetry breaking at finite temperature [151, 385–387, 392–399]. These dual observables relate the spectrum of the Dirac operator to the order parameter for confinement, namely the Polyakov loop. The introduction of these observables constitutes an important formal advance which allows us to gain a deeper insight into the underlying dynamics at the QCD phase boundary. However, they do not allow us to fully resolve the question regarding the relation of quark confinement and chiral symmetry breaking.

In the following we aim to shed more light on the question under which circumstances the chiral and the deconfinement transition lie close to each other. To this end, we analyze the deformation of the RG fixed-point structure of chiral four-fermion interactions due to confining gauge dynamics. Technically speaking, this means that we couple the order parameter for confinement to the RG flow of four-fermion interactions. As discussed in detail in Sect. 3.2, the latter can be related to the order parameter for chiral symmetry breaking by means of partial bosonization. As we shall see, this yields an intimate relation between the chiral and the deconfinement order parameter which suggests the existence of a dynamical locking mechanism for the chiral phase transition. To keep our discussion of the general mechanisms as simple as possible, we restrict ourselves to $N_f = 2$ massless quark flavors with N_c colors and employ the following ansatz for the effective action:

$$\Gamma_k[\bar{\psi}, \psi, \langle A_0 \rangle] = \int d^4x \left\{ \bar{\psi} (i\partial + \bar{g}\gamma_0 \langle A_0 \rangle) \psi + \frac{1}{2} \bar{\lambda}_\sigma [(\bar{\psi}\psi)^2 - (\bar{\psi}\vec{\tau}\gamma_5\psi)^2] \right\}, \quad (312)$$

where the τ_i represent the Pauli matrices and couple the spinors in flavor space.

The action (312) can be considered as an ansatz for a QCD low-energy model. In fact, we have discussed this action for $\langle A_0 \rangle \equiv 0$ in the context of QCD low-energy models in Sect. 5.2, where we have shown that the RG flow of the $\bar{\lambda}_\sigma$ -interaction decouples from the RG flows of other allowed four-fermion interaction channels in the large- N_c limit. Of course, fermionic self-interactions are fluctuation-induced in full QCD, e. g. by two-gluon exchange, and are therefore not fundamental, see our discussion in the previous sections. However, we are here rather interested in studying how the fixed-point structure of four-fermion interaction is deformed under the influence of confining dynamics. For such a general discussion, we expect the ansatz (312) to be sufficient.

Based on the action (312) we have discussed quantum and thermal phase transitions in QCD low-energy models in Sect. 5.2.2 for $\langle A_0 \rangle \equiv 0$. Let us now turn to a discussion of the fixed-point structure for finite $\langle A_0 \rangle$. The value of the background field $\langle A_0 \rangle$ is determined by the ground state of the associated order-parameter potential, see Refs. [351, 353]. As discussed above, this ground-state value $\langle A_0 \rangle$ is directly related to an order parameter for confinement, namely $\text{tr}_F L[\langle A_0 \rangle]$. In the following we do not need to know the exact values of $\langle A_0 \rangle$ and $\text{tr}_F L[\langle A_0 \rangle]$. We only need to know about some general properties of the confinement order parameter.

For temperatures much larger than the deconfinement phase-transition temperature T_d we have $\langle A_0 \rangle = 0$, i. e. $\text{tr}_F L[\langle A_0 \rangle] = 1$. On the other hand, the position $\langle A_0 \rangle$ of the ground state in the confined phase of pure $SU(N_c)$ Yang-Mills theory is uniquely determined up to center transformations by [351, 353]

$$\text{tr}_F (L[\langle A_0 \rangle])^n = 0 \quad (313)$$

with $(n \bmod N_c) = 1, \dots, N_c - 1$. These conditions determine the $N_c - 1$ coordinates $\{\phi^{(a)}\}$ of $\langle A_0 \rangle$:

$$\beta \bar{g} \langle A_0 \rangle = 2\pi \sum_{T^a \in \text{Cartan}} T^a \phi^{(a)} = 2\pi \sum_{T^a \in \text{Cartan}} T^a v^{(a)} |\phi|, \quad v^2 = 1, \quad (314)$$

where the T^a 's denote the generators of the underlying $SU(N_c)$ gauge group in the fundamental representation.⁸⁴ Concerning the parameterization of $\langle A_0 \rangle$, it turns out that it is convenient to introduce the eigenvalues ν_l of the hermitian matrix in Eq. (314):

$$\nu_l = \text{spec} \{ (T^a v^a)_{ij} \mid v^2 = 1 \} . \quad (315)$$

Finally, we have

$$\frac{1}{N_c} |\text{tr}_F(L[\langle A_0 \rangle])^n| \leq \frac{1}{N_c^n} \quad (316)$$

for $n \in \mathbb{N}$. Note that the ground-state value $\langle A_0 \rangle$ is shifted in QCD with dynamical quarks and yields a small but finite order parameter in the confined phase.

We now have set the stage for a discussion of the fixed-point structure of the four-fermion coupling λ_σ . The flow equation of the latter can be computed along the lines of Sect. 3.1. In the point-like limit we find [275]:

$$\beta_{\lambda_\sigma} \equiv \partial_t \lambda_\sigma = 2\lambda_\sigma - 16 \left(2 + \frac{1}{N_c} \right) v_3 \sum_{l=1}^{N_c} l_1^{(F),(4)}(\tau, 0, \nu_l | \phi) \lambda_\sigma^2 , \quad (317)$$

where $v_3 = 1/(8\pi^2)$ and $\lambda_\sigma = k^2 \bar{\lambda}_\sigma$. Since we work in the point-like limit, we have $\eta_\psi = 0$. To derive this equation we have employed a $3d$ regulator function; the definition of the background-field dependent threshold function can be found in App. D. Moreover, we have exploited the fact that the fermion propagator $(\Gamma^{(2)})^{-1}$ (inverse two-point function) can be spanned by the generators of the Cartan subalgebra as follows:

$$\left(\Gamma^{(2)}[\{\nu_l | \phi\}] \right)_{ij}^{-1} = \frac{1}{N_c} \left(\Gamma_0^{(2)}[\{\nu_l | \phi\}] \right)_{ij}^{-1} \mathbb{1}_{ij} + \sum_{T^a \in \text{Cartan}} \left(\Gamma_a^{(2)}[\{\nu_l | \phi\}] \right)_{ij}^{-1} T_{ij}^a . \quad (318)$$

Here, the T_{ij}^a 's denote the generators in the fundamental (color) representation. The expansion coefficients on the right-hand side can be computed straightforwardly by using $\text{tr}_F T^a T^b = \frac{1}{2} \delta_{ab}$ and $\text{tr}_F T^a = 0$.

For vanishing temperature as well as temperatures much larger than the deconfinement phase-transition temperature T_d , the fixed-point structure is identical to the one discussed in Sect. 5.2.2 since $\langle A_0 \rangle$ tends to zero for $T \gg T_d$ and $\langle A_0 \rangle \equiv 0$ for $T = 0$. For finite $\langle A_0 \rangle$, the pseudo fixed-point λ_σ^* depends on $\langle A_0 \rangle$ and the dimensionless temperature $\tau = T/k$. Within the present approximation, the value of the pseudo-fixed point λ_σ^* can be given in closed form:

$$\begin{aligned} \lambda_\sigma^*(\tau, \langle A_0 \rangle) &= \left(\frac{1}{\pi^2} \left(2 + \frac{1}{N_c} \right) \sum_{l=1}^{N_c} l_1^{(F),(4)}(\tau, 0, \nu_l | \phi) \right)^{-1} \\ &= \left(\frac{1}{\lambda_\sigma^*(0, 0)} + \frac{1}{6\pi^2} \left(2 + \frac{1}{N_c} \right) \sum_{n=1}^{\infty} (-N_c)^n \left[\text{tr}_F(L[\langle A_0 \rangle])^n \right. \right. \\ &\quad \left. \left. + \text{tr}_F(L^\dagger[\langle A_0 \rangle])^n \right] \left(1 + \frac{n}{\tau} \right) e^{-\frac{n}{\tau}} \right)^{-1} . \quad (319) \end{aligned}$$

The specific form in the second line has been obtained with the regulator function (349). However, we stress that the general form of the asymptotic series (319) holds for *any* regulator function, as can be shown by means of Poisson resummation techniques. Note that the series (319) effectively represents a low-temperature expansion and that the sum over the τ -dependent terms in the second line of Eq. (319) is closely related to the geometric series.

Using Eq. (313) it follows that all finite-temperature corrections to the (pseudo) fixed-point value vanish identically in the confined phase for $N_c \rightarrow \infty$, provided that the ground-state value $\langle A_0 \rangle$ is identical in

⁸⁴ The dimension of the Cartan subalgebra is $N_c - 1$.

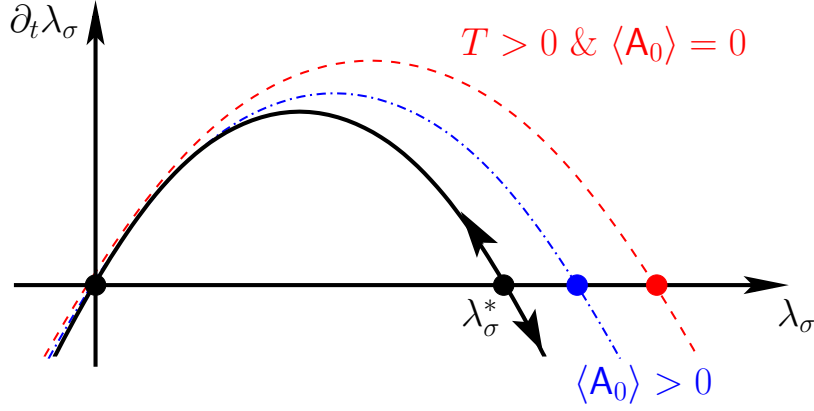


Fig. 25 Sketch of the β_{λ_σ} function of the four-fermion interaction for $T = 0$ (black/solid line), a given finite value of the temperature T and $\langle A_0 \rangle = 0$ (red/dashed line) and the same temperature T but $\langle A_0 \rangle > 0$ (blue/dashed-dotted line), see Ref. [275]. The arrows indicate the direction of the RG flow towards the infrared.

SU(N_c) Yang-Mills theory and QCD with dynamical fermions. Of course, this assumption is not exactly fulfilled but for physical quark masses it is reasonable to assume

$$\text{tr}_F L[\langle A_0 \rangle] \ll 1 \quad (320)$$

for $T \lesssim T_d$. Thus, we have found that

$$\lambda_\sigma^*(0, 0) \equiv \lambda_\sigma^*(\tau, \langle A_0 \rangle) \quad (321)$$

in the limit $N_c \rightarrow \infty$, independent of the temperature for $T \lesssim T_d$. On the other hand, we have

$$\lambda_\sigma^*(\tau, \langle A_0 \rangle) \rightarrow \lambda_\sigma^*(\tau, 0) \quad \text{for } \langle A_0 \rangle \rightarrow 0. \quad (322)$$

With the same reasoning it also follows that

$$\beta_{\lambda_\sigma}(0, 0) \equiv \beta_{\lambda_\sigma}(\tau, \langle A_0 \rangle) \quad (323)$$

for $T \lesssim T_d$ and $N_c \rightarrow \infty$, see also Fig. 25 for illustration. This means that for $T < T_d$ the question of whether chiral symmetry is spontaneously broken or not is in fact *independent* of the temperature, but depends only on the choice of the initial condition $\lambda_\sigma^{\text{UV}}$ relative to its fixed-point value λ_σ^* at $T = 0$. We add that Eqs. (321)-(323) are regularization-scheme independent statements and that $\lambda_\sigma^*(\tau, \langle A_0 \rangle)$ interpolates continuously for a given finite value of τ between $\lambda_\sigma^*(0, 0)$ and $\lambda_\sigma^*(\tau, 0)$. Note that we have not specified the precise value of T_d since it simply does not enter our analysis.

Provided that we choose an initial value $\lambda_\sigma^{\text{UV}} > \lambda_\sigma^*(0, 0)$, it follows immediately from Eq. (323) that

$$T_\chi \geq T_d \quad (324)$$

for $N_c \rightarrow \infty$, see Ref. [275]. This means that the chiral phase transition is locked in due to the confining dynamics in the gauge sector. Loosely speaking, thermal fluctuations of the quark fields, which tend to restore the chiral symmetry, are suppressed since they are directly linked to the deconfinement order parameter. Thus, we have found that the restoration of chiral symmetry is intimately connected to the confining dynamics in the gauge sector. These findings emerging from a non-perturbative analysis of the fermionic fixed-point structure confirm the results of a *mean-field* study by Meisinger and Ogilvie [277].

Let us now discuss how our (simplified) analysis relates to (full) QCD. In QCD, we only have a single input parameter, e. g. the value of the strong coupling g^2 at a given scale which then determines Λ_{QCD} . Thus, we have

$$T_\chi \sim \Lambda_{\text{QCD}},$$

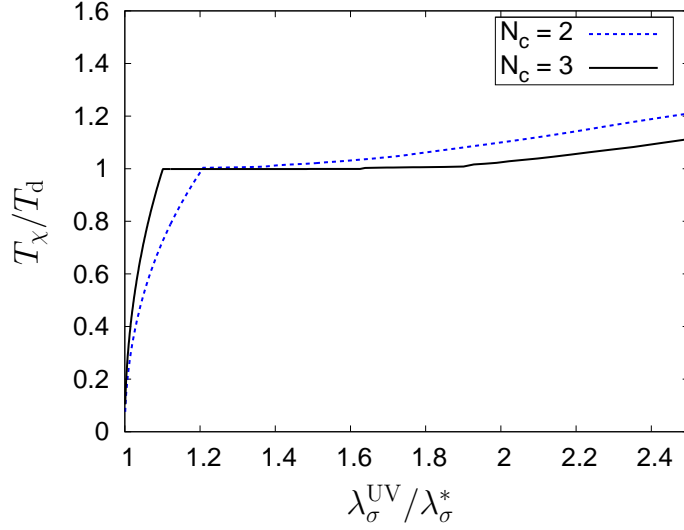


Fig. 26 Ratio T_χ/T_d of the chiral and the deconfinement phase transition temperature as a function of $\lambda_\sigma^{\text{UV}}/\lambda_\sigma^*$ for $N_c = 2, 3$. In the large- N_c limit, the lower end of the locking window (i. e. the regime with $T_\chi/T_d = 1$) is given by $\lambda_\sigma^{\text{UV}}/\lambda_\sigma^* = 1$. The figure has been taken from Ref. [275].

see also Sect. 6.2. In the present analysis the chiral transition temperature T_χ depends on two parameters, namely the value of the background field $\langle A_0 \rangle$ and the initial condition $\lambda_\sigma^{\text{UV}}$. Nevertheless, Eq. (324) is a parameter-free statement which simply follows from an analysis of the effect of gauge dynamics on the fixed-point structure in the matter sector. In particular, we have only made use of general properties of the deconfinement order parameter and the fact that $\lambda_\sigma^{\text{UV}} > \lambda_\sigma^*(0, 0)$ is a *necessary* condition for chiral symmetry breaking at $T = 0$ and $\langle A_0 \rangle = 0$. Of course, the initial condition $\lambda_\sigma^{\text{UV}}$ is not a free parameter in QCD but originally generated by quark-gluon interactions at high (momentum) scales. In a given regularization scheme the value of $\lambda_\sigma^{\text{UV}}$ can therefore in principle be related to the value of the strong coupling g^2 at, e. g., the τ mass scale, see our discussion of chiral symmetry breaking in the previous sections. We would like to point out that neither the value of g^2 at some scale nor the value of $\lambda_\sigma^{\text{UV}}$ on a given RG trajectory is a physical observable. However, their values can be related to physical low-energy observables. Recall that the value of $\lambda_\sigma^{\text{UV}}$ determines the critical scale k_{SB} which sets the scale for IR observables, see e. g. Eq. (235).

Since our general statements do not depend on the actual value of the deconfinement temperature T_d , one may wonder which role this quantity plays at all in our analysis. We have argued that T_χ depends on both $\lambda_\sigma^{\text{UV}}$ and $\langle A_0 \rangle$ in our study. The presence of the background field $\langle A_0 \rangle$ implies the existence of the transition temperature T_d which defines a scale in the theory. For $\langle A_0 \rangle = 0$, on the other hand, we have argued that $T_\chi \sim k_{\text{SB}}$. In this case, the scale k_{SB} is eventually determined by our choice for $\lambda_\sigma^{\text{UV}}$. If we now take into account the background field $\langle A_0 \rangle$, then the chiral phase transition temperature T_χ is locked in and we necessarily have $T_\chi \geq T_d$ in the large- N_c limit, see Eq. (324). Thus, the chiral phase transition temperature for all theories which would allow for $T_\chi \leq T_d$ for $\langle A_0 \rangle = 0$ is shifted such that $T_\chi \simeq T_d$. This observation allows us to define a “locking window” for the parameter $\lambda_\sigma^{\text{UV}}$ in which the chiral phase transition T_χ and the deconfinement phase transition T_d lie close to each other [275]. The upper end of this window can be estimated by the smallest value for $\lambda_\sigma^{\text{UV}}$ for which T_χ for $\langle A_0 \rangle = 0$ is still larger than T_d . The lower end of this window is given by $\lambda_\sigma^*(0, 0)$ in the large- N_c limit. Whereas λ_σ^* and $\lambda_\sigma^{\text{UV}}$ are scheme-dependent quantities, the mere existence of such a window in parameter space can be viewed as a universal statement. Since $\lambda_\sigma^{\text{UV}}$ sets the scale for physical low-energy observables, the existence of a “locking window” for $\lambda_\sigma^{\text{UV}}$ suggests the existence of a corresponding window for the

values of low-energy observables, such as the pion decay constant f_π . In Ref. [275] the existence of the latter has indeed been confirmed. It was also found that the physical value for the pion decay constant ($f_\pi \approx 90$ MeV) is compatible with the almost coinciding phase transition temperatures observed in lattice QCD simulations [360–363, 379, 382–384] and in functional first-principles studies [151, 400].

In our analysis we have concentrated on the limit $N_c \rightarrow \infty$. One may suspect that finite- N_c corrections alter our conclusions. In fact, we observe that terms with

$$n \bmod N_c = 0 \tag{325}$$

contribute to the right-hand side of Eq. (319) and to the RG flow of λ_σ , when we go beyond the large- N_c limit. Strictly speaking, Eq. (321) then holds only for $\tau \ll 1$ but not for arbitrary values of $\tau = T/k$. However, this does not necessarily imply that we do not have a finite range of values for the initial condition $\lambda_\sigma^{\text{UV}}$ anymore in which the chiral and the deconfinement phase transition are tightly linked. It only implies that the lower end of the window for $\lambda_\sigma^{\text{UV}}$ is shifted to larger values compared to the large- N_c limit where the lower end is given by $\lambda_\sigma^*(0, 0)$. In Ref. [275], finite- N_c corrections have been explicitly taken into account. It was found that the locking mechanism for the chiral phase transition is still present for finite N_c , in particular for $N_c = 2$ and $N_c = 3$. In Fig. 26 we show T_χ/T_d as a function of $\lambda_\sigma^{\text{UV}}/\lambda_\sigma^*$ for $N_c = 2, 3$. For the computation of T_χ/T_d , the results from Ref. [351] for $\langle A_0 \rangle$ for the corresponding $\text{SU}(N_c)$ Yang-Mills theory have been used to solve the flow equation for λ_σ , see Eq. (317).

We would like to close our discussion of confinement and chiral symmetry breaking with a few (critical) comments concerning the approximations underlying our present analysis. First, it is clear that the confinement order parameter in full QCD receives contributions from Feynman diagrams with at least one internal fermion line. These contributions tend to lower the deconfinement phase transition temperature.⁸⁵ We anticipate that our analytic findings are not (strongly) affected by this approximation since they rely on very general properties of the confinement order parameter. Therefore we still expect that a window in parameter space exists in which the chiral and the deconfinement phase transition lie close to each other. However, our estimate for the dependence of T_χ on $\lambda_\sigma^{\text{UV}}$ and the size of the “locking window” will change quantitatively when we take into account the corrections to the confinement order parameter due to quark fluctuations. Second, our ansatz (312) for the effective action is not complete with respect to Fierz transformations; for example, we have dropped the vector-channel interaction $\sim (\bar{\psi}\gamma_\mu\psi)^2$. Such interactions would also contribute to the RG flow of the four-fermion interaction λ_σ . At finite temperature the minimal set of point-like four-fermion interactions is larger than at vanishing temperature, since the Poincaré invariance is broken by the heat bath. If we allow for a finite $\langle A_0 \rangle$, the minimal set is even larger than in the case of a vanishing background field $\langle A_0 \rangle$. This is due to the fact that a finite background field $\langle A_0 \rangle$ distinguishes a direction in color space. For example, our expansion (318) of the fermion propagator suggests that a finite background field $\langle A_0 \rangle$ gives rise to additional point-like interactions of the type $\sim (\bar{\psi}T^{(3)}\psi)^2$ and $\sim (\bar{\psi}T^{(8)}\psi)^2$ for $N_c = 3$. However, the additional diagrams are of the same topology as the one shown in Fig. 15 (a), if we drop gluon-induced terms. We therefore expect that the inclusion of additional four-fermion interactions associated with a Fierz-complete basis is important for a quantitative computation of the chiral phase transition temperature beyond the large- N_c limit. Such an analysis is beyond the scope of this review. A study of the impact of the confinement order-parameter on contributions to the RG flow arising from 1PI diagrams with one- or two internal gluon lines, see Fig. 15 (b) and (c), certainly constitutes a further important improvement. As discussed in Sect. 6.5.2, the inclusion of such terms in the RG flow of four-fermion interactions opens up the possibility to remove the parameter $\lambda_\sigma^{\text{UV}}$, so that we are left with a single input parameter for the gauge and the matter sector, namely g^2 at a given UV scale. In any case, the locking mechanism for the chiral and deconfinement phase transition discussed here already provides a simple explanation for the observed almost-coincidence of both phase transitions.

⁸⁵ Recall that we only have a deconfinement crossover in the presence of dynamical quarks.

6.7 Fermions in Higher Representations and QED-like Theories

In this section we briefly discuss the applicability of the present approach to non-abelian gauge theories with fermions in higher representations, e. g. the adjoint representation, and to QED-like theories in $d = 2+1$ space-time dimensions. The latter class of theories is of great interest since the associated models may serve as effective theories for graphene, see e. g. Refs. [285–287]. The general discussion of scaling behavior in gauge theories in Sect. 6.3 indeed also holds for QED-like theories in $2 < d < 4$ space-time dimensions, as it essentially relies on only two assumptions (minimal requirements):

- (i) The existence of a non-trivial IR fixed-point of the gauge coupling for a large number of fermion flavors, i. e. in the chirally symmetric regime.
- (ii) The existence of an IR-attractive Gaussian as well as an IR-repulsive non-trivial fixed-point in the RG flows of the four-fermion couplings in the limit of vanishing gauge coupling.⁸⁶

These assumptions are fulfilled for QED in $2 < d < 4$ space-time dimensions.

The existence of a critical number $N_{f,cr}$ of fermion flavors in QED₃ has been confirmed in several studies, see e. g. Refs. [290–300]. However, the scaling behavior of physical observables as a function of N_f close to the quantum critical point $N_{f,cr}$ has not yet been analyzed in great detail. Only little is known about the (precise) size of the regime in which Miransky (exponential) scaling is dominant. It might well be that the critical exponent Θ associated with the gauge coupling is large at the phase transition (i. e. $|\Theta(N_{f,cr})| \gtrsim 1$). As a consequence, the scaling of physical observables close to $N_{f,cr}$ would be governed mainly by an exponential behavior, and the *universal* power-law corrections associated with Θ might be parametrically suppressed. An analysis of the presently available data for QED₃ in this direction as well as an independent RG study therefore seem to be worthwhile. Although N_f does not correspond to an experimentally accessible parameter of the theory, an analysis of the N_f -scaling behavior might provide us with important insights into the dynamics underlying chiral symmetry breaking in graphene.

A further fruitful extension of the discussed RG approach is represented by the study of gauge theories with fermions in higher representations, e. g. fermions in the adjoint representation. To this end, the use of computer algebra systems might be advisable [401]. Comprehension of these classes of gauge theories underlies (walking) technicolor-like scenarios for the Higgs sector and it is therefore important for our understanding of physics beyond the standard model. The quantum phase transition, which occurs in such theories for large N_f , has been studied using both Dyson-Schwinger equations as well as lattice simulations, see e. g. Refs. [85, 342, 344, 402–407]. An RG study in this direction can be used to benchmark presently available results for the critical number of fermion flavors in these theories and therefore contribute to a better understanding of dynamical symmetry breaking in gauge theories. Since $N_{f,cr}$ for a given number of colors is smaller in QCD with adjoint fermions than in QCD with fermions in the fundamental representation, it is tempting to speculate whether the dynamics close to the quantum phase transition is strongly affected by the confining dynamics in the gauge sector. In this respect, an analysis of the interrelation of confining and chiral dynamics along the lines of Sect. 6.6 could be rewarding.

7 Summary

We have reviewed RG approaches to various strongly interacting fermionic theories, ranging from non-relativistic many-body problems to relativistic gauge theories. We have shown that an analysis of the fixed-point structure of such theories allows us to study *universal* long-range behavior associated with quantum and thermal phase transitions in a clean and controlled way. Due to the intimate relation between phase transitions in a given theory and its fixed-point structure, evidence for the existence of fixed points can be verified in experiments. For example, we have shown in Sect. 4.1 that the existence of a non-trivial

⁸⁶ This assumption might be violated in $d = 2$, e. g., if the anomalous dimension of the fermions is zero in the limit of vanishing gauge coupling.

(IR repulsive) fixed-point in the four-fermion coupling is tightly linked to the observed universal behavior in experiments with ultracold atomic Fermi gases in the limit of a broad *Feshbach* resonance.

The analogue of the fixed-point associated with universal behavior in ultracold Fermi gases also exists in the Gross-Neveu model in $2 < d < 4$ space-time dimensions. For example, Gross-Neveu-type models play an important role in the context of (relativistic) superconductors. In any case, the existence of a non-trivial IR repulsive fixed-point in the Gross-Neveu model in $2 < d < 4$ space-time dimensions is associated with a second-order quantum phase transition, see Sect. 5.1. We have argued that theories with such a quantum phase transition are guaranteed to be asymptotically safe, i. e. nonperturbatively renormalizable. It is still an open question whether the converse is also true. An answer to this question might provide us with further insights into the asymptotic-safety scenario which underlies the quantization of gravity within a conventional path-integral approach.

In QCD low-energy models, we have seen that a non-trivial IR-repulsive fixed-point for the four-fermion couplings exists as well, see Sect. 5.2. In these models, the fermions play the role of (constituent) quarks. The mass of these fermions can be tuned by varying the four-fermion couplings. We have analyzed Fierz ambiguities in these models and shown that the dynamics close to the finite-temperature phase boundary can be easily understood in terms of the fixed-point structure of the theory.

In QCD-like gauge theories, the fermionic interactions do not represent free parameters. On the contrary, the running gauge coupling can drive the fermion sector to criticality, resulting in chiral symmetry breaking without any fine-tuning of the fermionic couplings, see Sect. 6. This is generically true for asymptotically free (chiral) gauge theories with N_f (massless) fermion flavors, such as QCD or even effective theories for graphene. A detailed analysis of the fixed-point structure in this class of theories provides a quantitative determination of the quantum phase transition that occurs for large values of N_f .

In Sects. 6.3 and 6.5 we have reviewed our understanding of phases of strongly-flavored gauge theories and the scaling behavior of their mass spectrum close to a quantum phase transition. We have discussed that essentially three different types of scaling behavior can occur close to such a phase transition: power-law behavior, exponential behavior, or a combination thereof. In the first and the third case, the scaling behavior in leading order is governed by a *universal* critical exponent which is determined by the symmetries and the dimensionality of the theory. Interestingly, this critical exponent also determines the infrared dynamics of the gauge sector. Therefore an analysis of the N_f -scaling behavior of observables in asymptotically free gauge theories allows us to probe the infrared gauge dynamics.

In summary, our review of universal aspects of various strongly interacting theories shows that a transfer of knowledge between studies of strongly-interacting hadronic matter and (non-relativistic) many-body problems is important and inspiring in order to gain a deeper insight into the dynamics which underlie the equation of state of hadronic matter as well as the generation of bound states in many-body problems.

Acknowledgements The author is deeply indebted to H. Gies, B. Klein and J. M. Pawłowski for uncountable discussions, encouragement and collaboration throughout the years. Moreover, the author is very grateful to C. S. Fischer, H. Gies, A. Janot, J. M. Pawłowski, J. Polonyi, D. D. Scherer and A. Schwenk for very enjoyable and fruitful collaborations on the topics presented here. It is also a great pleasure for the author to thank S. Diehl, D. D. Dietrich, J. E. Drut, A. Eichhorn, R. J. Furnstahl, T. K. Herbst, L. Janssen, M. Ku, M. P. Lombardo, H.-J. Pirner, F. Sannino, B.-J. Schaefer, M. M. Scherer and A. Wipf for various discussions which have left their traces in this manuscript. For critical comments on the manuscript, the author is very grateful to H. Gies and B. Klein. The author acknowledges support by DFG grant BR 4005/2-1 and the DFG research training group GRK 1523/1.

A Conventions

A.1 Units

In our studies of *relativistic* quantum field theories set $\hbar = c = k_B = 1$. As a consequence of this convention, the SI units for length (meter, m) and temperature (Kelvin, K) are related to the energy unit MeV as

follows

$$1 \text{ m} = 10^{15} \text{ fm} \approx 5.1 \times 10^{12} \frac{1}{\text{MeV}} \quad \text{and} \quad 1 \text{ K} \approx 8.6 \times 10^{-11} \text{ MeV}.$$

If not indicated otherwise, we set $\hbar = k_B = 2m = 1$ in our studies of *non-relativistic* quantum field theories, where m is the mass (parameter) of the fermions. As for relativistic quantum field theories, length and inverse momenta then have the same dimension, i. e.

$$[\text{length}] = [\text{momentum}]^{-1}.$$

Moreover, temperature and energy have the same dimension. From our choice $2m = 1$, it follows that the dimensions of energy and squared momenta are identical. Thus, we have

$$[\text{temperature}] = [\text{energy}] = 2 \times [\text{momentum}].$$

Finally is worth mentioning that in our conventions relativistic and non-relativistic spinors have the same mass dimension:

$$[\psi]_{\text{rel.}} = [\psi]_{\text{non-rel.}} = \frac{d}{2} \times [\text{momentum}],$$

where d denotes the number of space dimensions. Note that this is not true for the scalar fields ϕ . In this case, we have

$$[\phi]_{\text{rel.}} = \frac{d-1}{2} \times [\text{momentum}], \quad \text{and} \quad [\phi]_{\text{non-rel.}} = [\psi]_{\text{non-rel.}} = \frac{d}{2} \times [\text{momentum}].$$

A.2 Minkowski- and Euclidean Space-Time

The coordinates in d -dimensional Euclidean space-time and Minkowski (M) space-time are related by

$$\begin{aligned} x_{M,0} &= -ix_0, & x_{M,i} &= x_i, \\ g_M^{\mu\nu} x_{M,\mu} x_{M,\nu} &= x_{M,0}^2 - \vec{x}_M^2 = -x_0^2 - \vec{x}^2 = -g^{\mu\nu} x_\mu x_\nu = -x^2, \end{aligned}$$

where $\mu, \nu = 0, \dots, d-1$ and correspondingly for the momenta. The metric tensor in Euclidean space-time is given by the Kronecker-Delta, $g^{\mu\nu} = \delta^{\mu\nu}$, whereas we have the metric tensor $g_M^{\mu\nu} = \text{diag}(+, -, -, \dots, -)$ in Minkowski space-time.

A.3 Fourier Transformation

Our conventions for Fourier transformations in d -dimensional Euclidean space are summarized. For fermion fields we employ

$$\psi(x) = \int \frac{d^d p}{(2\pi)^d} \psi(p) e^{ip_\mu x_\mu}, \quad (326)$$

$$\bar{\psi}(x) = \int \frac{d^d p}{(2\pi)^d} \bar{\psi}(p) e^{-ip_\mu x_\mu}. \quad (327)$$

For bosonic fields we use

$$\phi(x) = \int \frac{d^d p}{(2\pi)^d} \phi(p) e^{ip_\mu x_\mu}. \quad (328)$$

Our conventions for the Fourier transformation of the fields imply that

$$\int d^d x e^{-ip_\mu x_\mu} = (2\pi)^d \delta^{(d)}(p). \quad (329)$$

B Dirac Algebra

B.1 Clifford Algebra in $d = 4$ (Euclidean) Space-Time Dimensions

We work exclusively in Euclidean space-time in this work and restrict our quantitative discussions to $d = 3$ and $d = 4$ space-time dimensions. The Dirac algebra is then defined through

$$\{\gamma_\mu, \gamma_\nu\} = \gamma_\mu \gamma_\nu + \gamma_\nu \gamma_\mu = 2\delta_{\mu\nu} \mathbb{1}, \quad (330)$$

$$(\gamma_\mu)^\dagger = \gamma_\mu, \quad (331)$$

$$\gamma_5 = \gamma_1 \gamma_2 \gamma_3 \gamma_0, \quad (332)$$

$$\sigma_{\mu\nu} = \frac{i}{2} [\gamma_\mu, \gamma_\nu] = \frac{i}{2} (\gamma_\mu \gamma_\nu - \gamma_\nu \gamma_\mu). \quad (333)$$

B.2 Clifford Algebra in $d = 3$ (Euclidean) Space-Time Dimensions

For our studies of quantum field theories in $d = 3$ Euclidean space-time dimensions, we employ a four-component representation for the γ -matrices. The explicit representation of our choice for the 4×4 representation of the Dirac algebra can be written as

$$\gamma_0 = \tau_3 \otimes \tau_3, \quad \gamma_1 = \tau_3 \otimes \tau_1, \quad \gamma_2 = \tau_3 \otimes \tau_2. \quad (334)$$

Here, the τ_i denote the Pauli matrices which satisfy $\tau_i \tau_j = \delta_{ij} \tau_0 + i\epsilon_{ijk} \tau_k$, with $i, j, k = 1, 2, 3$ and $\tau_0 = \mathbb{1}_2$ is a 2×2 unit matrix. The γ -matrices satisfy the anticommutation relation given in Eq. (330). Moreover, we have two additional 4×4 matrices which anticommute with all γ_μ and with each other:

$$\gamma_3 = -\tau_1 \otimes \tau_0, \quad \gamma_5 = \tau_2 \otimes \tau_0, \quad \gamma_3^2 = \gamma_5^2 = \mathbb{1}. \quad (335)$$

On the other hand, the matrix $\gamma_{35} \equiv i\gamma_3\gamma_5$ commutes with γ_μ and anticommutes with γ_3 and γ_5 .

B.3 Fierz Transformations

The Clifford Algebra defined in Sect. B.1 is spanned by 16 basis elements $\gamma^{(A)}$:

$$\{\gamma^{(A)}\} := \{\mathbb{1}, \gamma_0, \gamma_1, \gamma_2, \gamma_3, \sigma_{03}, \sigma_{13}, \sigma_{23}, \sigma_{01}, \sigma_{12}, \sigma_{20}, i\gamma_0\gamma_5, i\gamma_1\gamma_5, i\gamma_2\gamma_5, i\gamma_3\gamma_5, \gamma_5\}, \quad (336)$$

which obey

$$\text{tr} \left\{ \gamma^{(A)} \gamma^{(B)} \right\} = 4 \delta_{AB}. \quad (337)$$

This basis is complete:

$$\frac{1}{4} \sum_A \gamma_{ad}^{(A)} \gamma_{ef}^{(A)} = \delta_{af} \delta_{ed}. \quad (338)$$

From the completeness relation it is straightforward to expand two matrices, e. g. $M_{ab}^{(1)} M_{cd}^{(2)}$, in terms of the basis elements $\gamma^{(A)}$:

$$M_{ab}^{(1)} M_{cd}^{(2)} = \frac{1}{4} \sum_A \gamma_{ad}^{(A)} \sum_{e,f} (M_{ce}^{(2)} \gamma_{ef}^{(A)} M_{fb}^{(1)}). \quad (339)$$

This expression corresponds to the general expression given in Eq. (24). Defining

$$O_S = \mathbb{1}, \quad O_V = \gamma_\mu, \quad O_T = \frac{1}{\sqrt{2}} \sigma_{\mu\nu}, \quad O_A = \gamma_\mu \gamma_5 \quad \text{and} \quad O_P = \gamma_5, \quad (340)$$

we then obtain the following Fierz identities:

$$(\bar{\psi}_a O_X \psi_b) (\bar{\psi}_c O_Y \psi_d) = \sum_Y C_{XY} (\bar{\psi}_a O_Y \psi_d) (\bar{\psi}_c O_X \psi_b), \quad (341)$$

where $X, Y = S, V, T, A, P$ and

$$C_{XY} = \frac{1}{4} \begin{pmatrix} -1 & -1 & -1 & 1 & -1 \\ -4 & 2 & 0 & 2 & 4 \\ -6 & 0 & 2 & 0 & -6 \\ 4 & 2 & 0 & 2 & -4 \\ -1 & 1 & -1 & -1 & -1 \end{pmatrix}. \quad (342)$$

In Sect. 3, we study a NJL model with one fermion species at zero and at finite temperature. In this special case, the combination

$$(\bar{\psi}O_V\psi)^2 + (\bar{\psi}O_A\psi)^2$$

is invariant under Fierz transformations. Due to the relation

$$(\bar{\psi}O_V\psi)^2 - (\bar{\psi}O_A\psi)^2 + 2[(\bar{\psi}O_S\psi)^2 - (\bar{\psi}O_P\psi)] = 0, \quad (343)$$

we can transform the combination

$$(\bar{\psi}O_V\psi)^2 - (\bar{\psi}O_A\psi)^2$$

completely into scalar and pseudo-scalar channels.

C $SU(N)$ Algebra

In this appendix we give our conventions for the generators of the $SU(N)$ Lie-groups. The group $SU(N)$ of unitary matrices U of rank N with determinant $\det U = 1$ has $N^2 - 1$ generators T^a which obey the commutation relations

$$[T^a, T^b] = if^{abc}T^c, \quad (344)$$

where f^{abc} are the (anti-symmetric) structure constants of the group, and a, b, c take the values $1, \dots, N^2 - 1$. The normalization of the generators is given by

$$\text{Tr} \{T^a T^b\} = \frac{1}{2} \delta^{ab}. \quad (345)$$

Moreover, the generators fulfill the following (Fierz) identities:

$$\sum_a (T^a)_{\alpha\beta} (T^a)_{\gamma\delta} = \frac{1}{2} \delta_{\alpha\delta} \delta_{\beta\gamma} - \frac{1}{2N} \delta_{\alpha\beta} \delta_{\gamma\delta} \quad (346)$$

and

$$\sum_a \left\{ (T^a)_{\alpha\beta} (T^a)_{\gamma\delta} + \frac{1}{N} (T^a)_{\alpha\delta} (T^a)_{\beta\gamma} \right\} = \frac{N^2 - 1}{2N^2} \delta_{\alpha\delta} \delta_{\beta\gamma}. \quad (347)$$

For $SU(2)$, the generators are related to the Pauli matrices τ^a via $T^a = \frac{1}{2} \tau^a$ and the structure constants f^{abc} are given by the (standard) totally antisymmetric tensor ϵ^{abc} . The generators for the group $SU(3)$ can be expressed in terms of the Gell-Mann matrices λ^a via $T^a = \frac{1}{2} \lambda^a$.

D Regulator Functions and Threshold Functions

D.1 Regulator Functions

In the computation of the RG flow equations a regulator function needs to be specified which determines the regularization scheme. For explicit calculations we employ *optimized* regulator functions at zero and at finite temperature [129–131, 171, 172].

If not indicated otherwise, we employ the following so-called spatial regulator functions whenever we study a *relativistic* theory at zero *and* at finite temperature. To be specific, we choose

$$R_{\text{B}}(\vec{p}^2) = \vec{p}^2 \left(\frac{k^2}{\vec{p}^2} - 1 \right) \theta(k^2 - \vec{p}^2) \equiv \vec{p}^2 r_{\text{B}} \left(\frac{\vec{p}^2}{k^2} \right) \quad (348)$$

for the bosonic degrees of freedom, whereas we choose

$$R_{\psi}(\vec{p}) = -\not{\vec{p}} \left(\sqrt{\frac{k^2}{\vec{p}^2}} - 1 \right) \theta(k^2 - \vec{p}^2) \equiv -\not{\vec{p}} r_{\psi} \left(\frac{\vec{p}^2}{k^2} \right) \quad (349)$$

for the fermionic degrees of freedom. In many cases these regulator functions open up the possibility to perform analytically the Matsubara sums as well as the momentum integrals appearing in the 1PI diagrams.

For cases in which we consider a theory only at vanishing temperature, we use the following so-called covariant regulator functions for the bosons and fermions, respectively:

$$R_{\text{B}}(p^2) = p^2 \left(\frac{k^2}{p^2} - 1 \right) \theta(k^2 - p^2) \equiv p^2 r_{\text{B}} \left(\frac{p^2}{k^2} \right), \quad (350)$$

$$R_{\psi}(p) = -\not{p} \left(\sqrt{\frac{k^2}{p^2}} - 1 \right) \theta(k^2 - p^2) \equiv \not{p} r_{\psi} \left(\frac{p^2}{k^2} \right). \quad (351)$$

For our studies of *non-relativistic* fermionic many-body problems we use [27]

$$R_k^{\psi}(\vec{p}^2) = k^2 r_{\psi}(\mathcal{Z}) \quad \text{with} \quad \mathcal{Z} = (\vec{p}^2 - \mu)/k^2, \quad (352)$$

where

$$r_{\psi}(\mathcal{Z}) = (\text{sign}(\mathcal{Z}) - \mathcal{Z})\theta(1 - |\mathcal{Z}|) \quad (353)$$

and \vec{p}^2 denotes the square of the spatial momentum.

In the next two sections we list the threshold functions which appear in the RG flow equations. These functions represent the 1PI diagrams contributing to the RG flow of the studied couplings. Note that we have adopted the conventions introduced in Refs. [113]. The list of threshold functions in the two subsequent sections is not exhaustive. We only list those functions which have been employed explicitly in this review.

D.2 Threshold Functions for Covariant Regulators

In this section we give the general definition of the threshold functions as obtained for covariant regulators. For (explicit) evaluation of the momentum integrations we have used the (optimized) regulator functions defined in Eqs. (350) and (351). In order to define the threshold functions, it is convenient to define dimensionless propagators for the bosons (B) and the fermions (ψ), respectively:

$$\tilde{G}_{\text{B}}(\omega) = \frac{1}{x(1 + r_{\text{B}}) + \omega} \quad (354)$$

and

$$\tilde{G}_{\psi}(\omega) = \frac{1}{x(1 + r_{\psi})^2 + \omega}, \quad (355)$$

where $x = p^2/k^2$.

The threshold functions representing purely bosonic 1PI diagrams in the flow equations of bosonic self-interactions are given by

$$\begin{aligned} l_0^{(d)}(\omega; \eta_B) &= \frac{1}{2} \int_0^\infty dx x^{\frac{d}{2}} (\partial_t r_B - \eta_B r_B) \tilde{G}_B(\omega) \\ &= \frac{2}{d} \left(1 - \frac{\eta_B}{d+2}\right) \frac{1}{1+\omega}, \end{aligned} \quad (356)$$

where $\eta_B \equiv -\partial_t \ln Z_B$. Bosonic threshold functions of order n can then be obtained from Eq. (356) by taking derivatives with respect to the dimensionless mass parameter ω :

$$\frac{\partial}{\partial \omega} l_n^{(d)}(\omega; \eta_B) = -(n + \delta_{n,0}) l_{n+1}^{(d)}(\omega; \eta_B). \quad (357)$$

The threshold functions representing purely fermionic 1PI diagrams in the flow equations of bosonic self-interactions as well as fermionic self-interactions are given by

$$\begin{aligned} l_0^{(F),(d)}(\omega; \eta_\psi) &= \int_0^\infty dx x^{\frac{d}{2}} (\partial_t r_\psi - \eta_\psi r_\psi) (1 + r_\psi) \tilde{G}_\psi(\omega) \\ &= \frac{2}{d} \left(1 - \frac{\eta_\psi}{d+1}\right) \frac{1}{1+\omega}, \end{aligned} \quad (358)$$

where $\eta_\psi = -\partial_t \ln Z_\psi$. Again, higher-order fermionic threshold functions can be found by taking derivatives with respect to the dimensionless mass parameter ω :

$$\frac{\partial}{\partial \omega} l_n^{(F),(d)}(\omega; \eta_\psi) = -(n + \delta_{n,0}) l_{n+1}^{(F),(d)}(\omega; \eta_\psi). \quad (359)$$

Let us now turn to the threshold functions representing mixed boson-fermion diagrams. For example, these functions enter the flow equations of Yukawa couplings and flow equations of four-fermion couplings. We have

$$l_{1,1}^{(FB),(d)}(\omega_\psi, \omega_B; \eta_\psi, \eta_B) = -\frac{1}{2} \int_0^\infty dx x^{\frac{d-2}{2}} \tilde{\partial}_t \left[\tilde{G}_\psi(\omega_\psi) \tilde{G}_B(\omega_B) \right]. \quad (360)$$

In order to evaluate the integral over x , we use⁸⁷

$$\tilde{\partial}_t \Big|_\psi = \left(\frac{1}{x^{1/2}} - \eta_\psi \left(\frac{1}{x^{1/2}} - 1 \right) \right) \theta(1-x) \frac{\partial}{\partial r_\psi}, \quad (361)$$

$$\tilde{\partial}_t \Big|_B = \left(\frac{2}{x} - \eta_B \left(\frac{1}{x} - 1 \right) \right) \theta(1-x) \frac{\partial}{\partial r_B}, \quad (362)$$

where the first and the second line states how the formal derivative $\tilde{\partial}_t$ acts on the fermion and boson propagator, respectively. This yields

$$\begin{aligned} l_{1,1}^{(FB),(d)}(\omega_\psi, \omega_B; \eta_\psi, \eta_B) \\ = \frac{2}{d} \frac{1}{(1+\omega_\psi)(1+\omega_B)} \left\{ \left(1 - \frac{\eta_\psi}{d+1}\right) \frac{1}{1+\omega_\psi} + \left(1 - \frac{\eta_B}{d+2}\right) \frac{1}{1+\omega_B} \right\}. \end{aligned} \quad (363)$$

⁸⁷ Here, we only give the explicit expressions for the formal derivatives for the (optimized) regulator functions given in Eqs. (350) and (351).

The threshold function $l_{1,2}^{(\text{FB}),(\text{d})}$ is defined as follows:

$$\begin{aligned} l_{1,2}^{(\text{FB}),(\text{d})}(\omega_\psi, \omega_B; \eta_\psi, \eta_B) &= -\frac{1}{2} \int_0^\infty dx x^{\frac{d-2}{2}} \tilde{\partial}_t \left[\tilde{G}_\psi(\omega_\psi) \left(\tilde{G}_B(\omega_B) \right)^2 \right] \\ &= \frac{2}{d} \frac{1}{(1+\omega_\psi)(1+\omega_B)^2} \left\{ \frac{1}{1+\omega_\psi} \left(1 - \frac{\eta_\psi}{d+1} \right) \right. \\ &\quad \left. + \frac{2}{1+\omega_B} \left(1 - \frac{\eta_B}{d+2} \right) \right\}. \end{aligned} \quad (364)$$

The threshold functions entering the RG flow equations of the wave-function renormalizations read

$$\begin{aligned} m_{1,2}^{(\text{FB}),(\text{d})}(\omega_\psi, \omega_B; \eta_\psi, \eta_B) &= \frac{1}{2} \int_0^\infty dx x^{\frac{d}{2}} \tilde{\partial}_t \left[(1+r_\psi) \tilde{G}_\psi(\omega_\psi) \frac{d}{dx} \tilde{G}_B(\omega_B) \right] \\ &= \left(1 - \frac{\eta_B}{d+1} \right) \frac{1}{(1+\omega_\psi)(1+\omega_B)^2} \end{aligned} \quad (365)$$

and

$$\begin{aligned} m_4^{(\text{F}),(\text{d})}(\omega; \eta_\psi) &= -\frac{1}{2} \int_0^\infty dx x^{\frac{d+2}{2}} \tilde{\partial}_t \left[\frac{d}{dx} (1+r_\psi) \tilde{G}_\psi(\omega) \right]^2 \\ &= \frac{1}{(1+\omega)^4} + \frac{1-\eta_\psi}{d-2} \frac{1}{(1+\omega)^3} - \left(\frac{1-\eta_\psi}{2d-4} + \frac{1}{4} \right) \frac{1}{(1+\omega)^2}. \end{aligned} \quad (366)$$

Finally, we define the threshold functions which appear in the flow equations of fermionic theories with an explicitly broken chiral symmetry:

$$\begin{aligned} \tilde{l}_1^{(\text{F}),(\text{d})}(\omega; \eta_\psi) &= -\frac{\omega}{2} \int_0^\infty dx x^{\frac{d-2}{2}} \tilde{\partial}_t \left(\tilde{G}_\psi(\omega) \right)^2 \\ &\stackrel{(\eta_\psi=0)}{=} \frac{4}{d} \frac{\omega}{(1+\omega)^3} \end{aligned} \quad (367)$$

and

$$\begin{aligned} \tilde{l}_1^{(\text{F}),(\text{d})}(\omega; \eta_\psi) &= -\frac{1}{2} \int_0^\infty dx x^{\frac{d}{2}} \tilde{\partial}_t \left[(1+r_\psi)^2 \left(\tilde{G}_\psi(\omega) \right)^2 \right] \\ &\stackrel{(\eta_\psi=0)}{=} \frac{2}{d} \frac{1-\omega}{(1+\omega)^3}. \end{aligned} \quad (368)$$

Note that

$$l_1^{(\text{F}),(\text{d})}(\omega; \eta_\psi) = \tilde{l}_1^{(\text{F}),(\text{d})}(\omega; \eta_\psi) + \tilde{l}_1^{(\text{F}),(\text{d})}(\omega; \eta_\psi), \quad (369)$$

since

$$\tilde{\partial}_t \Big|_\psi = (\partial_t r_\psi - \eta_\psi r_\psi) \frac{\partial}{\partial r_\psi}. \quad (370)$$

Moreover, we have

$$\begin{aligned} b_1^{(\text{F}),(\text{d})}(\omega; \eta_\psi) &= -\frac{\omega}{2} \int_0^\infty dx x^{\frac{d-2}{2}} \tilde{\partial}_t \tilde{G}_\psi(\omega) \\ &\stackrel{(\eta_\psi=0)}{=} \frac{2}{d} \frac{\omega}{(1+\omega)^2}. \end{aligned} \quad (371)$$

D.3 Threshold Functions for Dimensionally Reduced Regulators

Spatial (or thermal) regulator functions are mostly applied in the context of finite-temperature studies. However, their application is not limited to these kind of investigations. Below we give the general definition of the resulting threshold functions employed in this review. For the (explicit) evaluation of the momentum integrations we have used the regulator functions given in Eqs. (348) and (349).

In order to define the threshold functions, it is convenient to define dimensionless propagators for the bosons (B) and the fermions (ψ), respectively:

$$\tilde{G}_B(x_0, \omega) = \frac{1}{\hat{z}_B x_0 + x(1 + r_B) + \omega} \quad (372)$$

and

$$\tilde{G}_\psi(x_0, \omega) = \frac{1}{\hat{z}_\psi^2 x_0 + x(1 + r_\psi)^2 + \omega}, \quad (373)$$

where $x = \bar{p}^2/k^2$. Here, we have dressed the ratio of the wave-function renormalizations longitudinal and transversal to the heat-bath, $\hat{z}_B = Z_B^\parallel/Z_B^\perp$ and $\hat{z}_\psi = Z_\psi^\parallel/Z_\psi^\perp$.

First, we define the threshold functions which appear in the RG flow equations for the bosonic self-interactions. For the purely bosonic loops, we find

$$\begin{aligned} l_0^{(d)}(\tau, \omega; \eta_B, \hat{z}_B) &= \frac{\tau}{2} \sum_{n=-\infty}^{\infty} \int_0^\infty dx x^{\frac{d-1}{2}} (\partial_t r_B - \eta_B r_B) \tilde{G}_B(\tilde{\omega}_n^2, \omega) \\ &= \frac{2}{d-1} \frac{1}{\sqrt{1+\omega}} \left(1 - \frac{\eta_B}{d+1}\right) \left(\frac{1}{2} + \bar{n}_B(\tau, \omega)\right), \end{aligned} \quad (374)$$

where $\eta_B \equiv -\partial_t \ln Z_B^\perp$, $\tau = T/k$ denotes the dimensionless temperature and $\tilde{\omega} = 2\pi n\tau$ denotes the dimensionless bosonic Matsubara frequencies. The function n_B represents the Bose-Einstein distribution function

$$\bar{n}_B(\tau, \omega) = \frac{1}{e^{\sqrt{1+\omega}/\tau} - 1}. \quad (375)$$

Bosonic threshold functions of order n can then be obtained from Eq. (374) by taking derivatives with respect to the dimensionless mass parameter ω :

$$\frac{\partial}{\partial \omega} l_n^{(d)}(\tau, \omega; \eta_B, \hat{z}_B) = -(n + \delta_{n,0}) l_{n+1}^{(d)}(\tau, \omega; \eta_B, \hat{z}_B). \quad (376)$$

For the purely fermionic loops contributing to the flow equations of the bosonic self-interactions but also to the RG flow of the four-fermion coupling, we find

$$\begin{aligned} l_0^{(F),(d)}(\tau, \omega, \mu; \eta_\psi, \hat{z}_\psi) &= \tau \sum_{n=-\infty}^{\infty} \int_0^\infty dx x^{\frac{d-1}{2}} (\partial_t r_\psi - \eta_\psi r_\psi)(1 + r_\psi) \tilde{G}_\psi((\tilde{\nu}_n + 2\pi\tau\mu)^2, \omega) \\ &= \frac{1}{d-1} \frac{1}{\sqrt{1+\omega}} \left(1 - \frac{\eta_\psi}{d}\right) (1 - \bar{n}_\psi(\tau, i\mu, \omega) - \bar{n}_\psi(\tau, -i\mu, \omega)). \end{aligned} \quad (377)$$

Here, we have introduced the dimensionless fermionic Matsubara frequencies $\tilde{\nu}_n = (2n+1)\pi\tau$ and $\eta_\psi \equiv -\partial_t \ln Z_\psi^\perp$. The function \bar{n}_ψ denotes the Fermi-Dirac distribution function:

$$\bar{n}_\psi(\tau, \mu, \omega) = \frac{1}{e^{(\sqrt{1+\omega}/\tau) + 2\pi\mu} + 1}. \quad (378)$$

Higher-order fermionic threshold functions can again be found by taking derivatives with respect to the dimensionless mass parameter ω :

$$\frac{\partial}{\partial \omega} l_n^{(F),(d)}(\tau, \omega, \mu; \eta_\psi, \hat{z}_\psi) = -(n + \delta_{n,0}) l_{n+1}^{(F),(d)}(\tau, \omega, \mu; \eta_\psi, \hat{z}_\psi). \quad (379)$$

Finally, we give the definition of the threshold function which appears in the RG flow equations of the Yukawa coupling. We have

$$l_{1,1}^{(\text{FB}),(\text{d})}(\tau, \omega_\psi, \omega_B; \eta_\psi, \eta_B, \hat{z}_\psi, \hat{z}_B) = -\frac{\tau}{2} \sum_{n=-\infty}^{\infty} \int_0^\infty dx x^{\frac{d-3}{2}} \tilde{\partial}_t \left[\tilde{G}_\psi(\tilde{\nu}_n^2, \omega_\psi) \tilde{G}_B(\tilde{\nu}_n^2, \omega_B) \right]. \quad (380)$$

To evaluate the integral over x (spatial momenta), we have to take derivatives with respect to the regulator function. For the regulator functions (348) and (349) these derivatives are given by

$$\tilde{\partial}_t \Big|_\psi = \left(\frac{1}{x^{1/2}} - \eta_\psi \left(\frac{1}{x^{1/2}} - 1 \right) \right) \theta(1-x) \frac{\partial}{\partial r_\psi}, \quad (381)$$

$$\tilde{\partial}_t \Big|_B = \left(\frac{2}{x} - \eta_B \left(\frac{1}{x} - 1 \right) \right) \theta(1-x) \frac{\partial}{\partial r_B}, \quad (382)$$

where the first and the second line defines how the formal derivative $\tilde{\partial}_t$ acts on the fermion propagator and the boson propagator, respectively. These expressions are only valid for the spatial regulator functions given in Eqs. (350) and (351). Recall that x refers to the squared *spatial* (loop) momentum. In this review, we have only used general properties of the threshold function $l_{1,1}^{(\text{FB}),(\text{d})}$ (for $\mu = 0$), but we have not employed it in the numerical evaluations of the flow equations. Therefore we only give the general definition of this function here.

References

- [1] P. Braun-Munzinger, D. Magestro, K. Redlich, and J. Stachel, Phys. Lett. **B518**, 41–46 (2001).
- [2] H. Feshbach, Annals of Physics **5**(4), 357–390 (1958).
- [3] M. W. Zwierlein, C. H. Schunck, A. Schirotzek, and W. Ketterle, Nature **442**, 54–58 (2006).
- [4] W. Partridge, Guthrie B. amd Li., R. I. Kamar, Y. a. Liao, and R. G. Hulet, Science **311**, 503–505 (2006).
- [5] G. B. Partridge, W. Li, Y. A. Liao, R. G. Hulet, M. Haque, and H. T. C. Stoof, Phys. Rev. Lett. **97**(19), 190407 (2006).
- [6] Q. Chen, C. A. Regal, M. Greiner, D. S. Jin, and K. Levin, Phys. Rev. A **73**(4), 041601 (2006).
- [7] S. Nascimbène, N. Navon, K. J. Jiang, F. Chevy, and C. Salomon, Nature **463**(7284), 1057–1060 (2010).
- [8] J. Carlson, S. Y. Chang, V. R. Pandharipande, and K. E. Schmidt, Phys. Rev. Lett. **91**(5), 050401 (2003).
- [9] G. E. Astrakharchik, J. Boronat, J. Casulleras, Giorgini, and S., Phys. Rev. Lett. **93**(20), 200404 (2004).
- [10] A. Bulgac, J. E. Drut, and P. Magierski, Phys. Rev. Lett. **96**, 090404 (2006).
- [11] A. Bulgac, J. E. Drut, and P. Magierski, Phys. Rev. Lett. **99**, 120401 (2007).
- [12] E. Burovski, N. Prokof'ev, B. Svistunov, and M. Troyer, Phys. Rev. Lett. **96**(16), 160402 (2006).
- [13] V. K. Akkineni, D. M. Ceperley, and N. Trivedi, Phys. Rev. B **76**(16), 165116 (2007).
- [14] A. Bulgac, J. E. Drut, and P. Magierski, Phys. Rev. A **78**, 023625 (2008).
- [15] R. Combescot and C. Mora, EPL (Europhysics Letters) **68**(1), 79 (2004).
- [16] F. Chevy, Phys. Rev. Lett. **96**(13), 130401 (2006).
- [17] F. Chevy, Phys. Rev. A **74**(6), 063628 (2006).
- [18] K. B. Gubbels, M. W. J. Romans, and H. T. C. Stoof, Phys. Rev. Lett. **97**(21), 210402 (2006).
- [19] W. Yi and L. M. Duan, Phys. Rev. A **73**(3), 031604 (2006).
- [20] A. Bulgac and M. M. Forbes, Phys. Rev. A **75**(3), 031605 (2007).
- [21] S. Diehl, H. Gies, J. M. Pawłowski, and C. Wetterich, Phys. Rev. A **76**, 053627 (2007).
- [22] S. Pilati and S. Giorgini, Phys. Rev. Lett. **100**(3), 030401 (2008).
- [23] K. B. Gubbels and H. T. C. Stoof, Phys. Rev. Lett. **100**(14), 140407 (2008).
- [24] A. Recati, C. Lobo, and S. Stringari, Phys. Rev. A **78**(2), 023633 (2008).
- [25] I. Bloch, J. Dalibard, and W. Zwerger, Rev. Mod. Phys. **80**(3), 885–964 (2008).
- [26] R. Haussmann and W. Zwerger, Phys. Rev. A **78**(6), 063602 (2008).
- [27] S. Diehl, S. Floerchinger, H. Gies, J. M. Pawłowski, and C. Wetterich, Annalen Phys. **522**, 615–656 (2010).
- [28] H. Gies and C. Wetterich, Phys. Rev. D **69**, 025001 (2004).
- [29] H. Gies and J. Jaeckel, Eur. Phys. J. C **46**, 433–438 (2006).
- [30] J. Braun and H. Gies, Phys. Lett. **B645**, 53–58 (2007).

- [31] J. Braun and H. Gies, JHEP **06**, 024 (2006).
- [32] J. Braun, Eur. Phys. J. **C64**, 459–482 (2009).
- [33] J. Braun, Phys. Rev. **D81**, 016008 (2010).
- [34] J. Bardeen, L. N. Cooper, and J. R. Schrieffer, Phys. Rev. **108**, 1175–1204 (1957).
- [35] L. P. Gorkov and T. K. Melik-Barkhudarov, Sov. Phys. JETP **13**, 1018 (1961).
- [36] H. Heiselberg, C. J. Pethick, H. Smith, and L. Viverit, Phys. Rev. Lett. **85**, 2418–2421 (2000).
- [37] P. B. Arnold and G. D. Moore, Phys. Rev. Lett. **87**, 120401 (2001).
- [38] V. A. Kashurnikov, N. V. Prokof'ev, and B. V. Svistunov, Phys. Rev. Lett. **87**, 120402 (2001).
- [39] J. P. Blaizot, R. Mendez Galain, and N. Wschebor, Europhys. Lett. **72**, 705–711 (2005).
- [40] R. Schmidt and T. Enss, Phys. Rev. **A83**, 063620 (2011).
- [41] M. Ku, J. Braun, and A. Schwenk, Phys. Rev. Lett. **102**, 255301 (2009).
- [42] M. Thies and K. Urlichs, Phys. Rev. **D67**, 125015 (2003).
- [43] P. de Forcrand and U. Wenger, PoS **LAT2006**, 152 (2006).
- [44] D. Nickel, Phys. Rev. **D80**, 074025 (2009).
- [45] T. Kojo, Y. Hidaka, L. McLerran, and R. D. Pisarski, Nucl. Phys. **A843**, 37–58 (2010).
- [46] G. Colangelo, S. Dürr, and R. Sommer, Nucl. Phys. Proc. Suppl. **119**, 254–256 (2003).
- [47] A. Ali Khan et al., Nucl. Phys. **B689**, 175–194 (2004).
- [48] G. Colangelo and S. Dürr, Eur. Phys. J. **C33**, 543–553 (2004).
- [49] M. Guagnelli et al., Phys. Lett. **B597**, 216–221 (2004).
- [50] G. Colangelo and C. Haefeli, Phys. Lett. **B590**, 258–264 (2004).
- [51] J. Braun, B. Klein, and H. J. Pirner, Phys. Rev. **D71**, 014032 (2005).
- [52] G. Colangelo, S. Dürr, and C. Haefeli, Nucl. Phys. **B721**, 136–174 (2005).
- [53] J. Braun, B. Klein, H. J. Pirner, and A. H. Rezaeian, Phys. Rev. **D73**, 074010 (2006).
- [54] J. Braun, B. Klein, and H. J. Pirner, Phys. Rev. **D72**, 034017 (2005).
- [55] J. Braun, B. Klein, and P. Piasecki, Eur. Phys. J. **C71**, 1576 (2011).
- [56] B. Klein, J. Braun, and B. J. Schaefer, PoS **LATTICE2010**, 193 (2010).
- [57] J. Braun, B. Klein, and B. J. Schaefer, in preparation (2010).
- [58] W. Kohn and L. J. Sham, Phys. Rev. **140**(4A), A1133–A1138 (1965).
- [59] J. Hubbard, Phys. Rev. Lett. **3**, 77–80 (1959).
- [60] R. Stratonovich, Dokl. Akad. Nauk. **115**, 1097 (1957).
- [61] T. N. De Silva and E. J. Mueller, Phys. Rev. A **73**(5), 051602 (2006).
- [62] R. Sensarma, W. Schneider, R. B. Diener, and M. Randeria, arXiv:0706.1741.
- [63] J. Dobaczewski, W. Nazarewicz, and P. G. Reinhard, Nucl. Phys. **A693**, 361–373 (2001).
- [64] M. V. Stoitsov, J. Dobaczewski, W. Nazarewicz, S. Pittel, and D. J. Dean, Phys. Rev. **C68**, 054312 (2003).
- [65] M. Bender, P. H. Heenen, and P. G. Reinhard, Rev. Mod. Phys. **75**, 121–180 (2003).
- [66] P. W. Anderson, The Theory of Superconductivity in the HighTc Cuprate Superconductors (Princeton University Press, Princeton, 1997).
- [67] P. Fulde, Electron Correlations in Molecules and Solids (Springer, Heidelberg, 1991).
- [68] C. Honerkamp, Eur. Phys. J. B **21**(1), 81–91 (2001).
- [69] C. Honerkamp, M. Salmhofer, and T. M. Rice, Eur. Phys. J. B **27**(1), 127–134 (2002).
- [70] R. Gersch, C. Honerkamp, D. Rohe, and W. Metzner, Eur. Phys. J. B **48**(3), 349–358 (2005).
- [71] M. Salmhofer, C. Honerkamp, W. Metzner, and Oliver, Progress of Theoretical Physics **112**(December), 943–970 (2004).
- [72] J. Mertsching and H. J. Fischbeck, physica status solidi (b) **103**(2), 783–795 (1981).
- [73] O. Schnetz, M. Thies, and K. Urlichs, Ann. Phys. **314**, 425–447 (2004).
- [74] J. E. Drut and D. T. Son, Phys. Rev. **B77**(7), 075115 (2008).
- [75] H. Gies and L. Janssen, Phys. Rev. **D82**, 085018 (2010).
- [76] H. Gies, L. Janssen, S. Rechenberger, and M. M. Scherer, Phys. Rev. **D81**, 025009 (2010).
- [77] J. Jaeckel, Effective actions for strongly interacting fermionic systems, PhD thesis, University of Heidelberg, 2003, hep-ph/0309090.
- [78] J. Braun and H. Gies, JHEP **05**, 060 (2010).
- [79] J. Braun, C. S. Fischer, and H. Gies, (to appear in Phys. Rev. D), arXiv:1012.4279.
- [80] S. Weinberg, Phys. Rev. **D19**, 1277–1280 (1979).
- [81] B. Holdom, Phys. Rev. **D24**, 1441 (1981).
- [82] D. K. Hong, S. D. H. Hsu, and F. Sannino, Phys. Lett. **B597**, 89–93 (2004).
- [83] F. Sannino and K. Tuominen, Phys. Rev. **D71**, 051901 (2005).
- [84] D. D. Dietrich, F. Sannino, and K. Tuominen, Phys. Rev. **D72**, 055001 (2005).
- [85] D. D. Dietrich and F. Sannino, Phys. Rev. **D75**, 085018 (2007).
- [86] T. A. Rytov and F. Sannino, Phys. Rev. **D76**, 105004 (2007).

- [87] O. Antipin and K. Tuominen, Phys. Rev. **D81**, 076011 (2010).
- [88] F. Sannino, Acta Phys. Polon. **B40**, 3533–3743 (2009).
- [89] K. G. Wilson, Phys. Rev. **B4**, 3174–3183 (1971).
- [90] K. G. Wilson, Phys. Rev. **B4**, 3184–3205 (1971).
- [91] K. G. Wilson and J. B. Kogut, Phys. Rept. **12**, 75–200 (1974).
- [92] F. J. Wegner and A. Houghton, Phys. Rev. **A8**, 401–412 (1973).
- [93] J. F. Nicoll and T. S. Chang, Phys. Lett. **A62**, 287–289 (1977).
- [94] J. Polchinski, Nucl. Phys. **B231**, 269–295 (1984).
- [95] C. Wetterich, Phys. Lett. **B301**, 90–94 (1993).
- [96] R. Shankar, Rev. Mod. Phys. **66**, 129–192 (1994).
- [97] D. F. Litim and J. M. Pawłowski, in *The Exact Renormalization Group*, Eds. Krasnitz et al., World Scientific, pp. 168 (1999), hep-th/9901063.
- [98] M. Salmhofer, Renormalization: An Introduction (Springer, Heidelberg, 1999).
- [99] C. Bagnuls and C. Bervillier, Phys. Rept. **348**, 91 (2001).
- [100] J. Berges, N. Tetradis, and C. Wetterich, Phys. Rept. **363**, 223–386 (2002).
- [101] J. Polonyi, Central Eur. J. Phys. **1**, 1–71 (2003).
- [102] S. K. Bogner, T. T. S. Kuo, and A. Schwenk, Phys. Rept. **386**, 1–27 (2003).
- [103] B. Delamotte, D. Mouhanna, and M. Tissier, Phys. Rev. **B69**, 134413 (2004).
- [104] J. M. Pawłowski, Annals Phys. **322**, 2831–2915 (2007).
- [105] H. Gies, hep-ph/0611146.
- [106] B. Delamotte, cond-mat/0702365.
- [107] S. K. Bogner, R. J. Furnstahl, and A. Schwenk, Prog. Part. Nucl. Phys. **65**, 94–147 (2010).
- [108] O. J. Rosten, arXiv:1003.1366.
- [109] P. Kopietz, L. Bartosch, and F. Schutz, Lect. Notes Phys. **798**, 1–380 (2010).
- [110] W. Metzner, M. Salmhofer, C. Honerkamp, V. Meden, and K. Schonhammer, arXiv:1105.5289.
- [111] P. M. Stevenson, Phys. Rev. **D23**, 2916 (1981).
- [112] S. Pokorski, Gauge field theories (Cambridge, UK: Univ. Press, 1987).
- [113] D. U. Jungnickel and C. Wetterich, Phys. Rev. **D53**, 5142–5175 (1996).
- [114] M. Bonini, M. D’Attanasio, and G. Marchesini, Nucl. Phys. **B437**, 163–186 (1995).
- [115] U. Ellwanger, M. Hirsch, and A. Weber, Z. Phys. **C69**, 687–698 (1996).
- [116] U. Ellwanger, M. Hirsch, and A. Weber, Eur. Phys. J. **C1**, 563–578 (1998).
- [117] M. Reuter, hep-th/9602012.
- [118] M. Reuter and C. Wetterich, Phys. Rev. **D56**, 7893–7916 (1997).
- [119] F. Freire, D. F. Litim, and J. M. Pawłowski, Phys. Lett. **B495**, 256–262 (2000).
- [120] T. R. Morris, JHEP **12**, 012 (2000).
- [121] S. Arnone, T. R. Morris, and O. J. Rosten, Eur. Phys. J. **C50**, 467–504 (2007).
- [122] L. F. Abbott, Nucl. Phys. **B185**, 189 (1981).
- [123] L. F. Abbott, Acta Phys. Polon. **B13**, 33 (1982).
- [124] H. Gies and C. Wetterich, Phys. Rev. **D65**, 065001 (2002).
- [125] H. Gies and C. Wetterich, Acta Phys. Slov. **52**, 215–220 (2002).
- [126] S. Floerchinger and C. Wetterich, Phys. Lett. **B680**, 371–376 (2009).
- [127] S. Floerchinger, Eur. Phys. J. **C69**, 119–132 (2010).
- [128] D. F. Litim and J. M. Pawłowski, Phys. Rev. **D66**, 025030 (2002).
- [129] D. F. Litim, Int. J. Mod. Phys. **A16**, 2081–2088 (2001).
- [130] D. F. Litim, Phys. Lett. **B486**, 92–99 (2000).
- [131] D. F. Litim, Phys. Rev. **D64**, 105007 (2001).
- [132] Y. Nambu and G. Jona-Lasinio, Phys. Rev. **122**, 345–358 (1961).
- [133] Y. Nambu and G. Jona-Lasinio, Phys. Rev. **124**, 246–254 (1961).
- [134] S. P. Klevansky, Rev. Mod. Phys. **64**, 649–708 (1992).
- [135] J. Berges, D. U. Jungnickel, and C. Wetterich, Phys. Rev. **D59**, 034010 (1999).
- [136] B. J. Schaefer and H. J. Pirner, Nucl. Phys. **A660**, 439–474 (1999).
- [137] J. Braun, K. Schwenzer, and H. J. Pirner, Phys. Rev. **D70**, 085016 (2004).
- [138] B. J. Schaefer and J. Wambach, Nucl. Phys. **A757**, 479–492 (2005).
- [139] E. Nakano, B. J. Schaefer, B. Stokic, B. Friman, and K. Redlich, Phys. Lett. **B682**, 401–407 (2010).
- [140] J. Jaeckel and C. Wetterich, Phys. Rev. **D68**, 025020 (2003).
- [141] J. D. Walecka, Oxford Stud. Nucl. Phys. **16**, 1–610 (1995).
- [142] K. I. Aoki, K. Morikawa, J. I. Sumi, H. Terao, and M. Tomoyose, Phys. Rev. **D61**, 045008 (2000).
- [143] N. Tetradis and C. Wetterich, Nucl. Phys. **B422**, 541–592 (1994).
- [144] D. F. Litim, Nucl. Phys. **B631**, 128–158 (2002).

- [145] C. Bervillier, A. Juttner, and D. F. Litim, Nucl. Phys. **B783**, 213–226 (2007).
- [146] F. Benitez et al., Phys. Rev. **E80**, 030103 (2009).
- [147] J. Goldstone, Nuovo Cim. **19**, 154–164 (1961).
- [148] J. Goldstone, A. Salam, and S. Weinberg, Phys. Rev. **127**, 965–970 (1962).
- [149] J. Gasser and H. Leutwyler, Phys. Lett. **B188**, 477 (1987).
- [150] J. Braun, H. Gies, and D. D. Scherer, Phys. Rev. **D83**, 085012 (2011).
- [151] J. Braun, L. M. Haas, F. Marhauser, and J. M. Pawłowski, Phys. Rev. Lett. **106**, 022002 (2011).
- [152] H. Gies, J. Jaeckel, and C. Wetterich, Phys. Rev. **D69**, 105008 (2004).
- [153] A. Eichhorn and H. Gies, arXiv:1104.5366.
- [154] J. Braun and B. Klein, Phys. Rev. **D77**, 096008 (2008).
- [155] J. Braun and B. Klein, Eur. Phys. J. **C63**, 443–460 (2009).
- [156] S. Ejiri et al., Phys. Rev. **D80**, 094505 (2009).
- [157] J. Engels and F. Karsch, arXiv:1105.0584.
- [158] V. A. Miransky and K. Yamawaki, Mod. Phys. Lett. **A4**, 129–135 (1989).
- [159] V. A. Miransky and K. Yamawaki, Phys. Rev. **D55**, 5051–5066 (1997).
- [160] V. L. Berezinskii, Sov. Phys. JETP **32**, 493 (1971).
- [161] V. L. Berezinskii, Sov. Phys. JETP **34**, 610 (1972).
- [162] J. M. Kosterlitz and D. J. Thouless, J. Phys. **C6**, 1181–1203 (1973).
- [163] D. B. Kaplan, J. W. Lee, D. T. Son, and M. A. Stephanov, Phys. Rev. **D80**, 125005 (2009).
- [164] H. Gies, (private communication).
- [165] J. Berges and J. Cox, Phys. Lett. **B517**, 369–374 (2001).
- [166] G. Aarts and J. Berges, Phys. Rev. **D64**, 105010 (2001).
- [167] J. Berges, AIP Conf. Proc. **739**, 3–62 (2005).
- [168] T. Gasenzer and J. M. Pawłowski, Phys. Lett. **B670**, 135–140 (2008).
- [169] R. Alkofer, H. Gies, and B. J. Schaefer (eds.), Aspects of non-equilibrium quantum field theory: From cosmology to table-top experiments. Proceedings, 46. Internationale Universitaetswochen fuer Theoretische Physik, Winter School, IUTP 46, Schladming, Austria, 2009.
- [170] J. Braun, (in preparation).
- [171] D. F. Litim and J. M. Pawłowski, JHEP **11**, 026 (2006).
- [172] J. P. Blaizot, A. Ipp, R. Mendez-Galain, and N. Wschebor, Nucl. Phys. **A784**, 376–406 (2007).
- [173] M. E. Fisher, The theory of critical point singularities, in: Varenna 1970, Proceedings, Critical Phenomena, edited by M. S. Green, (Academic Press, New York, 1971), pp. 1–99.
- [174] M. E. Fisher and M. N. Barber, Phys. Rev. Lett. **28**, 1516–1519 (1972).
- [175] N. Goldenfeld, Lectures on phase transitions and the renormalization group, Frontiers in physics (Addison-Wesley, Reading, USA, 1992).
- [176] J. Zinn-Justin, Int. Ser. Monogr. Phys. **113**, 1–1054 (2002).
- [177] F. Karsch, Prog. Theor. Phys. Suppl. **186**, 479–484 (2010).
- [178] D. D. Dietrich, Phys. Rev. **D82**, 065007 (2010).
- [179] L. Del Debbio and R. Zwicky, Phys. Lett. **B700**, 217–220 (2011).
- [180] L. Del Debbio and R. Zwicky, Phys. Rev. **D82**, 014502 (2010).
- [181] M. Salmhofer, C. Honerkamp, W. Metzner, and O. Lauscher, Progress of Theoretical Physics **112**(6), 943–970 (2004).
- [182] G. Hagen et al., Phys. Rev. **C76**, 034302 (2007).
- [183] T. Otsuka, T. Suzuki, J. D. Holt, A. Schwenk, and Y. Akaishi, Phys. Rev. Lett. **105**, 032501 (2010).
- [184] B. Friman and A. Schwenk, arXiv:1101.4858.
- [185] M. H. Anderson, J. R. Ensher, M. R. Matthews, C. E. Wieman, and E. A. Cornell, Science **269**(5221), 198–201 (1995).
- [186] C. C. Bradley, C. A. Sackett, J. J. Tollett, and R. G. Hulet, Phys. Rev. Lett. **75**(9), 1687–1690 (1995).
- [187] K. B. Davis, M. O. Mewes, M. R. Andrews, N. J. van Druten, D. S. Durfee, D. M. Kurn, and W. Ketterle, Phys. Rev. Lett. **75**(22), 3969–3973 (1995).
- [188] B. DeMarco and D. S. Jin, Science **285**(5434), 1703–1706 (1999).
- [189] J. J. Sakurai and J. Napolitano, Modern quantum physics (Addison-Wesley (Boston, USA), 2011).
- [190] S. Diehl, H. Gies, J. M. Pawłowski, and C. Wetterich, Phys. Rev. **A76**, 021602 (2007).
- [191] L. Bartosch, P. Kopietz, and A. Ferraz, Physical Review B **80**, 104514 (2009).
- [192] S. Floerchinger, M. Scherer, S. Diehl, and C. Wetterich, Phys. Rev. **B78**, 174528 (2008).
- [193] S. Floerchinger, M. M. Scherer, and C. Wetterich, Phys. Rev. **A81**, 063619 (2010).
- [194] M. M. Scherer, S. Floerchinger, and H. Gies, arXiv:1010.2890.
- [195] J. P. Blaizot, R. Mendez-Galain, and N. Wschebor, cond-mat/0311460.
- [196] J. P. Blaizot, arXiv:0801.0009.

- [197] J. P. Blaizot, R. Mendez Galain, and N. Wschebor, Phys. Lett. **B632**, 571–578 (2006).
- [198] J. P. Blaizot, R. Mendez-Galain, and N. Wschebor, Phys. Rev. **E74**, 051116 (2006).
- [199] J. P. Blaizot, R. Mendez-Galain, and N. Wschebor, Phys. Rev. **E74**, 051117 (2006).
- [200] S. Diehl and C. Wetterich, Phys. Rev. **A73**, 033615 (2006).
- [201] J. W. Lee, M. G. Endres, D. B. Kaplan, and A. N. Nicholson, PoS **LATTICE2010**, 197 (2010).
- [202] M. G. Endres, D. B. Kaplan, J. W. Lee, and A. N. Nicholson, arXiv:1106.5725.
- [203] J. Braun, S. Diehl, and M. M. Scherer, (in preparation).
- [204] P. Fulde and R. A. Ferrell, Phys. Rev. **135**(3A), A550–A563 (1964).
- [205] P. Hohenberg and W. Kohn, Phys. Rev. **136**(3B), B864–B871 (1964).
- [206] R. J. Furnstahl, nucl-th/0702040.
- [207] J. E. Drut, R. J. Furnstahl, and L. Platter, Progress in Particle and Nuclear Physics **64**(January), 120–168 (2010).
- [208] J. Engel, Phys. Rev. **C 75**(1), 014306 (2007).
- [209] B. G. Giraud, B. K. Jennings, and B. R. Barrett, Phys. Rev. **A 78**(3), 032507 (2008).
- [210] R. van Leeuwen, Adv. Quant. Chem. **43**, 25 (2003).
- [211] J. Polonyi and K. Sailer, cond-mat/0108179.
- [212] S. J. Puglia, A. Bhattacharyya, and R. J. Furnstahl, Nuclear Physics A **723**(1-2), 145 – 180 (2003).
- [213] R. Fukuda, T. Kotani, Y. Suzuki, and S. Yokojima, Progress of Theoretical Physics **92**(4), 833–862 (1994).
- [214] M. Valiev and G. W. Fernando, cond-mat/9702247.
- [215] J. Polonyi and K. Sailer, Phys. Rev. **B 66**(15), 155113 (2002).
- [216] A. Schwenk and J. Polonyi, nucl-th/0403011.
- [217] J. Braun, J. Polonyi, and A. Schwenk, (in preparation).
- [218] C. Alexandrou, J. Myczkowski, and J. W. Negele, Phys. Rev. **C39**, 1076–1087 (1989).
- [219] J. Braun, Functional renormalization group and density functional theory, (talk given at the ReisenbuRG workshop of DFG FOR 723), 2009.
- [220] A. Schwenk, RG for nuclear forces and nuclear structure, (talk given at the INT workshop on “New applications of the renormalization group method in nuclear, particle and condensed matter physics”), 2010.
- [221] S. Hands, S. Kim, and J. B. Kogut, Nucl. Phys. **B442**, 364–390 (1995).
- [222] P. Castorina, M. Mazza, and D. Zappala, Phys. Lett. **B567**, 31–38 (2003).
- [223] F. Hoffing, C. Nowak, and C. Wetterich, Phys. Rev. **B66**, 205111 (2002).
- [224] H. Gies and M. M. Scherer, Eur. Phys. J. **C66**, 387–402 (2010).
- [225] J. Zinn-Justin, Int. Ser. Monogr. Phys. **113**, 1–1054 (2002).
- [226] R. D. Pisarski and F. Wilczek, Phys. Rev. **D29**, 338–341 (1984).
- [227] M. Reuter, Phys. Rev. **D57**, 971–985 (1998).
- [228] D. F. Litim and J. M. Pawłowski, Phys. Lett. **B516**, 197–207 (2001).
- [229] D. F. Litim and D. Zappala, Phys. Rev. **D83**, 085009 (2011).
- [230] L. Karkkainen, R. Lacaze, P. Lacock, and B. Petersson, Nucl. Phys. **B415**, 781–796 (1994).
- [231] J. A. Gracey, Int. J. Mod. Phys. **A9**, 727–744 (1994).
- [232] S. Hands, A. Kocic, and J. B. Kogut, Ann. Phys. **224**, 29–89 (1993).
- [233] S. Weinberg, Lectures presented at Int. School of Subnuclear Physics, Ettore Majorana, Erice, Sicily, Jul 23 - Aug 8, 1976.
- [234] S. Weinberg, hep-th/9702027.
- [235] D. Dou and R. Percacci, Class. Quant. Grav. **15**, 3449–3468 (1998).
- [236] O. Lauscher and M. Reuter, Phys. Rev. **D65**, 025013 (2002).
- [237] D. F. Litim, Phys. Rev. Lett. **92**, 201301 (2004).
- [238] A. Codello and R. Percacci, Phys. Rev. Lett. **97**, 221301 (2006).
- [239] P. F. Machado and F. Saueressig, Phys. Rev. **D77**, 124045 (2008).
- [240] A. Codello, R. Percacci, and C. Rahmede, Int. J. Mod. Phys. **A23**, 143–150 (2008).
- [241] A. Eichhorn, H. Gies, and M. M. Scherer, Phys. Rev. **D80**, 104003 (2009).
- [242] K. Groh and F. Saueressig, J. Phys. **A43**, 365403 (2010).
- [243] A. Eichhorn and H. Gies, Phys. Rev. **D81**, 104010 (2010).
- [244] P. Fischer and D. F. Litim, AIP Conf. Proc. **861**, 336–343 (2006).
- [245] H. Gies, Phys. Rev. **D68**, 085015 (2003).
- [246] H. Gies, S. Rechenberger, and M. M. Scherer, Eur. Phys. J. **C66**, 403–418 (2010).
- [247] R. Percacci and O. Zanusso, Phys. Rev. **D81**, 065012 (2010).
- [248] M. Gell-Mann, Phys. Lett. **8**, 214–215 (1964).
- [249] G. Zweig, CERN-TH-401.
- [250] H. Fritzsch, M. Gell-Mann, and H. Leutwyler, Phys. Lett. **B47**, 365–368 (1973).
- [251] Y. Nambu, Phys. Rev. **D10**, 4262 (1974).

- [252] W. A. Bardeen and R. B. Pearson, Phys. Rev. **D14**, 547 (1976).
- [253] O. W. Greenberg and C. A. Nelson, Phys. Rept. **32**, 69–121 (1977).
- [254] R. Alkofer and H. Reinhardt, Chiral quark dynamics (Berlin, Germany: Springer, 1995).
- [255] K. Fukushima, Phys. Lett. **B591**, 277–284 (2004).
- [256] C. Ratti, M. A. Thaler, and W. Weise, Phys. Rev. **D73**, 014019 (2006).
- [257] C. Sasaki, B. Friman, and K. Redlich, Phys. Rev. **D75**, 074013 (2007).
- [258] V. Skokov, B. Stokic, B. Friman, and K. Redlich, Phys. Rev. **C82**, 015206 (2010).
- [259] T. K. Herbst, J. M. Pawłowski, and B. J. Schaefer, Phys. Lett. **B696**, 58–67 (2011).
- [260] V. Skokov, B. Friman, and K. Redlich, Phys. Rev. **C83**, 054904 (2011).
- [261] U. Vogl, M. F. M. Lutz, S. Klimt, and W. Weise, Nucl. Phys. **A516**, 469–495 (1990).
- [262] S. Klimt, M. F. M. Lutz, U. Vogl, and W. Weise, Nucl. Phys. **A516**, 429–468 (1990).
- [263] S. Klimt, M. F. M. Lutz, and W. Weise, Phys. Lett. **B249**, 386–390 (1990).
- [264] B. J. Schaefer and M. Wagner, Phys. Rev. **D79**, 014018 (2009).
- [265] K. Fukushima, Phys. Rev. **D77**, 114028 (2008).
- [266] T. Hell, S. Rossner, M. Cristoforetti, and W. Weise, Phys. Rev. **D81**, 074034 (2010).
- [267] D. U. Jungnickel and C. Wetterich, Eur. Phys. J. **C2**, 557–567 (1998).
- [268] L. Jendges, B. Klein, H. J. Pirner, and K. Schwenzer, hep-ph/0608056.
- [269] G. 't Hooft, Phys. Rev. **D14**, 3432–3450 (1976).
- [270] M. A. Shifman, A. I. Vainshtein, and V. I. Zakharov, Nucl. Phys. **B163**, 46 (1980).
- [271] E. V. Shuryak, Nucl. Phys. **B203**, 93 (1982).
- [272] T. Schafer and E. V. Shuryak, Rev. Mod. Phys. **70**, 323–426 (1998).
- [273] J. M. Pawłowski, Phys. Rev. **D58**, 045011 (1998).
- [274] M. A. Stephanov, PoS **LAT2006**, 024 (2006).
- [275] J. Braun and A. Janot, arXiv:1102.4841.
- [276] M. L. Goldberger and S. B. Treiman, Phys. Rev. **110**, 1178–1184 (1958).
- [277] P. N. Meisinger and M. C. Ogilvie, Phys. Lett. **B379**, 163–168 (1996).
- [278] R. D. Pisarski, Phys. Rev. **D62**, 111501 (2000).
- [279] A. Mocsy, F. Sannino, and K. Tuominen, Phys. Rev. Lett. **92**, 182302 (2004).
- [280] E. Megias, E. Ruiz Arriola, and L. L. Salcedo, Phys. Rev. **D74**, 065005 (2006).
- [281] B. J. Schaefer, J. M. Pawłowski, and J. Wambach, Phys. Rev. **D76**, 074023 (2007).
- [282] T. Hell, S. Roessner, M. Cristoforetti, and W. Weise, Phys. Rev. **D79**, 014022 (2009).
- [283] A. J. Mizher, M. N. Chernodub, and E. S. Fraga, Phys. Rev. **D82**, 105016 (2010).
- [284] T. Hell, K. Kashiwa, and W. Weise, Phys. Rev. **D83**, 114008 (2011).
- [285] V. P. Gusynin and S. G. Sharapov, Phys. Rev. Lett. **95**(14), 146801 (2005).
- [286] V. P. Gusynin, S. G. Sharapov, and J. P. Carbotte, Phys. Rev. Lett. **96**(25), 256802 (2006).
- [287] J. E. Drut and T. A. Lähde, Phys. Rev. B **79**(16), 165425 (2009).
- [288] W. E. Caswell, Phys. Rev. Lett. **33**, 244 (1974).
- [289] T. Banks and A. Zaks, Nucl. Phys. **B196**, 189 (1982).
- [290] R. D. Pisarski, Phys. Rev. **D29**, 2423 (1984).
- [291] T. W. Appelquist, M. J. Bowick, D. Karabali, and L. C. R. Wijewardhana, Phys. Rev. **D33**, 3704 (1986).
- [292] T. Appelquist, D. Nash, and L. C. R. Wijewardhana, Phys. Rev. Lett. **60**, 2575 (1988).
- [293] D. Atkinson, P. W. Johnson, and P. Maris, Phys. Rev. **D42**, 602–609 (1990).
- [294] M. R. Pennington and D. Walsh, Phys. Lett. **B253**, 246–251 (1991).
- [295] D. C. Curtis, M. R. Pennington, and D. Walsh, Phys. Lett. **B295**, 313–319 (1992).
- [296] C. J. Burden and C. D. Roberts, Phys. Rev. **D44**, 540–550 (1991).
- [297] P. Maris, Phys. Rev. **D52**, 6087–6097 (1995).
- [298] V. P. Gusynin, A. H. Hams, and M. Reenders, Phys. Rev. **D53**, 2227–2235 (1996).
- [299] P. Maris, Phys. Rev. **D54**, 4049–4058 (1996).
- [300] C. S. Fischer, R. Alkofer, T. Dahm, and P. Maris, Phys. Rev. **D70**, 073007 (2004).
- [301] E. Dagotto, A. Kocic, and J. B. Kogut, Nucl. Phys. **B334**, 279 (1990).
- [302] S. Hands and J. B. Kogut, Nucl. Phys. **B335**, 455 (1990).
- [303] S. J. Hands, J. B. Kogut, and C. G. Strouthos, Nucl. Phys. **B645**, 321–336 (2002).
- [304] S. J. Hands, J. B. Kogut, L. Scorzato, and C. G. Strouthos, Phys. Rev. **B70**, 104501 (2004).
- [305] K. i. Kondo, S. Shuto, and K. Yamawaki, Mod. Phys. Lett. **A6**, 3385–3396 (1991).
- [306] T. Appelquist, J. Terning, and L. C. R. Wijewardhana, Phys. Rev. Lett. **77**, 1214–1217 (1996).
- [307] T. Appelquist and S. B. Selipsky, Phys. Lett. **B400**, 364–369 (1997).
- [308] M. Velkovsky and E. V. Shuryak, Phys. Lett. **B437**, 398–402 (1998).
- [309] T. Appelquist, A. Ratnaweera, J. Terning, and L. C. R. Wijewardhana, Phys. Rev. **D58**, 105017 (1998).
- [310] M. Harada and K. Yamawaki, Phys. Rev. Lett. **86**, 757–760 (2001).
- [311] F. Sannino and J. Schechter, Phys. Rev. **D60**, 056004 (1999).

- [312] M. Harada, M. Kurachi, and K. Yamawaki, Phys. Rev. **D68**, 076001 (2003).
- [313] H. Terao and A. Tsuchiya, arXiv:0704.3659.
- [314] E. Poppitz and M. Unsal, JHEP **09**, 050 (2009).
- [315] A. Armoni, Nucl. Phys. **B826**, 328–336 (2010).
- [316] F. Sannino, Phys. Rev. **D80**, 065011 (2009).
- [317] F. Sannino, Nucl. Phys. **B830**, 179–194 (2010).
- [318] J. B. Kogut et al., Phys. Rev. Lett. **48**, 1140 (1982).
- [319] R. V. Gavai, Nucl. Phys. **B269**, 530 (1986).
- [320] M. Fukugita, S. Ohta, and A. Ukawa, Phys. Rev. Lett. **60**, 178 (1988).
- [321] F. R. Brown et al., Phys. Rev. **D46**, 5655–5670 (1992).
- [322] P. H. Damgaard, U. M. Heller, A. Krasnitz, and P. Olesen, Phys. Lett. **B400**, 169–175 (1997).
- [323] Y. Iwasaki, K. Kanaya, S. Kaya, S. Sakai, and T. Yoshie, Phys. Rev. **D69**, 014507 (2004).
- [324] S. Catterall and F. Sannino, Phys. Rev. **D76**, 034504 (2007).
- [325] T. Appelquist, G. T. Fleming, and E. T. Neil, Phys. Rev. Lett. **100**, 171607 (2008).
- [326] A. Deuzeman, M. P. Lombardo, and E. Pallante, Phys. Lett. **B670**, 41–48 (2008).
- [327] A. Deuzeman, M. P. Lombardo, and E. Pallante, Phys. Rev. **D82**, 074503 (2010).
- [328] T. Appelquist, G. T. Fleming, and E. T. Neil, Phys. Rev. **D79**, 076010 (2009).
- [329] Z. Fodor, K. Holland, J. Kuti, D. Negradi, and C. Schroeder, Phys. Lett. **B681**, 353–361 (2009).
- [330] Z. Fodor, K. Holland, J. Kuti, D. Negradi, and C. Schroeder, PoS **LAT2009**, 055 (2009).
- [331] E. Pallante, PoS **LAT2009**, 015 (2009).
- [332] T. DeGrand, arXiv:1010.4741.
- [333] Y. Kusafuka and H. Terao, arXiv:1104.3606.
- [334] V. A. Miransky, Nuovo Cim. **A90**, 149–170 (1985).
- [335] V. A. Miransky and P. I. Fomin, Sov. J. Part. Nucl. **16**, 203 (1985).
- [336] R. S. Chivukula, Phys. Rev. **D55**, 5238–5240 (1997).
- [337] T. Appelquist and F. Sannino, Phys. Rev. **D59**, 067702 (1999).
- [338] S. Bethke, Eur. Phys. J. **C64**, 689–703 (2009).
- [339] F. Karsch, E. Laermann, and A. Peikert, Nucl. Phys. **B605**, 579–599 (2001).
- [340] B. J. Schaefer, M. Wagner, and J. Wambach, Phys. Rev. **D81**, 074013 (2010).
- [341] J. Braun, hep-ph/0611145.
- [342] H. S. Fukano and F. Sannino, Phys. Rev. **D82**, 035021 (2010).
- [343] M. Jarvinen and F. Sannino, JHEP **02**, 081 (2011).
- [344] F. Sannino, Phys. Rev. **D80**, 017901 (2009).
- [345] T. DeGrand and A. Hasenfratz, Phys. Rev. **D80**, 034506 (2009).
- [346] M. Reuter and C. Wetterich, Nucl. Phys. **B417**, 181–214 (1994).
- [347] M. Reuter and C. Wetterich, hep-th/9411227.
- [348] H. Gies, Phys. Rev. **D66**, 025006 (2002).
- [349] J. M. Pawłowski, D. F. Litim, S. Nedelko, and L. von Smekal, Phys. Rev. Lett. **93**, 152002 (2004).
- [350] C. S. Fischer and H. Gies, JHEP **10**, 048 (2004).
- [351] J. Braun, H. Gies, and J. M. Pawłowski, Phys. Lett. **B684**, 262–267 (2010).
- [352] F. Marhauser and J. M. Pawłowski, arXiv:0812.1144.
- [353] J. Braun, A. Eichhorn, H. Gies, and J. M. Pawłowski, Eur. Phys. J. **C70**, 689–702 (2010).
- [354] A. Eichhorn, H. Gies, and J. M. Pawłowski, Phys. Rev. **D83**, 045014 (2011).
- [355] K. I. Kondo, Phys. Rev. **D82**, 065024 (2010).
- [356] D. F. Litim and J. M. Pawłowski, Phys. Lett. **B435**, 181–188 (1998).
- [357] T. van Ritbergen, J. A. M. Vermaseren, and S. A. Larin, Phys. Lett. **B400**, 379–384 (1997).
- [358] M. Czakon, Nucl. Phys. **B710**, 485–498 (2005).
- [359] U. Ellwanger, Phys. Lett. **B335**, 364–370 (1994).
- [360] Y. Aoki, G. Endrodi, Z. Fodor, S. D. Katz, and K. K. Szabo, Nature **443**, 675–678 (2006).
- [361] Y. Aoki, Z. Fodor, S. D. Katz, and K. K. Szabo, Phys. Lett. **B643**, 46–54 (2006).
- [362] M. Cheng et al., Phys. Rev. **D74**, 054507 (2006).
- [363] M. Cheng et al., Phys. Rev. **D81**, 054504 (2010).
- [364] F. Fucito, S. Solomon, and C. Rebbi, Phys. Rev. **D31**, 1460 (1985).
- [365] R. V. Gavai, J. Potvin, and S. Sanielevici, Phys. Rev. Lett. **58**, 2519 (1987).
- [366] F. R. Brown et al., Phys. Rev. Lett. **65**, 2491–2494 (1990).
- [367] F. Karsch, E. Laermann, and C. Schmidt, Phys. Lett. **B520**, 41–49 (2001).
- [368] M. Pepe and U. J. Wiese, Nuclear Physics B **768**(April), 21–37 (2007).
- [369] K. Holland, M. Pepe, and U. J. Wiese, Nuclear Physics B **694**(August), 35–58 (2004).
- [370] L. von Smekal, R. Alkofer, and A. Hauck, Phys. Rev. Lett. **79**, 3591–3594 (1997).
- [371] L. von Smekal, A. Hauck, and R. Alkofer, Ann. Phys. **267**, 1 (1998).

- [372] C. Lerche and L. von Smekal, Phys. Rev. **D65**, 125006 (2002).
- [373] R. Alkofer, C. S. Fischer, and F. J. Llanes-Estrada, Phys. Lett. **B611**, 279–288 (2005).
- [374] C. S. Fischer, A. Maas, and J. M. Pawłowski, Annals Phys. **324**, 2408–2437 (2009).
- [375] C. S. Fischer and J. M. Pawłowski, Phys. Rev. **D80**, 025023 (2009).
- [376] C. S. Fischer and J. M. Pawłowski, Phys. Rev. **D75**, 025012 (2007).
- [377] A. C. Aguilar, D. Binosi, J. Papavassiliou, and J. Rodriguez-Quintero, Phys. Rev. **D80**, 085018 (2009).
- [378] O. Gromenko, arXiv:0710.1591.
- [379] Y. Aoki et al., JHEP **06**, 088 (2009).
- [380] M. Panero, Phys. Rev. Lett. **103**, 232001 (2009).
- [381] S. Datta and S. Gupta, Phys. Rev. **D82**, 114505 (2010).
- [382] S. Borsanyi et al., arXiv:1011.4230.
- [383] A. Bazavov and P. Petreczky, PoS **LATTICE2010**, 169 (2010).
- [384] K. Kanaya, AIP Conf. Proc. **1343**, 57–62 (2011).
- [385] C. S. Fischer, Phys. Rev. Lett. **103**, 052003 (2009).
- [386] C. S. Fischer and J. A. Mueller, Phys. Rev. **D80**, 074029 (2009).
- [387] C. S. Fischer, A. Maas, and J. A. Muller, Eur. Phys. J. **C68**, 165–181 (2010).
- [388] J. M. Pawłowski, arXiv:1012.5075.
- [389] A. M. Polyakov, Phys. Lett. **B72**, 477–480 (1978).
- [390] J. Greensite, Prog. Part. Nucl. Phys. **51**, 1 (2003).
- [391] C. Gattringer, Phys. Rev. Lett. **97**, 032003 (2006).
- [392] F. Synatschke, A. Wipf, and C. Wozar, Phys. Rev. **D75**, 114003 (2007).
- [393] E. Bilgici, F. Bruckmann, C. Gattringer, and C. Hagen, Phys. Rev. **D77**, 094007 (2008).
- [394] K. Kashiwa, M. Matsuzaki, H. Kouno, Y. Sakai, and M. Yahiro, Phys. Rev. **D79**, 076008 (2009).
- [395] Y. Sakai, K. Kashiwa, H. Kouno, and M. Yahiro, Phys. Rev. **D77**, 051901 (2008).
- [396] E. Bilgici et al., Few Body Syst. **47**, 125–135 (2010).
- [397] B. Zhang, F. Bruckmann, C. Gattringer, Z. Fodor, and K. K. Szabo(2010).
- [398] T. K. Mukherjee, H. Chen, and M. Huang, Phys. Rev. **D82**, 034015 (2010).
- [399] R. Gatto and M. Ruggieri, Phys. Rev. **D82**, 054027 (2010).
- [400] C. S. Fischer, J. Luecker, and J. A. Mueller, Phys. Lett. **B702**, 438–441 (2011).
- [401] M. Q. Huber and J. Braun, arXiv:1102.5307.
- [402] S. Catterall, J. Giedt, F. Sannino, and J. Schneible, JHEP **11**, 009 (2008).
- [403] L. Del Debbio, A. Patella, and C. Pica, Phys. Rev. **D81**, 094503 (2010).
- [404] L. Del Debbio, B. Lucini, A. Patella, C. Pica, and A. Rago, Phys. Rev. **D80**, 074507 (2009).
- [405] F. Sannino, Phys. Rev. **D79**, 096007 (2009).
- [406] A. Patella, L. Del Debbio, B. Lucini, C. Pica, and A. Rago, PoS **LATTICE2010**, 068 (2010).
- [407] M. Mojaza, C. Pica, and F. Sannino, Phys. Rev. **D82**, 116009 (2010).